

Floodplain inundation mapping and modelling in the Flinders and Gilbert catchments

A technical report to the Australian Government from the CSIRO Flinders and Gilbert Agricultural Resource Assessment, part of the North Queensland Irrigated Agriculture Strategy

Dushmanta Dutta¹, Fazlul Karim¹, Catherine Ticehurst¹, Steve Marvanek² and Cuan Petheram¹

¹CSIRO Land and Water, Canberra

²CSIRO Land and Water, Adelaide

December 2013



Water for a Healthy Country Flagship Report series ISSN: 1835-095X

Australia is founding its future on science and innovation. Its national science agency, CSIRO, is a powerhouse of ideas, technologies and skills.

CSIRO initiated the National Research Flagships to address Australia's major research challenges and opportunities. They apply large scale, long term, multidisciplinary science and aim for widespread adoption of solutions. The Flagship Collaboration Fund supports the best and brightest researchers to address these complex challenges through partnerships between CSIRO, universities, research agencies and industry.

Consistent with Australia's national interest, the Water for a Healthy Country Flagship aims to develop science and technologies that improve the social, economic and environmental outcomes from water, and deliver \$3 billion per year in net benefits for Australia by 2030. The Sustainable Agriculture Flagship aims to secure Australian agriculture and forest industries by increasing productivity by 50 percent and reducing carbon emissions intensity by at least 50 percent by 2030.

For more information about Water for a Healthy Country Flagship, Sustainable Agriculture Flagship or the National Research Flagship Initiative visit <http://www.csiro.au/flagships>.

Citation

Dutta D, Karim F, Ticehurst C, Marvanek S and Petheram C (2013) Floodplain inundation mapping and modelling in the Flinders and Gilbert Catchments. A technical report to the Australian Government from the CSIRO Flinders and Gilbert Agricultural Resource Assessment, part of the North Queensland Irrigated Agriculture Strategy. CSIRO Water for a Healthy Country and Sustainable Agriculture flagships, Australia.

Copyright

© Commonwealth Scientific and Industrial Research Organisation 2013. To the extent permitted by law, all rights are reserved and no part of this publication covered by copyright may be reproduced or copied in any form or by any means except with the written permission of CSIRO.

Important disclaimer

CSIRO advises that the information contained in this publication comprises general statements based on scientific research. The reader is advised and needs to be aware that such information may be incomplete or unable to be used in any specific situation. No reliance or actions must therefore be made on that information without seeking prior expert professional, scientific and technical advice. To the extent permitted by law, CSIRO (including its employees and consultants) excludes all liability to any person for any consequences, including but not limited to all losses, damages, costs, expenses and any other compensation, arising directly or indirectly from using this publication (in part or in whole) and any information or material contained in it.

Flinders and Gilbert Agricultural Resource Assessment acknowledgments

This report was prepared for the Office of Northern Australia in the Australian Government Department of Infrastructure and Regional Development under the North Queensland Irrigated Agriculture Strategy <http://www.regional.gov.au/regional/ona/nqis.aspx>. The Strategy is a collaborative initiative between the Office of Northern Australia, the Queensland Government and CSIRO. One part of the Strategy is the Flinders and Gilbert Agricultural Resource Assessment, which was led by CSIRO. Important aspects of the Assessment were undertaken by the Queensland Government and TropWATER (James Cook University).

The Strategy was guided by two committees:

(i) the **Program Governance Committee**, which included the individuals David Crombie (GRM International), Scott Spencer (SunWater, during the first part of the Strategy) and Paul Woodhouse (Regional Development Australia) as well as representatives from the following organisations: Australian Government Department of Infrastructure and Regional Development; CSIRO; and the Queensland Government.

(ii) the **Program Steering Committee**, which included the individual Jack Lake (Independent Expert) as well as representatives from the following organisations: Australian Government Department of Infrastructure and Regional Development; CSIRO; the Etheridge, Flinders and McKinlay shire councils; Gulf Savannah Development; Mount Isa to Townsville Economic Development Zone; and the Queensland Government.

This report was reviewed by Dr Ian Watson (CSIRO), Dr Jai Vaze (CSIRO) and Dr Peter Stone (CSIRO).

Heinz Buettikofer (CSIRO), Ruth Palmer (CSIRO) and Daniel Aramini (CSIRO) are acknowledged for their assistance in the compilation of this report.

Director's foreword

Northern Australia comprises approximately 20% of Australia's land mass but remains relatively undeveloped. It contributes about 2% to the nation's gross domestic product (GDP) and accommodates around 1% of the total Australian population.

Recent focus on the shortage of water and on climate-based threats to food and fibre production in the nation's south have re-directed attention towards the possible use of northern water resources and the development of the agricultural potential in northern Australia. Broad analyses of northern Australia as a whole have indicated that it is capable of supporting significant additional agricultural and pastoral production, based on more intensive use of its land and water resources.

The same analyses also identified that land and water resources across northern Australia were already being used to support a wide range of highly valued cultural, environmental and economic activities. As a consequence, pursuit of new agricultural development opportunities would inevitably affect existing uses and users of land and water resources.

The Flinders and Gilbert catchments in north Queensland have been identified as potential areas for further agricultural development. The Flinders and Gilbert Agricultural Resource Assessment (the Assessment), of which this report is a part, provides a comprehensive and integrated evaluation of the feasibility, economic viability and sustainability of agricultural development in these two catchments as part of the North Queensland Irrigated Agricultural Strategy. The Assessment seeks to:

- identify and evaluate water capture and storage options
- identify and test the commercial viability of irrigated agricultural opportunities
- assess potential environmental, social and economic impacts and risks.

By this means it seeks to support deliberation and decisions concerning sustainable regional development.

The Assessment differs from previous assessments of agricultural development or resources in two main ways:

- It has sought to 'join the dots'. Where previous assessments have focused on single development activities or assets – without analysing the interactions between them – this Assessment considers the opportunities presented by the simultaneous pursuit of multiple development activities and assets. By this means, the Assessment uses a whole-of-region (rather than an asset-by-asset) approach to consider development.
- The novel methods developed for the Assessment provide a blueprint for rapidly assessing future land and water developments in northern Australia.

Importantly, the Assessment has been designed to lower the barriers to investment in regional development by:

- explicitly addressing local needs and aspirations
- meeting the needs of governments as they regulate the sustainable and equitable management of public resources with due consideration of environmental and cultural issues
- meeting the due diligence requirements of private investors, by addressing questions of profitability and income reliability at a broad scale.

Most importantly, the Assessment does not recommend one development over another. It provides the reader with a range of possibilities and the information to interpret them, consistent with the reader's values and their aspirations for themselves and the region.

Peter Stone

Dr Peter Stone, Deputy Director, CSIRO Sustainable Agriculture Flagship

The Flinders and Gilbert Agricultural Resource Assessment team

Project Director	Peter Stone
Project Leaders	Cuan Petheram, Ian Watson
Reporting Team	<u>Heinz Buettikofer</u> , <u>Becky Schmidt</u> , Maryam Ahmad, Simon Gallant, Frances Marston, Greg Rinder, Audrey Wallbrink
Project Support	<u>Ruth Palmer</u> , Daniel Aramini, Michael Kehoe, Scott Podger
Communications	<u>Leane Regan</u> , Claire Bobinskas, Dianne Flett ² , Rebecca Jennings
Data Management	<u>Mick Hartcher</u>

Activities

Agricultural productivity	<u>Tony Webster</u> , Brett Cocks, Jo Gentle ⁶ , Dean Jones, Di Mayberry, Perry Poulton, Stephen Yeates, Ainsleigh Wixon
Aquatic and riparian ecology	<u>Damien Burrows</u> ¹ , Jon Brodie ¹ , Barry Butler ¹ , Cassandra James ¹ , Colette Thomas ¹ , Nathan Waltham ¹
Climate	<u>Cuan Petheram</u> , Ang Yang
Instream waterholes	<u>David McJannet</u> , Anne Henderson, Jim Wallace ¹
Flood mapping	<u>Dushmanta Dutta</u> , Fazlul Karim, Steve Marvanek, Cate Ticehurst
Geophysics	<u>Tim Munday</u> , Tania Abdat, Kevin Cahill, Aaron Davis
Groundwater	<u>Ian Jolly</u> , <u>Andrew Taylor</u> , Phil Davies, Glenn Harrington, John Knight, David Rassam
Indigenous water values	<u>Marcus Barber</u> , Fenella Atkinson ⁵ , Michele Bird ² , Susan McIntyre-Tamwoy ⁵
Water storage	<u>Cuan Petheram</u> , Geoff Eades ² , John Gallant, Paul Harding ³ , Ahrim Lee ³ , Sylvia Ng ³ , Arthur Read, Lee Rogers, Brad Sherman, Kerrie Tomkins, Sanne Voogt ³
Irrigation infrastructure	<u>John Hornbuckle</u>
Land suitability	<u>Rebecca Bartley</u> , Daniel Brough ³ , Charlie Chen, David Clifford, Angela Esterberg ³ , Neil Enderlin ³ , Lauren Eyres ³ , Mark Glover, Linda Gregory, Mike Grundy, Ben Harms ³ , Warren Hicks, Joseph Kemei, Jeremy Manders ³ , Keith Moody ³ , Dave Morrison ³ , Seonaid Philip, Bernie Powell ³ , Liz Stower, Mark Sugars ³ , Mark Thomas, Seija Tuomi, Reanna Willis ³ , Peter R Wilson ²
River modelling	<u>Linda Holz</u> , <u>Julien Lerat</u> , Chas Egan ³ , Matthew Gooda ³ , Justin Hughes, Shaun Kim, Alex Loy ³ , Jean-Michel Perraud, Geoff Podger

Socio-economics

Lisa Brennan McKellar, Neville Crossman, Onil Banerjee,
Rosalind Bark, Andrew Higgins, Luis Laredo, Neil MacLeod,
Marta Monjardino, Carmel Pollino, Di Prestwidge, Stuart Whitten,
Glyn Wittwer⁴

Note: all contributors are affiliated with CSIRO unless indicated otherwise. Activity Leaders are underlined. ¹ TropWATER, James Cook University, ² Independent consultant, ³ Queensland Government, ⁴ Monash University, ⁵ Archaeological Heritage Management Solutions, ⁶ University of Western Sydney

Shortened forms

AEM	airborne electromagnetics
AHD	Australian Height Datum
APSIM	Agricultural Production Systems Simulator
AWRC	Australian Water Resources Council
CGE	Computable General Equilibrium
CSIRO	Commonwealth Scientific and Industrial Research Organisation
DEM	digital elevation model
GCMs	global climate models
GCM-ES	global climate model output empirically scaled to provide catchment-scale variables
IPCC AR4	the Fourth Assessment Report of the Intergovernmental Panel on Climate Change
IQQM	Integrated Quantity-Quality Model – a river systems model
Landsat TM	Landsat Thematic Mapper
MODIS	Moderate Resolution Imaging Spectroradiometer
NQIAS	North Queensland Irrigated Agriculture Strategy
NRM	natural resource management
ONA	the Australian Government Office of Northern Australia
OWL	the Open Water Likelihood algorithm
PAWC	plant available water capacity
PE	potential evaporation
RCP	representative concentration pathway
Sacramento	a rainfall-runoff model
SALI	the Soil and Land Information System for Queensland
SLAs	statistical local areas
SRTM	shuttle radar topography mission
TRaCK	Tropical Rivers and Coastal Knowledge Research Hub
WRON	CSIRO's Water Resource Observation Network

Units

MEASUREMENT UNITS	DESCRIPTION
GL	gigalitres, 1,000,000,000 litres
keV	kilo-electronvolts
kL	kilolitres, 1000 litres
km	kilometres, 1000 metres
L	litres
m	metres
mAHD	metres above Australian Height Datum
MeV	mega-electronvolts
mg	milligrams
ML	megalitres, 1,000,000 litres

Preface

The Flinders and Gilbert Agricultural Resource Assessment (the Assessment) aims to provide information so that people can answer questions such as the following in the context of their particular circumstances in the Flinders and Gilbert catchments:

- What soil and water resources are available for irrigated agriculture?
- What are the existing ecological systems, industries, infrastructure and values?
- What are the opportunities for irrigation?
- Is irrigated agriculture economically viable?
- How can the sustainability of irrigated agriculture be maximised?

The questions – and the responses to the questions – are highly interdependent and, consequently, so is the research undertaken through this Assessment. While each report may be read as a stand-alone document, the suite of reports must be read as a whole if they are to reliably inform discussion and decision making on regional development.

The Assessment is producing a series of reports:

- Technical reports present scientific work at a level of detail sufficient for technical and scientific experts to reproduce the work. Each of the 12 research activities (outlined below) has a corresponding technical report.
- Each of the two catchment reports (one for each catchment) synthesises key material from the technical reports, providing well-informed but non-scientific readers with the information required to make decisions about the opportunities, costs and benefits associated with irrigated agriculture.
- Two overview reports – one for each catchment – are provided for a general public audience.
- A factsheet provides key findings for both the Flinders and Gilbert catchments for a general public audience.

All of these reports are available online at <<http://www.csiro.au/FGARA>>. The website provides readers with a communications suite including factsheets, multimedia content, FAQs, reports and links to other related sites, particularly about other research in northern Australia.

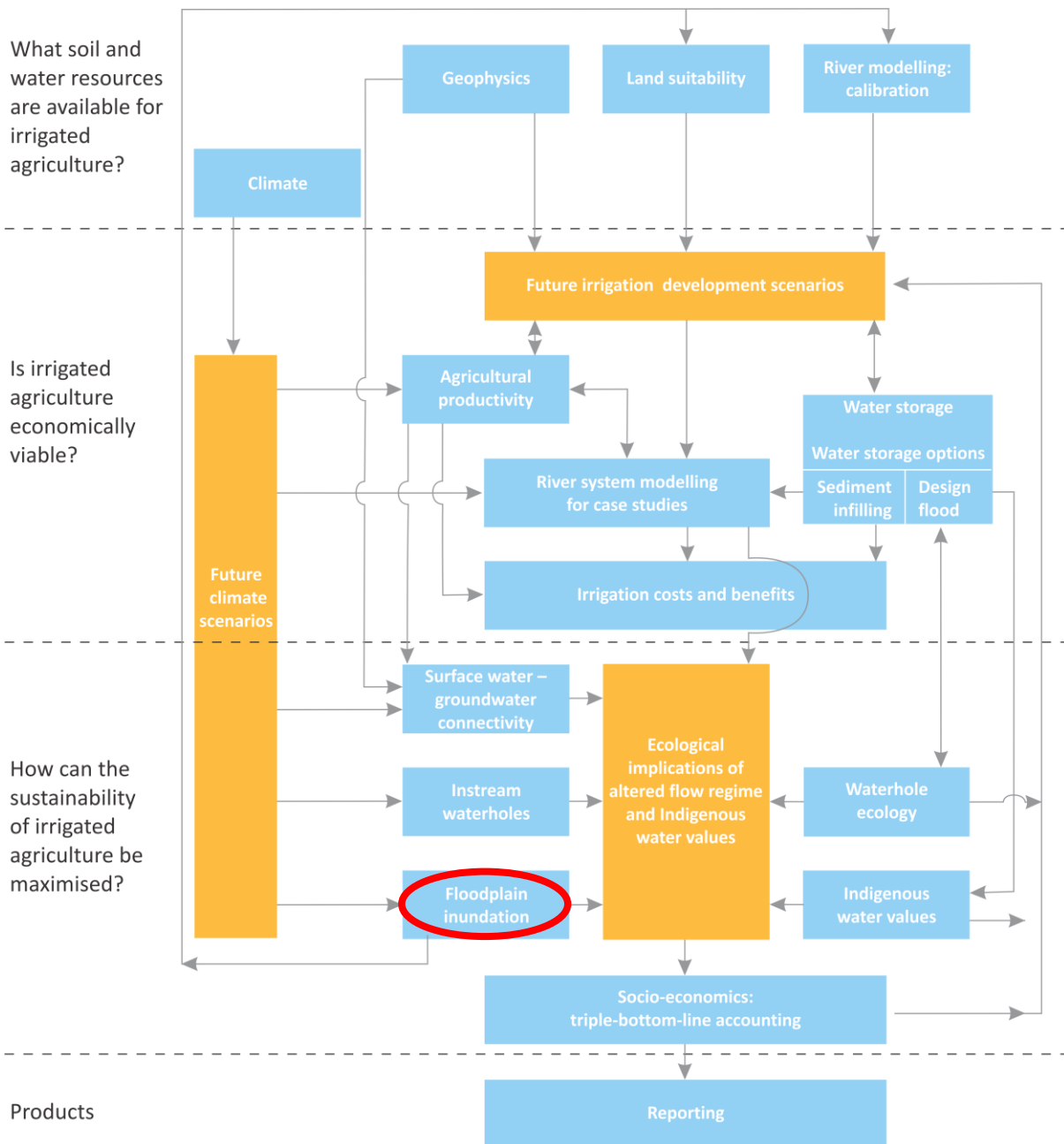
The Assessment is divided into 12 scientific activities, each contributing to a cohesive picture of regional development opportunities, costs and benefits. Preface Figure 1 illustrates the high-level linkages between the 12 activities and the general flow of information in the Assessment. Clicking on an ‘activity box’ links to the relevant technical report.

The Assessment is designed to inform consideration of development, not to enable particular development activities. As such, the Assessment informs – but does not seek to replace – existing planning processes. Importantly, the Assessment does not assume a given regulatory environment. As regulations can change, this will enable the results to be applied to the widest range of uses for the longest possible time frame. Similarly, the Assessment does not assume a static future, but evaluates three distinct scenarios:

- Scenario A – historical climate and current development
- Scenario B – historical climate and future irrigation development
- Scenario C – future climate and current development.

As the primary interest was in evaluating the scale of the opportunity for irrigated agriculture development under the current climate, the future climate scenario (Scenario C) was secondary in importance to scenarios A and B. This balance is reflected in the allocation of resources throughout the Assessment.

The approaches and techniques used in the Assessment have been designed to enable application elsewhere in northern Australia.



Preface Figure 1 Schematic diagram illustrating high-level linkages between the 12 activities (blue boxes)

This report is a technical report. The red oval in Preface Figure 1 indicates the activity (or activities) that contributed to this report.

The orange boxes indicate information used or produced by several activities. The red oval indicates the activity (or activities) that contributed to this technical report. Click on a box associated with an activity for a link to its technical report (or click on ‘Technical reports’ on <http://www.csiro.au/FGARA> for a list of links to all technical reports). Note that the Water storage activity has multiple technical reports – in this case the separate reports are listed under the activity title. Note also that these reports will be published throughout 2013, and hyperlinks to currently unpublished reports will produce an ‘invalid publication’ error in the CSIRO Publication Repository.

Executive summary

The Flinders and Gilbert catchments have large floodplains in their lower reaches that flood frequently. Wetlands with high biodiversity are located in these floodplains. While flooding can be catastrophic to agricultural production in terms of loss of stock, fodder and topsoil and damage to crops and infrastructure, the wetland ecosystems in these areas are thought to be largely dependent on “flood pulses”. Hydrological connectivity between floodplain wetlands and rivers is the principal mechanism for the diversity, productivity and interactions of the major biota in river-floodplain systems.

This report describes the characteristics of flooding in these catchments. It also reports on an investigation into the hydrological connectivity between floodplain wetlands and streamflow and the potential impacts of upstream irrigation development and climate change on flood regime and wetland connectivity in the Flinders and Gilbert catchments. The main aim of this activity of the Flinders and Gilbert Agricultural Resource Assessment was to map and model floods in the mid-to-lower reaches of the Flinders catchment and lower reaches of the Gilbert catchments for the purpose of:

1. Identifying areas susceptible to flooding.
2. Estimating inundation across the floodplains under future climate and development scenarios.
3. Quantifying hydrological connectivity of wetlands in terms of:
 - a. extent, timing and duration of connection of off-stream wetlands to main river channels
 - b. changes in connectivity as a result of changes to flow regime.
4. Establishing a relationship between streamflow and floodplain inundation to be used by the river system models for long term simulations.

This report details the flood mapping using satellite imagery and inundation modelling using 1- and 2-dimensional hydrodynamic models. Specifically the objectives of this technical report are to:

- Describe the methods used for mapping flooding using MODIS and Landsat TM imagery, document satellite data used and present the flood maps produced.
- Describe the hydrodynamic model used for inundation modelling, document the configuration of the hydrodynamic model and underlying assumptions, describe the hydro-meteorological data used in modelling.
- Describe the methods used for hydrological connectivity of floodplain wetlands to streamflows and quantify the connectivity under the historical climate and current levels of development.
- Present the results of calibration and validation of the hydrodynamic model.
- Evaluate floodplain inundation characteristics and wetland connectivity under the future climate and development and report the impacts of future climate and development on flood regime in the floodplains and wetland connectivity.

Flood Mapping

MODIS and Landsat satellite imagery were used for producing maps of surface water extents to identify lands subject to flooding in the Flinders and Gilbert catchments. MODIS satellite data of 500 m resolution acquired at daily interval from November 2000 until March 2011 were used for producing daily maps of surface water using the Open Water Likelihood (OWL) algorithm. Landsat data of 30 m resolution at 16 days interval were also used to produce water maps using the Canonical Variates Analysis tool. Composite maps of average, maximum and inundation duration were produced from daily MODIS water maps for each year from 2000 to 2011. The period captured the second largest flood event on record (January-February 2009) in the Flinders and Gilbert catchments. Event based inundation maps were produced for a selected number of flood events between 2000-2011 for the calibration and validation of the two-dimensional

hydrodynamic models. Cloud cover was a problem when producing event based inundation maps, particularly for the Gilbert catchment.

The Gilbert and Flinders floodplains show very similar flood patterns. The statistical summaries of the MODIS OWL water highlight the large flood in January/February 2009 for the Flinders and Gilbert catchments compared to the other years. The lower parts of the two catchments were inundated for more than 10 days during this flood. The 2010-2011 wet season was also reasonably wet for the two catchments, and the 2005-2006 and 2009-2010 wet seasons for the Flinders catchment only. The 2001-2002 and 2002-2003 wet seasons appear to have been particularly dry compared to the others, as was the 2006-2007 wet season except to the north of the lower Gilbert catchment.

There were significant variations in flooded areas with different OWL thresholds. Soil colour and type appear to have an influence on the MODIS OWL for low percentage water values. Overhead vegetation was another problem, particularly for the lower Gilbert catchment where the flooding was expected to be more extensive than was showing in the water maps.

The final MODIS flood map (which was generated from Maximum OWL flood maps from the relatively wet years of 2000, 2001, 2004, 2008, 2009, 2010 and 2011, with artefacts removed) was compared to the Queensland Department of Natural Resources and Mines QIFAO (Queensland Interim Floodplain Assessment Overlay) product. When the QIFAO flood map is compared to the MODIS flood map the QIFAO is showing much larger extent than the MODIS. There are a number of reasons for this: the QIFAO map is showing narrow drainage channels, many covered in vegetation, which are too fine for the MODIS to detect; the QIFAO appears to include the whole lower floodplain rather than what is visible to the satellite. There are also a few areas where the MODIS flood map is showing water, while the QIFAO is not. These areas are also mapping as water in the Landsat DERM imagery – although not as extensive as the MODIS flood map. They appear to be in very flat areas, which are not part of the drainage channels. The water mapped in these areas is likely to be very shallow, and possibly confused with moist soil in parts.

Set-up and calibration and validation of the hydrodynamic model

MIKE 21 two-dimensional and MIKE 11 one-dimensional hydrodynamic models of the MIKEFLOOD package were used in the Assessment. MIKE 21 was used for inundation modelling in the floodplains of the Flinders and Gilbert catchments. The total area of the hydrodynamic modelling domain of the Coastal floodplain of the Flinders river was 82,403 km² and that of the Coastal floodplain of the Gilbert River is 20,886 km². The spatial resolution of the hydrodynamic model was 150 m and 90 m for the coastal floodplains of Flinders and Gilbert rivers, respectively.

Based on the historical records and availability of data, four flood events in the Flinders catchment and two flood events in the Gilbert catchment over the past 12 years were selected for the calibration and validation of the two-dimensional model. In the Flinders catchment, the selected events were from 2001, 2004, 2009 and 2011, which represented large and small flood events. Flood maps derived from MODIS imagery were used to compare spatial metrics of inundation area across the floodplain. In addition, gauged water heights at key locations were used. In the Gilbert catchment, with the majority of the MODIS and Landsat imagery during the flood events obscured by cloud, only two events (of 2009 and 2011) were found to be suitable and the model was calibrated to one and validated to the other.

The pattern of simulated inundation extents by the hydrodynamic model was similar to the MODIS flood maps in the two catchments. In both calibration and validation of the hydrodynamic model, there are broad agreements between the simulated inundation extents and the MODIS flood maps with 5% thresholds. The main difference between the simulated inundation maps and the MODIS flood map was that the MODIS flood maps were unable to capture the fine scale flow paths, some of which were a single pixel in width. Considering the cloud covers, difference in resolutions of MODIS imagery (500 m) and hydrodynamic model (150 m in the Flinders and 90 m in the Gilbert), the cell-to-cell matching between the simulated flood maps and the MODIS flood maps with 5% and 10% thresholds was reasonably good.

The simulated stage heights had reasonably good agreement with the observed stage heights at the gauges located within the Flinders floodplain with R² values during calibration ranging between 0.40 - 0.72 and 0.45 - 0.78 at Canobie and Walker's Bend, respectively. During validation, R² values were 0.81 and 0.78 at

Canobie and Walker's Bend, respectively. No gauged stage height data were available in the lower Gilbert catchment.

One-dimensional hydrodynamic modelling was undertaken in the Flinders catchment using MIKE 11 hydrodynamic model. The simulated headwater and ungauged runoff by the Flinders river system model was used to define the initial and boundary conditions of the hydrodynamic model. The period of calibration was from 1981-1999 and validation was from 2000-2011.

The performance of the one-dimensional hydrodynamic model in simulating flood discharge in the Flinders catchment was excellent in terms of percentage bias (PBIAS) at all streamflow gauging stations (<10%) over the calibration period. NSE values for all streamflow gauging stations were good, ranging between 0.58-0.70 with the best performance at Walker's Bend. The model also performed well at simulating stage height, with low values of mean absolute error (MAE) and root mean squared error (RMSE) at all streamflow gauging stations except Etta Plains. The performance of the model was similar in the validation period.

Floodplain hydrologic matrix

The results of the MIKE21 model were used in conjunction with the MIKE 11 and the river system models to establish relationships between streamflow and floodplain inundation. In the Flinders floodplain, the relationships were derived for five sub-catchments located within the floodplain. A single relationship was derived for the entire Coastal floodplain of the Gilbert River. The best fitted relationships for most were linear functions for rising limb and power functions for falling limb of the hydrograph. These relationships can be applied to the output of the long term simulations from the river system model to assess how inundation extent may vary over the Assessment timeframe.

Wetland Connectivity

A number of data sources were explored to identify floodplain water bodies in the Flinders and Gilbert catchments. Eighty-five wetlands in the Flinders catchment and seven wetlands in Gilbert catchment were selected based on their ecological and indigenous values. Wetland connectivity analysis was undertaken for the two-dimensional hydrodynamic modelling domains of the Flinders and Gilbert catchments. Connectivity of wetlands with the major rivers were considered through floodplain flows (i.e. overbank flooding). Connection and disconnection during overbank flooding were identified using a threshold water depth of 30 cm. The threshold water depth was chosen to ensure continuous water connection across minor topographic variations in the landscape allowing movement of fish, which can be impeded at low water depths. Thirty centimetres was considered the minimum depth that could be assessed given the uncertainty in the digital elevation data. Time series information on wet or dry cells were first identified at each wetland and along the intervening floodplain pathways, from which the timing and duration of connection with surrounding water bodies and/or with the main stream were computed.

In the Flinders floodplain, four large wetlands, in close proximity to rivers, showed continuous connection with streams during floods. For the remaining wetlands, connectivity varied from 0 to 30 days depending on their locations on the floodplain and the magnitude of flood. The flood event of 2009 produced the highest duration of connectivity. However local variation in runoff and inflow from upstream can produce different results.

In the Coastal floodplain of the Gilbert River, all wetlands were connected to the river, some for short and some for longer periods of time during the three selected flood events. All wetlands maintained a high level of connectivity (more than 50% of time in a year) during the large 2009 flood, but also for relatively small flood events having a second peak (e.g. 2011).

Scenario Analyses

The calibrated two-dimensional hydrodynamic models for the coastal floodplains of Flinders and Gilbert rivers were used to undertake scenario modelling to analyse the impacts of future climate and potential reservoir developments on floodplain inundation and resulting changes in wetland connectivity in the two catchments. A number of scenarios were investigated in each catchment. These were:

- three future climate scenarios in both catchments (Scenario C);
- three future development scenarios in the Flinders catchment and six in the Gilbert catchment (Scenario B);
- three sea level rise (SLR) scenarios in both catchments (Scenario C); and
- three future climate and development scenarios in Gilbert catchment (Scenario D).

Three historical flood events of different magnitudes (2001, 2009 and 2011 flood events) were selected as the base-line events. The local runoff and upstream and downstream boundary conditions of the calibrated Flinders and Gilbert floodplain hydrodynamic models for the three selected events were updated representing the selected scenarios. The Sacramento rainfall-runoff model was used for generating local runoff under future climate. The Flinders and Gilbert river system models were used to generate upstream boundary conditions under future climate and potential development scenarios.

Impacts of future climate and development on floodplain inundation and wetland connectivity

Under the wet climate (Cwet) Scenario, the maximum inundation extent increased by up to 27% in the floodplains of the Flinders and Gilbert catchments. Compared to the extent of inundation, variation in average inundation depth was much lower, increasing only up to 4% in the Flinders and 3% in the Gilbert floodplains. The impact was less prominent on wetland connectivity. Under Scenario Cwet, wetland connectivity increased by up to 7.6% in the Flinders floodplain and 3% in the Gilbert floodplain. The lower magnitude flood events showed a larger increase in percentage of wetland connectivity under Scenario Cwet.

Under the dry climate (Cdry) Scenario, the maximum inundation extent decreased by up to 39% in the Flinders floodplain and 27% in the Gilbert floodplain. Similar to Scenario Cwet, variation in average inundation depth was lower decreasing by only 3% in the Flinders and 7% in the Gilbert floodplains. Under the same scenario, wetland connectivity decreased by up to 18% in the Flinders floodplain and 13% in the Gilbert floodplain with more reduction in connectivity during lower magnitude flood events.

Projected SLR caused a small increase in inundation extent and depth in the Flinders floodplain. The increase in the maximum inundation extent is less than 2% and average inundation depth is less than 3%, and was found to be higher for low magnitude flood events. Similarly, the impact on wetland connectivity was also found to be negligible. Under this scenario, wetland connectivity increased by only about 1%.

The impact of SLR is much more prominent in the Coastal floodplain of the Gilbert River compared to the Coastal floodplain of the Flinders River as significantly large portion of the Gilbert floodplain is situated along the coastal line and influenced by tide. The projected increase in the maximum area of inundation is up to about 5% and the average inundation depth is projected to increase by as much as 25%. As most of the wetlands in Gilbert were connected during the three selected flood events, SLR Scenario had little effect on wetland connectivity (<1.5% increase).

The impact of simulating an empty potential dam at Cave Hill resulted in a negligible reduction in inundation extent and depth (< 1% decrease) and wetland connectivity across the Flinders floodplain. This was mainly due to; i) the influence of local runoff generated on the Flinders floodplain on flood extent; and ii) the reservoir volume was small relative to the flood volumes.

The impact of simulating empty potential dams at Dagworth and Greenhills resulted in a notable change to the nature of flooding of the lower Gilbert floodplain. For the potential Dagworth reservoir, the maximum area of inundation and average depth of inundation during the 2001 flood event decreased by about 20% and 4% respectively. For the potential Greenhills dam, the maximum inundation area and average depth of inundation during the same flood event reduced by about 15% and 2% respectively. The impact of the dams on flooding was the largest during the lowest magnitude flood event (2001) and the lowest during the highest magnitude flood event (2009).

For the potential Dagworth dam (empty) under Scenario Cdry, the maximum area of inundation decreased by as much as 35% and the average inundation depth reduced by up to 8.3%.

Contents

Director’s foreword	i
The Flinders and Gilbert Agricultural Resource Assessment team	ii
Shortened forms.....	iv
Units	v
Preface	vi
Executive summary	viii
1 Introduction	1
1.1 Research Objectives	1
1.2 Assessment Area	1
1.3 Overview of approach	8
1.4 Hydrodynamic modelling domain	9
1.5 Report outline	12
2 Floodplain inundation mapping using remotely sensed data	13
2.1 Rationale for using remotely sensed data	13
2.2 Satellite Data, Image Acquisition & Pre-Processing.....	13
2.3 Methods for developing remotely sensed flood inundation maps	14
2.4 Results	16
2.5 Validation and uncertainty.....	22
2.6 Discussion.....	33
3 Calibration and validation of hydrodynamic models and floodplain hydrologic matrix	35
3.1 Rationale	35
3.2 Hydrodynamic modelling	35
3.3 Data preparation	36
3.4 Configuration of two-dimensional hydrodynamic model.....	49
3.5 Calibration and post-audit of two-dimensional hydrodynamic models	51
3.6 Configuration and calibration of one-dimensional hydrodynamic models	66
3.7 Floodplain hydrologic matrix	69
4 Floodplain inundation modelling under future climate and development scenarios	71
4.1 Introduction	71
4.2 Selection of Scenarios for inundation modelling	72
4.3 Results of Scenario Analyses.....	78

5	Assessment of Wetland connectivity	85
5.1	Rationale	85
5.2	Water assets for connectivity assessment.....	86
5.3	Method of Connectivity Analysis	89
5.4	Changes in Wetland Connectivity under future climate and development scenarios	99
6	Summary and Conclusions	101
6.1	Summary	101
6.2	Conclusions	103
7	References	105
Appendix A	IDL programs used to produce water maps	108
Appendix B	Locations of the river where cross-sections were measured	118
Appendix C		120
Appendix D		121

Figures

Preface Figure 1 Schematic diagram illustrating high-level linkages between the 12 activities (blue boxes). vii

Figure 1.1 A shaded relief map of the Flinders and Gilbert catchments. The Flinders and Gilbert catchments, the Gulf region is shown in the small thumbnail map in top left corner	3
Figure 1.2 Historical annual rainfall averaged over the Flinders (left) and Gilbert (right) catchments. The low-frequency smoothed line is the 10 year running mean	3
Figure 1.3 Historical monthly rainfall averaged over the Flinders (left) and Gilbert (right) catchments (A range is the 20th and 80th percentile monthly rainfall)	4
Figure 1.4 Historical annual areal potential evaporation averaged across the Flinders (left) and Gilbert (right) catchments. The low-frequency smoothed line is the 10 year running mean.....	4
Figure 1.5 Monthly potential area evaporation averaged over the Flinders (left) and Gilbert (right) catchments between 1965 and 2011(A range is the 20th and 80th percentile monthly potential areal evaporation)	4
Figure 1.6 Annual runoff (left) and monthly runoff (right) averaged over the Flinders catchment under Scenario A.....	5
Figure 1.7 Annual runoff (left) and monthly runoff (right) averaged over the Gilbert catchment under Scenario A.....	5
Figure 1.8 Observed daily water levels at Richmond (915008A) (top) and Walker’s Bend (915003A) (bottom) in the Flinders catchment highlighting the period of the minor (green line), moderate (yellow line) and major (red line) flooding as classified by the Bureau of Meteorology. The locations of Richmond and Walker’s Bend are shown Figure 1.10.	7
Figure 1.9 Observed daily water levels at Rockfields (917001D) (top) and Einasleigh (917106A) (bottom) in the Gilbert catchment highlighting the period of the minor (green line), moderate (yellow line) and major (red line) flooding as classified by Bureau of Meteorology. The locations of Rockfields and Einasleigh are shown Figure 1.10.	8
Figure 1.10 Hydrodynamic modelling domains for floodplain inundation modelling in the Flinders and Gilbert catchment.....	10
Figure 1.11 River network of the Flinders catchment used for one-dimensional hydrodynamic modelling....	11
Figure 1.12 River network of the Gilbert catchment used for one-dimensional hydrodynamic modelling	12
Figure 2.1 Flood event in the Gilbert HD domain from MODIS on the 17th March 2011 (left) and Landsat on the 9th February 2011 (right). Blue = water, White=cloud, overlaid on a “true colour” MODIS image. This MODIS water map was generated using the OWL with a 10% threshold. The Landsat water map shows a stripping pattern due to the linear gaps in the Landsat ETM imagery.....	17
Figure 2.2 Flood event in the Flinders HD domain from MODIS on the 19th February 2009 (left) and Landsat on the 18th to 20th February 2009 (right). Blue = water, White=cloud, overlaid on a “true colour” MODIS image. This MODIS water map was generated using the OWL with a 10% threshold. The Landsat water map shows a stripping pattern due to the linear gaps in the Landsat ETM imagery as well as cloud patterns.	17
Figure 2.3 Average percentage of water in a pixel (based on available images during the wet season). The year, as indicated, starts from November and goes until the end of April of the following year.....	19
Figure 2.4 Maximum percentage of water in a pixel (based on available images during the wet season). The year, as indicated, starts from November and goes until the end of April of the following year.....	20

Figure 2.5 The maximum number of consecutive days that a pixel is inundated with water (based on available images during the wet season). The year, as indicated, starts from November and goes until the end of April of the following year. The image in the bottom right corner is for all wet seasons from 2000 to March 2011.	21
Figure 2.6 Average percentage of time that a pixel was inundated (left) and maximum extent of inundation (right) based on all available Landsat data from DERM water maps.....	22
Figure 2.7 Landsat and MODIS water maps for nine test subsets.	24
Figure 2.8 Scatterplot of MODIS percentage water (vertical axis) and the equivalent Landsat percentage water (horizontal axis) for the nine test subsets. The 10-pixel moving average is also shown to indicate data trend.	25
Figure 2.9 Scatter plot of MODIS percentage water (vertical axis) and the equivalent Landsat percentage water (horizontal axis) for the nine test subsets combined. The 10-pixel moving average is also shown to indicate data trend.	26
Figure 2.10 Flinders Subset: left- NGRM water map, middle – OWL water map at 4% threshold, right – OWL water map at 1% threshold	28
Figure 2.11 Gilbert Subset: left- MD water map, middle – OWL water map at 4% threshold, right – OWL water map at 1% threshold	28
Figure 2.12 MODIS image (bands 721) of the Gilbert subset from 15 th February 2009.	28
Figure 2.13 DERM Landsat water map (left) and MODIS OWL water map with 4% threshold (right). Both images were for 26 th January 2009.	29
Figure 2.14 Final MODIS flood map generated from Maximum OWL flood maps from the relatively wet years of 2000, 2001, 2004, 2008, 2009, 2010 and 2011, with artefacts removed.....	30
Figure 2.15 Flood reclamation map produced by the Queensland Department of Natural Resources and Mines showing the areas of potential flood hazard.....	31
Figure 2.16 A MODIS flood-frequency image showing average proportion of water from 2000 to early 2011. Pixels with an average water proportion >2% show as black. A Google Earth image of the same subset is also shown.	32
Figure 2.17 Comparison between MODIS OWL, converted to a water map for different percentage water thresholds, and the Landsat DERM flood maps for the sites shown in Figure 2.7.....	33
Figure 3.1 Land cover map of the Flinders catchment with a simplified class structure separating riparian and non riparian zones	39
Figure 3.2 Land cover map of the Gilbert catchment with a simplified class structure separating riparian and non riparian zones	40
Figure 3.3 Comparison of SRTM DEM derived cross-sections with measured cross-sections at different gauging stations.....	42
Figure 3.4 Two sites of rivers where cross-sections were measured during the field trip	42
Figure 3.5 Map showing the locations of the stage height gauging stations in the Flinders catchment.....	43
Figure 3.6 Map showing the locations of the stage height gauging stations in the Gilbert catchment	44
Figure 3.7 Maps of the Sub-catchments used in two-dimensional hydrodynamic modelling in the Flinders Catchment	47
Figure 3.8 Maps of the Sub-catchments used in two-dimensional hydrodynamic modelling in the Gilbert Catchment	48
Figure 3.9 Hydrodynamic modelling domains for flood inundation modelling in the Flinders and Gilbert catchment.....	50

Figure 3.10 Comparison of the simulated inundation (without calibration of runoff factor) and flood maps derived from MODIS imagery with 5% threshold for different days of 2009 flood event. (Grey colour in MODIS flood map represents cloud cover)	53
Figure 3.11 Comparison of the simulated inundation (with calibrated runoff factor) and flood maps derived from MODIS imagery with 5% threshold for different days of 2009 flood event. (Grey colour in MODIS flood map represents cloud cover)	54
Figure 3.12 Comparison of the simulated inundation (with calibrated runoff factor) and flood maps derived from MODIS imagery with 5% threshold for different days of 2011 flood event. (Grey colour in MODIS flood map represents cloud cover)	55
Figure 3.13 Comparison of total number of inundated cells by hydrodynamic model and in the flood maps generated from MODIS with 1%, 5% and 10% thresholds in OWL for the flood events of 2009 and 2011	55
Figure 3.14 Cell-to-cell matching of inundated cells between the hydrodynamic model and the flood maps generated from MODIS with 1%, 5% and 10% thresholds in OWL for 2009 and 2011 flood events.	56
Figure 3.15 Comparison of the observed and simulated stage heights at Canobie (915212A), Etta plains (915012A), Walker’s Bend (915003A) for 2009 and 2011 flood events.....	57
Figure 3.16 Comparison of the simulated inundation (with calibrated runoff factor) and flood maps derived from MODIS imagery with 5% threshold for different days of 2001 flood event.....	58
Figure 3.17 Comparison of the simulated inundation (with calibrated runoff factor) and flood maps derived from MODIS imagery with 5% threshold for different days of 2006 flood event.....	59
Figure 3.18 Comparison of total number of inundated cells by hydrodynamic model and in the flood maps generated from MODIS with 1%, 5% and 10% thresholds in OWL for flood events of 2001 and 2006.	60
Figure 3.19 Cell-to-cell matching of inundated pixels between the hydrodynamic model and the flood maps generated from MODIS with 1%, 5% and 10% thresholds in OWL for flood events of 2001 and 2006.	60
Figure 3.20 Comparison of the observed and simulated stage heights at Canobie (915212A) and Walker’s Bend (915003A) for different flood events of 2001 and 2006	61
Figure 3.21 Spatial extent and temporal variation of inundation during the simulated flood events of 2001, 2004, 2006, 2008, 2009 and 2011	62
Figure 3.22 Comparison of the simulated inundation (left) and flood map derived from MODIS imagery (using a 5% threshold) (right) on 15 th January 2009	63
Figure 3.23 Comparison of the simulated inundation and flood maps derived from MODIS imagery (using a 5% threshold) for 17 and 18 March 2011.....	64
Figure 3.24 Cell-to-cell matching of inundated pixels and total number of inundation cells between the hydrodynamic model and the flood maps generated from MODIS with 1%, 5% and 10% thresholds in OWL for 15 January 2009	65
Figure 3.25 Cell-to-cell matching of inundated pixels and total number inundation cells between the hydrodynamic model and the flood maps generated from MODIS with 1%, 5% and 10% thresholds in OWL for 2011.....	65
Figure 3.26 Total inundation extent and spatial variation in floodplain total inundation duration in n the Gilbert floodplain during the flood events of 2001, 2008, 2009 and 2011.....	66
Figure 3.27 Subcatchments of Flinders River System model within the two-dimensional hydrodynamic modelling domain of Flinders floodplain.....	69
Figure 4.1 Comparison of total runoff within the hydrodynamic modelling domain in the Flinders catchment from 1999 to 2011 (period over which hydrodynamic model was calibrated and validated under scenarios A, Cwet and Cdry)	73

Figure 4.2 Comparison of total runoff within the hydrodynamic modelling domain of the Gilbert catchment during the periods of calibration and validation (1999-2011) of the hydrodynamic model for a) current climate, b) future climate, Cwet, c) future climate, Cdry.	74
Figure 4.3 Simulated streamflow by the Gilbert river system model at the end of the system for the periods of three different flood events (2001, 2009 and 2011) for current and future climate	75
Figure 4.4 Cave Hill catchment area, streamflow gauging station and location of proposed dam site (Source: Lee et al., 2013)	76
Figure 4.5 Dagworth and Greenhills catchments, streamflow gauging stations and location of proposed dam sites (Source: Lee et al., 2013).....	77
Figure 4.6 Simulated streamflow by the Gilbert river system model at the end of the system for the periods of 2001, 2009 and 2011 flood events under current condition and Dagworth dam reservoir empty scenario	78
Figure 4.7 6-hourly time series of number of cells inundated in the Flinders floodplain during the 2001, 2009 and 2011 flood events under scenarios A, Cwet and Cdry.....	79
Figure 4.8 6-hourly time series of the number of cells inundated in the Gilbert floodplain during the 2001, 2009 and 2011 flood events under scenarios A, Cwet and Cdry.....	79
Figure 4.9 6-hourly time series of number of cells inundated during the 2001, 2009 and 2011 flood events under current condition and Cave Hill reservoir empty scenario in the Flinders floodplain	80
Figure 4.10 6-hourly time series of number of cells inundated during 2001, 2009 and 2011 flood events under current condition and Dagworth and Greenhills reservoirs empty scenarios in the Gilbert floodplain.....	81
Figure 4.11 6-hourly time series of number of cells inundated during 2001, 2009 and 2011 flood events under current condition and SLR scenario in the Flinders floodplain	82
Figure 4.12 6-hourly time series of number of cells inundated during 2001, 2009 and 2011 flood events under current condition and SLR scenario in the Gilbert floodplain.....	83
Figure 4.13 6-hourly time series of number of cells inundated during 2001, 2009 and 2011 flood events under current condition and Cdry and Dagworth reservoir empty scenario in the Gilbert floodplain	84
Figure 5.1 Spatial representation of important ecological assets across the Assessment region	87
Figure 5.2 A schematic representation of wetland connectivity based on water depth and wetland bank height. Connection to the flood waters and surrounding water bodies starts at time t1 and ends at t2 when the depth of inundation falls below the wetland bank height.....	90
Figure 5.3 Map showing locations of the wetlands and major streams in the Flinders Catchment. The red rectangle shows the hydrodynamic modelling boundary.....	91
Figure 5.4 Map showing location of the wetlands and major streams in the Gilbert Catchment. The hydrodynamic study (red rectangle) was limited to lower Gilbert floodplain only.	92
Figure 5.5 Typical example of spatial variation in inundation duration across the floodplain for the flood in 2009.	94
Figure 5.6 Timing and duration of connectivity of selected wetlands in the Flinders Catchment for (a) 2001, (b) 2009 and (c) 2011 flood events.....	95
Figure 5.7 Typical example of spatial variation in inundation duration across the lower Gilbert floodplain for the flood in 2009.....	97
Figure 5.8 Timing and duration of connectivity of wetlands to the Gilbert River for floods of different magnitudes, a) 2001 flood, b) 2009 (2 nd largest in records) and 2011.....	98

Tables

Table 2.1 Example of how the flood duration is calculated during cloudy periods.	15
Table 2.2 Flood event dates, and number of available MODIS/Landsat images for the Flinders catchment..	16
Table 2.3 Flood event dates, and number of available MODIS/Landsat images for the Gilbert catchment. ..	16
Table 2.4 Classification accuracy of the MODIS OWL for different water percentage thresholds when compared to the NGRM water map for the Gulf region (All), Flinders and Gilbert catchments.	26
Table 3.1 Aggregation of DCLD classes.....	38
Table 3.2 Manning’s roughness coefficients for different land cover types.....	40
Table 3.3 List of the gauging stations in the Flinders catchments and the current status	43
Table 3.4 List of the gauging stations in the Flinders catchments and the current status	45
Table 3.5 Selected flood events for Flinders two-dimensional HD model calibration/validation	51
Table 3.6 selected flood events for Gilbert two-dimensional HD model calibration/validation	52
Table 3.7 Performance of the Flinders one-dimensional hydrodynamic model at simulating discharge over the calibration period.....	68
Table 3.8 Performance of the Flinders one-dimensional hydrodynamic model simulating stage height over the calibration period.....	68
Table 3.9 Performance of the Flinders one-dimensional hydrodynamic model at simulating discharge over the validation period	68
Table 3.10 Performance of the Flinders one-dimensional hydrodynamic model at simulating stage height over the validation period	68
Table 3.11 Relationship between streamflow and inundation areas for different reaches of the Flinders floodplain.....	70
Table 3.12 Relationship between streamflow and inundation areas for different reaches of the Flinders floodplain.....	70
Table 4.1 Locations and physical properties of the proposed top three dams at the Flinders and Gilbert Catchments.....	71
Table 4.2 Impact of future climate (Cdry and Cwet) on inundation area and depth for flood events of different magnitudes in the Flinders floodplain.....	79
Table 4.3 Impact of future climate (Cdry and Cwet) on inundation area and depth for flood events of different magnitudes in the Gilbert floodplain	80
Table 4.4 Impact of the Cave Hill dam on inundation area and depth for flood events of different magnitude in the Flinders floodplain	80
Table 4.5 Impacts of Dagworth and Greenhills dams on inundation area and depth for flood events of different magnitudes in the Gilbert floodplain	81
Table 4.6 Impact of the SLR on inundation area and depth for flood events of different magnitudes in the Flinders floodplain	82
Table 4.7 Impact of SLR on inundation area and depth for flood events of different magnitude in the Gilbert floodplain.....	83
Table 4.8 Impacts of the Cdry and Dagworth dam on inundation area and depth for flood events of different magnitudes in the Gilbert floodplain	84
Table 5.1 List of wetlands in the Flinders and their physical properties.....	87

Table 5.2 List of wetlands in the Gilbert catchment and their physical properties.	89
Table 5.3. List of streams that were used to assess connectivity with wetlands in Flinders and Gilbert catchments.	92
Table 5.4. Summary of connectivity status for 85 wetlands studied in the Flinders catchment. Results are presented as a percentage of total wetlands.....	96
Table 5.5 An overview of wetland connectivity level in the Gilbert catchment for observed climate conditions.	98
Table 5.6 Summary of connectivity for flood events studied for the current climate.	99
Table 5.7 Predicted changes in connectivity for different floods due to climate change and future development	99
Apx Table C.1 Statistical measures used to evaluate model performance (Moriassi et al., 2007).....	120
Apx Table D.1 Estimates of connectivity (number of days) of wetlands to streams in the Flinders floodplain for the flood events of 2001, 2009 and 2011.....	121
Apx Table D.2 Estimates of connectivity of wetlands to streams in the Gilbert floodplain for the flood events of 2001, 2009 and 2011	124

1 Introduction

Floods are the most frequent and costly natural disasters in Australia and world-wide causing serious social-economic damage (BTE, 2001; Guha-Sapir and Santos, 2013). There are also benefits associated with floods particularly in rural floodplains and wetlands, which are a critical part of the natural environment. Floodplains and wetlands play important ecological and hydrological roles in river basins (Bullock and Acreman 2003; Pringle, 2001). Flood flows provide an opportunity for off-stream wetlands to be connected to the main river channel. The environmental benefits of water flowing into wetlands and over floodplains depend on the extent, depth, duration and frequency of the inundation. The Flinders and Gilbert catchments have large floodplains in the low-lying middle and lower parts, where floods occur regularly. Many wetlands with high biodiversity are located in these floodplains. While flooding can be catastrophic to agricultural production in terms of loss of stock, fodder and topsoil and damage to crops and infrastructure, the wetland ecosystems in these areas are thought to be largely dependent on “flood pulses”, which allow for biophysical exchanges to occur between the main channel and wetlands (Warfe et al., 2011).

Conceptual node-link hydrological models, such as river system models typically simulate 100 years of hydrological data for large catchments in less than an hour. They are not, however, spatially explicit and do not usually model floodplain processes well. For simulating floodplain processes, traditionally (physically based) two-dimensional hydrodynamic models are used (Dutta, 2012). While hydrodynamic models are able to better simulate floodplain processes they require much longer computational time than river system models (i.e. see companion technical report on river system modelling, calibration; Lerat et al. 2013). Depending upon the hydrodynamic model resolution and floodplain size, hydrodynamic model simulations may take as long as ¼ of real time (i.e. an 8 day flood event would take 2 days to simulate). It is, therefore, impractical to use two-dimensional hydrodynamic models to assess the connectivity of wetlands to the main channel over large areas and for long simulation periods. Instead the approach undertaken in this study was to develop relationships between river discharge and floodplain inundation derived from simulation results of one and two dimensional hydrodynamic models and then for these relationships to be utilised in conjunction with simulated streamflow data generated from the river system models.

1.1 Research Objectives

This activity of the Flinders and Gilbert Agricultural Resource Assessment was undertaken to address the following key research questions:

1. How frequently are key wetlands connected to the main river channels?
2. How will flood regime and wetland connectivity in the floodplains be affected by climate change and potential dams constructed upstream of the floodplain?
3. Can a hydrodynamic model be utilised to develop relationships between streamflow simulated using a river system model and floodplain inundation computed using a hydrodynamic model?

1.2 Assessment Area

1.2.1 GENERAL

The Assessment area encompasses the Flinders and Gilbert catchments, which are located in the Gulf region of North Queensland (Figure 1.1).

The Flinders catchment has an area of 109,000 km² and a population of about 6,000 people. The Flinders River, the longest of the Gulf Rivers and sixth longest Australian river overall, rises in the Great Dividing

Range north-east of Hughenden, nearly 1,000 km from its entry to the Gulf of Carpentaria. The river flows initially in a westerly direction towards Julia Creek, before flowing north to the vast savannah country downstream of Canobie Station. It passes through its delta and finally into the Gulf of Carpentaria, 25 km west of Karumba. The Cloncurry and Corella Rivers, its major tributaries, enter the river from the southwest above Canobie. The other major tributaries are: Dugald, Williams, McKinlay and Saxby Rivers (refer to Figure 1.11).

The Gilbert catchment has an area of 46,354 km² and a population of about 1,200 people. The Gilbert catchment is comprised of two major rivers, the Gilbert and the Einasleigh. The Gilbert River rises in the Great Dividing Range approximately 150 km southeast of Georgetown. The river flows in a north-westerly direction and is joined by its major tributary, the Einasleigh River, downstream of Strathmore Station, before finally entering the Gulf of Carpentaria in a river delta 100 kilometres wide. The other main tributary, the Etheridge River, joins the Einasleigh River downstream of Georgetown.

Both catchments have a maximum elevation of about 1,050 m. While the Gilbert catchment is undulating in its mid-to-upper reaches the Flinders catchment is predominantly flat (Figure 1.1). The land use in the two catchments is mainly cattle grazing; only a small part is being used for cropping.

1.2.2 CLIMATE

The Flinders and Gilbert catchments have a semi-arid tropical climate. The mean and median annual rainfall spatially averaged across the Flinders catchment is 492 mm and 454 mm, respectively. However, the historical annual rainfall series for the Flinders catchment shows considerable variation between water years (Figure 1.2). The mean and median annual rainfall spatially averaged across the Gilbert catchment is 775 mm and 739 mm, respectively. Spatially, mean annual rainfall varies from about 1,050 mm at the coast to about 650 mm in the south-east of the catchment.

The highest catchment average annual rainfall (1,310 mm in the Flinders and 2,187 mm in the Gilbert) occurred in 1974, and was nearly three times the median annual rainfall value (see companion technical report on climate, Petheram and Yang, 2013).

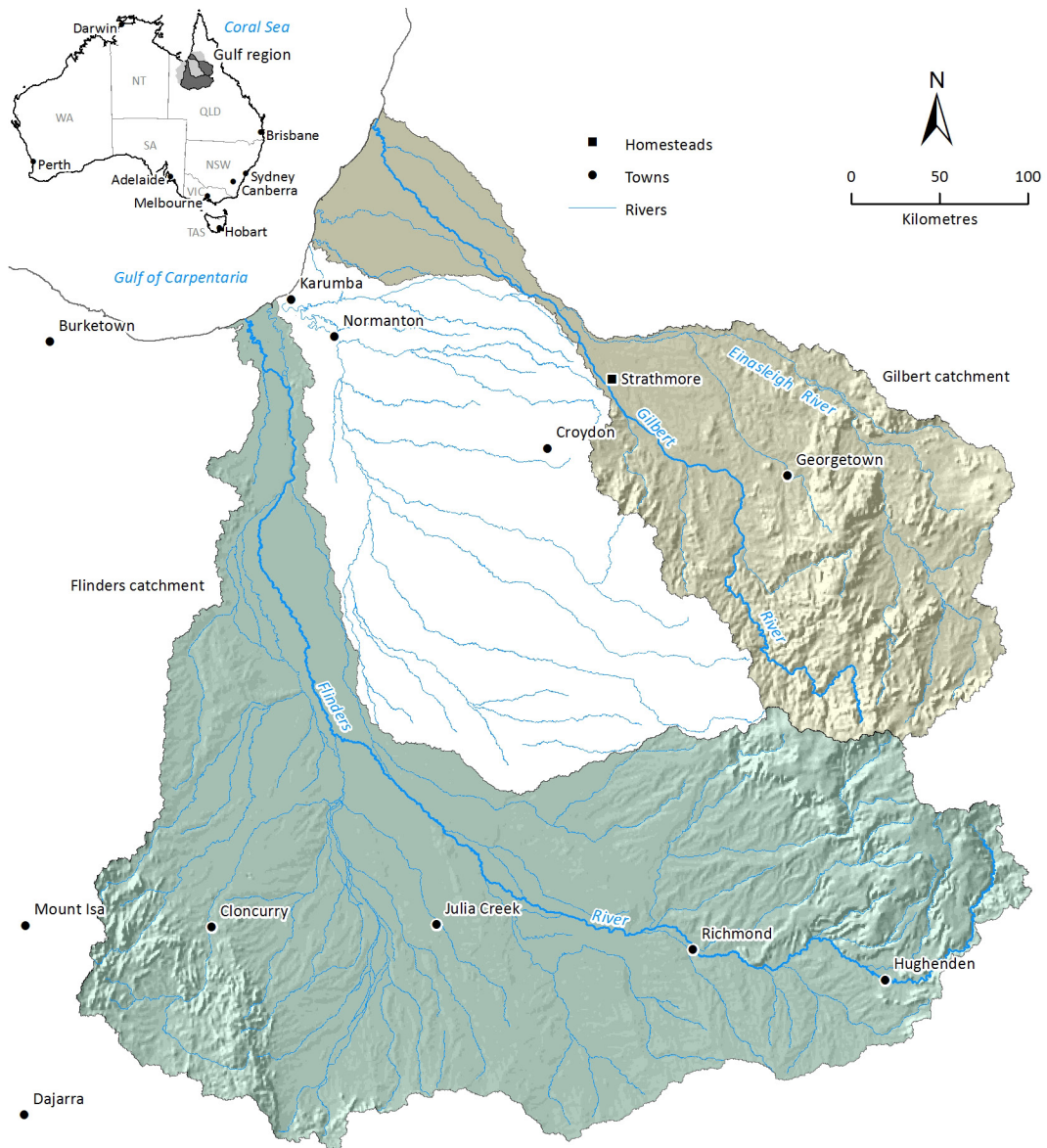


Figure 1.1 A shaded relief map of the Flinders and Gilbert catchments. The Flinders and Gilbert catchments, the Gulf region is shown in the small thumbnail map in top left corner

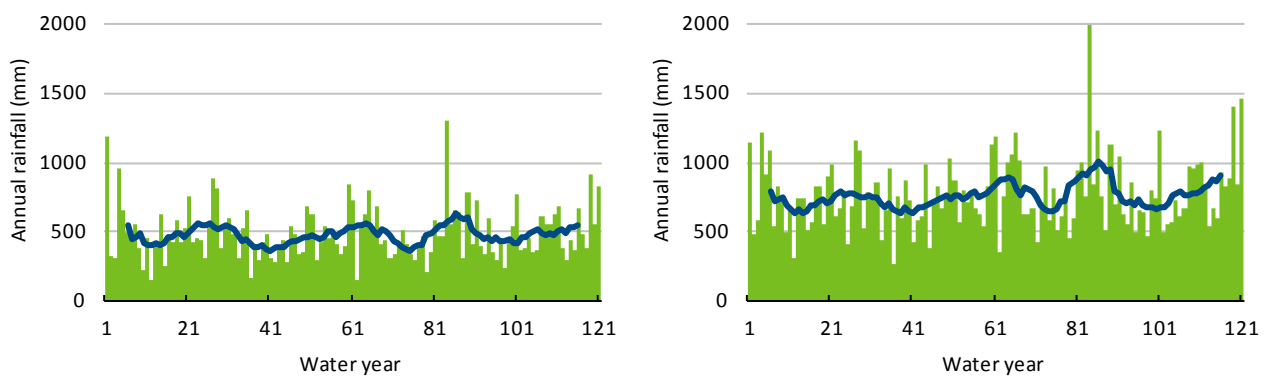


Figure 1.2 Historical annual rainfall averaged over the Flinders (left) and Gilbert (right) catchments. The low-frequency smoothed line is the 10 year running mean

A defining characteristic of the Flinders and Gilbert catchments' climate is the seasonality of rainfall with more than 80% of rainfall (88% in the Flinders and 93% in the Gilbert) occurring during the wet season (November to April inclusive) (Figure 1.3). The highest median monthly rainfall in the two catchments

occurs during the months of January and February (~100 mm in Flinders and ~ 200 mm in Gilbert). The months with the lowest median rainfall are July and August (~ 0.5 mm) (Petheram and Yang, 2013).

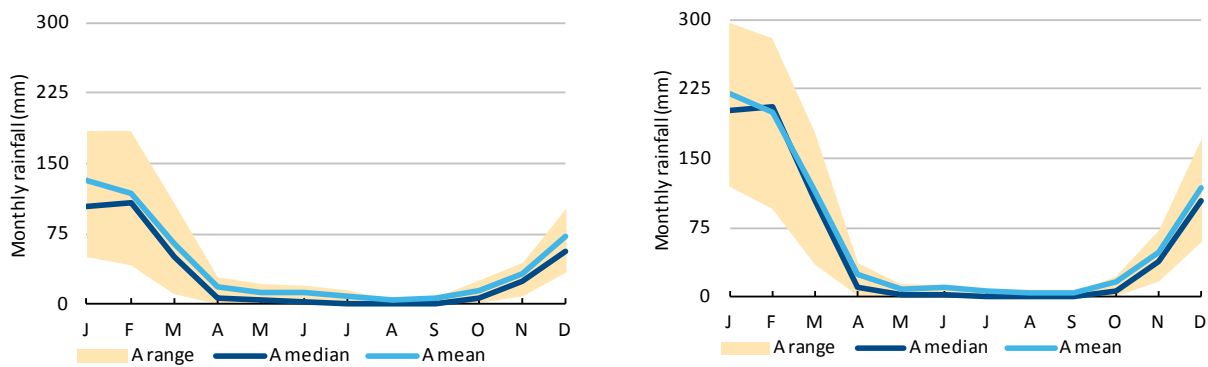


Figure 1.3 Historical monthly rainfall averaged over the Flinders (left) and Gilbert (right) catchments (A range is the 20th and 80th percentile monthly rainfall)

Areal potential evaporation in the two catchments exceeds 1,800 mm in most years. The Flinders catchment has a mean annual potential evaporation of 1,862 mm. Mean wet and dry season potential evaporation are 1,115 mm and 762 mm respectively. The Gilbert catchment has a mean annual potential evaporation of 1,868 mm. Mean wet and dry season potential evaporation is 1,067 mm and 815 mm respectively (Figure 1.4). Potential evaporation in the two catchments exhibits a strong seasonal pattern, ranging from 200 mm per month during the build up and the wet season (October to January), to about 100 mm per month during the middle of the dry season (June to July) (Figure 1.5). The majority of the Flinders and Gilbert catchments experience a mean annual rainfall deficit of greater than 600 mm. Consequently, both catchments have a high proportion of landscape with a semi-arid climate (Petheram and Yang, 2013).

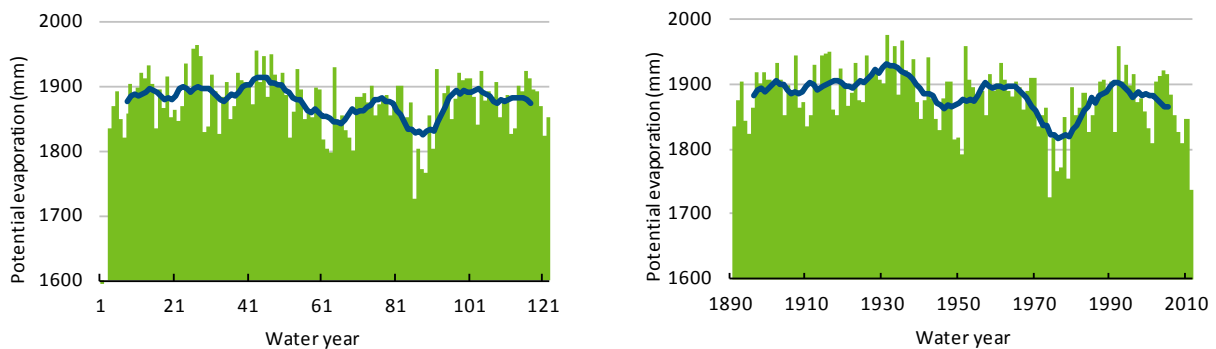


Figure 1.4 Historical annual areal potential evaporation averaged across the Flinders (left) and Gilbert (right) catchments. The low-frequency smoothed line is the 10 year running mean

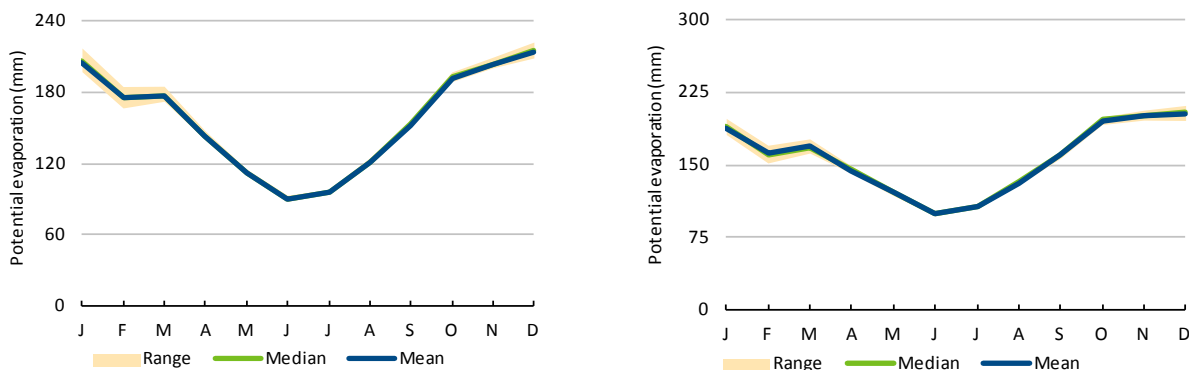


Figure 1.5 Monthly potential area evaporation averaged over the Flinders (left) and Gilbert (right) catchments between 1965 and 2011 (A range is the 20th and 80th percentile monthly potential areal evaporation)

1.2.3 SURFACE RUNOFF AND STREAMFLOW

Like rainfall, streamflow is highly variable and seasonal in the Flinders and Gilbert catchments. Flooding during summer and cessation of flows during the rest of the year are common characteristics of most of these streams in the two catchments.

In the Flinders catchment, approximately 96% of runoff occurs during the wet season, with the majority of runoff occurring during the months January to March. Figure 1.6 illustrates the large inter-annual and intra-annual variability in runoff in the Flinders catchment.

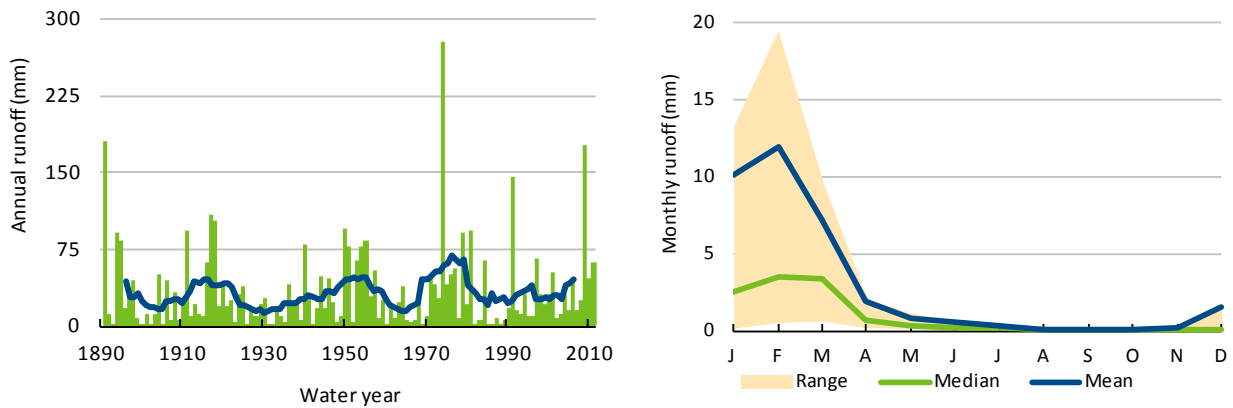


Figure 1.6 Annual runoff (left) and monthly runoff (right) averaged over the Flinders catchment under Scenario A

In the Gilbert catchment, approximately 97% of runoff occurs during the wet season, with the majority of runoff occurring during the months January to March. Figure 1.7 illustrates the large monthly variability in runoff in the Gilbert catchment.

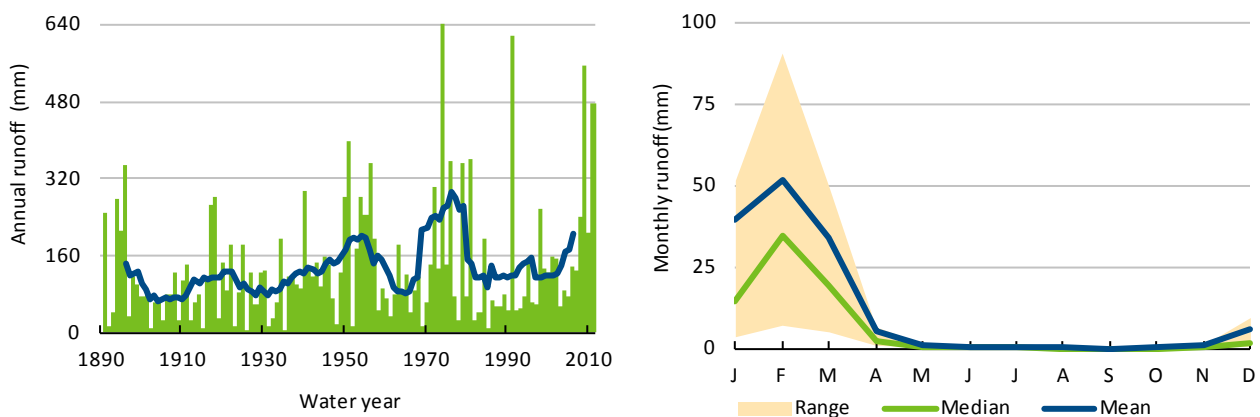


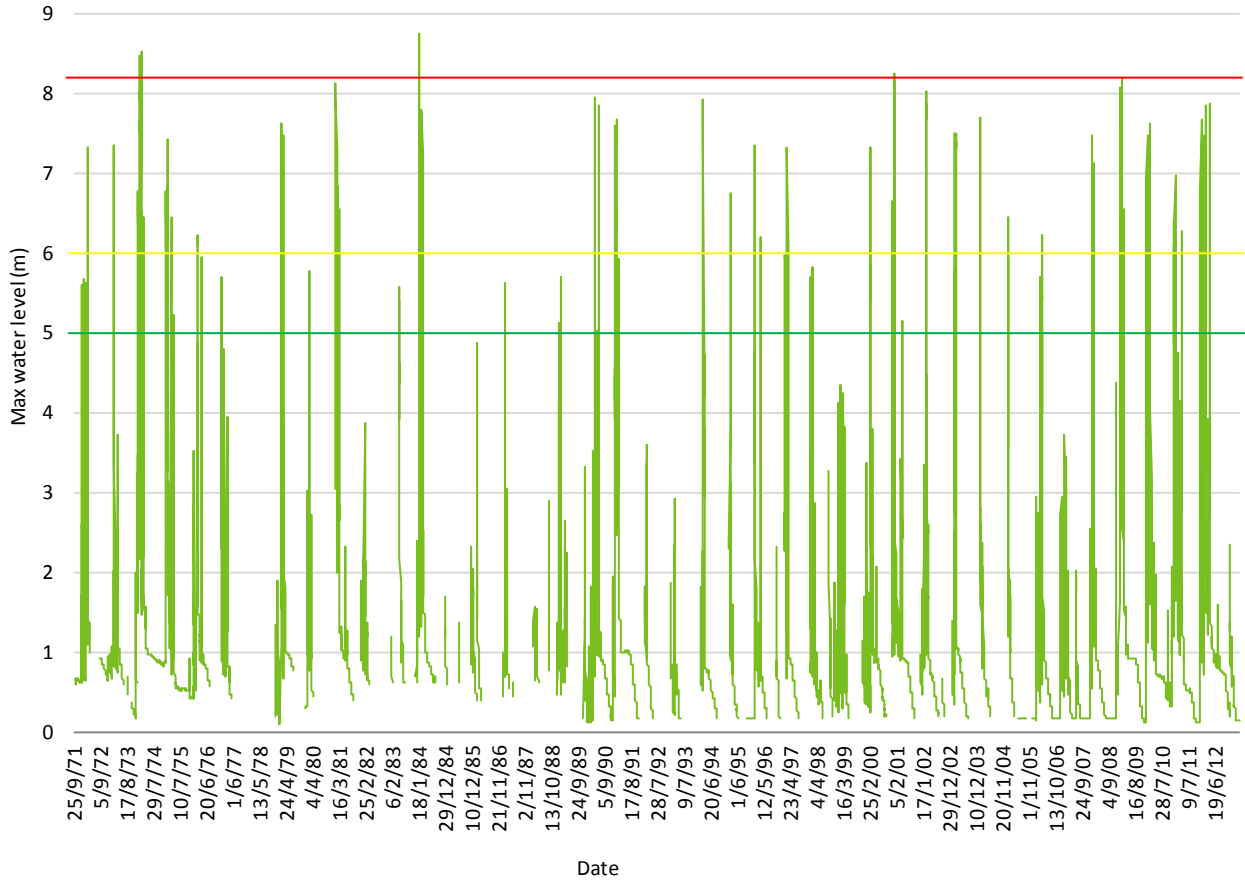
Figure 1.7 Annual runoff (left) and monthly runoff (right) averaged over the Gilbert catchment under Scenario A

The streamflow and catchment runoff of the Flinders and Gilbert catchments are described in more detail in a companion technical report on River System modelling (Lerat et al., 2013) (Preface Figure 1).

1.2.4 FLOODING

Floods occur regularly in parts of the Flinders and Gilbert catchments. In the Flinders catchment, floods normally develop in the headwaters of the Flinders, Cloncurry and Corella Rivers. General heavy rainfall situations can develop from cyclonic influences in the Gulf of Carpentaria which cause widespread flooding, particularly in the lower reaches below Canobie (refer to Figure 1.10). Figure 1.8 shows the recorded daily water levels at two gauging stations, Richmond (915008A) and Walker's Bend (915003A), highlighting flood events of different magnitudes. Each river height station has a pre-determined flood classification which details heights on gauges at which minor, moderate and major flooding commences.

Richmond



Walker's Bend

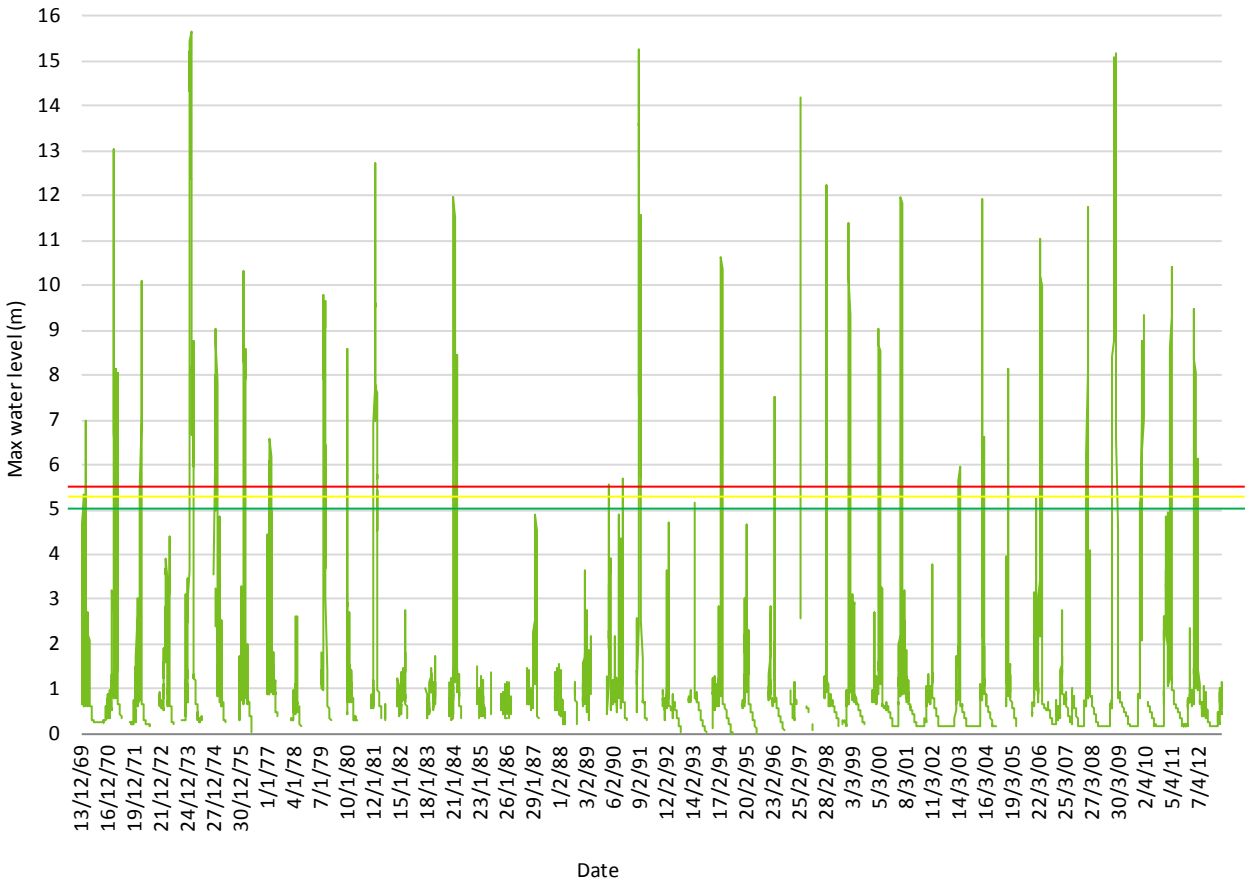
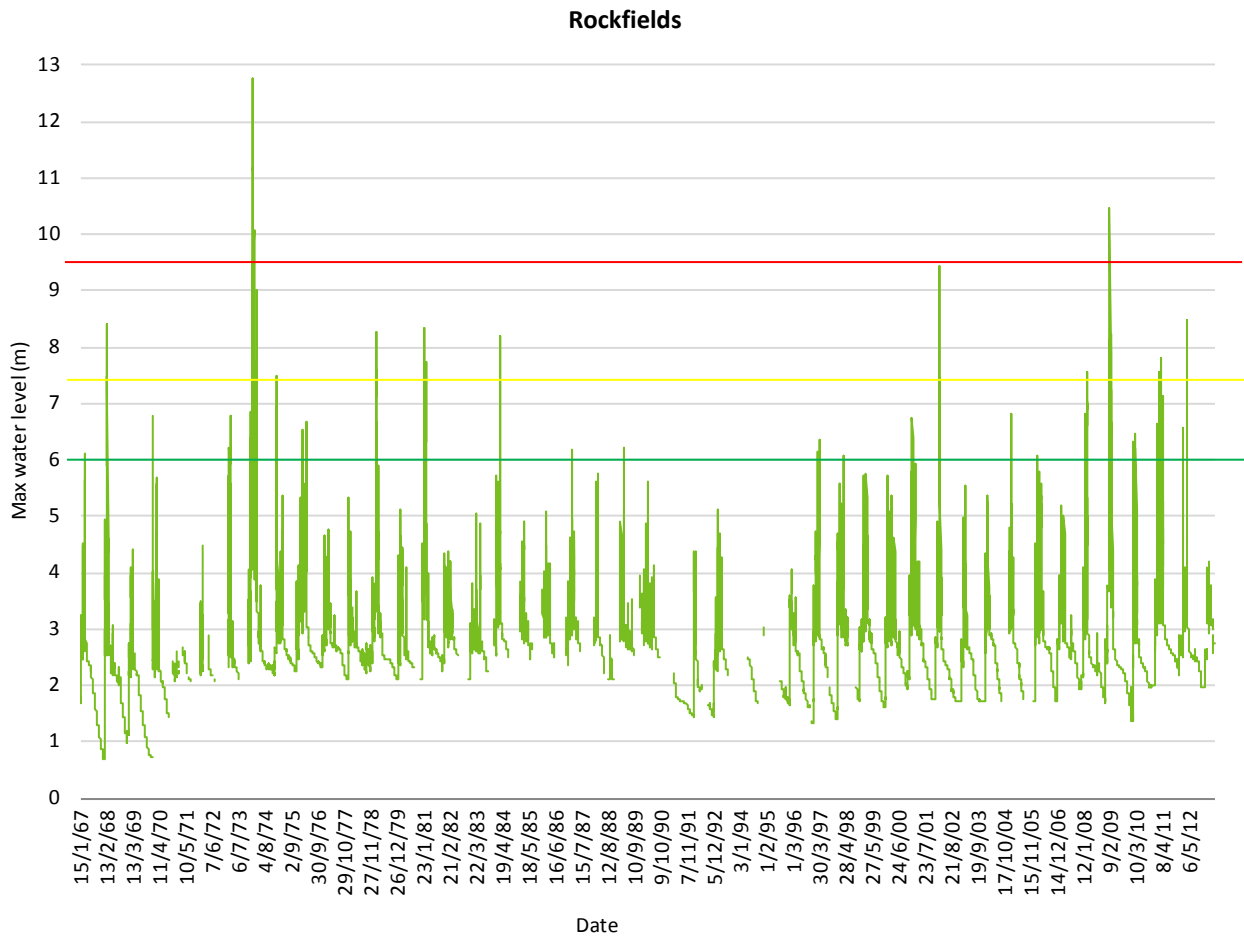


Figure 1.8 Observed daily water levels at Richmond (915008A) (top) and Walker’s Bend (915003A) (bottom) in the Flinders catchment highlighting the period of the minor (green line), moderate (yellow line) and major (red line) flooding as classified by the Bureau of Meteorology. The locations of Richmond and Walker’s Bend are shown Figure 1.10.

In the Gilbert catchment, floods normally develop in the headwaters of the Gilbert and Einasleigh rivers, however, heavy rainfall due to tropical cyclones also causes widespread flooding, particularly in the lower reaches below Strathmore (refer to Figure 1.10), where the Gilbert and Einasleigh rivers converge before entering the Gulf of Carpentaria. Peak flood heights are available at selected streamflow gauging stations from the early 1970s, including the major events recorded in 1974, 1991 and 2009. Figure 1.9 shows the recorded daily water levels at two streamflow gauging stations (Rockfields, 917001D and Einasleigh, 917106A) highlighting historical flood events of different magnitudes.



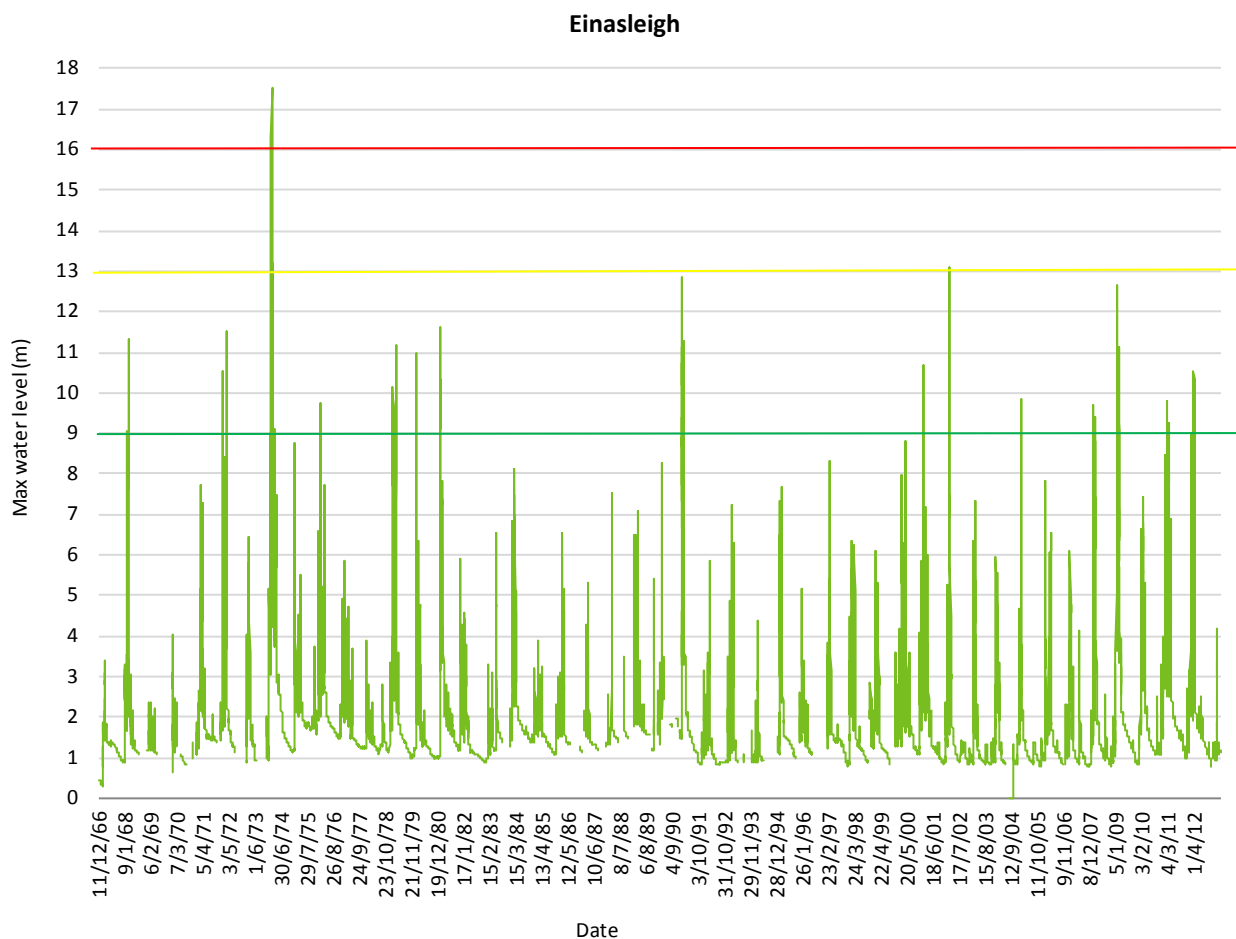


Figure 1.9 Observed daily water levels at Rockfields (917001D) (top) and Einasseigh (917106A) (bottom) in the Gilbert catchment highlighting the period of the minor (green line), moderate (yellow line) and major (red line) flooding as classified by Bureau of Meteorology. The locations of Rockfields and Einasseigh are shown Figure 1.10.

The extent and magnitude of 1974 flooding in the Gulf region was estimated as the biggest in more than 100 years. In January and February 2009, the region was severely affected by big floods. The prolonged flooding was a result of several periods of intense rainfall. The overall extent and magnitude of the flooding in this region was estimated as the second biggest in more than 100 years, only second to the record flooding in 1974 (BOM, 2009). The 2009 flood had serious impacts on the local communities in the Gulf area. Apart from causing damage to the local industries, the floods also cut off local communities for a long period, causing many daily essentials to be in short supply for prolonged periods. Even clean water supply became a problem in some areas, as water supply systems were damaged by the flooding (ABC, 2009a&b).

1.3 Overview of approach

Hydrodynamic models have been in common use for several decades worldwide, for the simulation of flood events for engineering, planning and risk assessment studies (Nicholas, 2003). Both one and two dimensional hydrodynamic model are used for simulation of floodplain inundation (Horritt and Bates, 2002; Bales et al., 2007). The strength of these models includes use of water equilibrium equations, such as St. Venant’s equations, to model water movement in river channel and floodplain and to estimate inundation extent, duration, depth and frequency of wetting. Based on the modelling objectives and availability of data and resources one can select a one-dimensional or two-dimensional model or very recently coupled one- and two-dimensional models. To be useful, hydrodynamic models need to be calibrated. Traditionally flood models are calibrated by comparing in-stream water heights (commonly gauge records) and floodplain inundation (commonly water marks on trees, buildings and electric poles). However, for relatively remote

and sparsely populated catchments like the Flinders and Gilbert, it is often not possible to collect the field data that are necessary to sufficiently calibrate the model. This serves as a major constraint to the use of hydrodynamic models in remote and data sparse areas.

In recent years there have been major advances in flood inundation mapping through the use of satellite and airborne remote sensing. Bates et al. (1997) and Smith (1997) present a good review of the active and passive remote sensing studies of flood inundation. While the satellite imagery based approaches have several limitations including an inability to develop detailed understanding of floodplain hydrology (such as water balance) and hydraulics (e.g. changing floodplain dynamics), these techniques indeed provide very useful calibration data sets for the flood inundation hydraulic models that can simulate a variety of historical and likely future conditions. However, until relatively recently hydrodynamic modelling and remote sensing for flood mapping have been largely separate disciplines without any clear connection. Interest in integrating these two fields have increased in recent years with the availability of MODIS imagery data, which are freely available near-global and frequent (twice a day).

In this assessment, a combination of hydrodynamic modelling and remote sensing was used to quantify floodplain inundation, the connectivity (in terms of extent, timing and duration) of the main river channels to off-stream wetlands and assess how connectivity may change as a result of upstream regulation and climate change. The following are the major tasks that were performed:

- Task 1: use remote sensing techniques to map flood hazard in the Flinders and Gilbert catchments.
- Task 2: use a hydrodynamic model to simulate floodplain inundation under future climate and development scenarios.
- Task 3: use a hydrodynamic model and geographical information system (GIS) techniques to quantify the hydrological connectivity (in terms of extent, timing and duration) of the main river channels to off-stream wetlands and assess how this connectivity may change as a result of changes to flow regime.
- Task 4: use a hydrodynamic model to derive relationships between streamflow and floodplain inundation for river system modelling in floodplain reaches.

The subsequent chapters of this report present details of the methods and models used for undertaking the above tasks.

1.4 Hydrodynamic modelling domain

MODIS imagery (refer to Chapter 2) indicates large areas of the Flinders and Gilbert catchments are inundated during flood events. As hydrodynamic modelling is computationally intensive, we focused modelling inundation in those parts of the catchments that are most susceptible to flooding. In the Flinders catchment large flood events occur in the mid-to-lower reaches, while in the Gilbert catchment large flood events appear to be confined to the coastal region below Strathmore station. Hydrodynamic modelling was undertaken in the two modelling domains covering the floodplains of the two catchments as shown in Figure 1.10. These domains were defined based on historical streamflow data and preliminary flood inundation mapping using MODIS imagery. The two modelling domains of two dimensional hydrodynamic models include parts of the floodplains of several catchments adjacent to the Flinders (i.e. Nicholson, Leichhardt, Morning Inlet, Norman) and Gilbert catchments (i.e. Norman, Staaten and Mitchell) as floodplains of these catchments are connected during large flood events. The total area of the modelling domain of the Flinders floodplain is 82,403 km² and that of the Gilbert floodplain is 20,886 km².

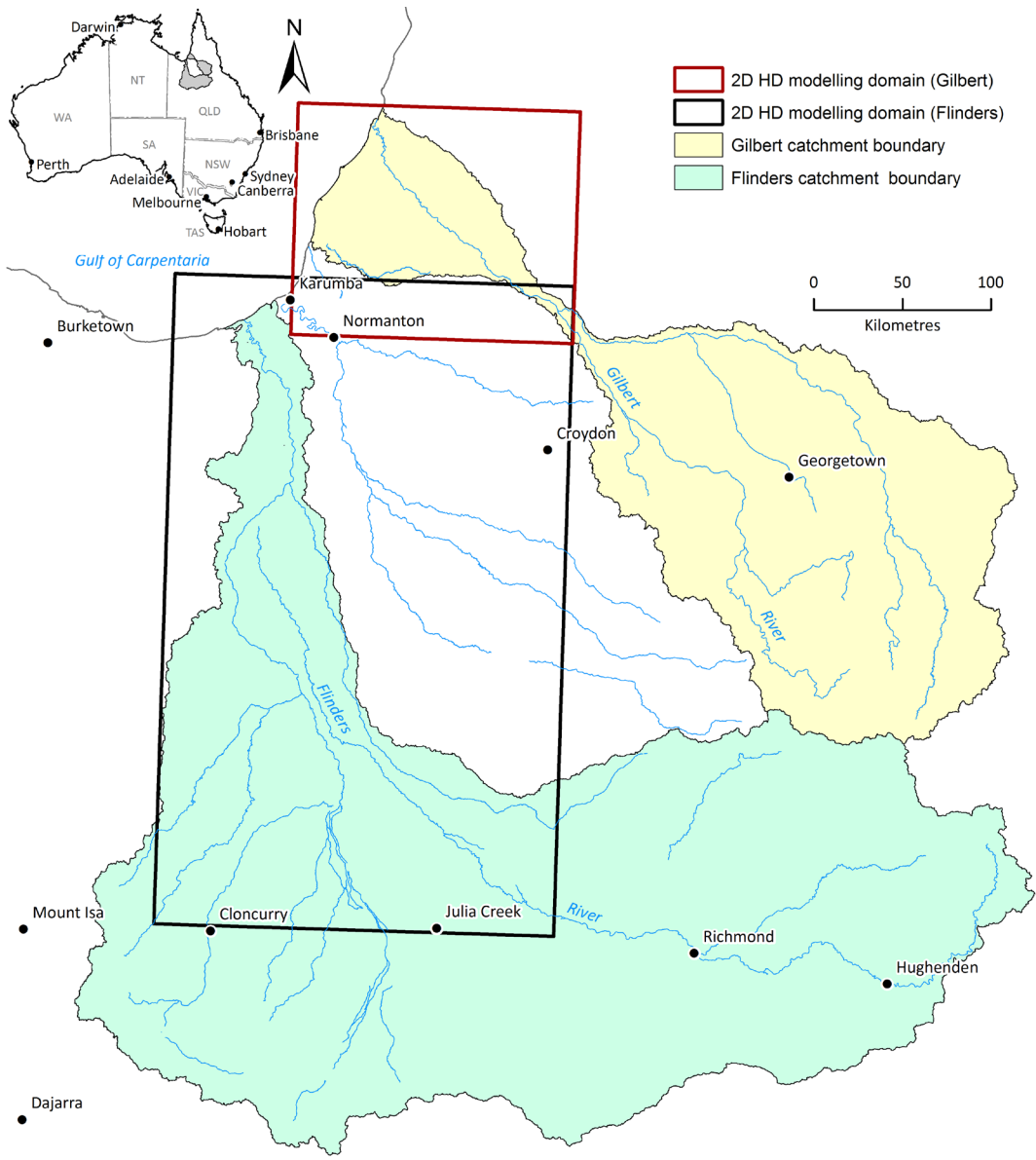


Figure 1.10 Hydrodynamic modelling domains for floodplain inundation modelling in the Flinders and Gilbert catchment

A one-dimensional hydrodynamic model was constructed to cover the entire river systems of the two catchments. Figure 1.11 and Figure 1.12 show the river network used for 1D hydrodynamic modelling of the Flinders Gilbert catchment respectively. These two networks align well with the river networks of the two catchments used in the river system modelling activity (see companion technical report on river system modelling, Lerat et al., 2013).

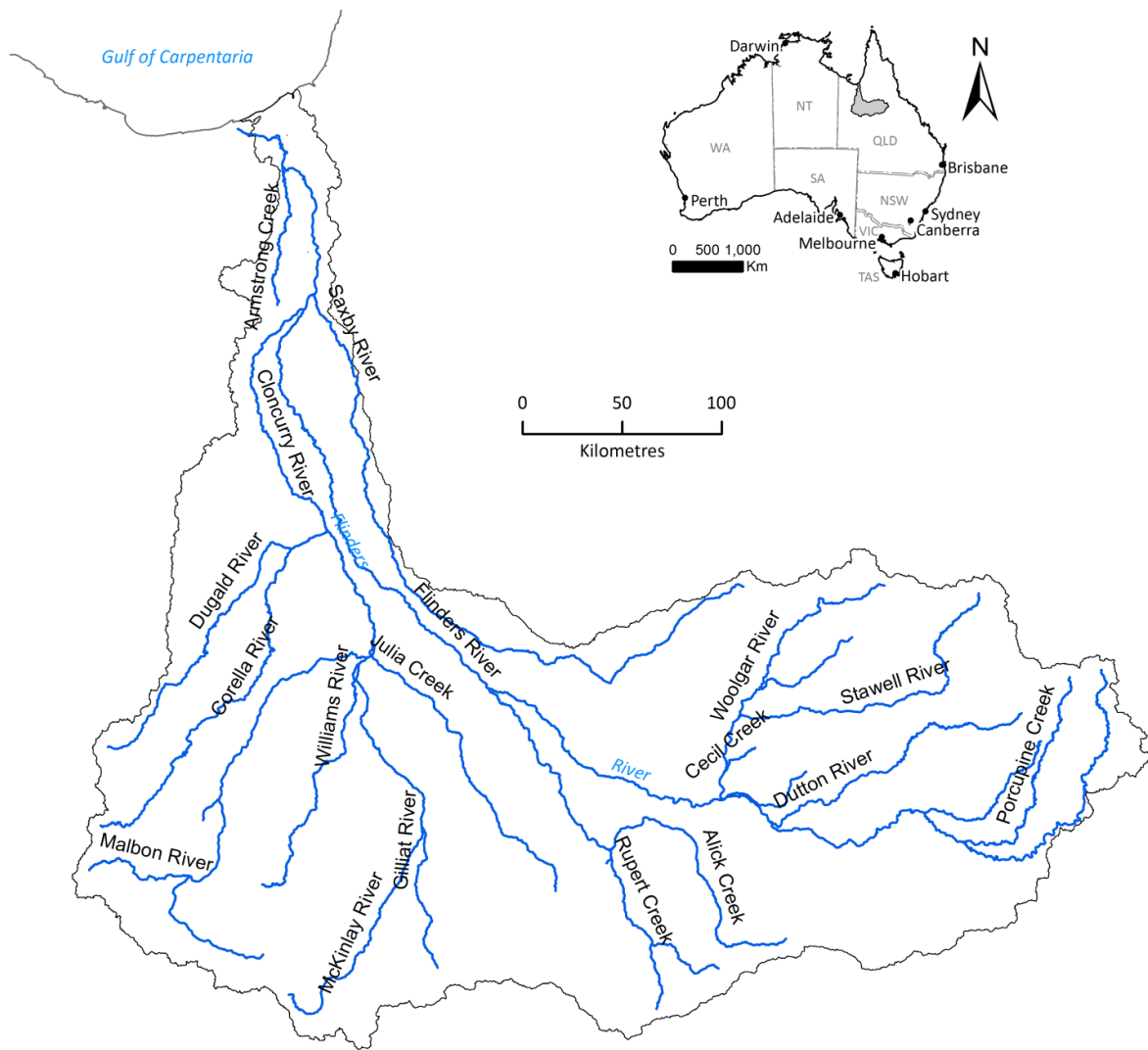


Figure 1.11 River network of the Flinders catchment used for one-dimensional hydrodynamic modelling

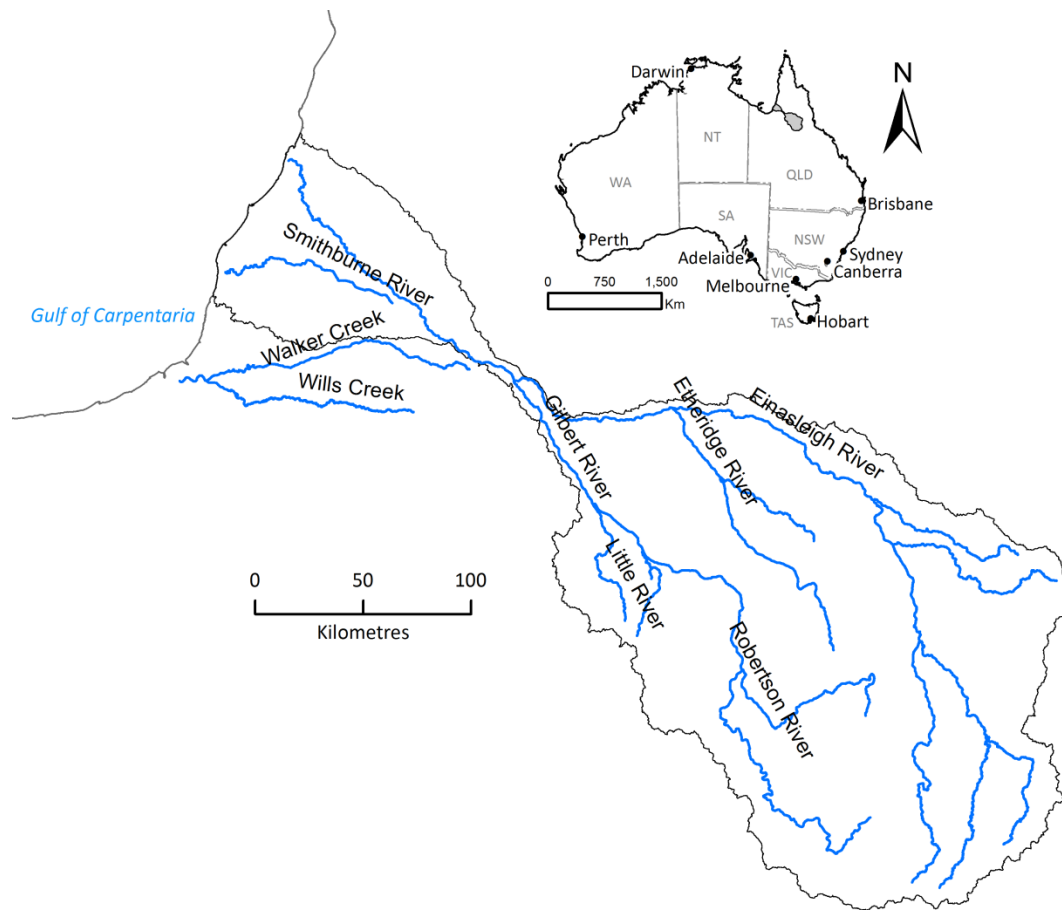


Figure 1.12 River network of the Gilbert catchment used for one-dimensional hydrodynamic modelling

1.5 Report outline

This report has been prepared to provide information on the results of the flood mapping and modelling activity of the Assessment. It is intended to guide discussion of flood hazards, wetland connectivity and impact of proposed development and climate change on flooding and wetland connectivity and opportunities during high flow events within the study area.

The report is structured as follows:

- the background, objectives, study area and scope of the study, overview of methodology (Chapter 1)
- methods and results of flood mapping using remote sensing imagery (Chapter 2)
- methods, calibration and post-audit of hydrodynamic modelling and establishment of relationship between streamflow and floodplain discharge for river system modelling in floodplain (Chapter 3)
- floodplain inundation modelling for future climate and development scenarios (Chapter 4)
- methods and results of wetland connectivity analysis (chapter 5)
- final conclusions and recommendations (Chapter 6)

2 Floodplain inundation mapping using remotely sensed data

2.1 Rationale for using remotely sensed data

Daily surface water maps, and derivations thereof, for the entire Flinders and Gilbert catchments were required to provide a spatial summary of water extent and movement during the wet seasons to identify lands subject to flooding at a regional scale. Regular maps of surface water were also required to help calibrate and validate the two-dimensional hydrodynamic models used to simulate flood events for the lower parts of the Flinders and Gilbert catchments. These maps were produced using satellite imagery from the MODIS and Landsat sensors.

2.2 Satellite Data, Image Acquisition & Pre-Processing

MODIS satellite data (MODERate resolution Imaging Spectroradiometer) were used for producing daily maps of surface water. The MODIS sensor is an optical/infrared sensor from NASA. There are two MODIS sensors currently orbiting the earth (TERRA since 2000 and AQUA since 2002). They acquire daytime images of Australia around 10 am (TERRA) and 2 pm (AQUA). The MODIS data, as used here, have a pixel size of 500 m x 500 m. The TERRA and AQUA MODIS surface reflectance data, named MOD09GA and MYD09GA respectively, were available for free download from the NASA LP DAAC (Land Processes Distributed Active Archive Centre) website: <http://reverb.echo.nasa.gov/reverb>. All available images from November 2000 until March 2011 were downloaded for the wet season (start of November until the end of April). The data were downloaded as sinusoidal projected georeferenced tiles, where tiles H31V10 and H31V11 were required to cover the Gulf region. The tiles (in .hdf format) were reprojected into geographic latitude/longitude on WGS'84 datum, with a pixel size of 0.004697 degrees (approximately 500 m), using IDL code (*MRT_Multiple_resample.pro* – which also requires the freely available NASA MODIS Reprojection Tool MRT to be installed). This program also extracted the reflectance and cloud masking bands that are required to produce water maps. [Note that all IDL programs are included in Appendix A].

Landsat data were also required for mapping surface water when available. These data are at a much finer spatial resolution (30 m pixels) than MODIS, which is better suited to narrow or small water features. However, Landsat data are only available every 16 days at best. This is usually less frequent due to cloud cover and missing data. Landsat 5 data (also called Thematic Mapper or TM) and Landsat 7 data (also called Enhanced Thematic Mapper or ETM) are available for free download from the NASA GloVIS website (<http://glovis.usgs.gov/>). Fortunately we were able to use Landsat data already processed into water maps by the Queensland Department of Environment and Resource Management (DERM) (Muir and Danaher, 2008). All available Landsat data were provided, with some tiles starting from the 1980s, however there were significant time gaps across the region. Since the data were provided in compressed ERDAS format, they were all converted to ENVI format which consists of a flat binary file and header file (*ERDAS_to_ENVI_multi.pro*).

2.3 Methods for developing remotely sensed flood inundation maps

2.3.1 CALCULATING INUNDATION EXTENT USING MODIS

Algorithm used

The method used here for mapping open surface water with MODIS was developed by Guerschman et al., (2011) based on empirical statistical modelling and is summarized below. It calculates fraction of water (which also could be interpreted as the likelihood that the pixel contains water) within a MODIS pixel using Equations 2 and 3:

$$f_w = \frac{1}{1 + \exp(z)} \quad (2)$$

where,
$$z = \beta_0 + \sum_{i=0}^5 B_i \cdot x_i \quad (3)$$

and

β_0 =	-3.41375620	x_1 =	SWIR band 6 (reflectance*1000)
β_1 =	-0.000959735270	x_2 =	SWIR band7 (reflectance*1000)
β_2 =	0.00417955330	x_3 =	NDVI
β_3 =	14.1927990	x_4 =	NDWI (Gao, 1996)
β_4 =	-0.430407140	x_5 =	MrVBF (Gallant and Dowling, 2003)
β_5 =	-0.0961932990		

A further threshold is also applied using the modified NDWI (Xu 2006) where $f_w=1$ for all mNDWI>0.8 (Guerschman et al., 2011). This method is also referred to as the OWL (Open Water Likelihood) version 2.04. A cloud mask is also applied using the accompanying MODIS state band which contains information on cloud and cloud-shadow location. This algorithm was applied to the MODIS reflectance bands using IDL code (*MODIS_OWLv2p4.pro*).

The daily MODIS OWL water maps (one from TERRA – MOD, and AQUA – MYD) were combined into a single daily water map based on best available data (using *MODIS_tile_OWL_Daily.pro* and *MODIS_tile_OWL_Daily_Pt2.pro*). This was where any null data (clouds or no-data) were replaced by the other image data when available. When there were data for a pixel from both the MOD and MYD water maps, then the maximum OWL value was used. This is based on the assumption that pixels closest to the sensor (i.e. not on the edge of the swath) are of better quality and result in a higher equivalent OWL value (Chen et al., 2013). The daily MODIS OWL water maps, still based on the two tiles (H31V10 and H31V11), were then stitched together and subset for the Gulf region (using *MODIS_stitch_OWL.pro*).

Event Maps

The daily MODIS maps were subset for the Flinders and Gilbert catchment's HD domains for flood events in the following years: 2000-2001, 2003-2004, 2005-2006, 2007-2008, 2008-2009 and 2010-2011. The MODIS OWL water maps then needed to be converted into a map of water and non-water pixels. Three different water percentage thresholds were tested to map pixels as water. All pixels above the OWL threshold of 1%, 5% and 10% were mapped as water (1), with non-water (0) and nulls (255), and converted to an ascii GRID format for use in the hydrodynamic models. The water maps also needed to be converted to MGA Zone 54 coordinate system and 90 or 150 metre pixel size for the Gilbert and Flinders HD domains, respectively.

Composite maps

Composite maps were also produced for the Gulf region. These were statistical summaries of the MODIS OWL water maps for each year as well as for all the MODIS data (from November 2000 to March 2011). The average, maximum and inundation duration were calculated using *MODIS_OWL_frequency_stats.pro*. The inundation duration maps were based on the length of time that a pixel was under water. Firstly it required

the OWL percentage water map be converted into a water/non-water map. A threshold of 10% was adopted such that any value equal to or above this was determined to be water.

The length of time that a pixel was under water was calculated from these daily water maps (based on the 10% threshold). For pixels subject to cloud cover, if they were wet before the cloudy pixel day(s), and wet when the pixel was no longer in cloud, then the pixel was assumed to be wet for the full duration. However if the pixel was dry once it was no longer in cloud, the pixel was assumed to be dry during the cloudy period. This is illustrated in Table 2.1 below.

Table 2.1 Example of how the flood duration is calculated during cloudy periods.

DAY 1	DAY 2	DAY 3	... DAY X	INUNDATION LENGTH (DAYS)
Wet	Cloud	Cloud	Wet	X
Wet	Cloud	Cloud	Dry	1

These maps provide a spatial summary of pixel wetness compared to its surrounds. The average OWL water map provides a comparative indication of how wet a pixel is through time. The maximum OWL water maps shows how wet the pixel can get when flooded. For example some pixels may only have up to a maximum of 50% water in it, while other pixels can be fully flooded. However the maximum OWL water map does not indicate how frequently this occurs, unlike the average OWL water map. The inundation water maps indicate the maximum number of consecutive days that a pixel has been flooded (i.e. between November 2000 and March 2011). For clarity, the inundation lengths were divided into classes of 0, 1, 2-5, 5-10 and >10 wet days.

2.3.2 FOR LANDSAT TM

Algorithm used

The Landsat water maps were produced by DERM (Muir and Danaher, 2008). These maps were produced for the whole of Queensland. In summary the data were produced from the Queensland SLATS vegetation monitoring work which involved a thorough orthorectification and radiometric standardization of all images. In order to separate water from non-water, the Canonical Variates Analysis tool was used on spectral signatures collected throughout the Queensland area. This resulted in a water index, where a threshold of less than 70 was determined to be water. The data were provided as row/path images as a water index, and also as a water mask which had clouds masked out. The Muir and Danaher (2008) analysis found water features were detected with a 96% user’s accuracy and a 70% producer’s accuracy for single date comparisons with 2.5 metre SPOT 5 imagery for water features > 3 Landsat pixels. The Producer’s accuracy provides a probability of how many water pixels were classified as such, while the User’s accuracy provides a measure of the number of pixels classified as water really being water on the ground. Overall the accuracy was estimated to be 99%.

Event maps

Landsat water maps for selected flood events (i.e. years 2000-2001, 2003-2004, 2005-2006, 2007-2008, 2008-2009, 2010-2011) were examined to determine if they were relatively free of cloud. In some situations, the Landsat cloud mask appeared to be masking water instead of cloud, so the water index (thresholded at <70) was used to map water when the outline was obvious. These were then converted to the same ascii GRID format and pixel size as the MODIS water maps for input into the hydrodynamic models.

Composite maps

Due to the large number of Landsat images, which were all of different sizes, a program was written to resample each image for each path/row to the same size and location (*ENVI_same_size.pro*). The average and maximum water maps were produced from the Landsat water maps (*Multi_Image_Stats.pro*). Since these maps are already water/non-water maps, the average water maps are the average proportion of time that the pixel is flooded (based on all available data), and the maximum water map is the maximum extent of inundation based on all available data.

2.4 Results

2.4.1 EVENT BASED INUNDATION MAPS

Cloud cover was a problem when producing event based inundation maps, particularly for the Gilbert catchment. Both MODIS and Landsat water maps were used for the selected flood events even when there was a small percentage of cloud-free data within the HD domain (Table 2.3 and Table 2.2). The flood events were for 2000-2001, 2003-2004, 2005-2006, 2007-2008, 2008-2009 and 2010-2011.

Table 2.2 Flood event dates, and number of available MODIS/Landsat images for the Flinders catchment.

FLOOD EVENT DATE	NO. OF MODIS IMAGES	NO. OF LANDSAT IMAGES
09/03/2011-12/04/2011	10	0
02/01/2009-24/02/2009	12	2
20/03/2006-23/04/2006	4	1
27/12/2000-26/01/2001	7	2

Table 2.3 Flood event dates, and number of available MODIS/Landsat images for the Gilbert catchment.

FLOOD EVENT DATE	NO. OF MODIS IMAGES	NO. OF LANDSAT IMAGES
09/3/2011-12/4/2011	6	2
09/1/2009-08/02/2009	1	1
29/12/2000 - 10/01/2001	0	0

Cloud cover is often a problem when trying to map flood events using optical remote sensing data. The Flinders, and particularly the Gilbert, catchments have this same issue. Figure 2.1 and Figure 2.2 show examples of a flood event occurring in the Gilbert and Flinders HD domains on a relatively cloud-free day for the MODIS and Landsat water maps.

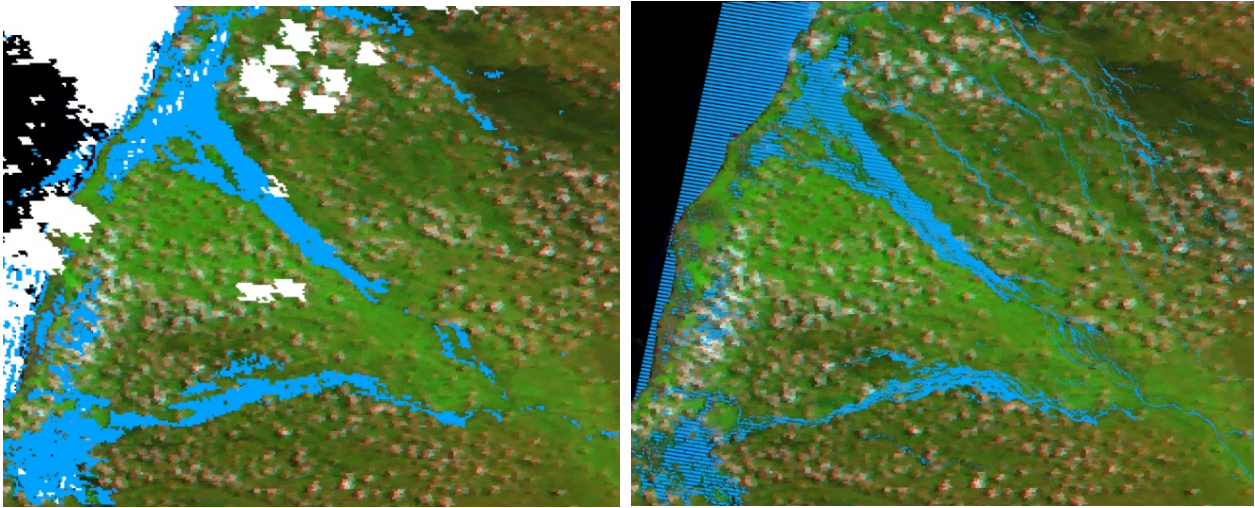


Figure 2.1 Flood event in the Gilbert HD domain from MODIS on the 17th March 2011 (left) and Landsat on the 9th February 2011 (right). Blue = water, White=cloud, overlaid on a “true colour” MODIS image. This MODIS water map was generated using the OWL with a 10% threshold. The Landsat water map shows a stripping pattern due to the linear gaps in the Landsat ETM imagery.

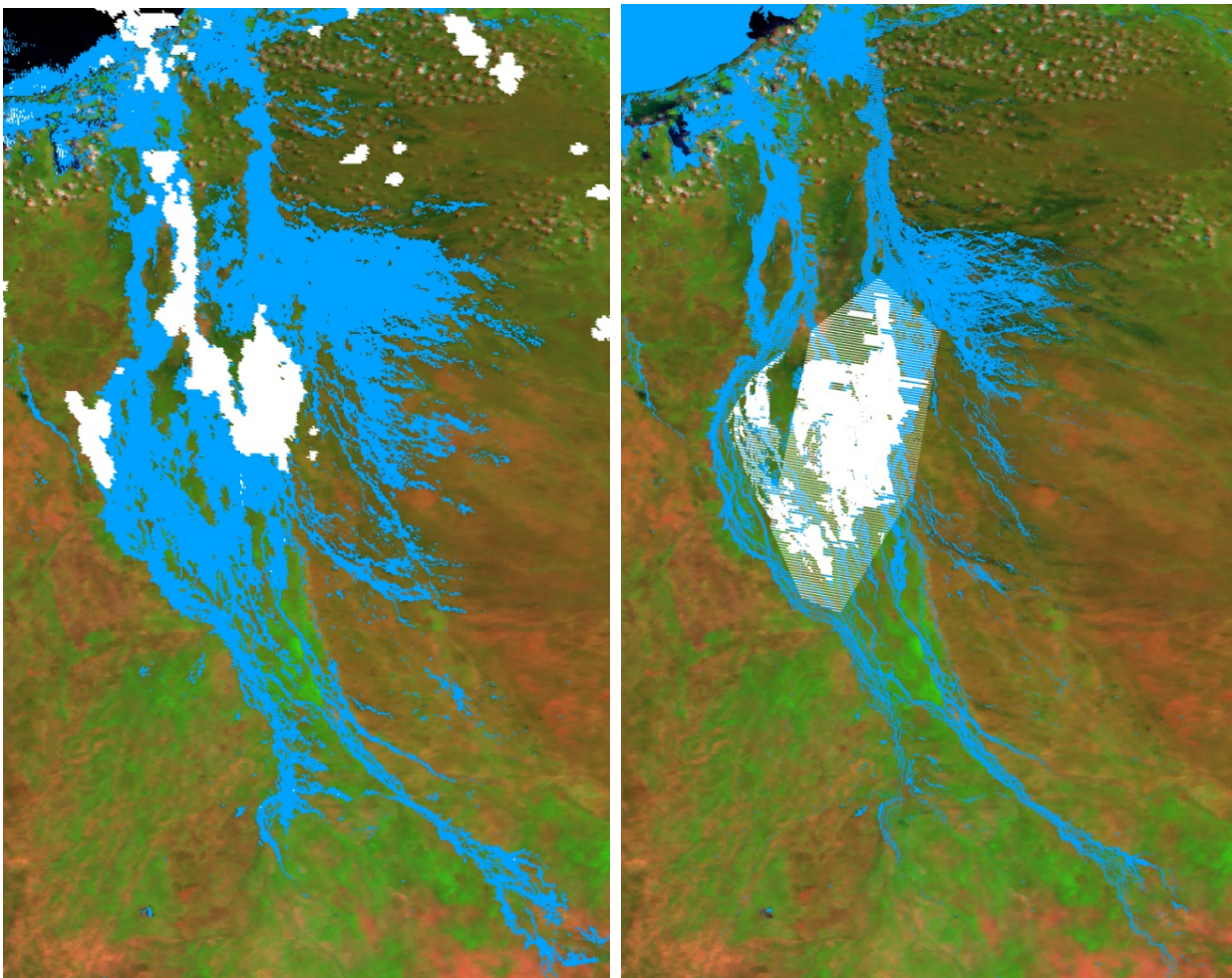


Figure 2.2 Flood event in the Flinders HD domain from MODIS on the 19th February 2009 (left) and Landsat on the 18th to 20th February 2009 (right). Blue = water, White=cloud, overlaid on a “true colour” MODIS image. This MODIS water map was generated using the OWL with a 10% threshold. The Landsat water map shows a stripping pattern due to the linear gaps in the Landsat ETM imagery as well as cloud patterns.

Both the Flinders and Gilberts HD domains (Figure 2.1 and Figure 2.2) show very similar flood patterns in both the MODIS OWL and the Landsat water maps. The Landsat image was a month before the MODIS

image shown for the Gilbert catchment, however the water appears to be flooding in the same channels. The area of water mapped in the Gilbert HD domain (excluding the ocean) from the MODIS water maps are 4,210 km², 1,640 km² and 1,365 km² for the 1%, 5% and 10% thresholds, respectively. The Landsat scene for the Gilbert, which is a month earlier than the MODIS, measures an area of 970 km², however this is reduced somewhat due to the stripped Null values. These are estimated to be up to 20% of the pixels in the water areas hence the real area of water mapped by the Landsat could be up to 1,213 km², which compares well with the 10% threshold. The MODIS water map for the Flinders shows a slightly larger flood compared to the Landsat, despite these images being acquired around the same time, however the areas where flooding occurs are still very similar. The area for the MODIS water maps in the Flinders HD domain (excluding the ocean) is 5,018 km², 2,475 km², and 1,985 km² for the 1%, 5% and 10% thresholds respectively. The area from the Landsat imaged around the same time is 1,056 km², or up to 1,320 km² allowing for the stripped Nulls accounting for 20% of the values. Hence a 10% threshold of the OWL percentage water is more similar to the Landsat water maps than the 1% and 5% thresholds.

2.4.2 STATISTICS

The statistical summaries of the MODIS OWL water maps for each year (based on November to the following April) were calculated. The average percentage of water in a pixel for each wet season (November until April) is shown in Figure 2.3. This is a good indication of which years were wet, and the distribution of water during those wet years. It highlights the large flood in January/February 2009 (during the 2008 wet season) compared to the other years. The 2005-2006 wet season was also reasonably wet for the Norman and Flinders catchments, and the 2009-2010 and 2010-2011 wet seasons for the Norman catchment only.

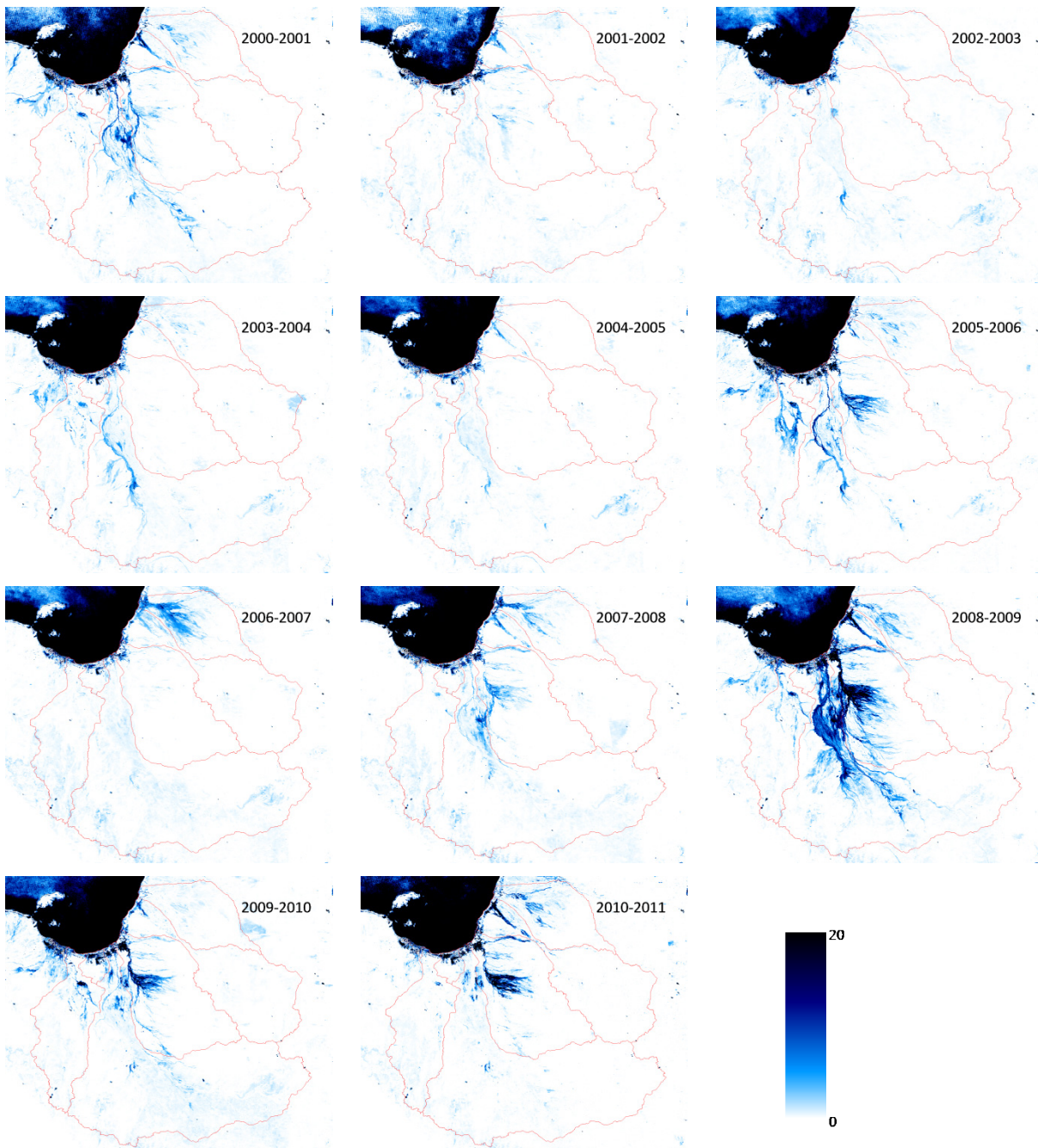


Figure 2.3 Average percentage of water in a pixel (based on available images during the wet season). The year, as indicated, starts from November and goes until the end of April of the following year.

The maximum percentage of water in a pixel for each wet season is shown in Figure 2.4. It shows how wet a pixel can get during the flood season. In particular the black areas show where a MODIS pixel (of 500 m x 500 m in size) is fully flooded. This figure shows just how large the February/March 2009 flood (2008-2009 wet season) was compared to the other years.

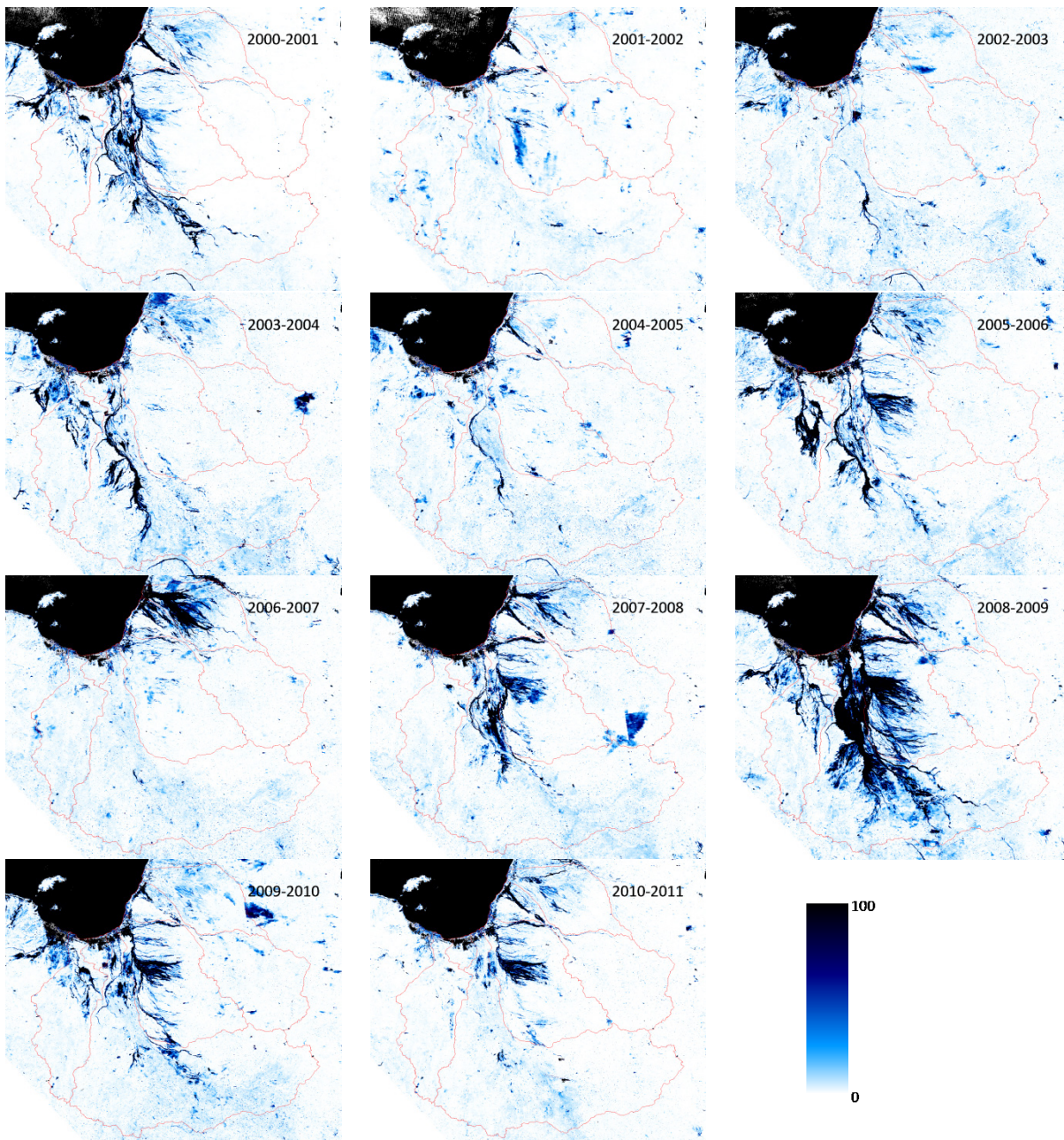


Figure 2.4 Maximum percentage of water in a pixel (based on available images during the wet season). The year, as indicated, starts from November and goes until the end of April of the following year.

Both the average (Figure 2.3) and maximum (Figure 2.4) images are showing some areas of low average and maximum values that are mapped as having some water when there is likely to be none. This is due to soil colour, in particular dark soils, which tend to be mistaken as dark water. There are also artefacts in the images which are particularly visible in the maximum bands. These are not easy to automatically detect, however they are clearly visible in the images in that they show as having a high proportion of water for one year only and nothing in any of the other years. These tend to be along the edge of the MODIS swaths (i.e. pixels that are furthest from the sensor) where the OWL accuracy reduces, or around thin clouds that aren't automatically masked. Keeping this in mind, and possibly including the use of a flood likelihood mask, these images are still useful in interpreting the wet and dry years as well as their distribution within each catchment.

Figure 2.5 shows the number of consecutive days that each pixel is inundated. It has been divided into classes (2-5 days, 5-10 days and > 10 days) for clarity of interpretation. Areas inundated for only 1 day are not shown, to eliminate the artefacts visible in the Maximum images (Figure 2.4). The images are shown for each wet season (November to April), as well as for all wet seasons from 2000 to March 2011. It is

indicating that the lower parts of the Flinders and Norman catchments were inundated for more than 10 days during the large flood in February/March 2009 (2008-2009 wet season). The lower Gilbert catchment also had areas under water for more than 10 days. The 2001-2002 and 2002-2003 wet seasons appear to have been particularly dry compared to the others, as was the 2006-2007 wet season except to the north of the lower Gilbert catchment.

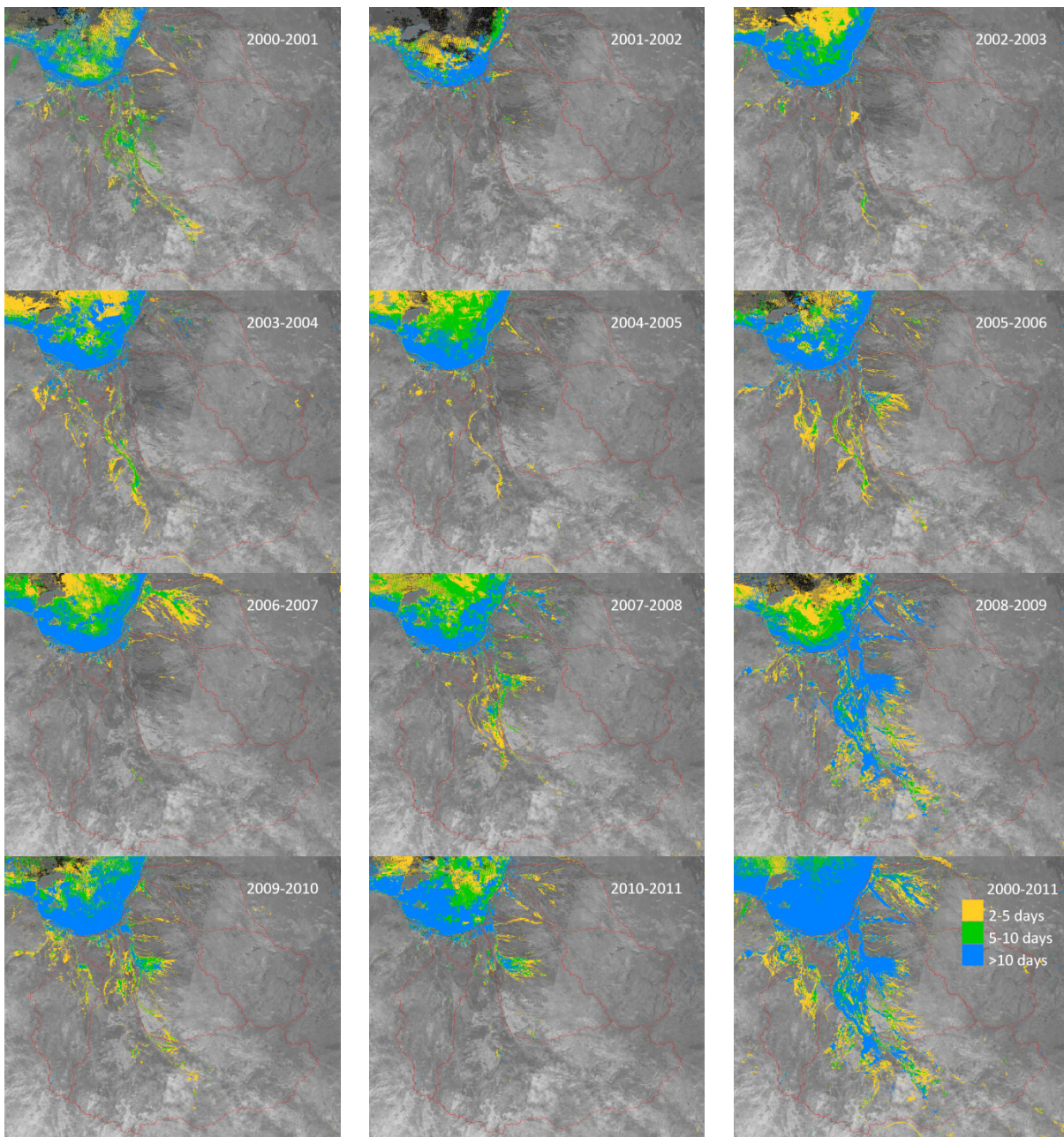


Figure 2.5 The maximum number of consecutive days that a pixel is inundated with water (based on available images during the wet season). The year, as indicated, starts from November and goes until the end of April of the following year. The image in the bottom right corner is for all wet seasons from 2000 to March 2011.

For the Landsat statistical summaries, the average water maps (i.e. the average proportion of time that the pixel is flooded - based on all available data), and the maximum water maps (i.e. the maximum extent of inundation based on all available data) are shown in

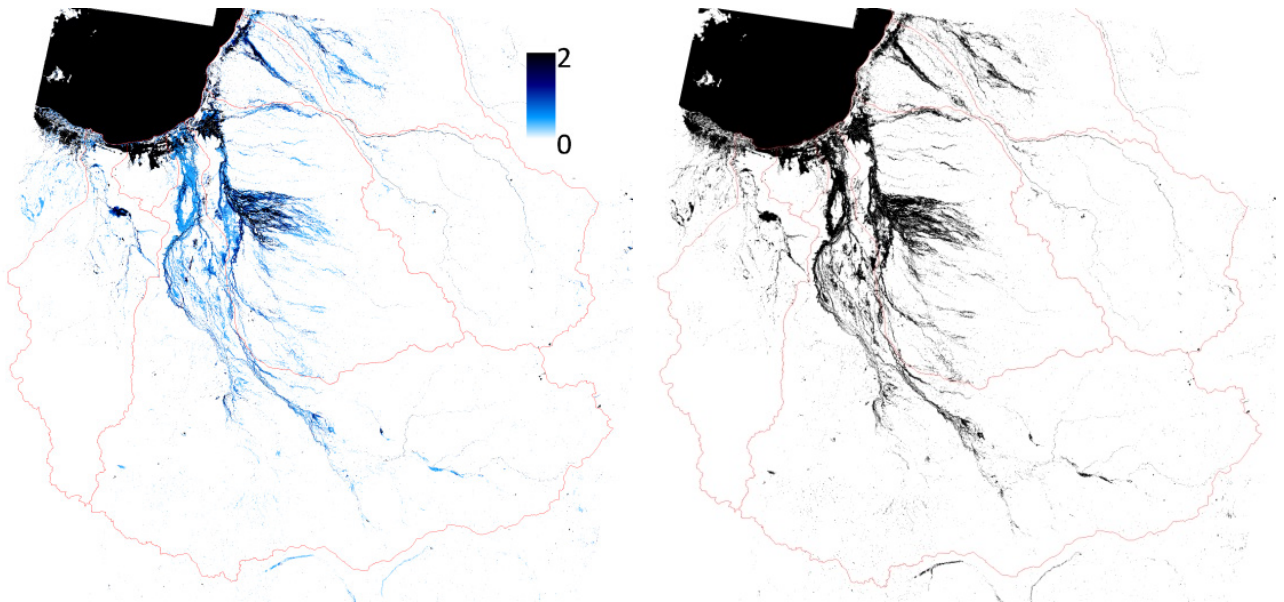


Figure 2.6. The data was available from the late 1980s up until 2011, however it was patchy and temporally inconsistent. When compared to the MODIS summary images (Figure 2.5), they both show significant flooding in the lower Norman catchment. They also show minimal inundation extent in the lower Gilbert catchment. However due to the large temporal gaps in the Landsat data, not all flood events are captured, and hence the maximum inundation extent can vary from the ones seen in the MODIS flood maps.

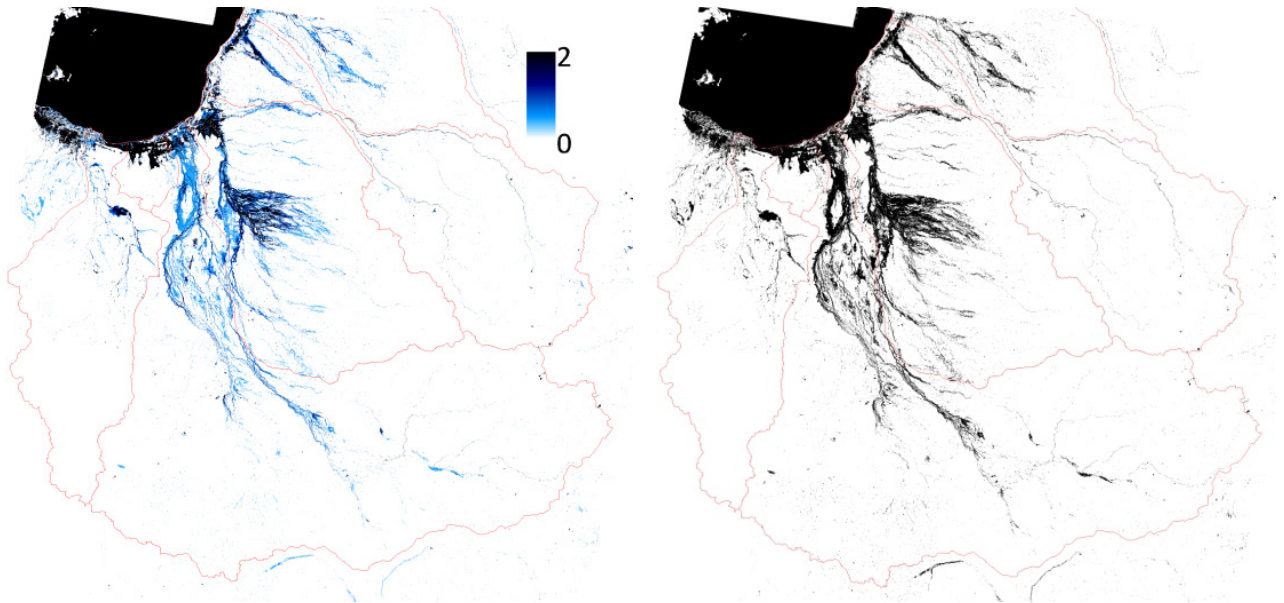


Figure 2.6 Average percentage of time that a pixel was inundated (left) and maximum extent of inundation (right) based on all available Landsat data from DERM water maps.

2.5 Validation and uncertainty

Some validation analyses were performed to assess: how well the MODIS water maps are mapping water percentage compared to the DERM Landsat water maps; how well the MODIS water maps compare to independent water maps at the same spatial scale; and what is the best threshold in the MODIS OWL water maps to define a pixel as having water or not. These three issues are discussed in the following sections.

2.5.1 VALIDATION OF MODIS OWL VERSION 2.4 USING DERM LANDSAT WATER MAPS FOR THE GILBERT AND FLINDERS RIVERS IN NORTHERN AUSTRALIA

The cloud-free Landsat scenes from the DERM Landsat water maps collection were selected (due to the high occurrence of cloud cover, the number of available images was very limited). Small subsets of the Landsat images were created such that they were completely cloud-free, didn't contain any null data (since all suitable Landsat images were Landsat ETM with the large striping effect around the edge, the scene centre was used), and contained sufficient amounts of surface water to cover the MODIS pixel. MODIS images from the same day and time were then selected (these were Terra images as they coincided best with the Landsat overpass times) before being resampled to the same pixel size as the Landsat images (i.e. 30m). Overall nine subsets were extracted, six for the Gilbert catchment and three for the Flinders catchment.

The MODIS subsets needed to be georeferenced to the Landsat subsets as accurately as possible. This was done using the IDL programs *MODIS_landsat_OWL_match.pro* and *MODIS_Landsat_OWL_match_part2.pro*. In these programs the Landsat image was shifted by small amounts compared to the MODIS pixel to determine the best overlap between the two images by calculating water proportion in the Landsat image for an equivalent MODIS pixel size. The highest correlation between the MODIS and Landsat water proportions determined the best spatial match between the two, which was then used for subsequent analysis.

The DERM Landsat water maps were used for validation of the corresponding MODIS OWL water maps. While the DERM water maps are still based on remote sensing data, they are completely independent of the method used to calculate the OWL, and the DERM water maps have been assessed to be accurate to 99% based on a Queensland-wide analysis.

The linear relationship between the MODIS water proportion and Landsat water proportion (generated by resampling the higher-resolution MODIS image) were examined for all nine sites. The MODIS and Landsat images of the nine sites (Figure 2.7) show the MODIS pixels don't effectively map water along narrow water features. If the water features are too narrow, they are not detected at all. What is also very apparent in Figure 2.7, is that MODIS is mapping pixels as having a small percentage of water, while the Landsat image has not mapped any water at all. Such an example can be seen for subset G2011-3, which shows a large patch of flooded pixels in the MODIS OWL (top left of image) that does not show in the Landsat imagery. This may be due to confusion of the MODIS OWL algorithm with moist soil for the pixels having very low proportions of water in them.

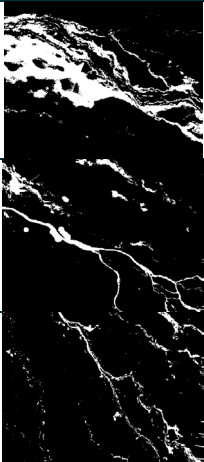
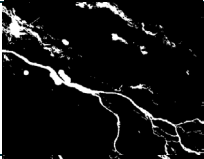
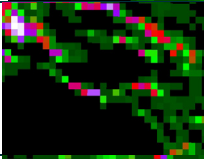
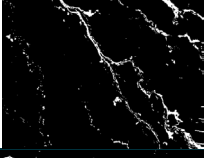
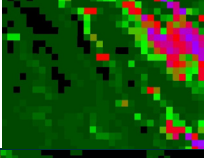
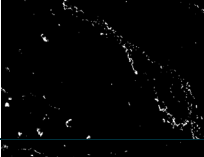
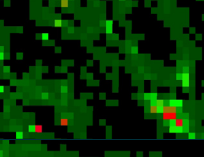
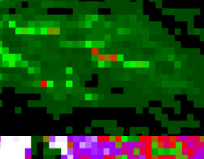
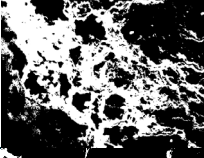
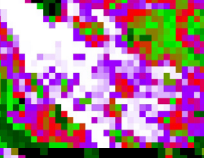
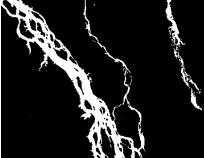
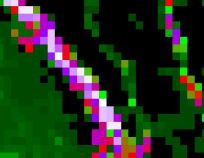
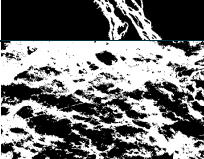
Name	Landsat water map	MODIS water proportion
G2011-1		
G2011-2		
G2011-3		
G2010-1		
G2010-2		
G2010-3		
F2009-1		
F2009-2		
F2009-3		

Figure 2.7 Landsat and MODIS water maps for nine test subsets.

The linear relationships between the MODIS and Landsat water percentages for the nine test subsets are shown in Figure 2.8. The Root Mean Square Error (RMSE) and R^2 of the 1:1 linear relationships are also shown.



Figure 2.8 Scatterplot of MODIS percentage water (vertical axis) and the equivalent Landsat percentage water (horizontal axis) for the nine test subsets. The 10-pixel moving average is also shown to indicate data trend.

Sites G2011-1 and F2009-2 show the best RMSE and R^2 results when the MODIS OWL percentage water are compared to the Landsat water maps. Inspection of the water maps (Figure 2.7) shows these subsets have water features which are large enough to be detected in the MODIS pixel, but the water is still confined to the river channels. This is in contrast to F2009-1 and F2009-3, which have the largest RMSE values, and where the water has spread onto the floodplain. F2009-3 has a strong relationship between MODIS percentage water and Landsat percentage water, however it is not a 1:1 relationship. The MODIS is consistently overestimating the percentage water compared to Landsat resulting in a high RMSE=34.3. The Landsat scene (RGB=Bands 543) is also shown here to help explain these differences (Figure 2.7). What is apparent from the image is that most of the area is in flood, and what isn't flooded appears to be very wet. Since it is very difficult to determine where there is flooding under vegetation in optical remote sensing data, it is difficult to know whether the MODIS is mapping flooding occurring under the vegetation, or if it is just mapping wet soil. Either way, the MODIS is still mapping the correct patterns of water distribution, but is over mapping the percentage of water in areas of vegetation. Any mismatch between the MODIS and Landsat subsets will also degrade the results. G2011-1 has a high RMSE (22.4) due to the edge of water bodies not directly coinciding for the MODIS and Landsat subsets. For example, one MODIS pixel is 81% water, but just on the edge of the water body with only 1% water in the corresponding Landsat image.

When results from all sites are combined (Figure 2.9), the final RMSE is 22.8 and $R^2=0.7$. The reasonably poor RMSE can be explained by the F2009-1 and F2009-3 sites which are almost entirely flooded, except for reasonably small patches which are not classified as having water in the Landsat scene. Particularly for F2009-3 the MODIS percentage water is consistently higher than the Landsat percentage water – even though it is a strong linear, but not 1:1, relationship for most parts.

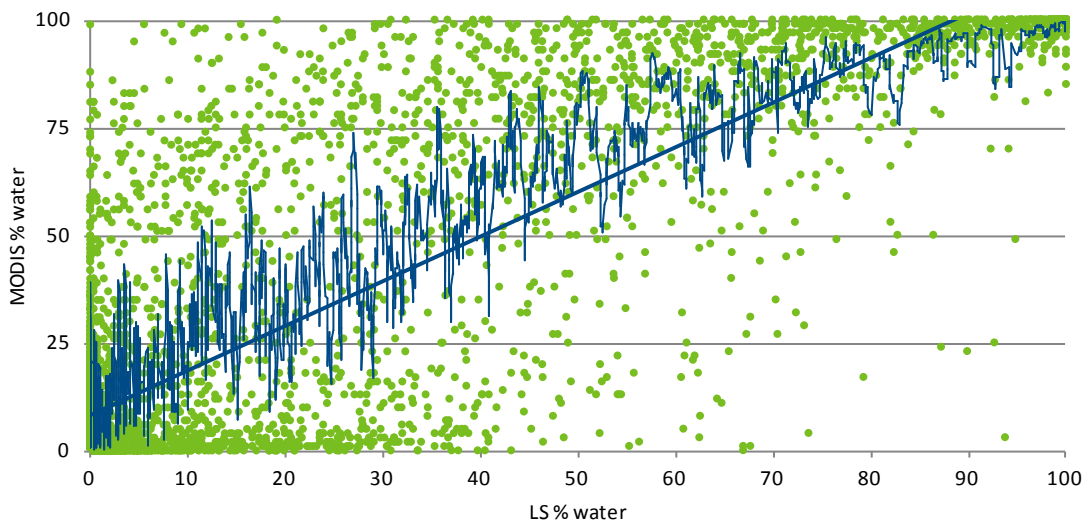


Figure 2.9 Scatter plot of MODIS percentage water (vertical axis) and the equivalent Landsat percentage water (horizontal axis) for the nine test subsets combined. The 10-pixel moving average is also shown to indicate data trend.

2.5.2 COMPARISON BETWEEN MODIS OWL AND INDEPENDENT FLOOD MAPS OF SIMILAR SPATIAL SCALE FOR FEBRUARY/MARCH 2009

A flood map from the large February/March 2009 flood was produced by Mike Digby (Northern Gulf Resource Management Group) using daily MODIS data. The map (which will be referred to as the NGRM map) provided length of duration that a pixel was flooded, and divided into 1-5 days, 5-10 days and >10 days duration.

To enable a comparison between the NGRM map and MODIS OWLs, all daily MODIS OWLs for February and March 2009 were used such that any pixel flooded for more than 1 day was mapped. The NGRM shape file were also converted so all pixels flooded for more than 1 day were mapped. The OWL and NGRM flood maps were then compared for the whole Flinders/Gilbert/Norman catchments, and individually for the Flinders and Gilbert catchments. OWL threshold values of 1 to 5% were used to produce water maps and compared to the NGRM maps for analysis.

The percentage of OWL pixels identically classified as the NGRM map for different OWL percentage water thresholds are shown in Table 2.4. It can be seen that a threshold of 2% water in an OWL image provides results most similar to the NGRM maps. For the Flinders catchment only this threshold is 5%, and for the Gilbert it is 1%.

Table 2.4 Classification accuracy of the MODIS OWL for different water percentage thresholds when compared to the NGRM water map for the Gulf region (All), Flinders and Gilbert catchments.

OWL % THRESHOLD	ALL	FLINDERS	GILBERT
1	72.1	71.3	67.7
2	75.6	84.9	58.1
3	75.0	86.7	55.4
4	74.4	87.1	54.0
5	73.9	87.2	53.2

When a spatial comparison is done, the Flinders subset compares reasonably well when an OWL threshold of 4% is used (

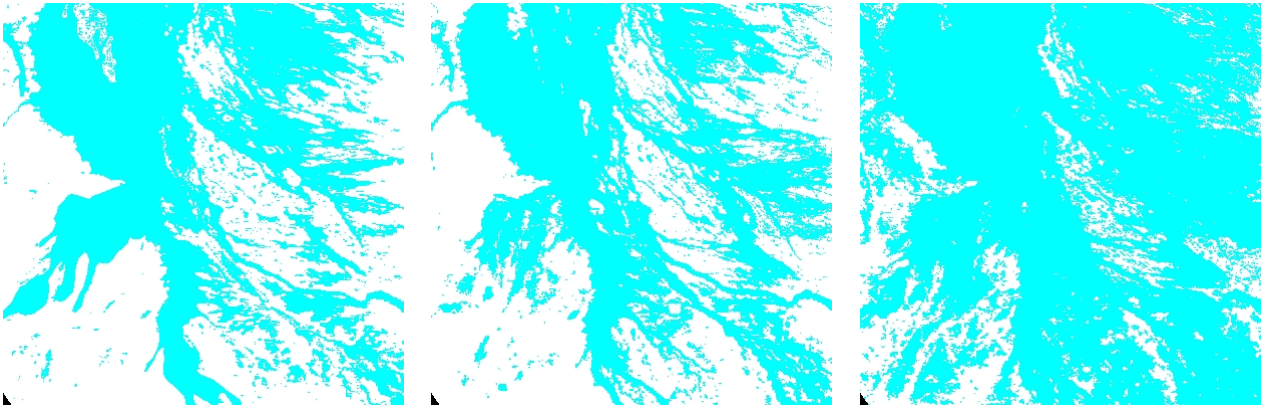


Figure 2.10). When the 1% OWL threshold is used, the number of water pixels is much greater than the NGRM map. The greatest difference between the OWL water map and the NGRM map occurs in the Gilbert River catchment (

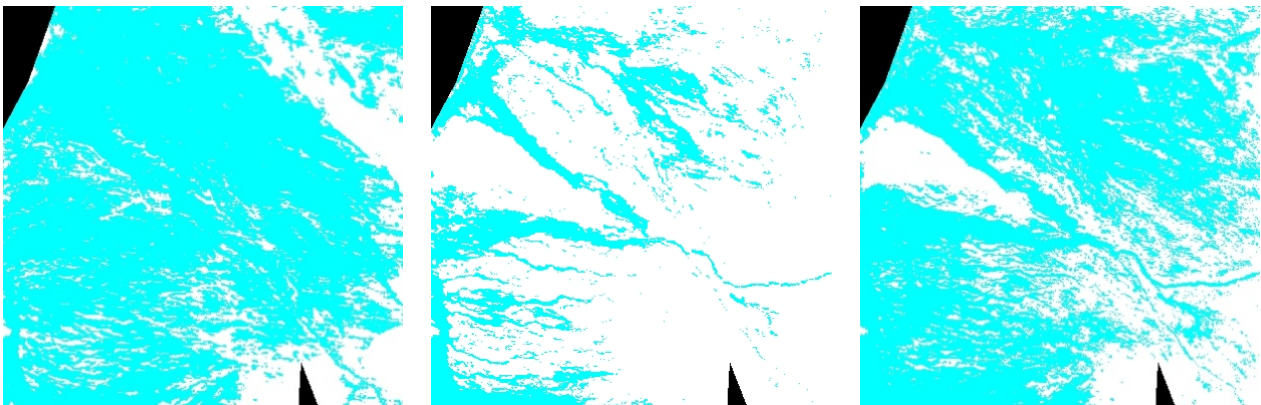


Figure 2.11). A threshold of 4% in the OWL water map shows far fewer pixels are mapped as water compared to the NGRM map. A threshold of 1% results in a more similar map, however there is still a patch of pixels mapped as non-water in the left of the OWL water map, which is completely mapped as water in the NGRM map. Inspection of the MODIS image (Figure 2.12) shows this area is heavily vegetated and it is possible that if water were present it is not being detected in the open water algorithm (which was designed to map open water). On the western side of the Gilbert subset image, the OWL with the 4% threshold is mapping very little water compared to the NGRM map, while more water is showing in the 1% OWL map. However, caution must be taken when using a 1% OWL threshold since it has been shown to be confused with soil colour (see example in the following sections). Furthermore, the accuracy of the NGRM map in this area is unknown.

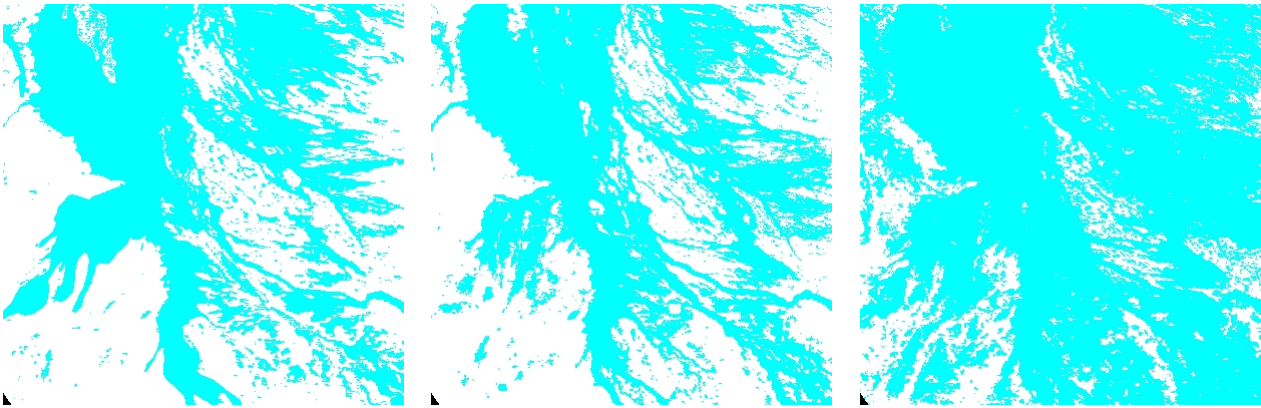


Figure 2.10 Flinders Subset: left- NGRM water map, middle – OWL water map at 4% threshold, right – OWL water map at 1% threshold

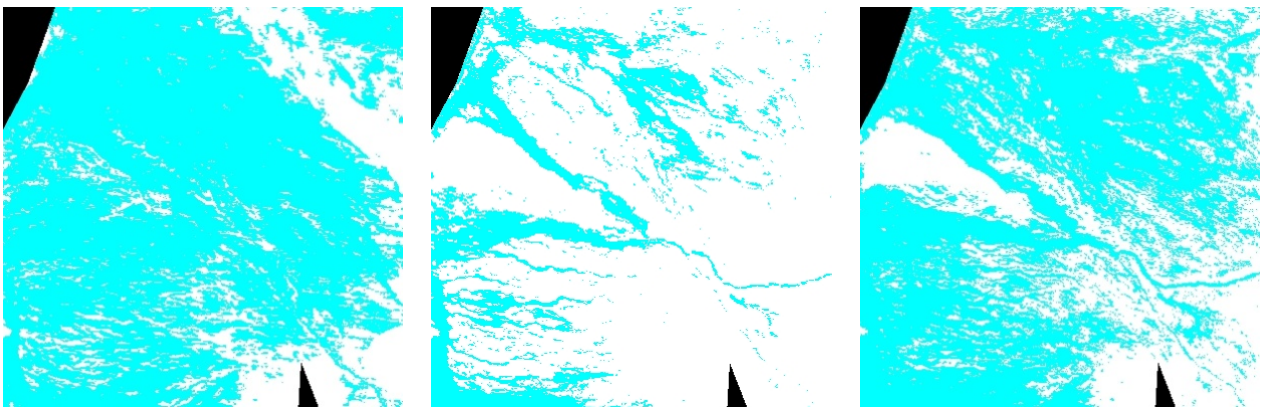


Figure 2.11 Gilbert Subset: left- MD water map, middle – OWL water map at 4% threshold, right – OWL water map at 1% threshold

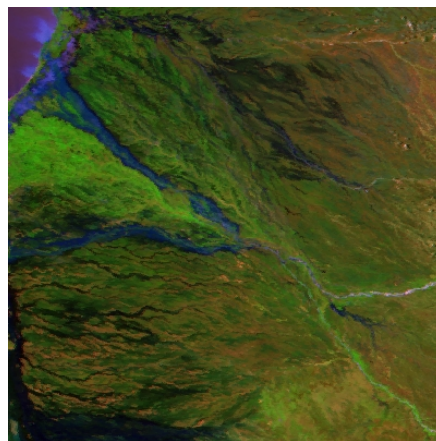


Figure 2.12 MODIS image (bands 721) of the Gilbert subset from 15th February 2009.

There was no accuracy assessment available for the NGRM water map so while we can compare the MODIS OWL water maps with the NGRM map, we cannot state which one is more accurate. Hence, as a further comparison for the Gilbert catchment, the DERM Landsat water maps were also examined since they had an estimated accuracy of 99%. Although they were very limited around the lower Gilbert catchment due to clouds, an example in Figure 2.13 shows a comparison of the MODIS OWL with the independently derived DERM Landsat map for the same day. Unfortunately the MODIS data is extremely cloudy, however what is visible does show some agreement with the Landsat water map. In particular, the Landsat water map shows large areas in the centre of the image that are not flooded, unlike the NGRM water map, which gives us some confidence in the OWL water maps.

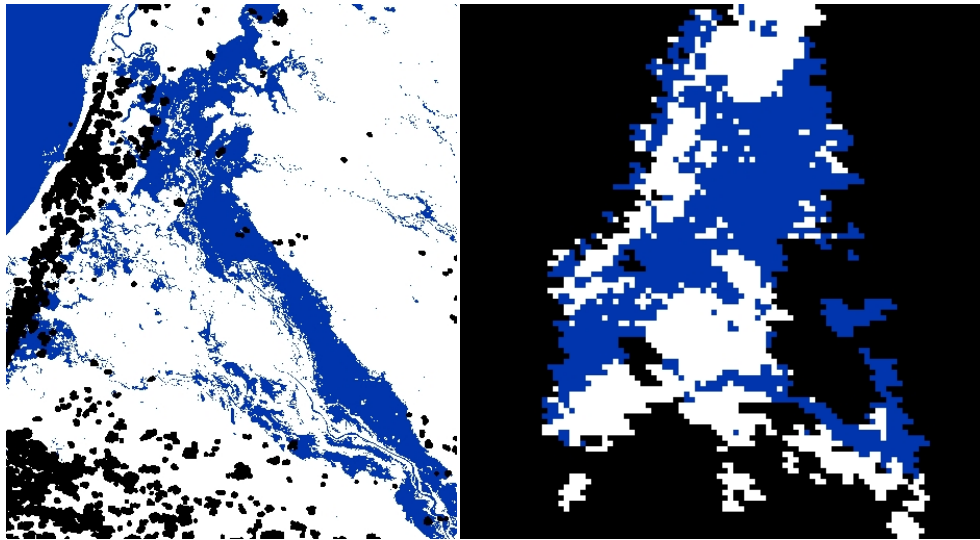


Figure 2.13 DERM Landsat water map (left) and MODIS OWL water map with 4% threshold (right). Both images were for 26th January 2009.

2.5.3 HOW THE MODIS IMAGERY COMPARED TO THE OTHER PRODUCTS EG QUEENSLAND GOVERNMENT FLOOD RECLAMATION

The final MODIS flood map, Figure 2.14, (which was generated from Maximum OWL flood maps from the relatively wet years of 2000, 2001, 2004, 2008, 2009, 2010 and 2011, with artefacts removed) was compared to the Queensland Department of Natural Resources and Mines QIFAO (Queensland Interim Floodplain Assessment Overlay) product. The QIFAO flood map, Figure 2.15, was developed to show areas of potential flood hazard. It was generated using a combination of drainage information, historical flood records, vegetation and soil maps and airborne and satellite imagery (aerial photography, SPOT and Landsat). When the QIFAO flood map is compared to the MODIS flood map the QIFAO is showing much larger extent than the MODIS. There are a number of reasons for this: the QIFAO map is showing narrow drainage channels, many covered in vegetation, which are too fine for the MODIS to detect; the QIFAO appears to include the whole lower floodplain rather than what is visible to the satellite. There are also a few areas where the MODIS flood map is showing water, while the QIFAO is not. These areas are also mapping as water in the Landsat DERM imagery – although not as extensive as the MODIS flood map. They appear to be in very flat areas, which are not part of the drainage channels. The water mapped in these areas is likely to be very shallow, and possibly confused with moist soil in parts.

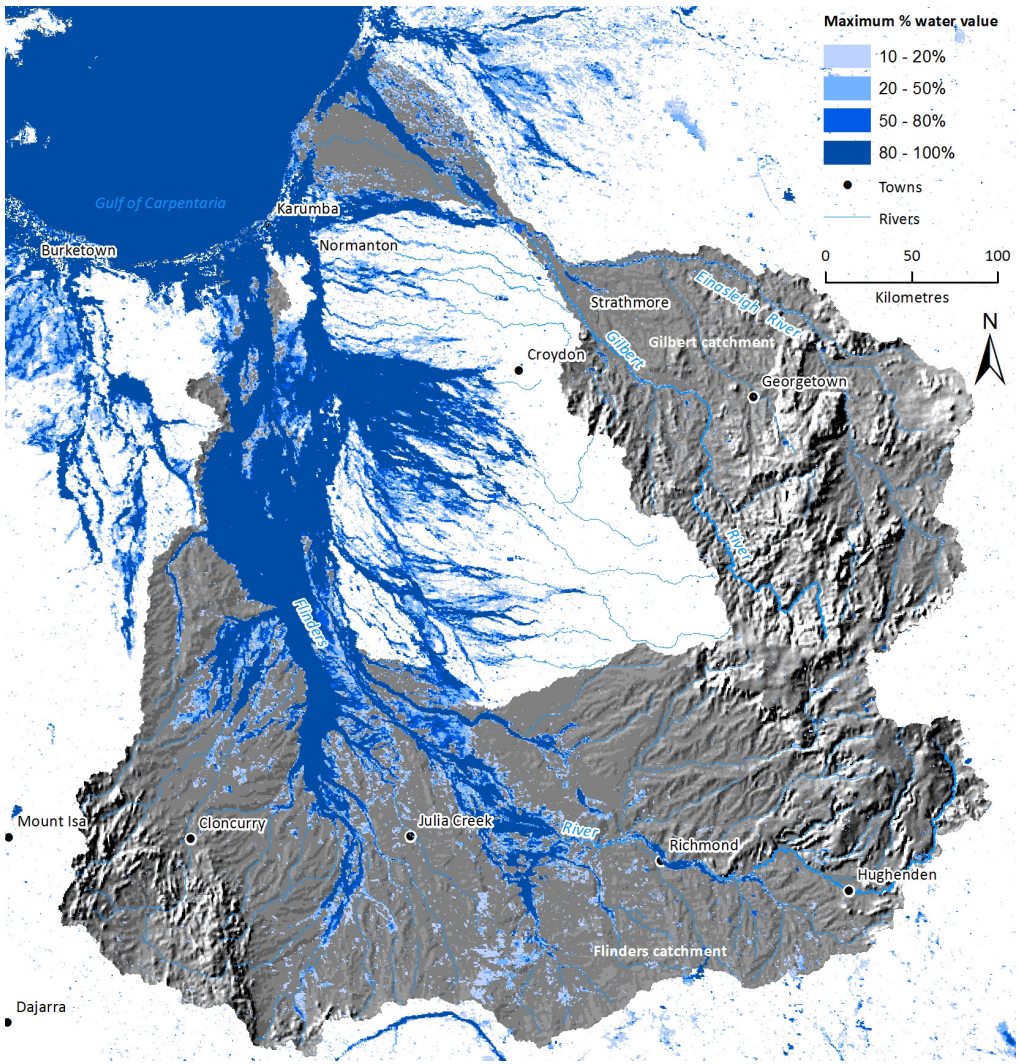


Figure 2.14 Final MODIS flood map generated from Maximum OWL flood maps from the relatively wet years of 2000, 2001, 2004, 2008, 2009, 2010 and 2011, with artefacts removed

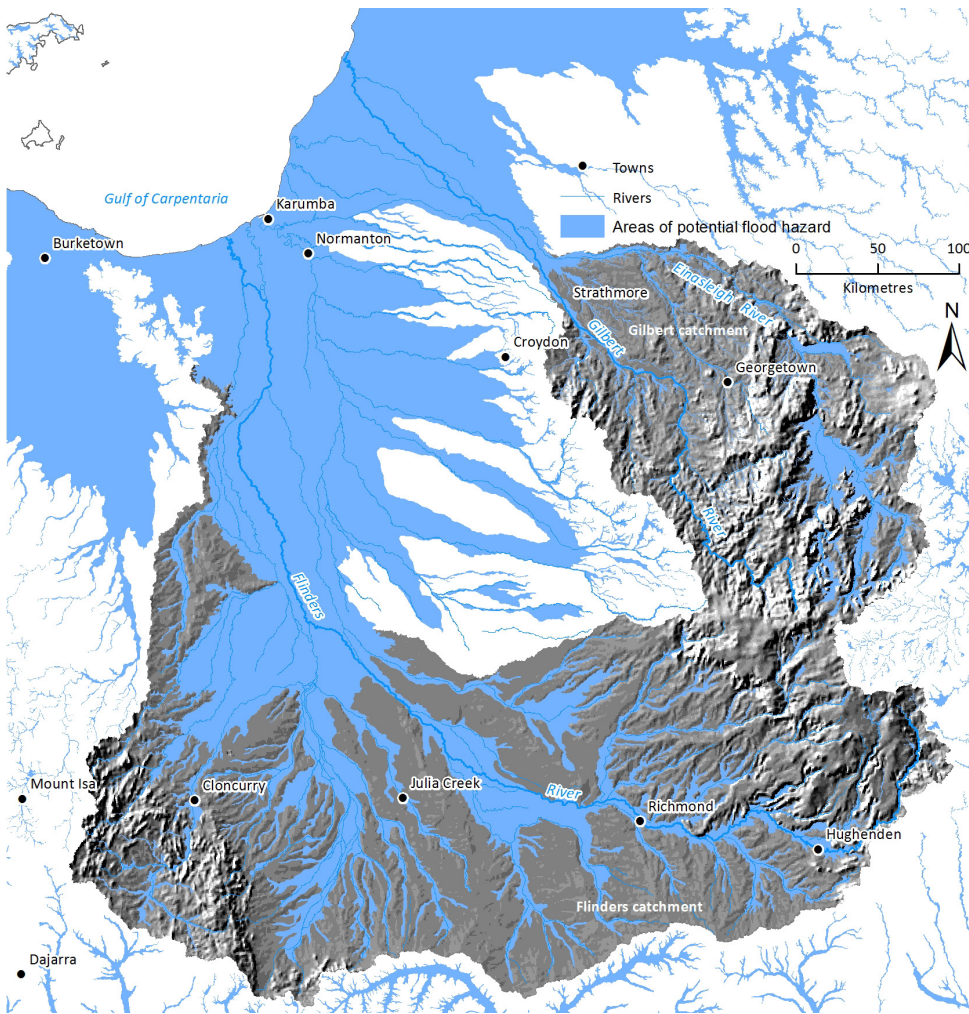


Figure 2.15 Flood reclamation map produced by the Queensland Department of Natural Resources and Mines showing the areas of potential flood hazard

2.5.4 INFLUENCE OF SOIL COLOUR ON OWL

Soil colour and type appear to have an influence on the MODIS OWL for low percentage water values. Figure 2.16 shows the average likelihood of pixels containing surface water, or average proportion of water within a pixel, for the Gulf catchments (called a MODIS flood-frequency image). While the light-blue values are very low (around 0.4% water and below) there are distinct regions showing a higher likelihood of containing surface water compared to its surroundings (for example marked in a red X in Figure 2.16), even though it is not expected to be wetter.

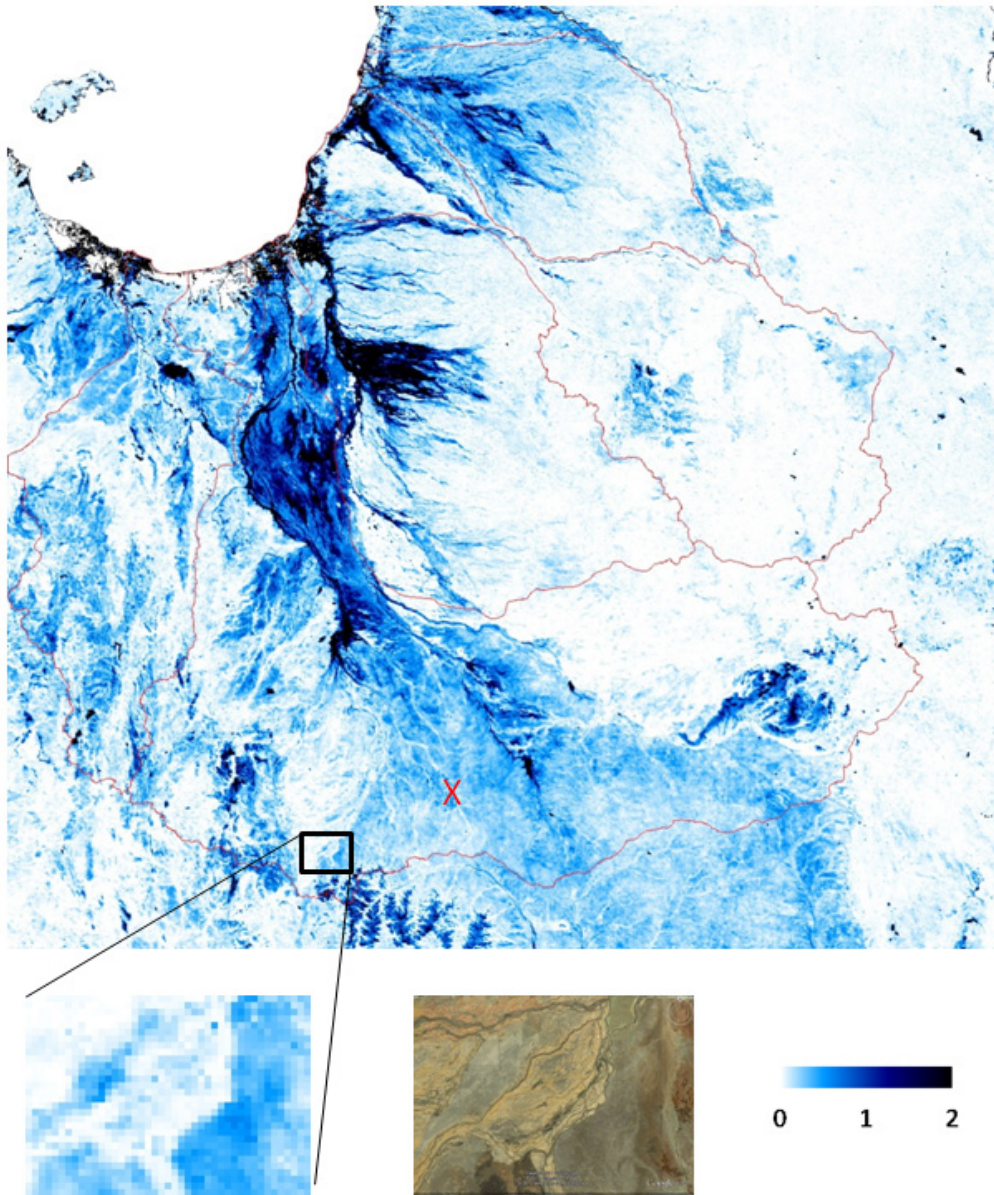


Figure 2.16 A MODIS flood-frequency image showing average proportion of water from 2000 to early 2011. Pixels with an average water proportion >2% show as black. A Google Earth image of the same subset is also shown.

This appears to be due to different soils rather than surface water. The region in the subset from the above image has been extracted from Google earth (Figure 2.16), and shows an obvious difference in soil colour matching the pattern in the MODIS flood-frequency image. The area showing as less wet in the MODIS image is of slightly lower altitude than the surrounding dark soil so we would expect it to be wetter than its surrounds rather than the other way around.

Fortunately individual daily MODIS surface water images usually only map these ‘wetter’ areas as 1-2% likelihood of containing water (or 1-2% water within the pixel). Due to noise in the MODIS data, and confusion between the algorithm mapping surface water and wet soil, pixels containing <3% water are usually removed from further flood analysis.

2.5.5 SELECTING A PERCENTAGE THRESHOLD FOR WATER IN AN OWL PIXEL

A number of factors need to be considered in determining the best OWL water percentage threshold to use. Soil colour has been seen to have an influence on the OWL for values of 2% and less so this also needs

to be considered. The nine subset sites were examined to help determine the best threshold to define a MODIS OWL pixel as inundated or not. This was done by increasing the MODIS OWL percentage water threshold incrementally from 1 to 100%, and comparing it to the Landsat water maps (Figure 2.17). The higher thresholds compare well to the Landsat DERM flood maps where the accuracy increases significantly for the first 3-4% thresholds and then levels off and peaks anywhere between 5 and 90%. Its peak depends on the surface water size and distribution.

A threshold around 10% appears to work well based on all the evidence and past experience. However this threshold may vary depending on the individual characteristics of an area, as well as the requirements of the water map.

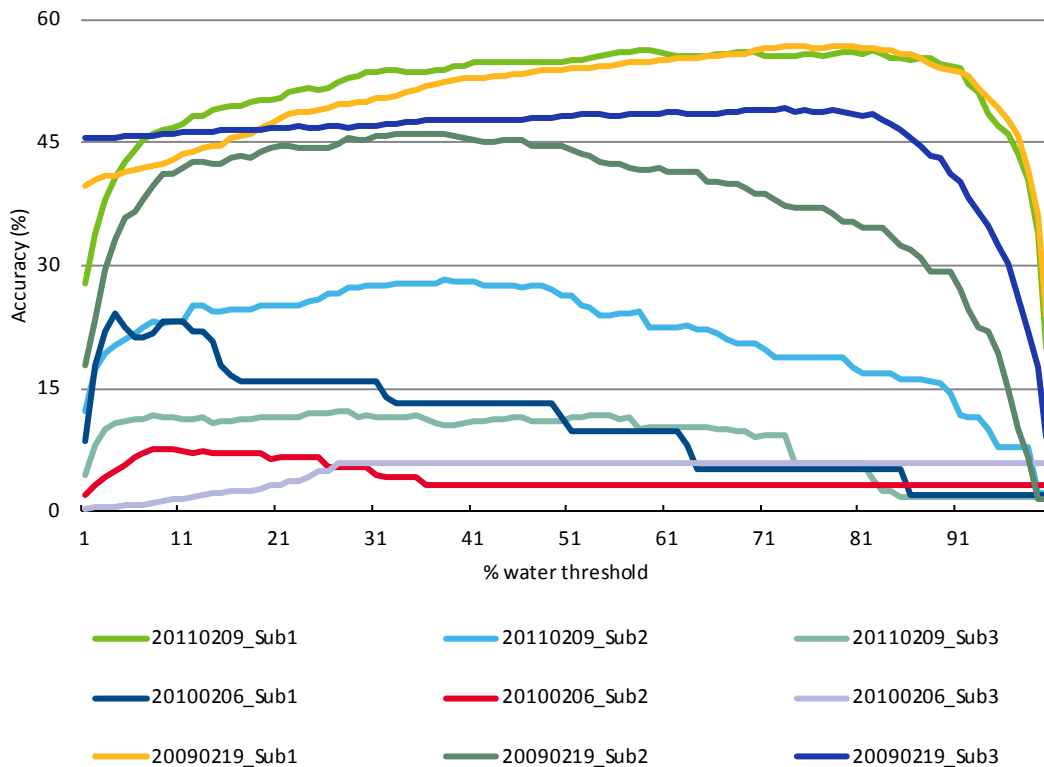


Figure 2.17 Comparison between MODIS OWL, converted to a water map for different percentage water thresholds, and the Landsat DERM flood maps for the sites shown in Figure 2.7.

2.6 Discussion

Water maps generated from remote sensing imagery are particularly useful for covering large areas at a reasonable temporal frequency. While MODIS is able to provide daily water maps, it is of a poorer spatial resolution (250 m – 1 km pixel size) compared to Landsat (30 m pixels). The suitability of MODIS for use in flood analysis is very much dependent on the user’s requirements. The MODIS maps of surface water are not of sufficient detail to map narrow water features of less than 1 pixel in width. This problem is even more exaggerated when the narrow river channel is covered by vegetation, which obscures the water from the sensor. The best results from the MODIS water maps were in the lower catchments during the large flood events.

Overhead vegetation was still a problem, particularly for the lower Gilbert catchment where the flooding was expected to be more extensive than was showing in the water maps. Even though the MODIS sensors were imaging at a sub-daily interval, cloud cover is still a major problem when mapping flood events, particularly before the flood peak. The lower Gilbert catchment appeared to be covered in cloud more often than the Flinders catchment. Like most case studies, most of the cloud-free water maps were available during the floods recession.

Care must be taken when interpreting the MODIS water maps due to artefacts in the imagery and confusion with dark soils. Unusual water features appearing in only one image need to be treated with caution, and a flood-likelihood mask would greatly benefit interpretation of the data.

The Landsat DERM water maps are very useful for detecting fine water features, however the temporal infrequency of the imagery made it difficult in analysing flood events. The large volume of data also made it difficult for examining the whole Gulf region. Fortunately the Landsat water maps were of similar water surface shape and location to the MODIS water maps (based on a 10% OWL threshold) when images from a similar date were examined near the peak of a large flood event in the Gilbert and Flinders rivers. However, like MODIS, the Landsat water maps will also be affected by the same difficulties in detecting water under flooded vegetation.

3 Calibration and validation of hydrodynamic models and floodplain hydrologic matrix

3.1 Rationale

Hydrodynamic modelling can be used to simulate floodplain inundation using both one-dimensional and two-dimensional modelling schemes (Horritt and Bates, 2002). The strength of the hydrodynamic models includes use of shallow water unsteady flow equations to calculate flood levels and flow patterns to estimate inundation extent, duration, depth and frequency of wetting. Hydrodynamic models can also simulate the complex effects of backwater, overtopping of embankments, waterway confluences, bridge constrictions and other hydraulic structure behaviour. There are various models available for hydraulic simulation ranging from simple to complex. Based on the modelling objectives and availability of data and resources one can select one-dimensional and two-dimensional or coupled one- and two-dimensional models. Technical considerations include the scale of the model domain, irregularity in land topography, availability of topography data, and complexity of the hydraulic regime.

3.2 Hydrodynamic modelling

For hydrodynamic modelling in the Assessment, MIKE 21 two-dimensional and MIKE 11 one-dimensional hydrodynamic models of the MIKEFLOOD package (DHI, 2007) were used. MIKE 21 was used for floodplain inundation modelling and MIKE21 in conjunction with MIKE 11 was used to produce relationships between simulated streamflow and modelled floodplain inundation. A brief description of the two models is presented below.

3.2.1 MIKE 11 MODEL

MIKE 11 is a one-dimensional model that can be used for modelling streamflow, tidal effects, inundation extent, duration and depth, flow exchange and flood mapping (DHI, 2009a). It includes options for incorporating simple and advanced structures for performing hydraulic simulations. The model is primarily developed for hydraulic modelling of streamflow in the rivers, channels and runners. However, MIKE 11 modelling can also be performed across the floodplain using wide cross-sections for preliminary assessment of the floodplain behaviour.

The model solves the following St-Venant's equations.

$$\frac{\partial A}{\partial t} + \frac{\partial Q}{\partial x} = q \quad (1)$$

$$A \frac{\partial Q}{\partial t} + Q^2 \frac{\partial \beta}{\partial x} - 2\beta Q \frac{\partial A}{\partial t} - \frac{\beta Q^2}{A} \frac{\partial A}{\partial x} + gA^2 \frac{\partial H}{\partial x} + gA^2 \frac{Q^2}{\left[\sum \frac{A}{n} R^{2/3} \right]^2} = 0 \quad (2)$$

Where, t = time; x = distance along the longitudinal axis of the water course; A = cross-sectional area; Q = discharge through A ; q = lateral inflow or outflow distributed along the x -axis of the watercourse; β = momentum factor; g = gravitational acceleration constant; H = water surface level with reference to datum; R = hydraulic radius; and n = Manning's roughness coefficient.

The model estimates outflow based on the dynamic simulated water level at the outflow boundary. Key model input data includes stream/river network, cross-section geometry, riverbed friction, initial and

boundary conditions. Key model output data includes water level and velocity at the cross-section locations and discharge at mid-points between the successive cross-sections.

3.2.2 MIKE 21 MODEL

MIKE21 two-dimensional hydrodynamic (HD) model is the basic computational hydrodynamic module that simulates the water level variation and streamflow in response to a variety of forcing functions in floodplains lakes, estuaries, bays and coastal areas (DHI, 2009b). The water levels and flows are resolved on either a rectilinear grid, a curvilinear grid, a triangular element mesh or any combination of these three.

The model solves the following St-Venant's equations.

$$\frac{\partial h}{\partial t} + \frac{\partial M}{\partial x} + \frac{\partial N}{\partial y} = q_i \quad (3)$$

$$\frac{\partial M}{\partial t} + \frac{\partial uM}{\partial x} + \frac{\partial vM}{\partial y} + gh \frac{\partial H}{\partial x} + \frac{1}{\rho} \tau_x(b) = 0 \quad (4)$$

$$\frac{\partial N}{\partial t} + \frac{\partial uN}{\partial x} + \frac{\partial vN}{\partial y} + gh \frac{\partial H}{\partial y} + \frac{1}{\rho} \tau_y(b) = 0 \quad (5)$$

where,

H and h : water level and depth respectively; u and v : flow velocity in x and y directions respectively; g and ρ : gravitational acceleration and density of water respectively; M and N : flux of discharge of x and y directions ($M= uh$, $N=vh$) respectively; q_i : effective rainfall intensity on surface grid; $\tau_x(b)$ and $\tau_y(b)$: bottom shear stress in x and y directions, respectively

MIKE 21 numerical procedure uses Alternating Direction Implicit technique (ADI) to solve the mass and momentum stiffness matrix at each time step (Abbott et al., 1973). The boundary conditions in MIKE21 can vary in both time and space. Point sources and sinks can also be incorporated into the MIKE 21 Model. Model input data includes bathymetry (obtained from the DEM), boundary conditions, wind speed and direction (constant and/or varying in time and space), atmospheric pressure maps, bed resistance (constant or spatially variable), flux or velocity based eddy viscosity and radiation stresses. Rainfall, evaporation and surface infiltration data varying in time and space can be incorporated in MIKE 21. Model output includes spatial and temporal variations of water depth and flux densities in x - and y -direction.

The model has been widely used all over the world including Australia for the floodplain hydraulics and flood discharge estimation. The main strength of the model is its ability to cope with wetting and drying of floodplain in the time evolution of an overbank flow event and the model can handle a large number of computational grids (in the range of millions). The main limitation is the poor representation of stream channels and therefore the model is not suitable for predicting channelized or a very small overbank event. Like other two-dimensional models, computational time is a big issue using MIKE 21 model.

3.3 Data preparation

Hydrodynamic models are data intensive. A large amount of spatial and temporal data is required for constructing and calibrating a hydrodynamic model. Data required for one- and two-dimensional hydrodynamic models include:

- land topography;
- landcover map and surface roughness;
- stream network and cross-section data (for 1D model);
- stage height and streamflow data;
- tidal data; and

- surface runoff.

3.3.1 TOPOGRAPHY DATA

High resolution topography data are one of the most important spatial datasets required for hydrodynamic modelling. Teng et al. (2013) showed that the quality of the inundation simulation by two-dimensional hydrodynamic are highly correlated to the digital elevation model (DEM) and the modelling resolution. They found LiDAR DEM at 2 to 5 m resolution to be most suitable for inundation modelling in flat floodplains.

In the Flinders and Gilbert catchments, existing LiDAR data coverage was limited to the lower region covering a very small part of the modelling domains. For this reason the Assessment was limited to using the 30 m resolution digital elevation model (DEM) derived from Shuttle Radar Topography Mission (SRTM) to define the floodplain topography of the Flinders and Gilbert catchments. The hydrologically corrected 30 m DEM was resampled to 150 m and 90 m resolution computational grids in the hydrodynamic modelling domains of the Flinders and Gilbert catchments, respectively. It was necessary to resample the SRTM DEM to a more coarse resolution to cover the most of floodplain by keeping computation time reasonable.

3.3.2 LANDCOVER AND SURFACE ROUGHNESS

In 2010 Geoscience Australia in collaboration with the Australia Bureau of Resources Economics and Sciences (ABARES) released the Dynamic Land Cover Dataset (DLCD) (Lymburner et al., 2010). The 34 DLCD land cover classes conform to the 2007 International Standards Organisation (ISO) Land Cover Standard (19144–2) and reflect the structural character of vegetation, ranging from cultivated and managed land covers (crops and pastures) to natural land covers such as closed forest and sparse, open grasslands. While the DLCD is currently the most comprehensive and best validated national land cover product in Australia, it was considered too detailed for this application. The large number of land cover classes and the lack of any riparian-non riparian distinction suggested that a simplified and spatially constrained version of the data may be more suitable. The 34 DLCD classes were aggregated into eight general land cover classes (Table 3.1). For example, six agriculture classes (irrigated cropping, irrigated pasture, rain fed cropping, rain fed pasture, irrigated sugar and rain fed sugar) were merged into a single class called agriculture.

Table 3.1 Aggregation of DCLD classes

DCLD LAND COVER CLASS	MODIFIED CLASS STRUCTURE	
Extraction sites	Bare areas	
Bare ground		
Inland water bodies	Water	
Salt lakes		
Irrigated cropping	Agriculture	
Irrigated pasture		
Irrigated sugar		
Rain fed cropping		
Rain fed pasture		
Rain fed sugar		
Wetlands	Wetlands	
Forbs open	Savannah	
Forbs sparse		
Tussock grasses – closed		
Alpine grasses – open		
Hummock grasses – open		
Sedges – open		
Tussock grasses –open		
Grassland – scattered		
Tussock grasses - scattered		
Grassland – sparse		
Hummock grasses - sparse		
Tussock grasses - sparse		
Shrubs – closed		Shrubs
Shrubs – open		
Chenopod shrubs open		
Shrubs - scattered		
Chenopod shrubs – scattered		
Shrubs – sparse		
Chenopod shrubs - sparse		
Trees - closed	Trees	
Trees – open	Scattered trees	
Trees - scattered		
Trees - sparse		

In order to create a mapping product that differentiated riparian versus non-riparian zones within the DCLD land cover classes, the SRTM derived blue line network was buffered to a distance of 150 m. The coverage from the buffered blue line network was then used to partition a classification process using the object based image analysis software, eCognition. The new simplified class structure with the riparian and non

riparian zones. Figure 3.1 and Figure 3.2 show the updated land cover maps for the Flinders and Gilbert catchments.

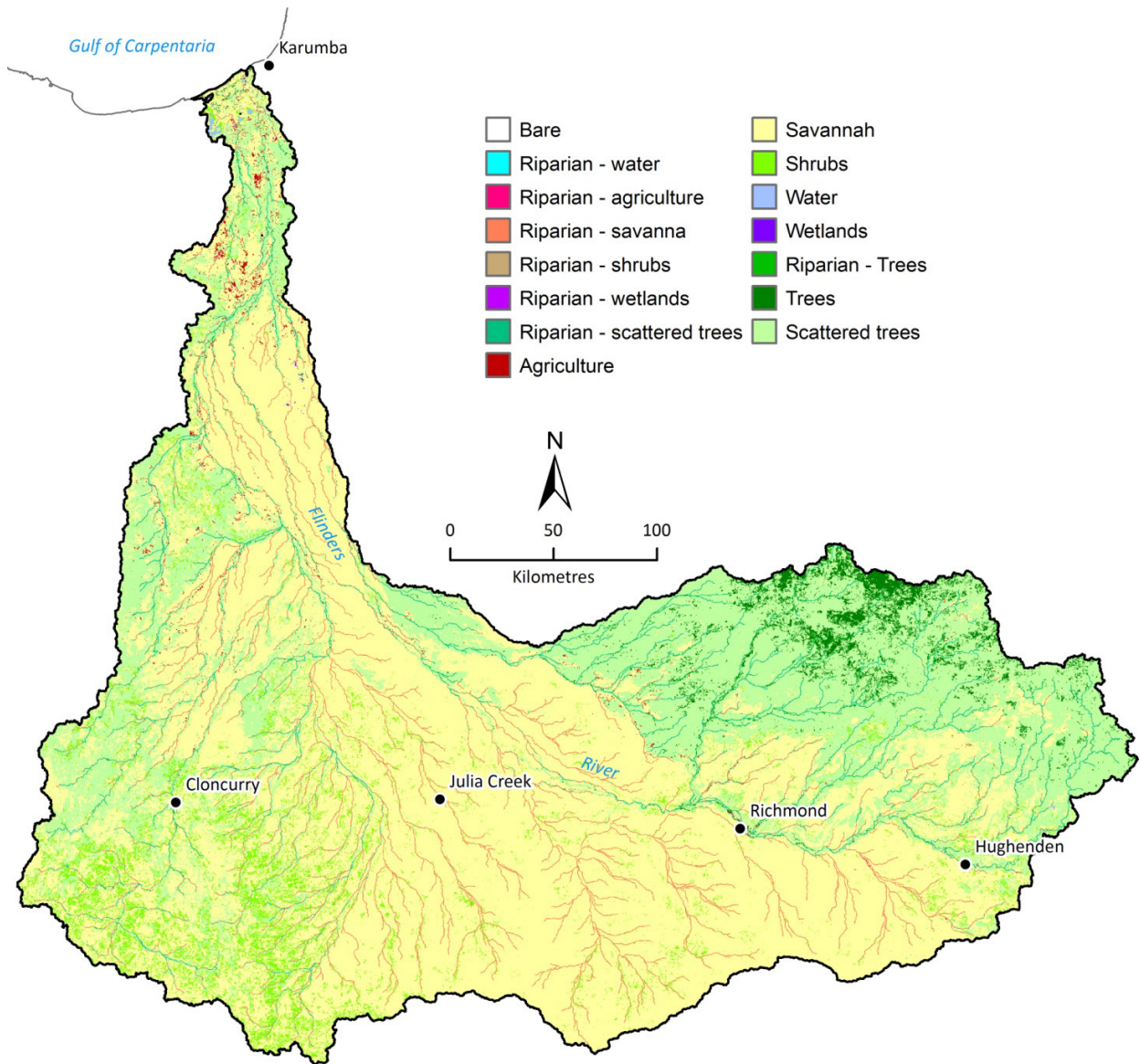


Figure 3.1 Land cover map of the Flinders catchment with a simplified class structure separating riparian and non riparian zones

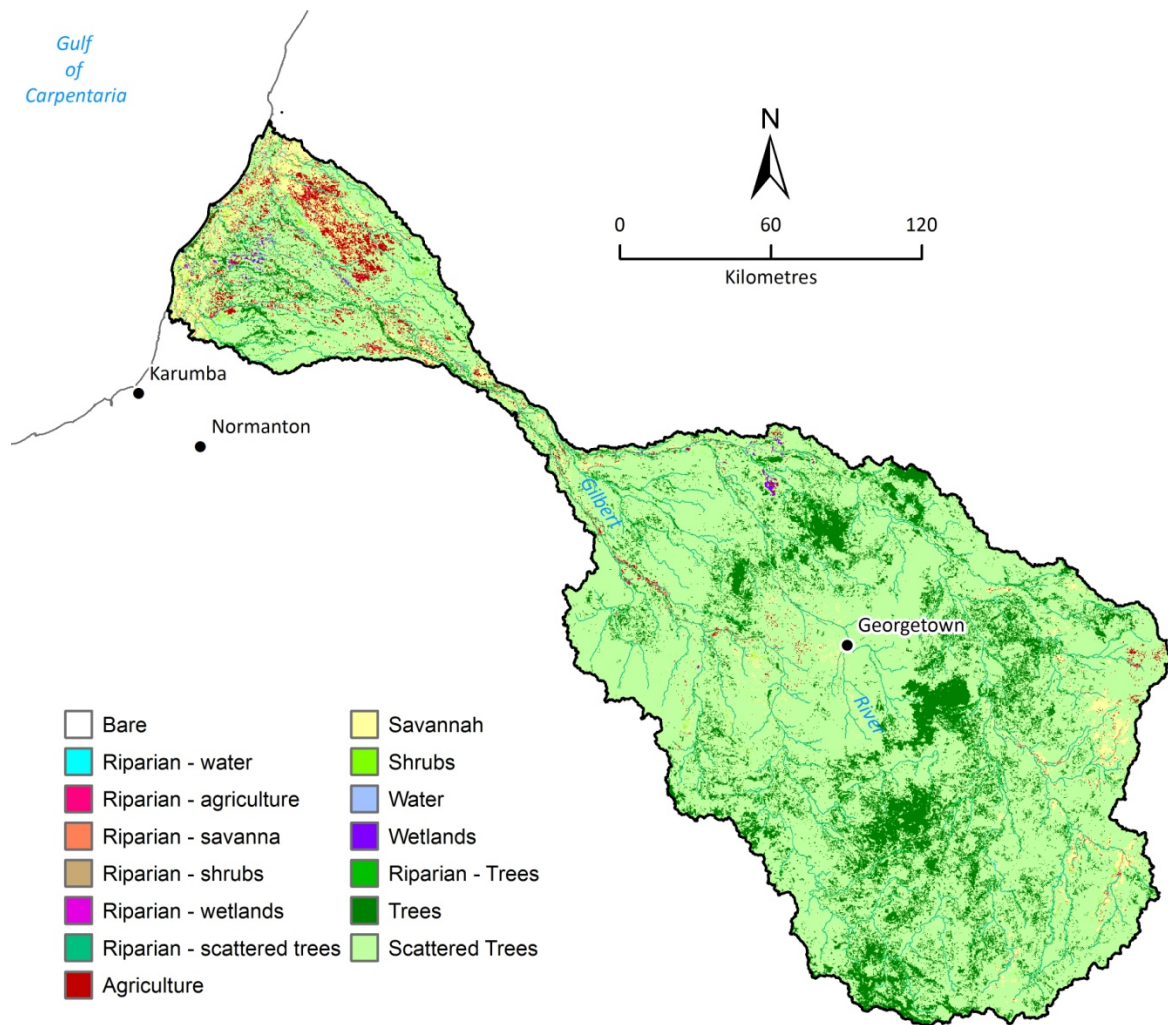


Figure 3.2 Land cover map of the Gilbert catchment with a simplified class structure separating riparian and non riparian zones

The updated landcover maps of the two catchments were resampled to the modelling resolution of the two-dimensional hydrodynamic model to estimate Manning’s roughness coefficient (n) to represent the hydraulic roughness of the land surface to the propagating flood wave. Initial roughness coefficients were estimated based on published literature (e.g. Arcement and Schneider, 1989; Land and Water Australia, 2009) and then refined as part of calibration process (Table 3.2).

Table 3.2 Manning’s roughness coefficients for different land cover types

LAND COVER TYPE	MANNING’S ROUGHNESS COEFFICIENT
Bare areas	0.060
Open water	0.025
Agriculture	0.065
Wetlands	0.040
Savannah	0.080
Shrubs	0.070
Trees	0.090
Scattered trees	0.090

3.3.3 STREAM NETWORK AND CROSS-SECTIONS

The stream network was derived from the projected SRTM and cross-checked with the watercourses lines in the topographic mapping “Hydrography feature dataset” from Australian Hydrological Geospatial Fabric (AHGF), a specialised Geographic Information System (BoM, 2012). The SRTM derived network agreed with the topographic mapping for the most part but some correction to flow direction was needed in the low lying flat areas where there is a lot of river braiding to ensure the DEM derived stream lines for main rivers followed the channel path depicted in the topographic mapping. A visual assessment of Google Earth Pro imagery was used to identify the significant drainage lines in the landscape and select a subset of “major” rivers from the DEM derived network to be used in the analysis. Cross-section of each reach of a river network needs to be defined in one-dimensional hydrodynamic modelling. Cross-section data are only available at the stream gauges of the main rivers in the Flinders and Gilbert catchments. An attempt was made to derive cross-section data from 30 m SRTM DEM for different sections of the stream networks of the two catchments. By comparing the generated cross-sections from the SRTM DEM with the measured cross-sections at the gauging locations, it was found that the cross-section derived from the SRTM 30m DEM did not represent the shape of the measured cross-sections in the mid and lower part of the river networks in the Flinders and Gilbert catchments (Figure 3.3).

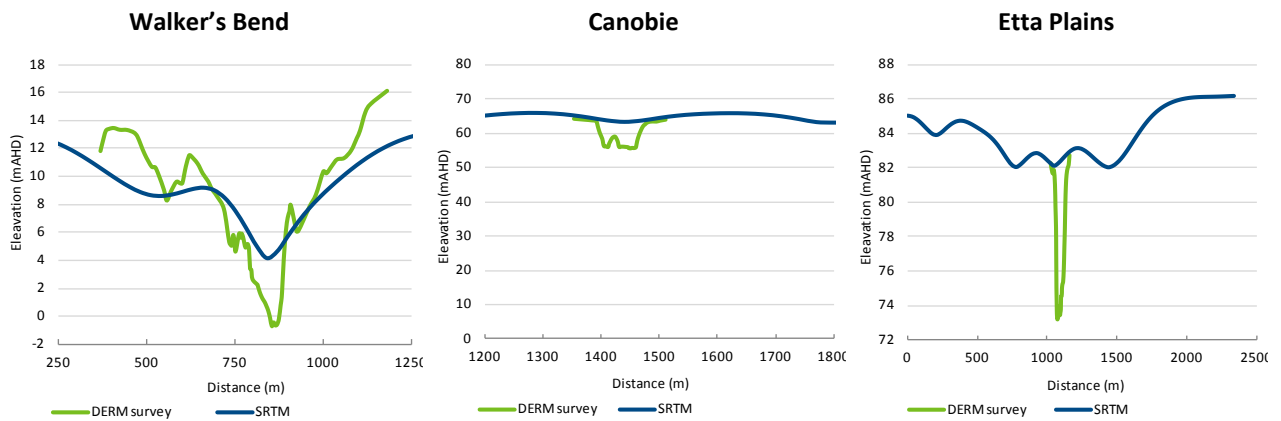
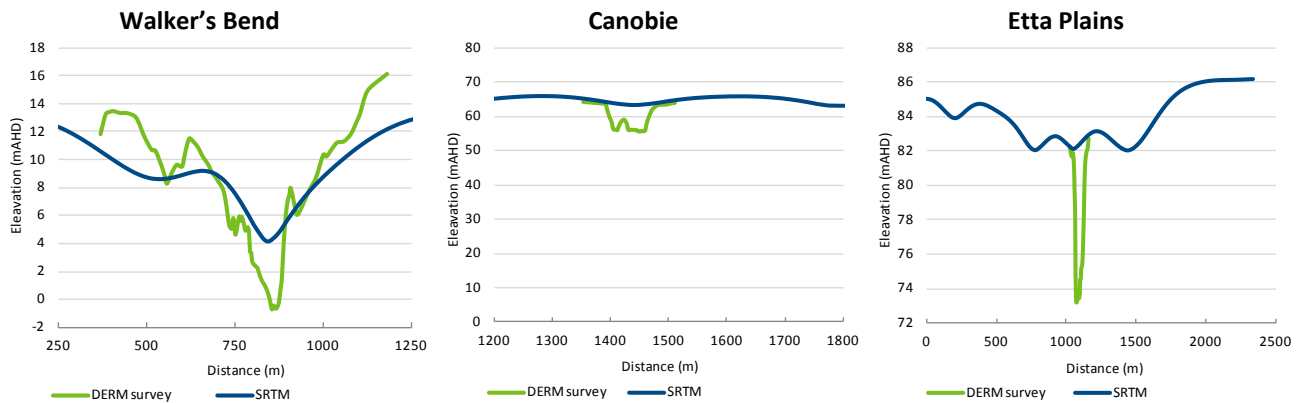


Figure 3.3



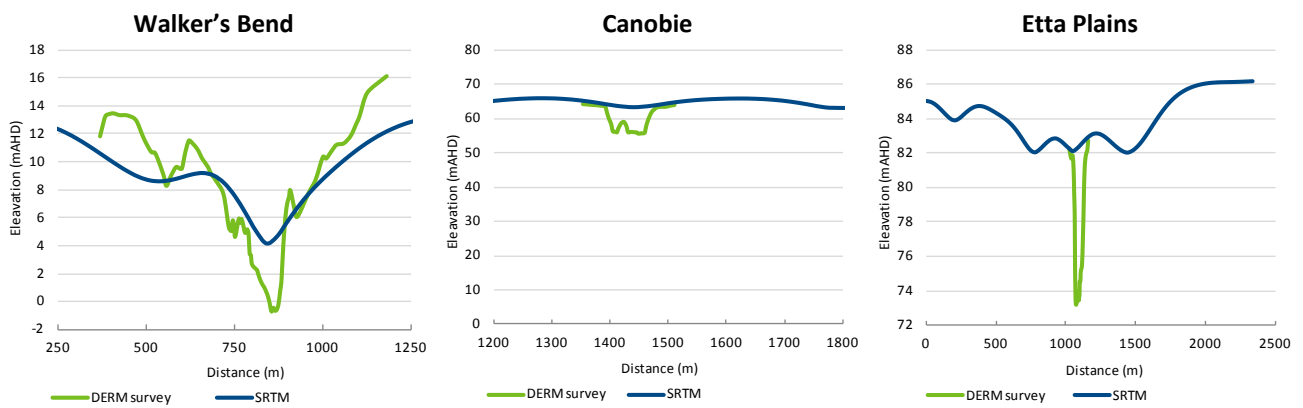


Figure 3.3 Comparison of SRTM DEM derived cross-sections with measured cross-sections at different gauging stations

A four-day field trip to the Flinders and Gilbert was undertaken by the hydrodynamic modelling team during 22-25 October 2012 to visit different parts of the catchments and survey the cross-section where possible. During this trip, the cross-sections of different rivers at 56 locations (that were accessible by roads) were measured (mostly the width and depths at few locations along the cross-section). For example, Figure 3.4 shows photographs of two sites at the Flinders and Gilbert Rivers respectively, where cross-section measurements were undertaken. The list of all measurement sites is presented in Appendix B . These data were used to update the cross-sections derived from SRTM DEM for different sections of the river networks of the two catchments for one-dimensional hydrodynamic modelling.



Figure 3.4 Two sites of rivers where cross-sections were measured during the field trip

3.3.4 STAGE HEIGHT AND STREAMFLOW DATA

Water level and streamflow data were used both as boundary conditions in the one- and two-dimensional hydrodynamic models as well as for their calibration and validation. Figure 3.5 shows the names, identification numbers (IDs) and locations of the gauging stations in the Flinders catchment. There were a total of 26 stations, all stations except one (915203A) were open between 1968 and 1972. Ten stations are currently open (Table 3.3).

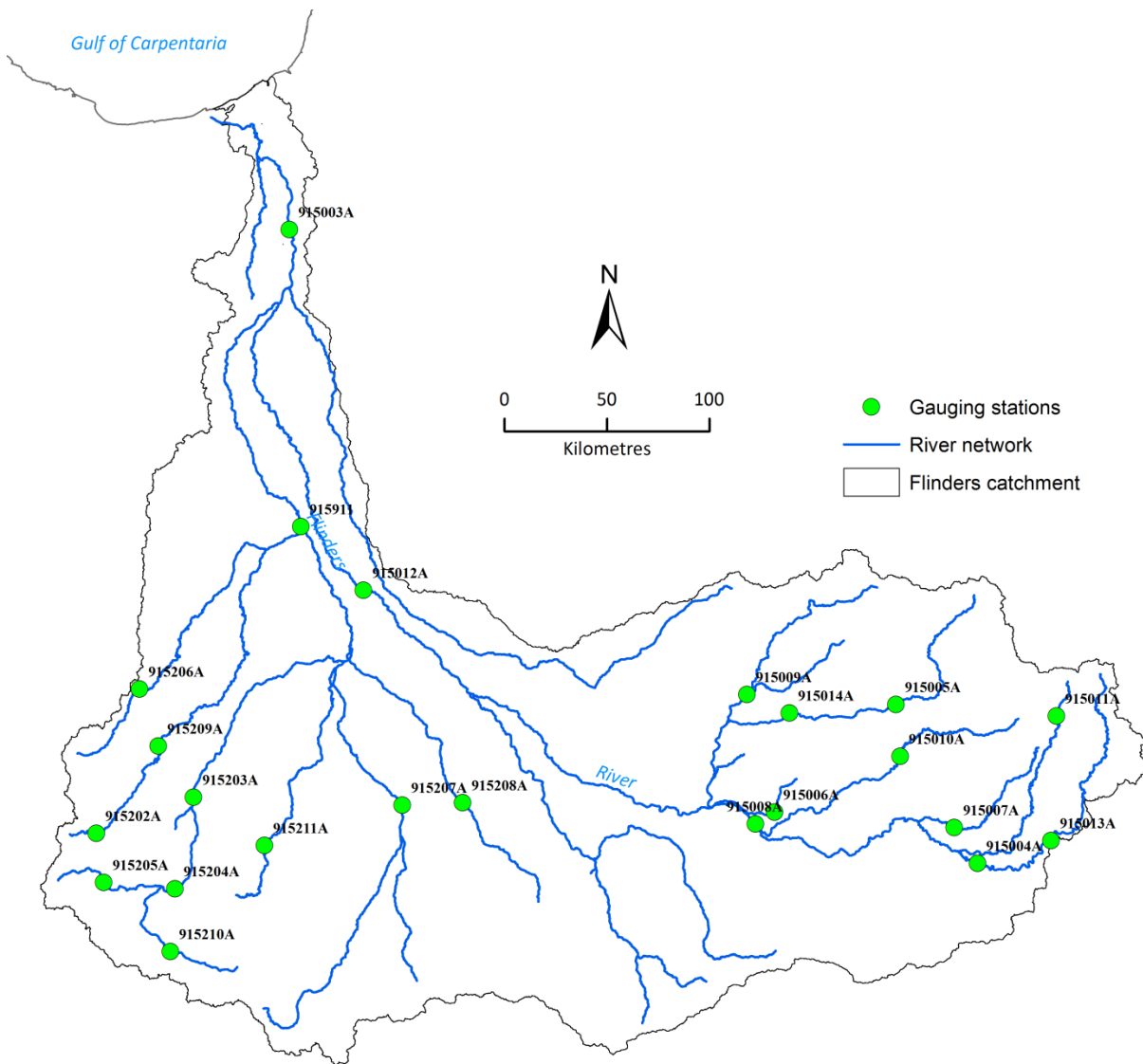


Figure 3.5 Map showing the locations of the stage height gauging stations in the Flinders catchment

Table 3.3 List of the gauging stations in the Flinders catchments and the current status

GAUGE ID	GAUGE NAME	CATCHMENT AREA (KM ²)	PERIOD OF RECORD	CURRENT STATUS
915003A	Flinders River at Walker's Bend	106,300	1969 ~	Open
915008A	Flinders River at Richmond	17,380	1971 ~	Open
915011A	Porcupine Creek at Mt Emu Plains	540	1971 ~	Open
915012A	Flinders River at Etta Plains	46,130	1972 ~	Open
915015A	Flinders River at Glendower Crossing	2,146	2012 ~	Open
915203B	Cloncurry River at Cloncurry	5,859	1994 ~	Open
915206A	Dugald River at Railway Crossing	660	1969 ~	Open
915208A	Julia Creek at Julia Creek	1,353	1970 ~	Open
915211A	Williams River at Landsborough Highway	415	1970 ~	Open
915212A	Cloncurry River at Canobie	41,220	1972 ~	Open

915001A	Mitchell Grass Catchment at Richmond	6	1968 - 1991	Closed
915004A	Flinders River at Hughenden	2,519	1969 - 1988	Closed
915005A	Stawell River at Thirty Mile Hut	2,274	1971 - 1988	Closed
915006A	Mountain Creek at Revenue Downs	203	1970 - 1988	Closed
915007A	Betts Gorge Creek at Alstonvale	1,077	1969 - 1988	Closed
915009A	Woolgar River at Patience Creek	3,391	1971 - 1988	Closed
915010A	Dutton River at Perisher	1,458	1971 - 1988	Closed
915013A	Flinders River at Glendower	1,958	1972 - 2011	Closed
915014A	Stawell River at Walker's Park	3,852	1972 - 1988	Closed
915202A	Corella River at Lake Corella	331	1973 - 1983	Closed
915203A	Cloncurry River at Cloncurry	5,975	1968 - 1994	Closed
915204A	Cloncurry River at Damsite	4240	1968 - 2001	Closed
915205A	Malbon River at Black Gorge	425	1971 - 1988	Closed
915207A	Gilliat River at Gilliat	6,073	1969 - 1988	Closed
915209A	Corella River at Main Road	1,587	1971 - 1988	Closed
915210A	Cloncurry River at Agate Downs	1,089	1971 - 1988	Closed

In the Gilbert catchment, there are a total of 29 stage height gauging stations (Figure 3.6), eight of which are currently open. Table 3.3 lists all the stations and period of data record available.

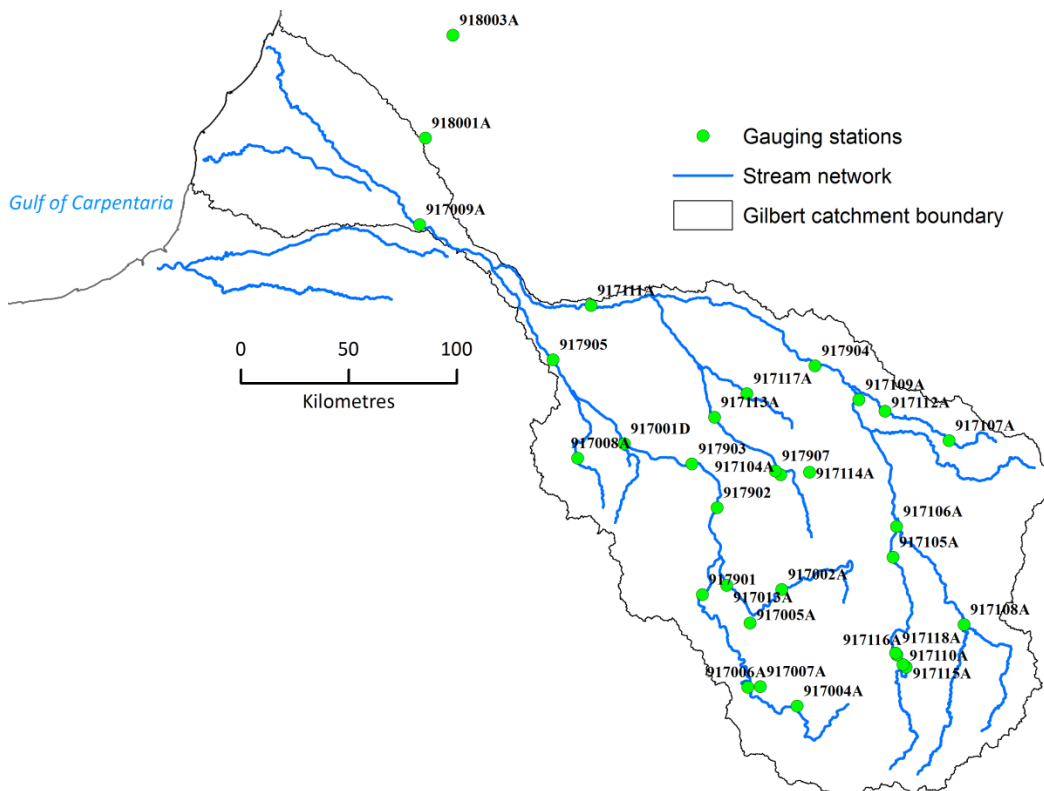


Figure 3.6 Map showing the locations of the stage height gauging stations in the Gilbert catchment

Table 3.4 List of the gauging stations in the Flinders catchments and the current status

GAUGE ID	GAUGE NAME	CATCHMENT AREA (KM ²)	PERIOD OF RECORD	CURRENT STATUS
917001D	Gilbert River at Rockfields	10,990	1967 ~	Open
917104A	Etheridge River at Roseglen	867	1967 ~	Open
917106A	Einasleigh River at Einasleigh	276	1966 ~	Open
917107A	Elizabeth Creek at Mount Surprise	651	1968 ~	Open
917114A	Routh Creek at Beef Road	81	1972 ~	Open
917115A	Copperfield River at Spanner Waterhole	1,199	1983 ~	Open
917116A	Copperfield River at Kidston Dam Headwater	1,250	1985 ~	Open
917118A	Copperfield River at Kidston Dam Tailwater	1,252	1984 ~	Open
917002A	Robertson River at Robin Hood	1,019	1966 - 1988	Closed
917003A	Gilbert River at Green Hills	8,339	1972 - 1973	Closed
917004A	Gilbert River at Gilberton	1,892	1968 - 1988	Closed
917005A	Agate Creek at Cave Creek Junction	218	1969 - 1988	Closed
917006A	Gilbert River at Percy Junction	3,317	1970 - 1988	Closed
917007A	Percy River at Ortana	526	1969 - 1988	Closed
917008A	Little River at Inorunie	436	1971 - 1993	Closed
917009A	Gilbert River at Miranda Downs	38,620	1971 - 1989	Closed
917011A	Smithburne River at Lotus Vale	195	1970 - 1973	Closed
917013A	Robertson River at North Head	1,888	1972 - 1988	Closed
917101A	Etheridge River at Georgetown	1,518	1949 - 1956	Closed
917102A	Einasleigh River at Carpentaria Downs	3,225	1949 - 1957	Closed
917103A	Copperfield River at Narrawa No 1	3,055	1953 - 1961	Closed
917105A	Copperfield River at Narrawa No 2	2,910	1966 - 1988	Closed
917108A	Mckinnons Creek at Possum Pad	1,572	1968 - 1988	Closed
917109A	Einasleigh River at Cowana Lake	12,150	1968 - 1988	Closed
917110A	Copperfield River at Middle Creek Gap	1,212	1969 - 1988	Closed
917111A	Einasleigh River at Minnies Dip	21,280	1971 - 1988	Closed
917112A	Elizabeth Creek at Cabana	1,288	1972 - 1988	Closed
917113A	Etheridge River at Huonfels	2,358	1972 - 1988	Closed
917117A	Camp Oven Creek at Maureen	28	1977 - 1988	Closed

The quality of the gauged data and the uncertainty associated with gauging stations are detailed in the companion report of the River System Modelling Activity (Lerat et al., 2013).

3.3.5 TIDE DATA

Tidal data are used in the one- and two-dimensional hydrodynamic models as the boundary conditions at the downstream end of streams and floodplains that are connected to estuary or sea. Tide data for Queensland are owned by the Tidal Unit of the Maritime Safety Queensland, Department of Transport and Main Roads (DTMR). Data of 10-minute time interval were obtained for two stations, Karumba and Weipa.

Based on proximity to model seaside boundaries of Flinders and Gilbert, tide data at Karumba was used as the downstream boundary condition.

3.3.6 SURFACE RUNOFF

Runoff generated by Sacramento rainfall-runoff model (Burnash et al., 1973) was used to compute sub-catchment runoff within the modelling domain and at model boundaries where river system model data were unavailable. Gridded runoff simulation was performed between 1 July 1890 and 30 June 2011 for 0.05° (~ 5 km) resolution grids using the daily SILO gridded climate data (Jeffrey et al., 2001). Morton areal wet potential evaporation was used to compute potential evaporation. The calibrated parameters from the most downstream gauge (Walker's Bend; 915003A) were used for gridded simulation of runoff for the hydrodynamic modelling domain of the Flinders catchment. For the hydrodynamic modelling domain of the Gilbert catchment, the calibrated parameters from the gauged catchment of Mentana Creek at Mentana Yards (918002A) were used for runoff simulation.

The two-dimensional hydrodynamic modelling domains of the Flinders and Gilbert catchments were divided into 196 and 90 subcatchments as shown in Figure 3.7 and Figure 3.8, respectively. The simulated gridded runoff was averaged to subcatchment runoff by assigning SILO cells to the subcatchments based on the intersecting cells. Averaged runoff was incorporated into the hydrodynamic model as a point source at the outlet of each sub-catchment. Sub-catchment boundaries and pour points were generated using 30 m grid SRTM data from arbitrarily located pour points, typically located at the stream junctions/inflow to main rivers. Runoff from upper catchments were obtained from stream gauge records (where available) and added as inflow boundary to the model.

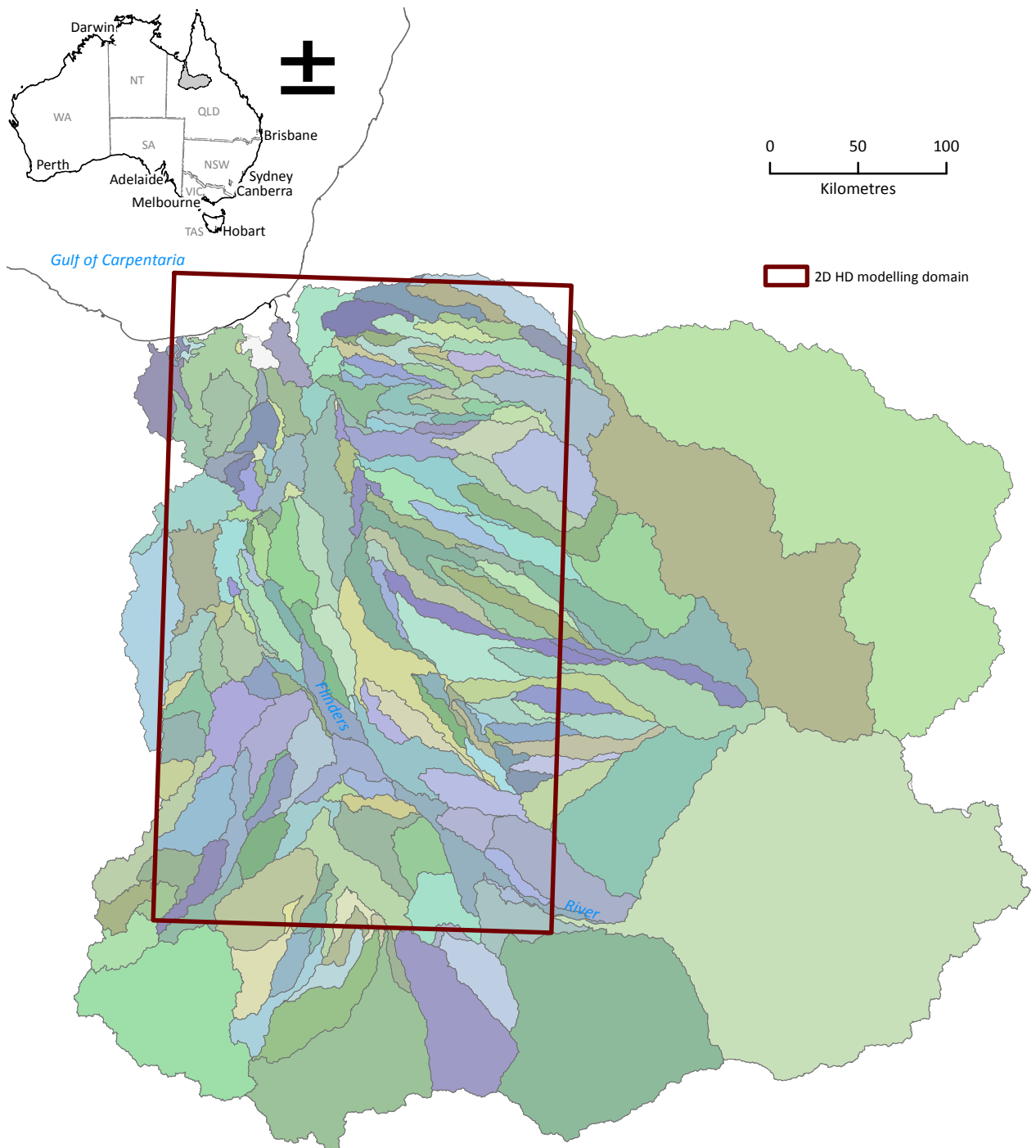


Figure 3.7 Maps of the Sub-catchments used in two-dimensional hydrodynamic modelling in the Flinders Catchment

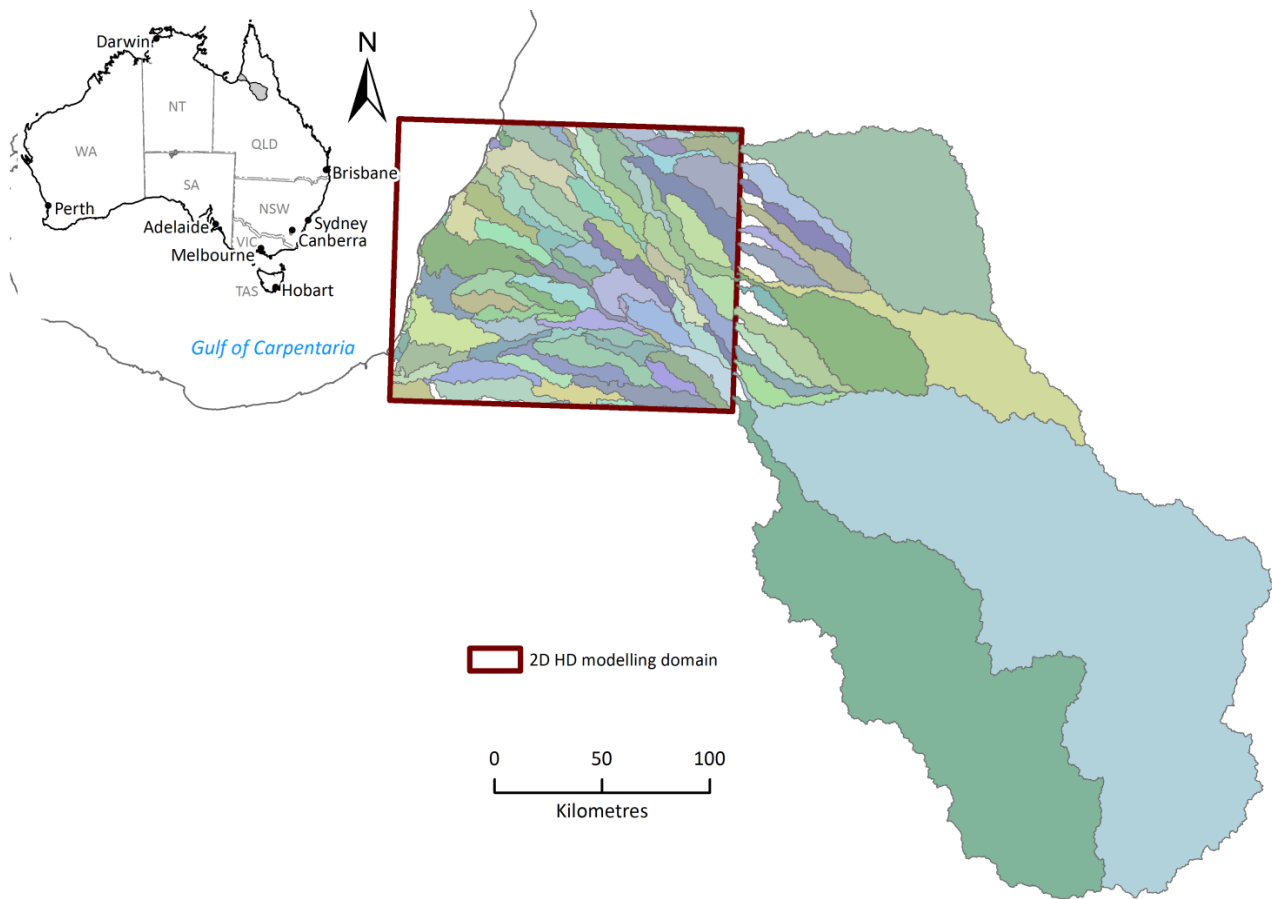


Figure 3.8 Maps of the Sub-catchments used in two-dimensional hydrodynamic modelling in the Gilbert Catchment

For one-dimensional hydrodynamic modelling, ungauged runoff for different modelling reaches was obtained from the locally calibrated Sacramento Rainfall-runoff model. A residual calibration approach was undertaken for local calibration of the Sacramento rainfall-runoff model for each reach as part of the River System Modelling Activity (see companion technical report on river system modelling; Lerat et al., 2013).

3.3.7 QUESTIONNAIRE SURVEY FOR FLOOD INUNDATION

Records of historical flood events and their inundation characteristics (e.g. depths, duration, extents) are required for proper calibration and validation of a hydrodynamic model. Ground-based data for historical flood events in the Flinders and Gilbert Catchments are very limited. A questionnaire survey was conducted to collect additional information on historical floods in the modelling areas for validation of the two-dimensional hydrodynamic model. Owners of different homesteads in the floodplains were approached by telephone for the survey and they were asked for the following information related to historical and recent floods (including some of the major historical floods in 1974, 2001 and 2009).

- Inundation extent (how far from river)
- Flood depth (incl. location)
- Flood duration
- Flow velocity (did the water move fast or slow?)
- Roads/bridges affected? For how long?

The information gathered from the survey for the Gilbert Catchment was used in conjunction with the flood maps generated from the remote-sensing imagery was used in the calibration and validation of the hydrodynamic model in the Gilbert floodplain.

3.4 Configuration of two-dimensional hydrodynamic model

3.4.1 FLINDERS AND GILBERT TWO-DIMENSIONAL HYDRODYNAMIC MODELLING

The hydrodynamic modelling domains for the Flinders and Gilbert catchments are shown in Figure 3.9. The MIKE21 two-dimensional hydrodynamic model was configured for the modelling domain in the Flinders catchment that included mid and lower parts of the Flinders and Norman catchments covering the floodplains of the two catchments, which are connected during floods with floodwater cross over from the Norman catchment to the Flinders. The spatial resolution of the model was 150 m and the modelling domain consisted of approximately 3.7 million grids (1509 × 2427) of 150 m resolution. There are 11 upstream inflow boundary points contributing runoff to the modelling domain from the upper catchment. Gauged streamflow data were available at three of these boundary points (Cloncurry River at Cloncurry, 915203B; Julia Creek at Julia Creek, 915208A; and Dugald River at Railway crossing, 915206A), which were used as the boundary condition for these three gauges. The missing data points in the gauged records were filled in by the simulated flow by the river system model (see companion technical report on river modelling calibration Lerat et al., 2013). For rest of the boundary points, simulated runoff time series were used.

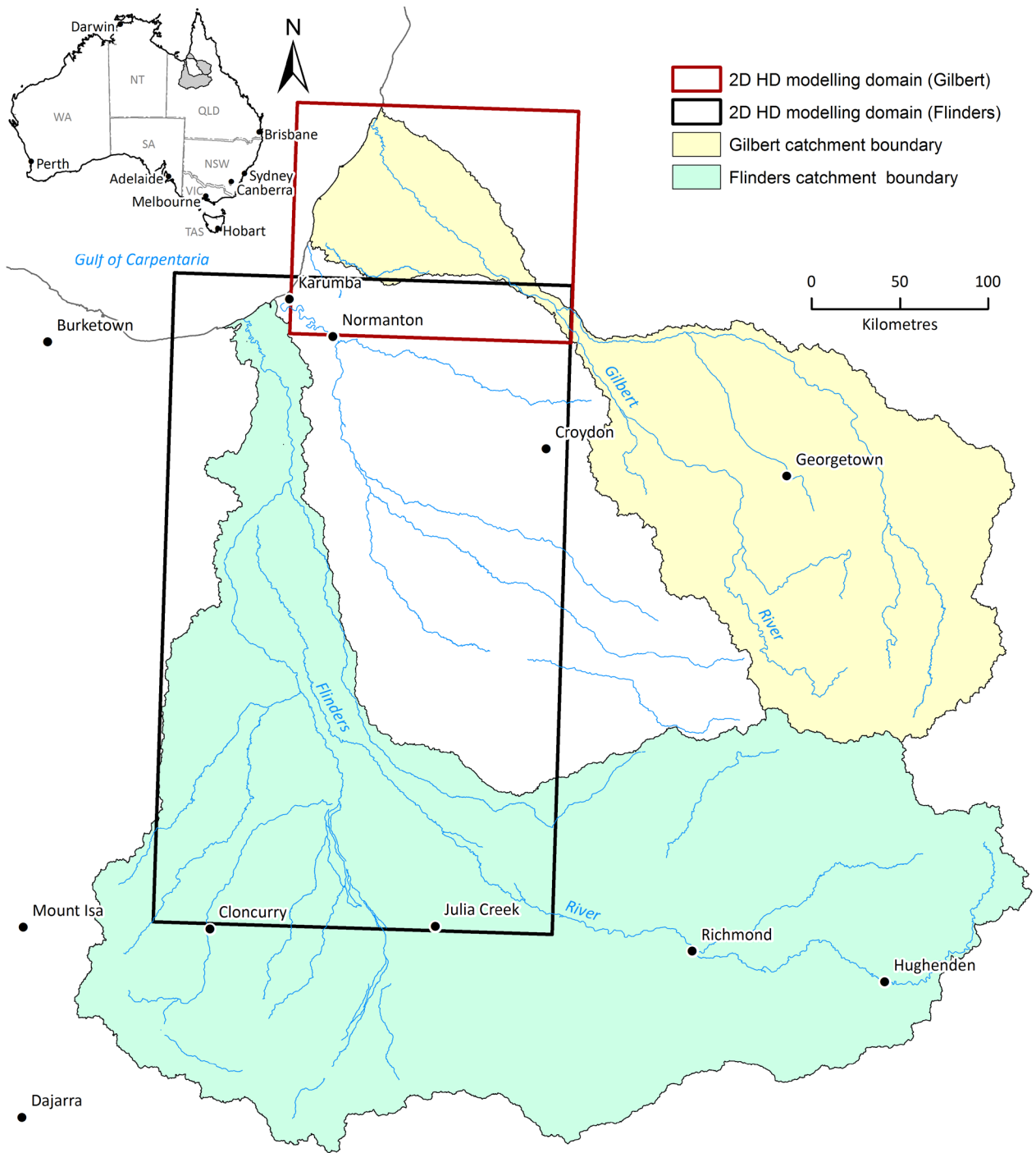


Figure 3.9 Hydrodynamic modelling domains for flood inundation modelling in the Flinders and Gilbert catchment

MIKE21 model was configured for the modelling domain of the Gilbert catchment that included the lower part of the Gilbert catchment and a small part of the Norman catchment, where flood water from Gilbert crosses over to the Norman. The spatial resolution of the model was 90 m and the modelling domain consists of approximately 2.58 million 90 m resolution grids (1782 × 1447). There was only one upstream boundary point where streamflow from upper Gilbert Catchment enters to the Gilbert floodplain. As there was no streamflow gauging station at this model boundary, simulated streamflow data from the Gilbert Source river system model was used (see companion technical report on river model calibration; Lerat et al., 2013). There were also three inflows from the Staaten catchment to the lower Gilbert floodplain. For these boundaries, simulated runoff time series were used. The observed tidal data at Karumba was used to define the boundary conditions at the grids located along the coastline at the Gulf of Carpentaria.

3.5 Calibration and post-audit of two-dimensional hydrodynamic models

Hydrodynamic models, like any other mathematical models, need to be calibrated to fine tune some of the model parameters prior to their use for simulation. Traditionally flood models are calibrated by comparing in-stream water heights (commonly gauge records) and floodplain inundation (commonly water marks on trees, buildings and electric poles). However, for the Flinders and Gilbert catchments, the available data and information on historical flood were very limited except for the gauged stage heights at three gauges in the floodplains of the Flinders. There were no gauged data available within the modelling domain of the Gilbert catchment. The flood maps derived from MODIS satellite imagery provided one means of evaluating the models performances at predicting temporal and spatial inundation dynamics. The flood maps from the remote sensing data were used along with the gauged stage height data (where available) to calibrate the hydrodynamic model.

Based on the historical records and availability of data, several flood events over the past 12 years were selected for the calibration and validation of the two-dimensional model. Table 3.5 and Table 3.6 present the events selected for calibration, validation and simulation of the two-dimensional hydrodynamic model at the Flinders and Gilbert catchments, respectively. Due to the long computational time, the two-dimensional model was run to cover the rising and falling limbs of the flood hydrographs.

Flood events in the Flinders catchment were selected on the basis of: i) the availability of the observed stage height data at the three gauging stations within the two-dimensional hydrodynamic modelling domain of the catchment (Cloncurry River at Canobie, 915212A; Flinders River at Etta Plains, 915012A and Flinders River at Walker’s Bend, 915003A); ii) the availability of cloud free MODIS and Landsat data; and iii) the magnitudes of the flood event. In the Flinders catchment two events were used for calibrating the model and two events were used for validating the model (Table 3.5). Flood maps derived from MODIS imagery were used to compare spatial metrics of inundation area across the floodplain. In addition, gauged water heights at key locations (e.g. Canobie, Etta Plains and Walker’s Bend) were used.

A similar set of criteria to the Flinders catchment was used to select flood events for calibration and validation in the Gilbert catchment. However, the absence of stage height data in the model domain mean the model was only calibrated using satellite imagery. Unfortunately the quality of the satellite imagery was poor in the Gilbert catchment with the majority of the MODIS and Landsat imagery during the flood events obscured by cloud. Only two events were found to be suitable and the model was calibrated to one and validated to the other (Table 3.6).

Table 3.5 Selected flood events for Flinders two-dimensional HD model calibration/validation

START DATE	END DATE	DURATION (DAYS)	PEAK FLOW AT WALKERS BEND (M ³ /S)	DATE OF PEAK FLOW	RANKED SIZE OF THE EVENT	USED FOR
27/12/2000	26/01/2001	30	3,612	31/12/2000	7	Validation/simulation
18/01/2004	31/01/2004	14	3,570	25/01/2004	9	Simulation
20/03/2006	23/04/2006	34	3,045	28/03/2006	12	Validation
10/01/2008	31/01/2008	22	3,416	18/01/2008	10	Simulation
21/01/2009	24/02/2009	35	5,883	17/02/2009	2	Calibration/simulation
09/03/2011	12/04/2011	34	2,646	23/03/2011	14	Calibration/simulation

Table 3.6 selected flood events for Gilbert two-dimensional HD model calibration/validation

START DATE	END DATE	DURATION (DAYS)	PEAK FLOW AT ROCKFIELDS (M ³ /S)	DATE OF PEAK FLOW	RANKED SIZE OF THE EVENT	USED FOR
29/12/2000	10/01/2001	12	1978	1/01/2001	11	Simulation
10/01/2008	22/01/2008	12	1,954	15/01/2008	7	Simulation
09/01/2009	31/01/2009	22	6,389	27/01/2009	2	Calibration/simulation
09/03/2011	29/03/2011	20	2,912	11/03/2011	3	Validation/ simulation

The computational time step was derived after satisfying numerical stability criteria for the flood flow of different magnitudes. The time step varied for different events due to the varied magnitude of streamflow of the flood events. The shortest time step was three seconds and six seconds for the hydrodynamic models of the Flinders and Gilbert catchments, respectively. These were for the 2009 flood events, which was the largest streamflow event used for calibration of each of the models and the second largest flood event on the record. The Flinders model took about 15 days of computer time to simulate the 2009 flood event, which lasted 54 days. At the boundaries, daily time step stage heights and discharges were specified. The model uses an inbuilt interpolation technique to derive streamflow variables at each computational time step. An initial water level map was generated by running the model on dry land for a constant inflow. Initial discharges at all computational grids were specified as zero. To avoid any effects of initial conditions, simulations for the first six hours were excluded from analyses and interpretations of the results. Model outputs include water surface elevation, depth, velocity and flow flux for each computational grid. Simulated outputs can be saved at the computational time step or a desired time step, which is a multiple of the computational time step (6-hour time step was used here).

During the manual calibration process, floodplain topography was modified at locations having steep land slopes to ensure model stability. A slight adjustment was also made at the interface between river and floodplain. Grids that represent streams were carefully checked and manually edited to ensure continuous stream channel.

The final calibration was undertaken by fine tuning the Manning’s roughness coefficients for different landcover types to attain i) an accurate reproduction of the MODIS imagery; and then ii) a good match between observed and simulated water depths and the observed and simulated time of peak arrival at different locations on the floodplain. Surface roughness coefficients were varied iteratively for the major land covers (e.g. Savanna) within the recommended range (Table 3.2). Our first effort was to reproduce the inundation area.

3.5.1 RESULTS OF CALIBRATION IN FLINDERS

Inundation Extent

Figure 3.10 presents the simulated inundation extents and the flood maps derived from MODIS imagery using the OWL algorithm with a 5% threshold for different days during the 2009 flood event in the Flinders catchment. The days were selected based on the availability of MODIS images not obscured by cloud. The 2009 flood event in the Flinders catchment had the highest number of unobstructed MODIS images. This comparison shows that the hydrodynamic model underestimated the flooded area considerably compared to the MODIS imagery. This was due to the low runoff coefficient (~0.05) used to generate local runoff by the Sacramento rainfall-runoff model on the Flinders floodplain. The runoff coefficient was adjusted using a multiplication factor of 2 to improve the simulation. Figure 3.11 illustrates the final calibrated results using the revised runoff. It can be seen that the overall pattern of the simulated inundation extent in different parts of the Flinders floodplain is similar to the MODIS flood maps. The inundation maps from the hydrodynamic model show numerous thin lines of the channelized flow paths, which don’t appear in the MODIS flood maps. This is mainly due to the resolution of the MODIS imagery, which was 500 m compared

to the 150 m resolution of the hydrodynamic model. There are some differences in the extent of the simulated flood with the MODIS flood maps on different dates on the eastern part of the catchment. For example, on 19th February 2009, the MODIS map shows discontinuity in the inundation in the middle part, which is due to the cloud cover in the area.

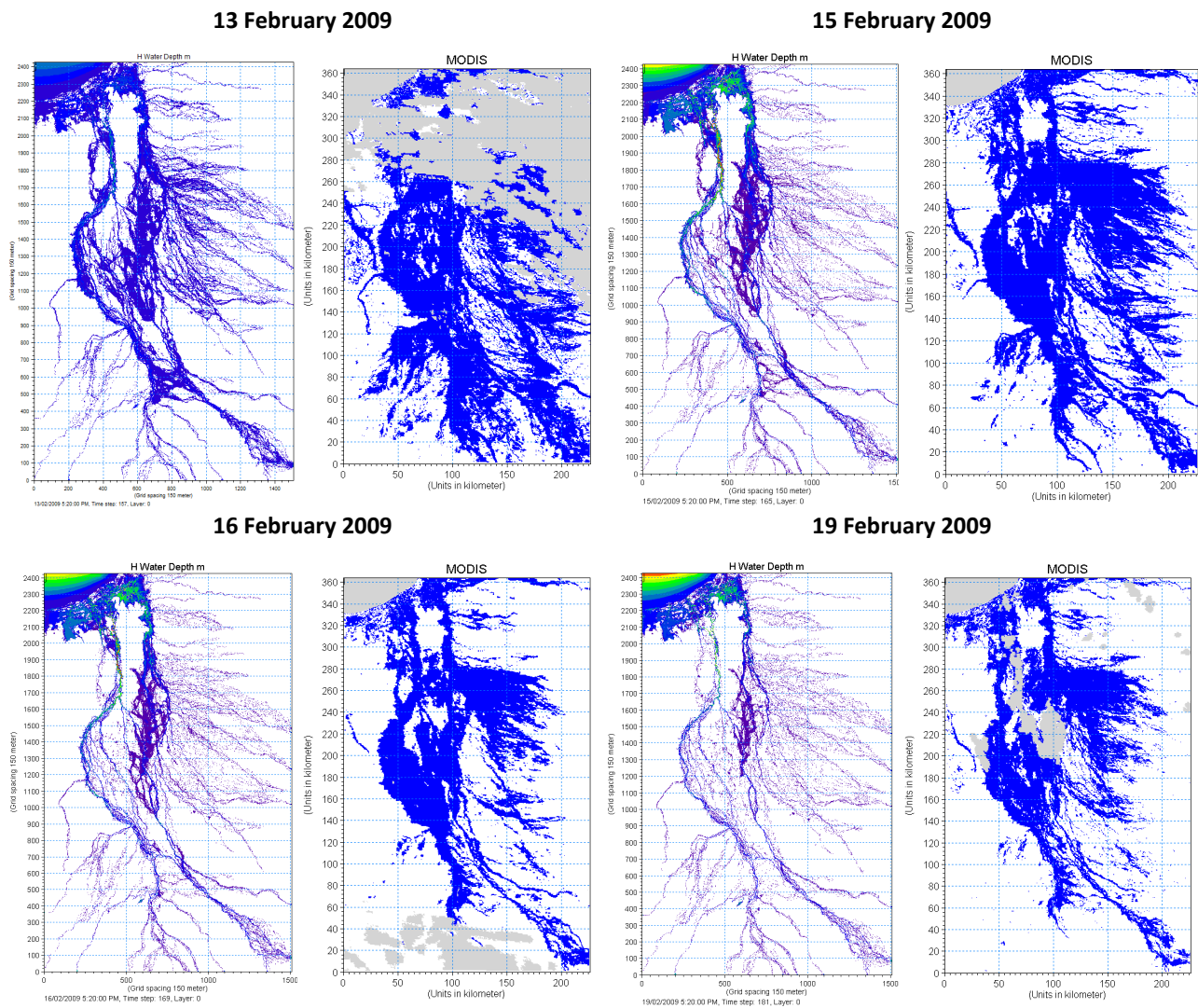
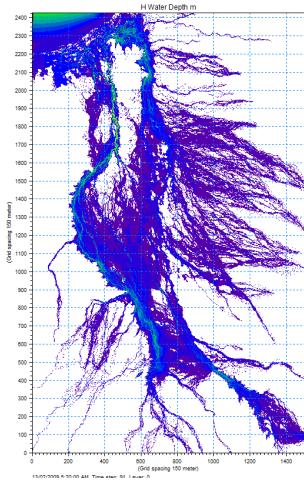
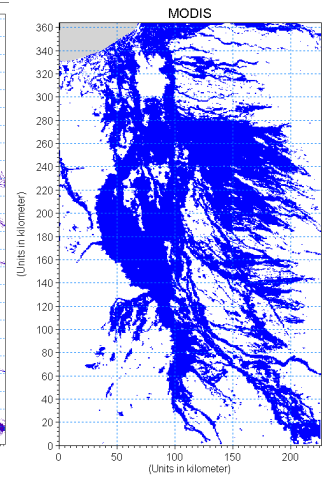
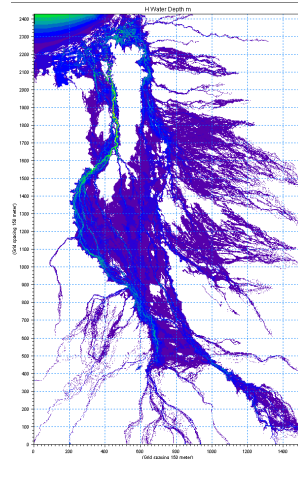
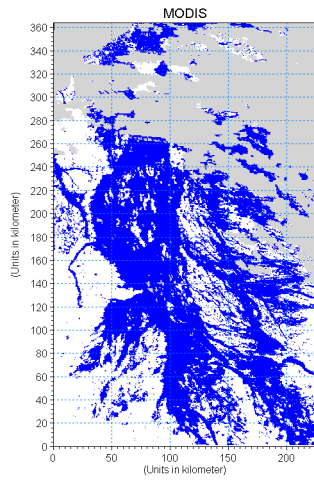


Figure 3.10 Comparison of the simulated inundation (without calibration of runoff factor) and flood maps derived from MODIS imagery with 5% threshold for different days of 2009 flood event. (Grey colour in MODIS flood map represents cloud cover)

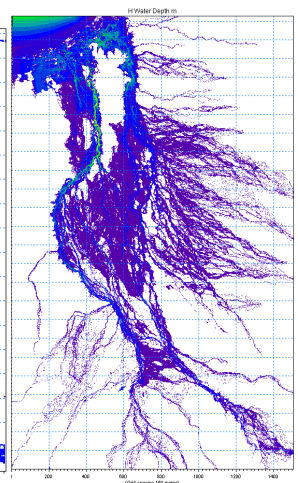
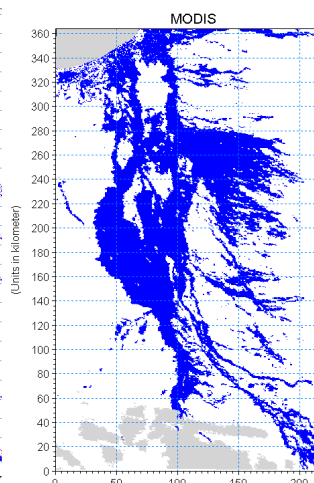
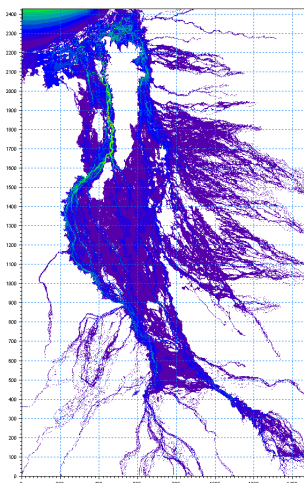
13 February 2009



15 February 2009



16 February 2009



19 February 2009

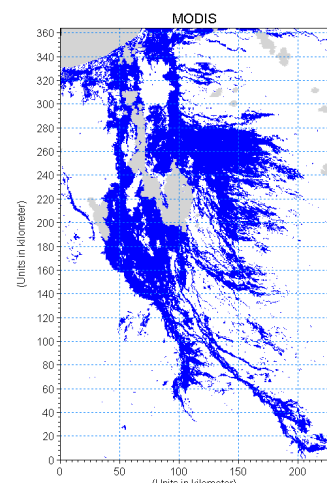


Figure 3.11 Comparison of the simulated inundation (with calibrated runoff factor) and flood maps derived from MODIS imagery with 5% threshold for different days of 2009 flood event. (Grey colour in MODIS flood map represents cloud cover)

Figure 3.12 shows the simulated inundation extents and the flood maps derived from the MODIS imagery on a limited number of days during the flood event of 2011 for which good quality MODIS data were available.

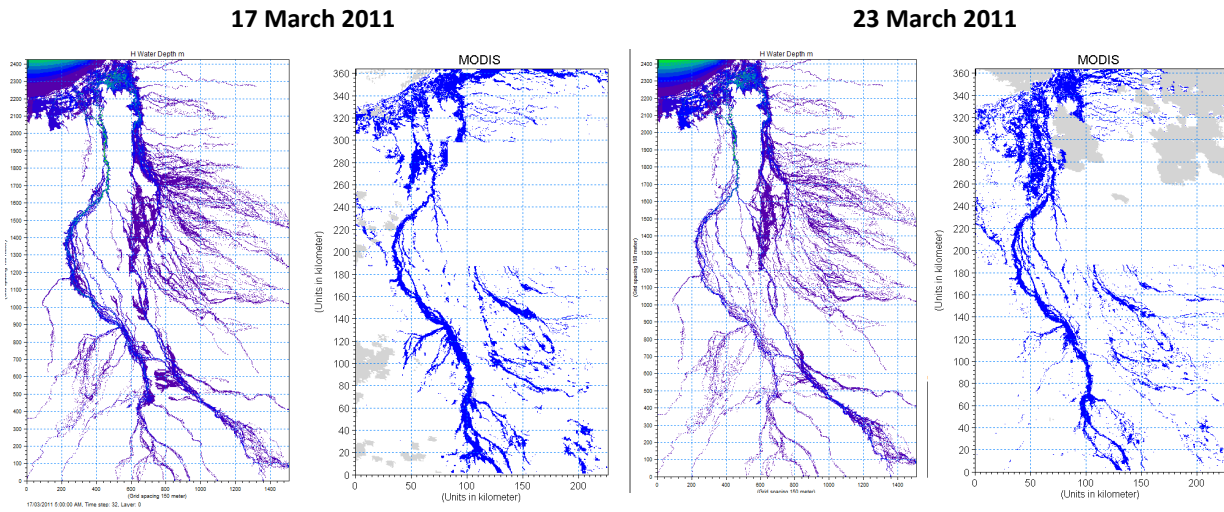


Figure 3.12 Comparison of the simulated inundation (with calibrated runoff factor) and flood maps derived from MODIS imagery with 5% threshold for different days of 2011 flood event. (Grey colour in MODIS flood map represents cloud cover)

The pattern of simulated inundation extents by the hydrodynamic model is similar to the MODIS flood maps, except that the MODIS flood maps do not identify inundation in the upper middle part of the catchment along Flinders River, which is possibly obscured by vegetation cover.

Figure 3.13 compares the total inundation areas (in terms of number of cells inundated) simulated by the hydrodynamic models with that of the MODIS flood maps of 1%, 5% and 10% thresholds on different days of the 2009 and 2011 flood events. There are significant variations in the inundation areas in the MODIS flood maps with different threshold values, with 1% threshold flood maps producing the largest area inundation area and 10% threshold maps producing the smallest inundation area. However, the differences between 5% and 10% threshold flood maps are considerably smaller than the differences using the 1% and 5% threshold maps. For the 2009 flood event, the simulated inundation areas by the hydrodynamic model are similar to 10% threshold MODIS flood maps for five out of the seven days compared. However, for the 2011 flood event, the estimated inundation areas by MODIS imagery were significantly lower than the inundation area simulated by the hydrodynamic model, which is due to the cloud covers in the MODIS imagery in 2011.

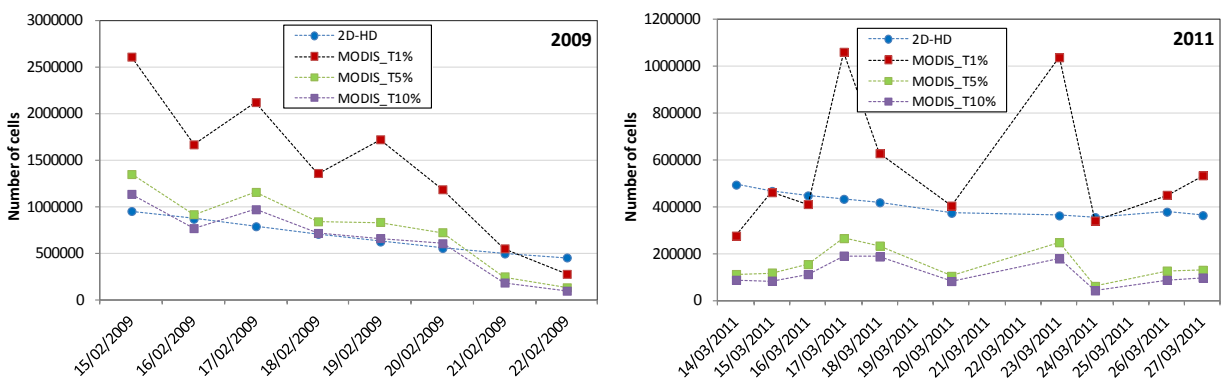


Figure 3.13 Comparison of total number of inundated cells by hydrodynamic model and in the flood maps generated from MODIS with 1%, 5% and 10% thresholds in OWL for the flood events of 2009 and 2011

Figure 3.14 shows the results of cell-to-cell comparison between the inundation maps simulated by the hydrodynamic model and the MODIS flood maps with 1%, 5% and 10% thresholds for 2009 and 2011 flood events. Although 1% threshold showed the largest areas of inundation, the cell-to-cell matching of the inundated cells between the flood maps from the hydrodynamic model and MODIS flood map of 1% threshold was lowest for the both events. The cell-cell matching of the inundation areas between the

hydrodynamic model and the MODIS flood map with 5% threshold varied between 39- 66% with an average of 54% for 2009 and varied between 45- 65% with an average of 53% for 2011. The matching of the simulated inundation area with the MODIS flood maps with 10% threshold varied between 44- 72% with average of 59% for 2009 and between 52- 72% with an average of 59% for 2011. Considering the cloud covers, difference in resolution of MODIS imagery (500m) and hydrodynamic model (150m), the cell-to-cell matching between the simulated flood maps by the hydrodynamic model and the MODIS flood maps with 5% and 10% thresholds are reasonably good for both 2009 and 2011 flood events.

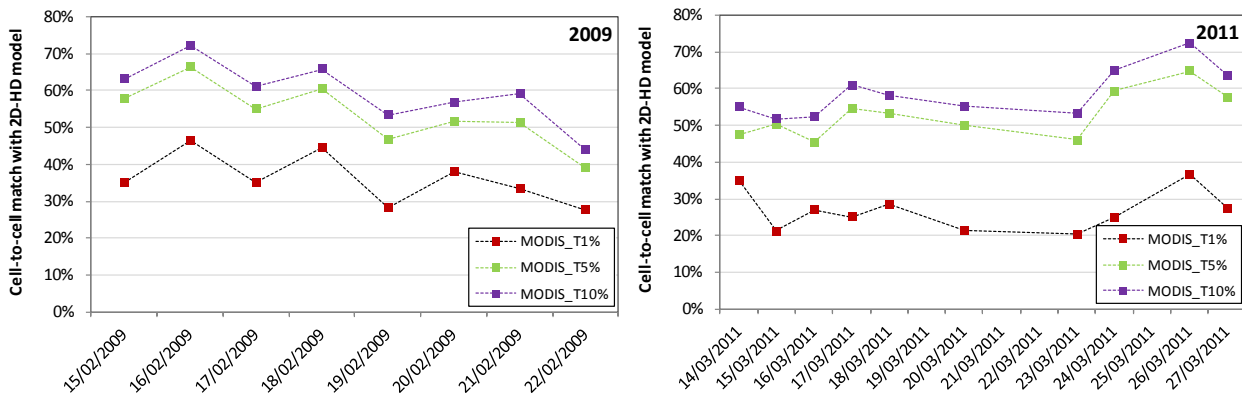


Figure 3.14 Cell-to-cell matching of inundated cells between the hydrodynamic model and the flood maps generated from MODIS with 1%, 5% and 10% thresholds in OWL for 2009 and 2011 flood events.

Stage height

Figure 3.15 compares the observed and simulated flood stage heights at Canobie, Etta Plains and Walker’s Bend for the flood events of 2009 and 2011. The results show reasonably good agreement between the observed and simulated stage heights at Canobie and Walker’s Bend for both 2009 and 2011 flood events. There are close agreements between the simulated and observed peaks. Although, the overall agreement between the simulated and observed stage heights at Etta Plain is not as good as the other gauges, the simulated peak are reasonably close to the observed peaks at Etta Plains for 2011.

The correlation coefficient (R^2) between the observed and simulated stage heights for the calibration and validation events varied between 0.40 to 0.72 and 0.45 to 0.78 at Canobie and Walker’s Bend, respectively.

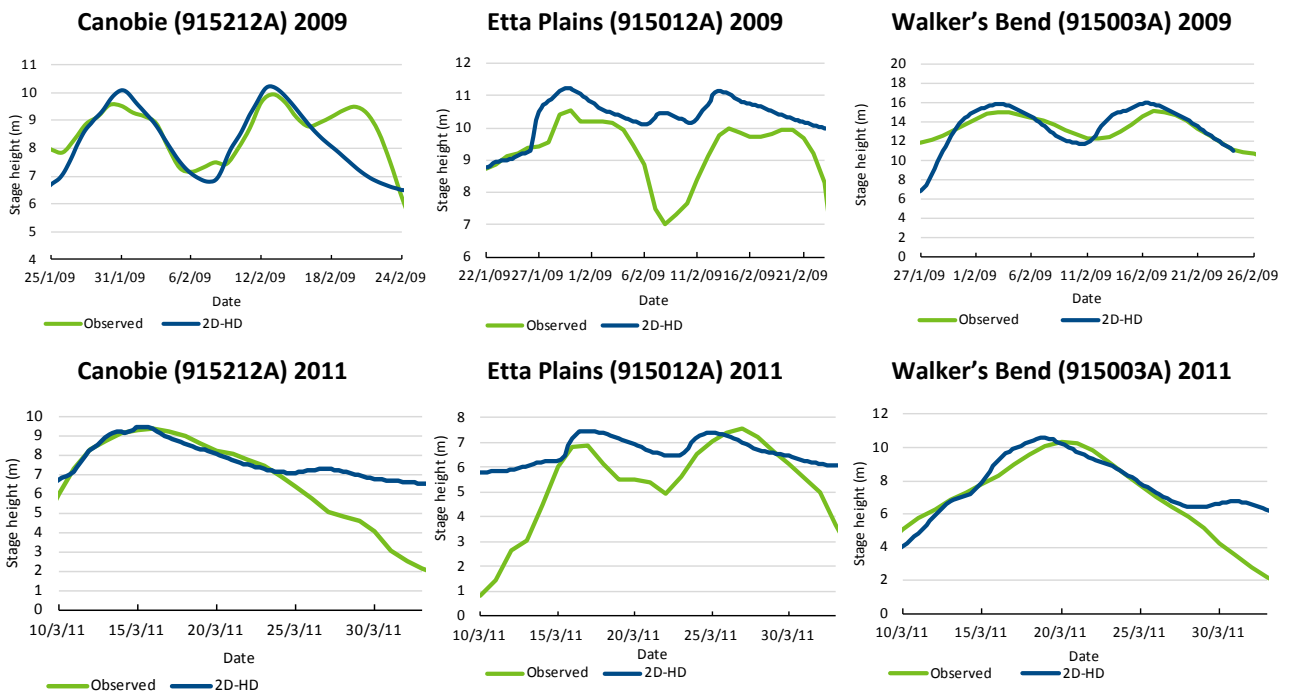


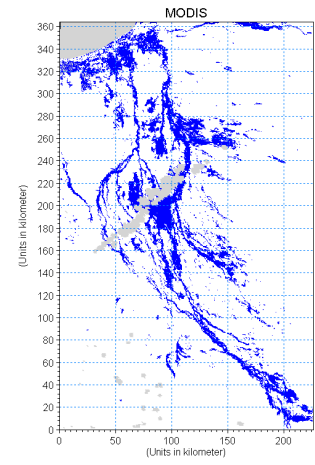
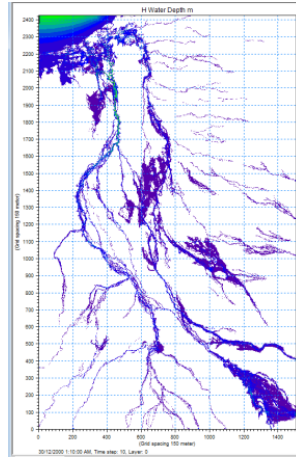
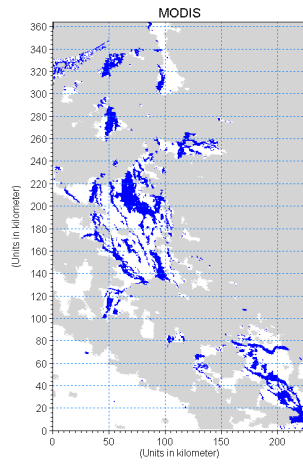
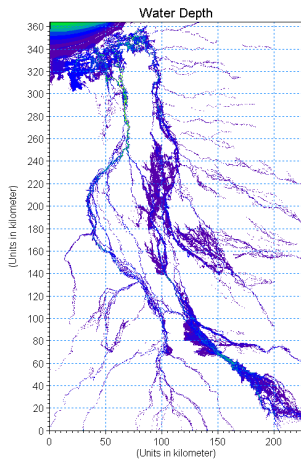
Figure 3.15 Comparison of the observed and simulated stage heights at Canobie (915212A), Etta plains (915012A), Walker's Bend (915003A) for 2009 and 2011 flood events

3.5.2 VALIDATION RESULTS FOR THE FLINDERS

The calibrated model was validated for the flood events of 2001 and 2006, which were relatively smaller events compared to the 2009 flood event. Figure 3.16 and Figure 3.17 show the comparison of the simulated inundation areas (with the calibrated runoff factor) and the MODIS flood maps with 5% threshold for different days of 2001 and 2006 flood events, respectively. Similar to the calibration results, the overall patterns of the simulated inundation on most of the days are similar to the MODIS flood maps, however, simulated flood maps included thin streamlines as inundated cells, which were not captured by the MODIS flood maps.

31 December 2000

5 January 2001



6 January 2001

7 January 2001

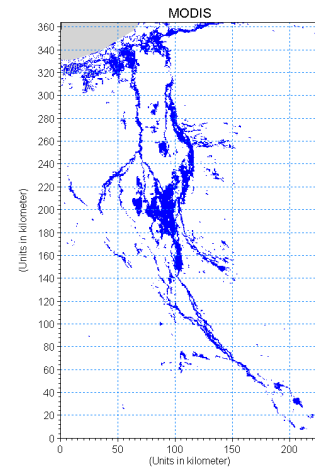
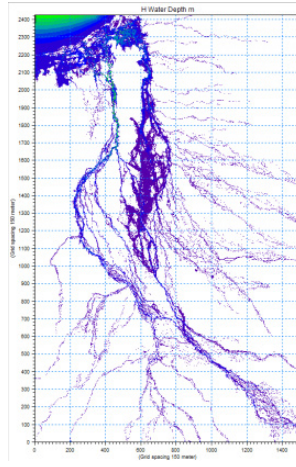
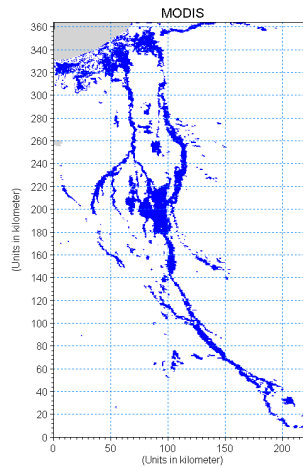
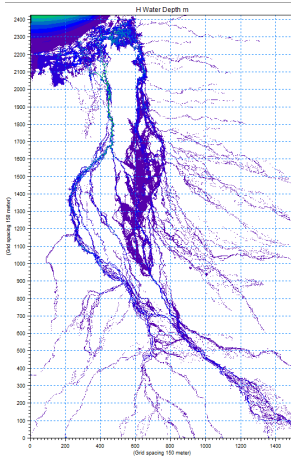


Figure 3.16 Comparison of the simulated inundation (with calibrated runoff factor) and flood maps derived from MODIS imagery with 5% threshold for different days of 2001 flood event.

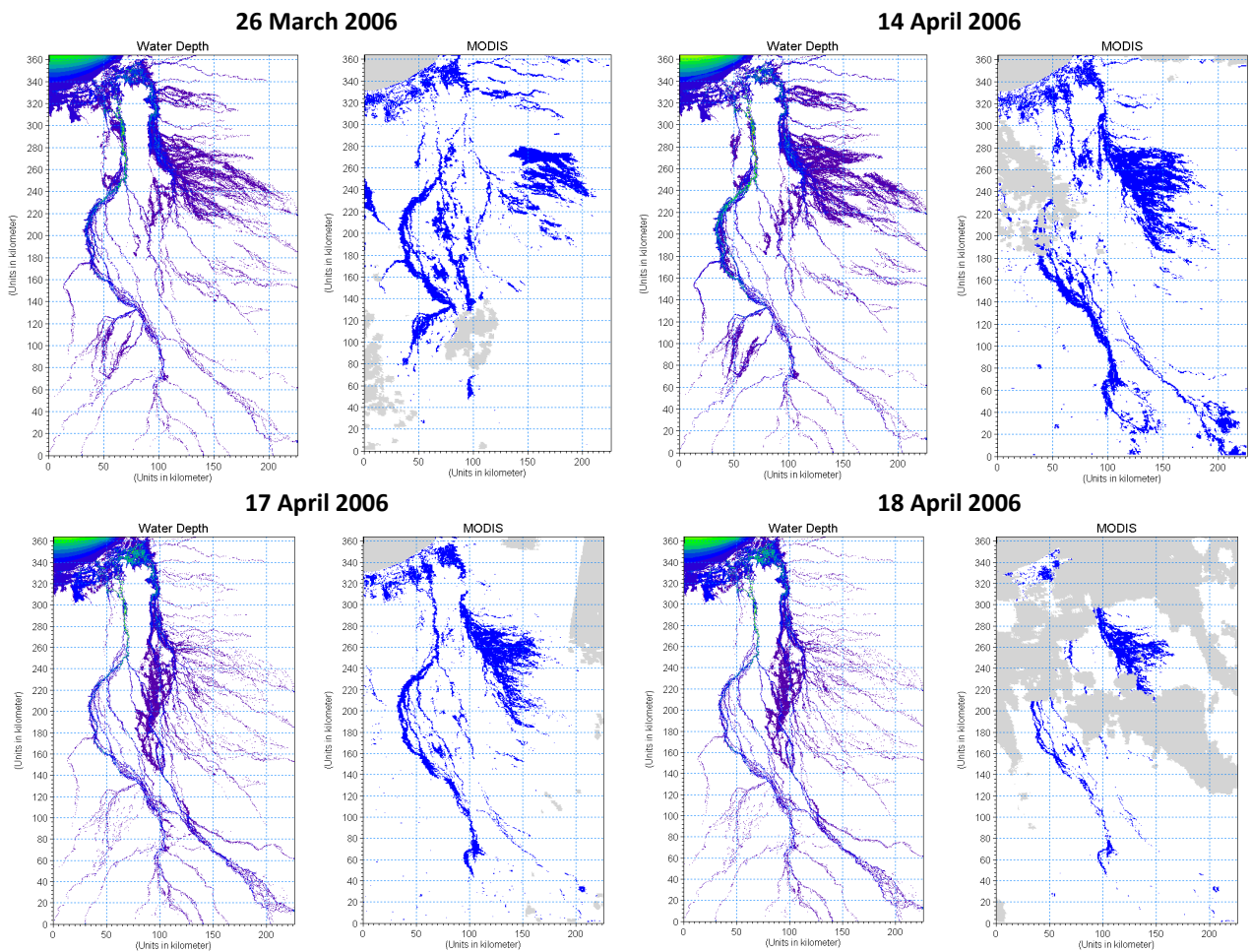


Figure 3.17 Comparison of the simulated inundation (with calibrated runoff factor) and flood maps derived from MODIS imagery with 5% threshold for different days of 2006 flood event.

Figure 3.18 compares the total inundation areas computed using the hydrodynamic model and using the MODIS flood maps with 1%, 5% and 10% thresholds for different days of the 2001 and 2006 flood events. The level of agreement between the simulated total inundation area and MODIS flood maps with different threshold is similar to the calibration events. The 1% threshold MODIS flood maps produced much larger flooded areas compared to the hydrodynamic model. MODIS flood maps with 5% threshold have better agreement with the hydrodynamic model results in most of the days in 2001 with 10% threshold MODIS flood maps having the highest agreement. The agreements are a bit lower for 2006, which is due to the cloud covers in MODIS image in 2006.

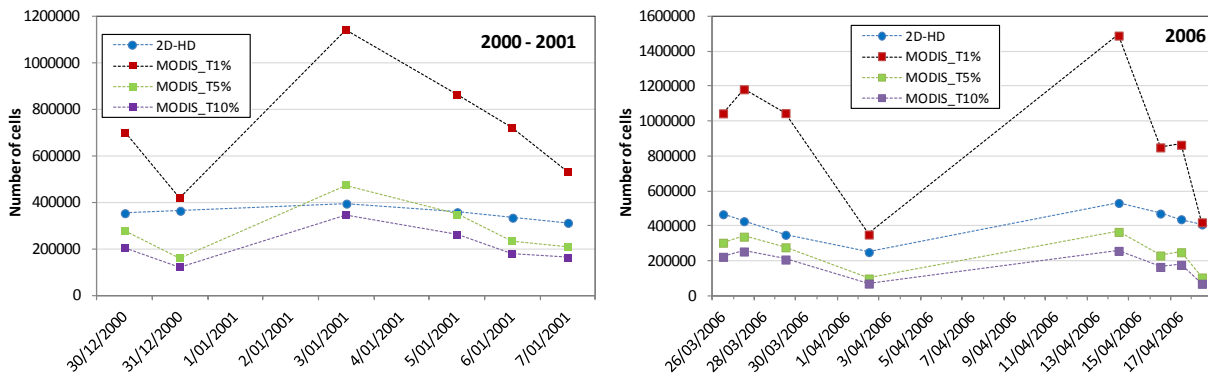


Figure 3.18 Comparison of total number of inundated cells by hydrodynamic model and in the flood maps generated from MODIS with 1%, 5% and 10% thresholds in OWL for flood events of 2001 and 2006

The cell-to-cell agreement between the simulated flood maps and the MODIS flood maps with 5% threshold varied between 33-60% with an average of 45% for 2001. The agreement between the simulated flood map and MODIS flood map with 10% threshold varied between 38-66% with an average of 51% for the same event (Figure 3.19). During the 2006 event, agreement between the simulated flood maps and the MODIS flood maps varied between 48-56% with an average of 52% for with 5% MODIS flood maps and between 53-63% with an average of 59% for 10% threshold.

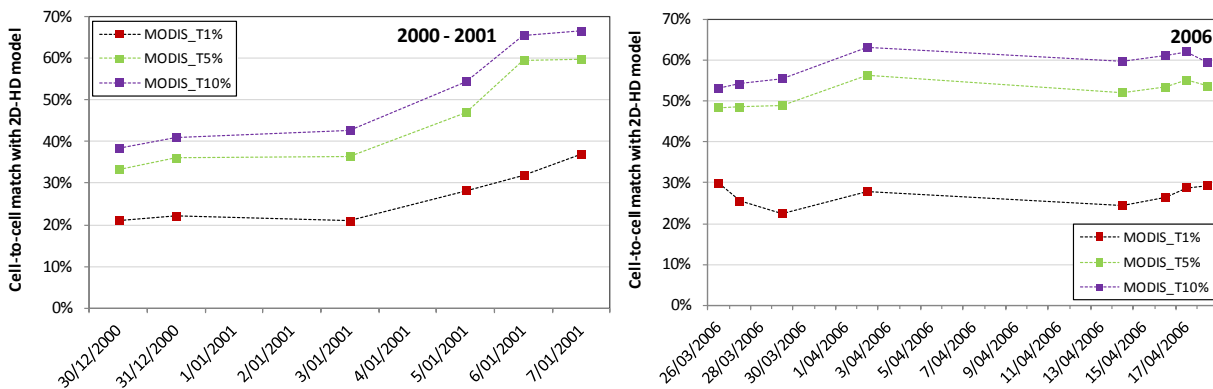


Figure 3.19 Cell-to-cell matching of inundated pixels between the hydrodynamic model and the flood maps generated from MODIS with 1%, 5% and 10% thresholds in OWL for flood events of 2001 and 2006

Figure 3.20 shows a comparison of the simulated and observed flood stage heights at Walker’s Bend for 2001 and 2006 and at Canobie for 2006. There were no observed data for any other gauges. The results show the performance of the model at Walker’s Bend was similar to the calibration period with a good match between the simulated and the observed stage heights. At Canobie in 2006, the simulated flood peaks match well with the observed flood peaks, but the model overestimated the stage heights between the two peaks. For the 2006 event, the correlation coefficients (R^2) were 0.81 and 0.78 at Canobie and Walker’s Bend, respectively.

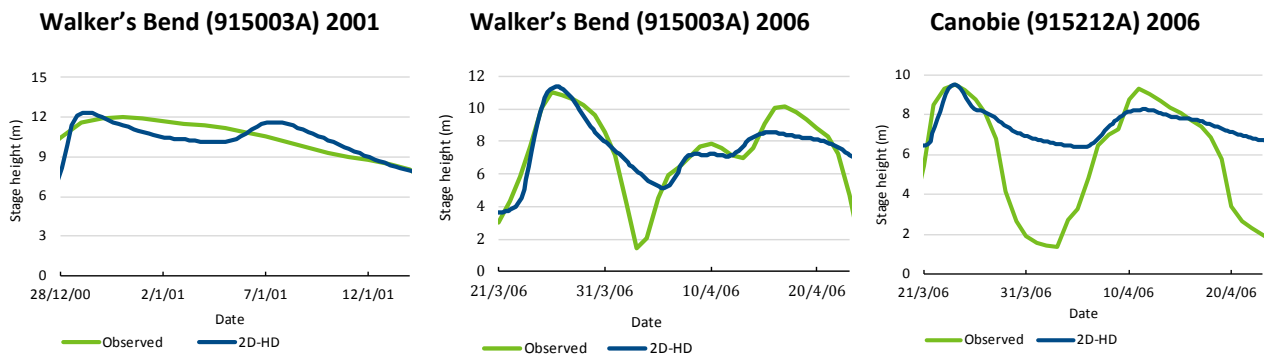


Figure 3.20 Comparison of the observed and simulated stage heights at Canobie (915212A) and Walker's Bend (915003A) for different flood events of 2001 and 2006

3.5.3 INUNDATION DURATION IN THE FLINDERS

The spatial extent and temporal variation of inundation for the six simulated flood events (2001, 2004, 2006, 2008, 2009 and 2011) are shown in Figure 3.21. The 2009 flood event was the largest in terms of total inundation area (35,161 km²) and inundation duration. Many areas in the floodplain were under water for more than 10 days in total and considerably large areas were inundated for greater than 20 days.

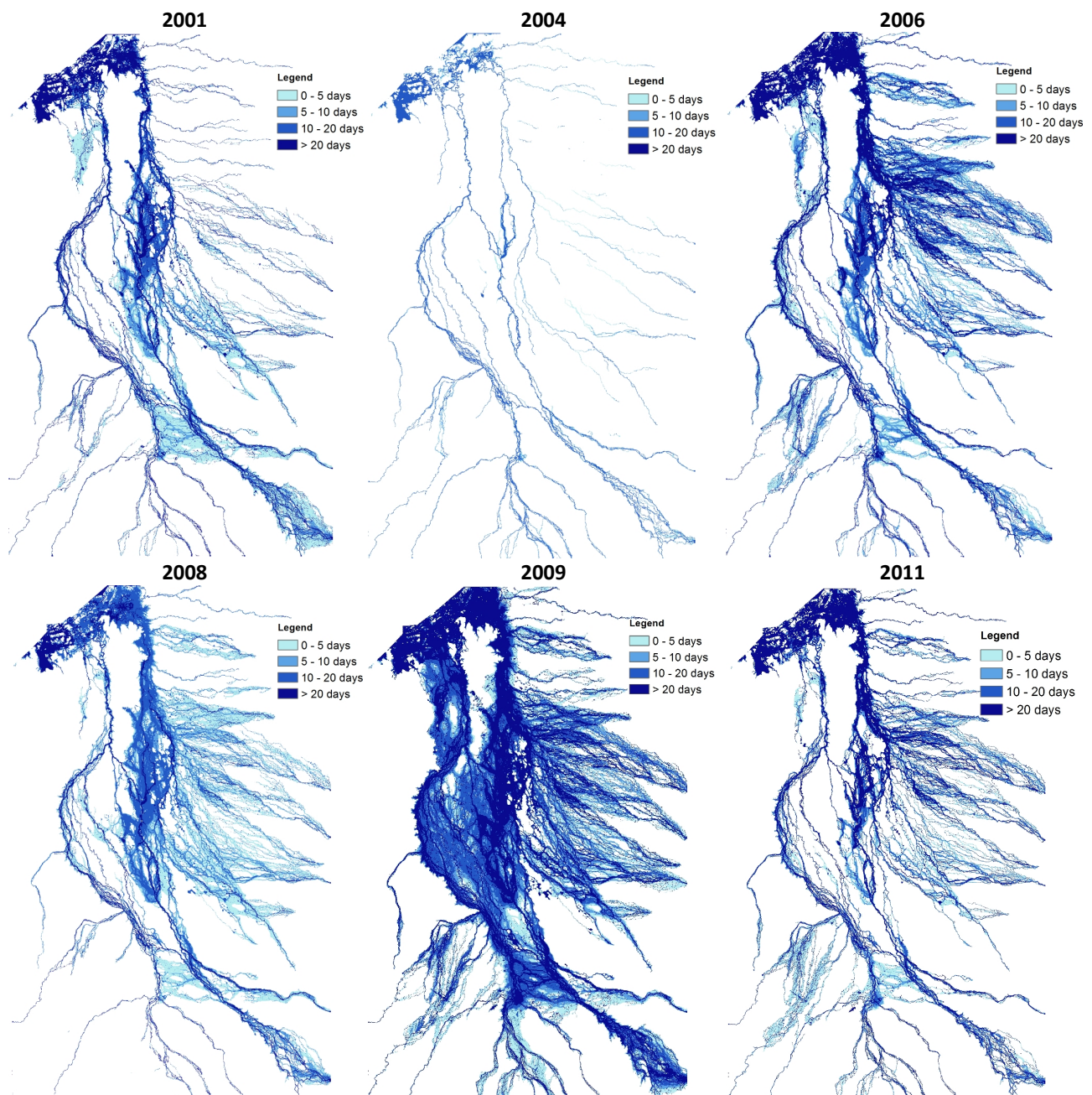


Figure 3.21 Spatial extent and temporal variation of inundation during the simulated flood events of 2001, 2004, 2006, 2008, 2009 and 2011

3.5.4 RESULTS OF CALIBRATION AND VALIDATION IN GILBERT

Inundation extent

There were few cloud free MODIS images available during the flood events in the Gilbert catchment. After reviewing the quality of the images, only a single image (15th January, 2009), during the 2009 flood event, was found to be suitable for the calibration of the two-dimensional hydrodynamic model in the Gilbert catchment. During the 2011 event, several images were available, but the quality of the images was low, except for the images on the 17th and 18th March 2011. Flood maps derived from these images were the only datasets available for the calibration and validation of the hydrodynamic model as all the gauging stations in the Gilbert River catchment are located outside the modelling domain. The two-dimensional hydrodynamic model was mainly calibrated using the flood map derived from the MODIS image of 15th January 2009. Figure 3.22 and Figure 3.23 show a comparison of the simulated inundation and the MODIS flood maps with 5% threshold value for 2009 and 2011, respectively. This visual comparison shows the

overall pattern of the simulated inundation extents is similar to the MODIS flood maps for the selected days of the two flood events. The main difference was that the MODIS flood maps were unable to capture the fine scale flow paths, some of which were a single pixel in width.

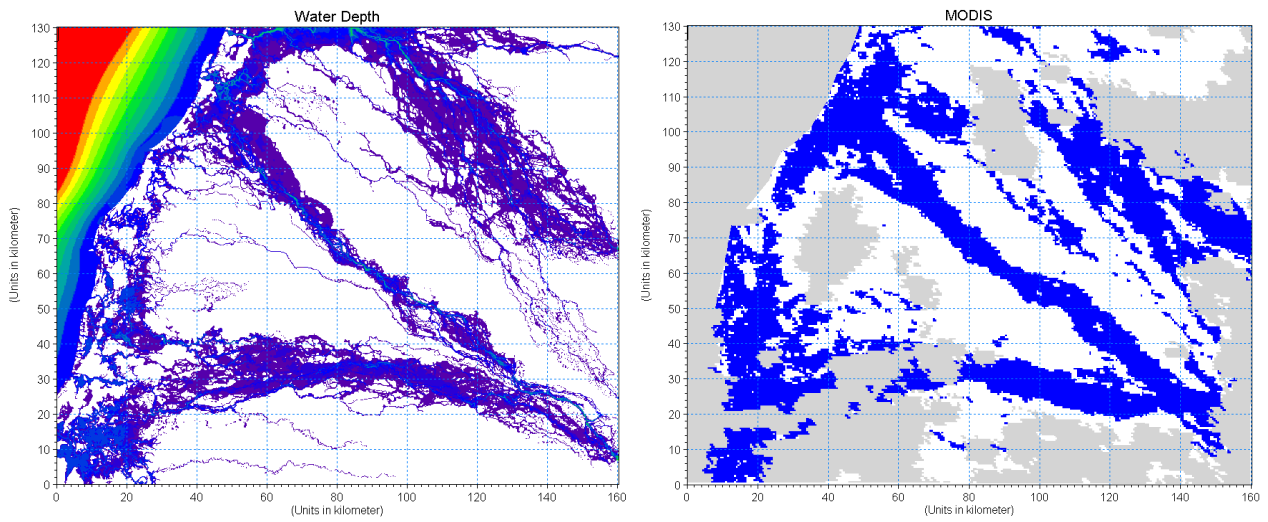
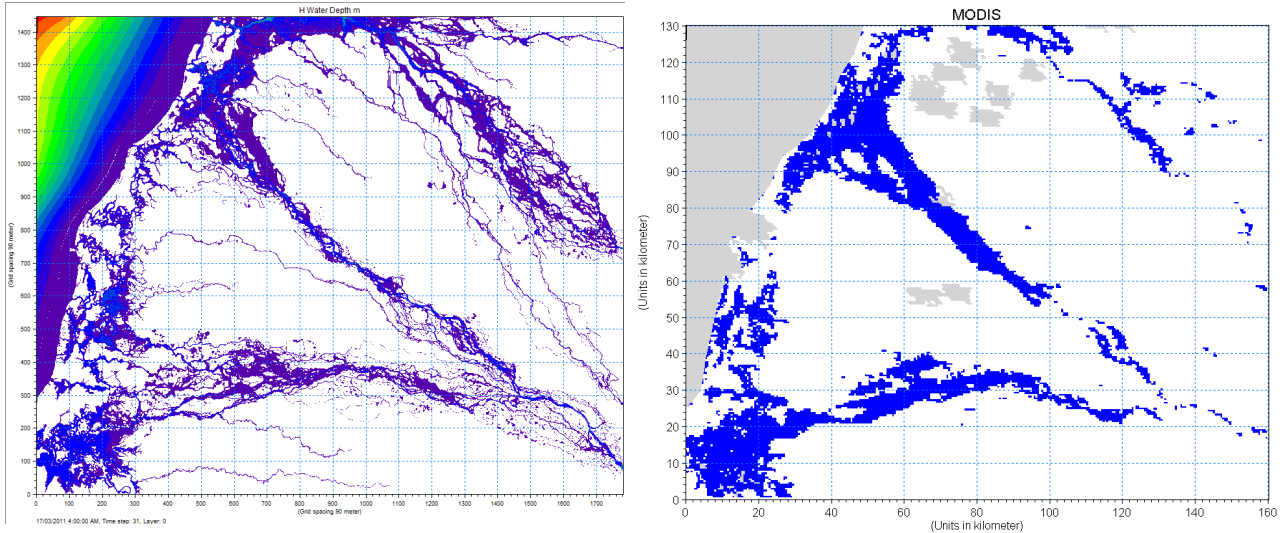


Figure 3.22 Comparison of the simulated inundation (left) and flood map derived from MODIS imagery (using a 5% threshold) (right) on 15th January 2009

17 March 2011



18 March 2011

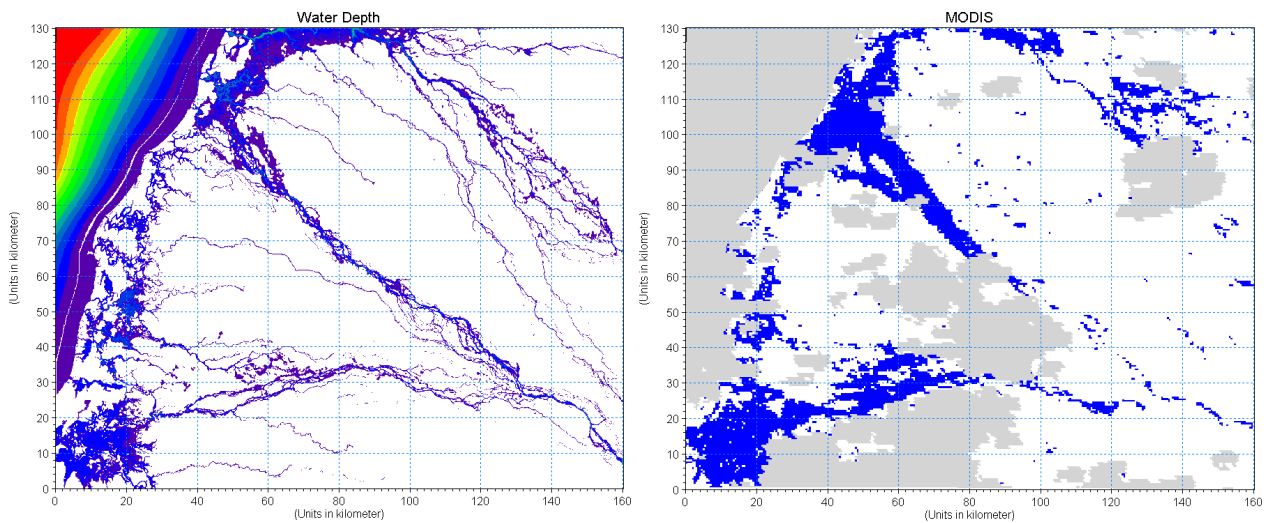


Figure 3.23 Comparison of the simulated inundation and flood maps derived from MODIS imagery (using a 5% threshold) for 17 and 18 March 2011

The comparison of the total inundation area between the simulated inundation results and the MODIS flood maps with 1%, 5% and 10% on 15th January 2009 (Figure 3.24) show that the MODIS flood maps with 5% and 10% thresholds have better agreement with the simulated results compared to 1% threshold. As per the results for the Flinders catchment, the 1% threshold flood map for the Gilbert was considerably larger than the simulated extent. Similarly, cell-to-cell agreement between the simulated and MODIS flood maps were higher (above 60%) using 5% and 10% threshold values. Similar agreement was obtained for 2011 as well (Figure 3.25).

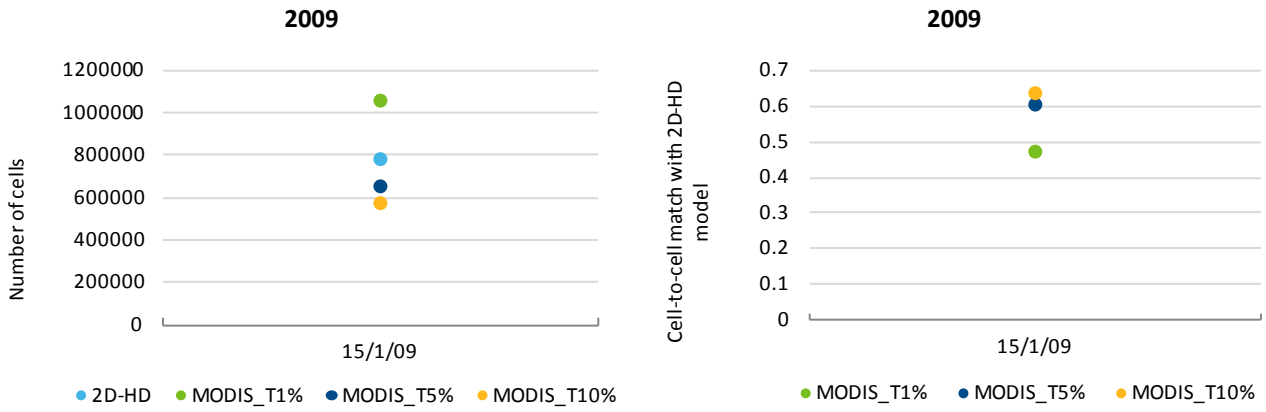


Figure 3.24 Cell-to-cell matching of inundated pixels and total number of inundation cells between the hydrodynamic model and the flood maps generated from MODIS with 1%, 5% and 10% thresholds in OWL for 15 January 2009

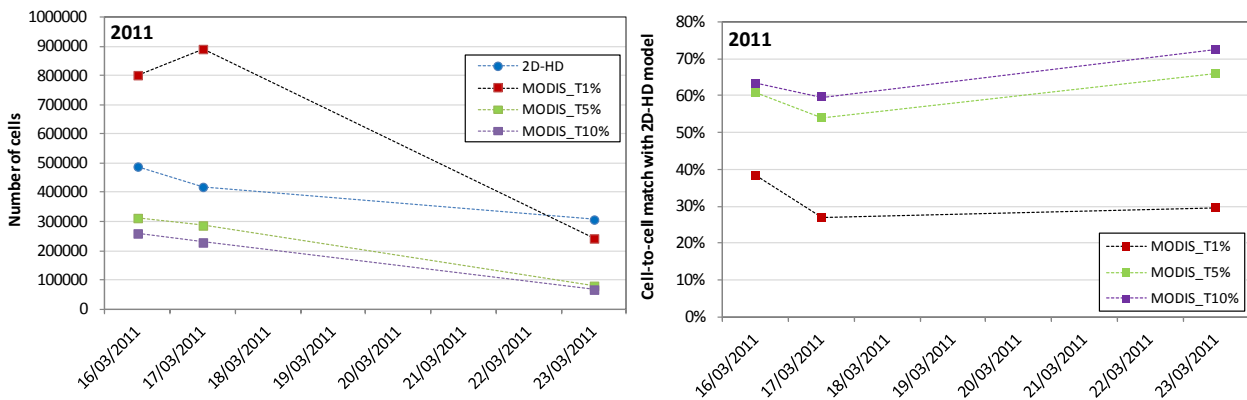


Figure 3.25 Cell-to-cell matching of inundated pixels and total inundation cells between the hydrodynamic model and the flood maps generated from MODIS with 1%, 5% and 10% thresholds in OWL for 2011

3.5.5 INUNDATION DURATION IN THE GILBERT FLOODPLAIN

The spatial extent and temporal variation of inundation for the four simulated flood events (2001, 2008, 2009 and 2011) are shown in Figure 3.26. The 2009 flood event was the largest in terms of total inundated area (8707 km²) and inundation duration. Relatively large areas were inundated for more than 20 days during this flood event. The flood event of 2011 was the second largest with 5781 km² of total inundation area. The results obtained from the model agree with the information gathered from the questionnaire survey. For example, the total duration of the simulated inundation was more than 20 days in Double Lagoon area and between 10-20 days in Vanrook for the 2009 flood event, which were similar to the observation made by the local people.

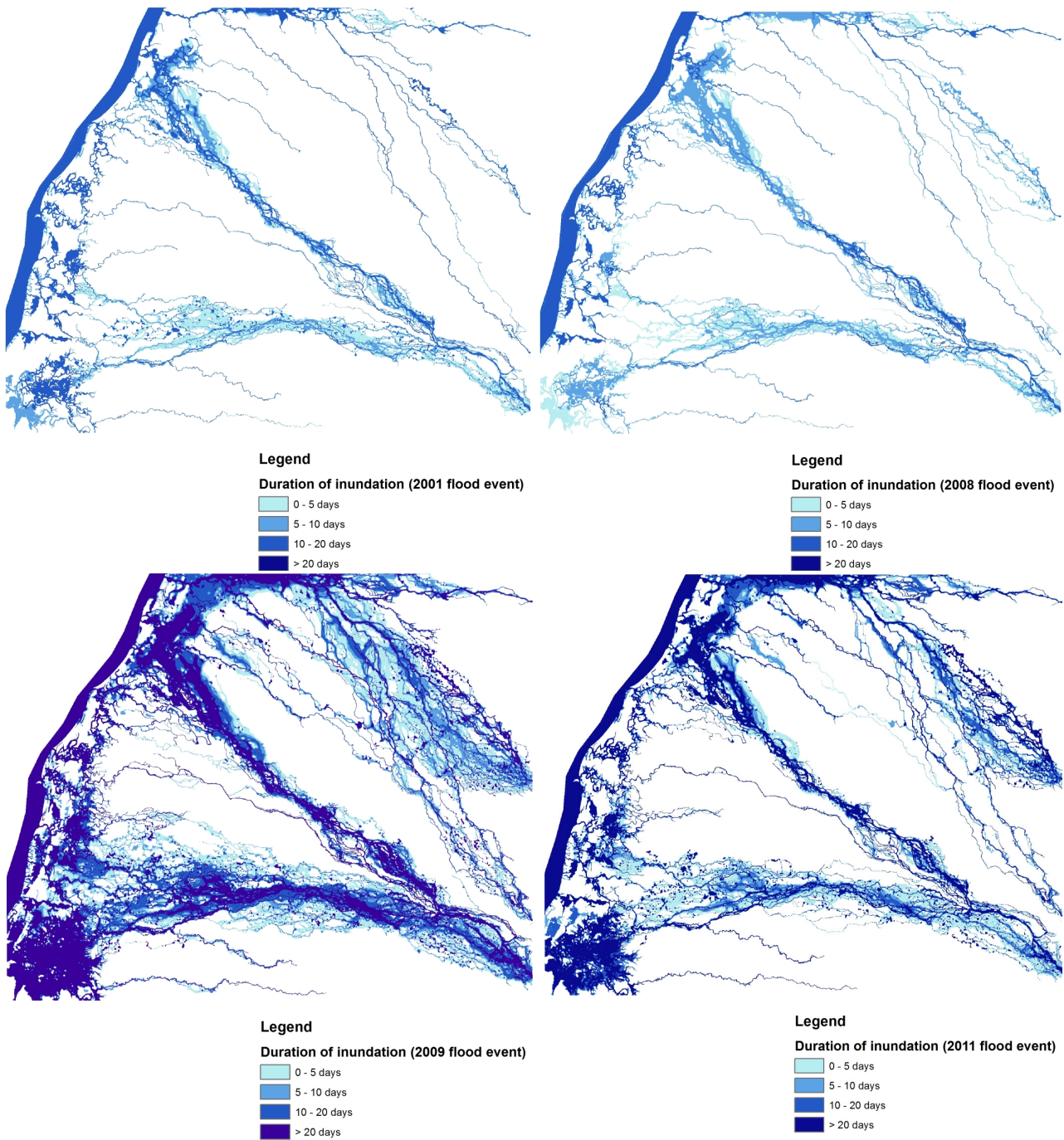


Figure 3.26 Total inundation extent and spatial variation in floodplain total inundation duration in the Gilbert floodplain during the flood events of 2001, 2008, 2009 and 2011

3.6 Configuration and calibration of one-dimensional hydrodynamic models

Two-dimensional hydrodynamic modelling is computationally expensive and it is not possible to run the model for long periods for multiple scenarios. To overcome this problem, relationships between streamflow and inundation area were developed by linking river discharge (above bank-full threshold) from the one-dimensional MIKE11 model to floodplain inundation area from the two-dimensional MIKE21 model, for different floodplain reaches. These relationships can then be applied to the output of the long term simulations from the river system model (see companion technical report on river system calibration; Lerat et al. 2013) to assess how inundation extent may vary over the Assessment timeframe.

In the Flinders catchment, the one-dimensional hydrodynamic model network was setup to mirror the river system model network, as shown in Figure 1.11. However, in the Flinders river system model, Walker's Bend (915003A) was the end-of-system of the modelling network (see companion technical report on river system modelling, calibration; Lerat et al., 2013). For the one-dimensional hydrodynamic modelling, the river network was extended up to the Gulf of Carpentaria.

The upstream boundary of the two-dimensional hydrodynamic model of the Gilbert floodplain was located at the end of the river network of the Gilbert river system model (see companion technical report on river system modelling, calibration; Lerat et al., 2013). The Gilbert river model end-of-system flows were then used to provide the upstream boundary inflow for the two-dimensional hydrodynamic modelling. Thus, the simulated discharge by the river system model could be directly related to the inundation characteristic in the Gilbert floodplain by establishing a relationship between streamflow and floodplain inundation. It was therefore, not necessary to develop a coupled one-dimensional, two-dimensional hydrodynamic modelling framework for the Gilbert catchment.

The one-dimensional hydrodynamic model for the Flinders catchment was setup using the simulated headwater and ungauged runoff by the river system model. The simulated headwater runoff was used as the upstream boundary condition and the simulated ungauged runoff for each river reach was added at the downstream point of the reach in hydrodynamic modelling as flux input. In the absence of other data, the river cross-section data surveyed as part of the Assessment were used to define the model river cross-sections. The main calibration parameter was Manning's roughness coefficient. The model was calibrated against the observed discharge and water levels at three streamflow gauging stations located on the floodplain reaches (Canobie, Etta Plains, Walker's Bend). The period of calibration was from 1981-1999 and validation was from 2000-2011. Calibration was undertaken using a manual approach.

3.6.1 CALIBRATION OF ONE-DIMENSIONAL HYDRODYNAMIC MODEL FOR FLINDERS CATCHMENT

Three commonly used statistical measures namely, Nash-Sutcliffe efficiency (NSE), goodness of fit (R^2) and percentage bias, were used for evaluating model performance in discharge simulation. R^2 , mean absolute error (MAE) and root mean squared error (RMSE) were used for the evaluation of model performance at simulating stage heights. These performance metrics are described in Appendix C .

Table 3.7 and Table 3.8 present a statistical summary of the model calibration performance at different gauges for river discharge and river stage height, respectively. The performance of the model at simulating flood discharge was excellent in terms of percentage bias (PBIAS) at all streamflow gauging stations. NSE values for all streamflow gauging stations were good ranging between 0.58-0.70 with the best performance at Walker's Bend. The model also performed well at simulating stage height, with low values of MAE and RMSE at all streamflow gauging stations except Etta Plains.

The calibrated model simulated river discharge and stage height well over the independent validation period. As shown in Table 3.9 , the NSE values of the model in discharge simulation were similar to the calibration period. Although the PBIAS values were higher over the validation period compared to the calibration period, the model performance was still very good at two of the streamflow gauging stations. In another three streamflow gauging stations, the performance of the model was satisfactory. Similar to the calibration period, the model performed well at simulating stage height at all streamflow gauging stations with low MAE and RMSE except in Etta Plains (Table 3.10).

Table 3.7 Performance of the Flinders one-dimensional hydrodynamic model at simulating discharge over the calibration period

Gauge	Gauge ID	NSE (daily)	R ²	Bias (%)
Flinders River at Walker's Bend	915003A	0.70	0.71	-1.6
Flinders River at Richmond	915008A	0.61	0.70	-3.7
Flinders River at Etta Plains	915012A	0.65	0.66	-9
Cloncurry River at Cloncurry	915203B	0.64	0.66	-4
Cloncurry River at Canobie	915212A	0.58	0.59	-0.2

Table 3.8 Performance of the Flinders one-dimensional hydrodynamic model simulating stage height over the calibration period

Gauge	Gauge ID	R ²	MAE (m)	RMSE (m ²)
Flinders River at Walker's Bend	915003A	0.94	0.24	0.6
Flinders River at Richmond	915008A	0.75	0.59	0.74
Flinders River at Etta Plains	915012A	0.76	2.4	2.44
Cloncurry River at Cloncurry	915203B	0.67	0.26	0.39
Cloncurry River at Canobie	915212A	0.53	0.64	1.03

Table 3.9 Performance of the Flinders one-dimensional hydrodynamic model at simulating discharge over the validation period

Gauge	Gauge ID	NSE (daily)	R ²	Bias (%)
Flinders River at Walker's Bend	915003A	0.72	0.77	8
Flinders River at Richmond	915008A	0.60	0.67	25.7
Flinders River at Etta Plains	915012A	0.76	0.78	-24.8
Cloncurry River at Cloncurry	915203B	0.76	0.78	-24.8
Cloncurry River at Canobie	915212A	0.52	0.54	-2.8

Table 3.10 Performance of the Flinders one-dimensional hydrodynamic model at simulating stage height over the validation period

Gauge	Gauge ID	R ²	MAE (m)	RMSE (m ²)
Flinders River at Walker's Bend	915003A	0.95	0.23	0.59
Flinders River at Richmond	915008A	0.76	0.61	0.75
Flinders River at Etta Plains	915012A	0.8	2.4	2.32
Cloncurry River at Cloncurry	915203B	0.68	0.24	0.33
Cloncurry River at Canobie	915212A	0.58	0.77	1.51

3.7 Floodplain hydrologic matrix

Figure 3.27 shows the sub-catchments of the Flinders river system model within the two-dimensional hydrodynamic modelling domain. An attempt was made to develop relationship between streamflow simulated by the one-dimensional hydrodynamic model and the inundation area simulated by two-dimensional model. This was undertaken for five major sub-catchments (915000, 9150030, 9150120, 9152120 and 9152121). Simulated inundation areas for all six flood events by two-dimensional hydrodynamic model (2001, 2004, 2006, 2008, 2009 and 2011) were used to establish best-fit relationships between discharge and inundation areas for these sub-catchments representing different reaches of the river system model.

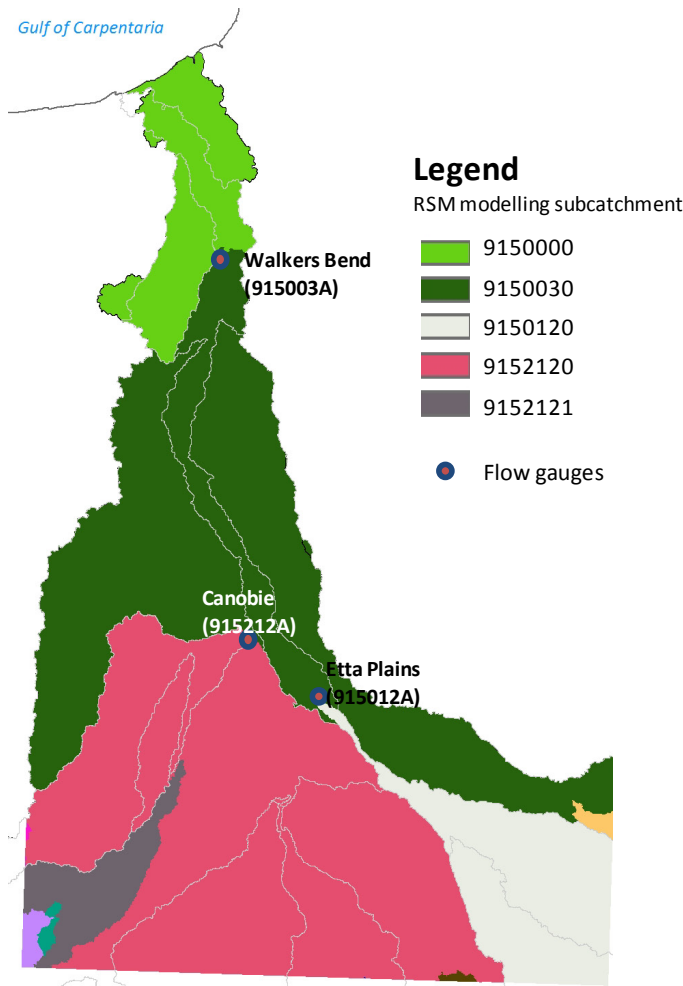


Figure 3.27 Subcatchments of Flinders River System model within the two-dimensional hydrodynamic modelling domain of Flinders floodplain

From the correlation analysis it was found that relationships between streamflow (above overbank flow threshold) and inundation area were different for rising and falling limbs of flood hydrographs. Therefore, it was decided to develop two sets of relationships one for rising limb and another for falling limb of flood hydrographs. Table 3.11 presents the established relationships between streamflow and inundation area for different subcatchments. The best fitted relationships for most of the subcatchments were linear functions for rising limb of the flood hydrograph with R^2 values ranging between 0.53-0.77. Whereas for falling limbs, power functions were better fitted with R^2 values ranging between 0.69-0.85.

Table 3.11 Relationship between streamflow and inundation areas for different reaches of the Flinders floodplain

RIVER SYSTEM MODELLING SUB-CATCHMENT	FOR RISING LIMB OF FLOW HYDROGRAPH		FOR FALLING LIMB OF FLOW HYDROGRAPH	
River System modelling sub-catchment	Relationship between streamflow (Q, m ³ /sec) and inundation area (A, km ²)	R ²	Relationship between streamflow (Q, m ³ /sec) and inundation area (A, km ²)	R ²
Sub-catchments (9152120 and 9152121) above Canobie	$A = 0.9944Q$	0.77	$A = 0.6525Q$	0.75
Sub-catchment (9150120) above Etta Plains	$A = 26.987Q^{0.5008}$	0.55	$A = 14.438Q^{0.6302}$	0.73
Sub-catchment (9150030) above Walker's Bend	$A = 0.9305Q$	0.53	$A = 28.52Q^{0.6041}$	0.69
Sub-catchment (9150000) below Walker's Bend	$A = 0.2954Q$	0.53	$A = 29.966Q^{0.4603}$	0.85

Only one relationship was established between streamflow and inundation area by relating the simulated streamflow by the Gilbert river system model at the end of the system and the simulated inundation by the two dimensional hydrodynamic model for the Gilbert floodplain modelling domain. The simulated inundation results of the hydrodynamic model for all four flood events (2001, 2008, 2009 and 2011) were used for best-fit analysis. Table 3.12 presents the relationship between streamflow (above overbank flow threshold) and inundation area for rising and falling limb of flow hydrograph for Gilbert floodplain.

Table 3.12 Relationship between streamflow and inundation areas for different reaches of the Flinders floodplain

RIVER SYSTEM MODELLING SUB-CATCHMENT	FOR RISING LIMB OF FLOW HYDROGRAPH		FOR FALLING LIMB OF FLOW HYDROGRAPH	
River System modelling sub-catchment	Relationship between streamflow (Q, m ³ /sec) and inundation area (A, km ²)	R ²	Relationship between streamflow (Q, m ³ /sec) and inundation area (A, km ²)	R ²
Sub-catchment below EOS of river system model	$A = 0.5315Q$	0.97	$A = 715.91Q^{0.1606}$	0.93

4 Floodplain inundation modelling under future climate and development scenarios

4.1 Introduction

Climatic variables are generally considered, together with soil data, to be the most important environmental factors in determining the suitability of particular locations for agriculture. And because climate is so very closely linked to hydrology and water availability, understanding of climate and its variability is especially important in assessments of semi-arid and subtropical sites in northern Australia for irrigated land use. In a companion technical report, Petheram and Yang, 2013 used 15 global climate models (GCMs) to study the impact of climate change on rainfall and other climate variables in the Flinders and Gilbert catchments. It was reported that approximately half the GCMs were found to result in a spatially averaged increase in mean annual rainfall (by up to 17% in the Flinders and 22% in the Gilbert) and half resulted in a decrease (by up to 33% in both the Flinders and Gilbert), relative to the historical climate. The potential changes in rainfall in the future will have impact on the streamflow and local runoff, which in turn, is likely to affect the flooding characteristics in the floodplains.

Tidal influence is prominent in the lower part of the river system in the floodplains of the Flinders and Gilbert catchments. According to the IPCC, global sea-level is projected to rise by 18 to 59 cm by 2100, with a possible additional contribution from melting ice sheets of 10 to 20 cm (IPCC, 2007). The sea-level rise on parts of the coastline around the Gulf of Carpentaria is projected to be up to 25 mm above the global average sea-level rise by 2070 (this value is calculated using the SRES A1B or medium emissions scenario) (CSIRO, 2008).

In the Assessment, 22 potential dam sites were investigated in the Flinders and Gilbert catchments (see companion technical report on water storage; Petheram et al. 2013). The sizes of the potential dams and their catchment areas vary. In each catchment three potential dams were short-listed for further investigation. These were Cave Hill, O’Connell Creek off-stream storage and Porcupine Creek potential dam sites in the Flinders catchment and Copperfield Gorge River Dam (raising the height of current dam), Dagworth and Greenhills potential dam sites in the Gilbert catchment (Table 4.1). It is possible that the potential dams with large reservoir volumes, if built, may perturb downstream flood events.

Table 4.1 Locations and physical properties of the proposed top three dams at the Flinders and Gilbert Catchments

CATCHMENT	PROPOSED DAM	LOCATION	CATCHMENT AREA (KM ²)	CAPACITY (GL)
Flinders	Cave Hill Dam	Cloncurry River	5,265	248
Flinders	O’Connell Creek Off-stream	O’Connell Creek	1,508	127
Flinders	Porcupine Gorge	Porcupine Creek	1,051	31
Gilbert	Raising Copperfield River Gorge Dam	Copperfield River	1,244	25
Gilbert	Dagworth	Einasleigh River	15,351	498
Gilbert	Green Hills	Gilbert River	8,310	271

In this section, the calibrated two dimensional hydrodynamic models for the Flinders and Gilbert catchments were used to simulate floodplain inundation under projected future climate and potential

development scenarios. This was undertaken to analyse the possible impacts of these scenarios on floodplain inundation and connectivity of wetlands to the main river system.

4.2 Selection of Scenarios for inundation modelling

The calibrated two-dimensional hydrodynamic models for the Flinders and Gilbert floodplains were used to undertake scenario modelling to analyse the impacts of future climate and potential reservoir developments on floodplain inundation and resulted changes in wetland connectivity in the two catchments. A number of scenarios were investigated in each catchment. These were:

- three future climate scenarios in each (Scenario C);
- three future development scenarios in the Flinders catchment and six in the Gilbert catchment (Scenario B);
- three sea level rise (SLR) scenarios in each (Scenario C); and
- three future climate and development scenarios in Gilbert (Scenario D).

Three historical flood events of different magnitudes (2001, 2009 and 2011 flood events) were selected as the base-line events. The local runoff and upstream and downstream boundary conditions of the calibrated Flinders and Gilbert floodplain hydrodynamic models for the three selected events were updated representing the selected scenarios. The Sacramento rainfall-runoff model was used for generating local runoff under future climate. The Flinders and Gilbert river system models were used to generate upstream boundary conditions under future climate and potential development scenarios.

4.2.1 FUTURE CLIMATE SCENARIOS (DRY AND WET SCENARIOS)

In a companion technical report, Petheram and Yang (2013) used empirically scaled rainfall data from 15 Global Climate Models (GCMs) to generate runoff for the Flinders and Gilbert catchments under future climate scenarios. The runoff results were ranked in order of increasing catchment average mean annual runoff. The GCMs corresponding to the 10th, 50th and 90th catchment average mean annual runoff were selected for the Cwet, Cmid and Cdry future climates. The GCMs' used for the Gilbert catchments under scenarios Cwet, Cmid and Cdry were cccma_t47, ncar_ccsm and mri respectively. The GCMs used for the Flinders catchment under scenarios Cwet, Cmid and Cdry were giss_aom, gfdl and miub respectively. The catchment average mean annual runoff under Scenario Cmid was similar to the catchment average mean annual runoff under Scenario A (historical climate). For this reason it was deemed unnecessary to further investigate this scenario using the hydrodynamic model.

Figure 4.1 shows the projected changes in the runoff in the Flinders catchment under scenario A, Cwet and Cdry from 1999 to 2011 (the two-dimensional hydrodynamic model was calibrated and validated for flood events within this period). Under Scenario Cwet the total annual catchment average runoff increased by 2% and the average peak runoff increased by 25%. Under Scenario Cdry mean annual runoff decreased by 3% and peak runoff increased by 37%. The highest peak in 2009 increased by 24% in under Scenario Cwet and decreased by 32% under Scenario Cdry.

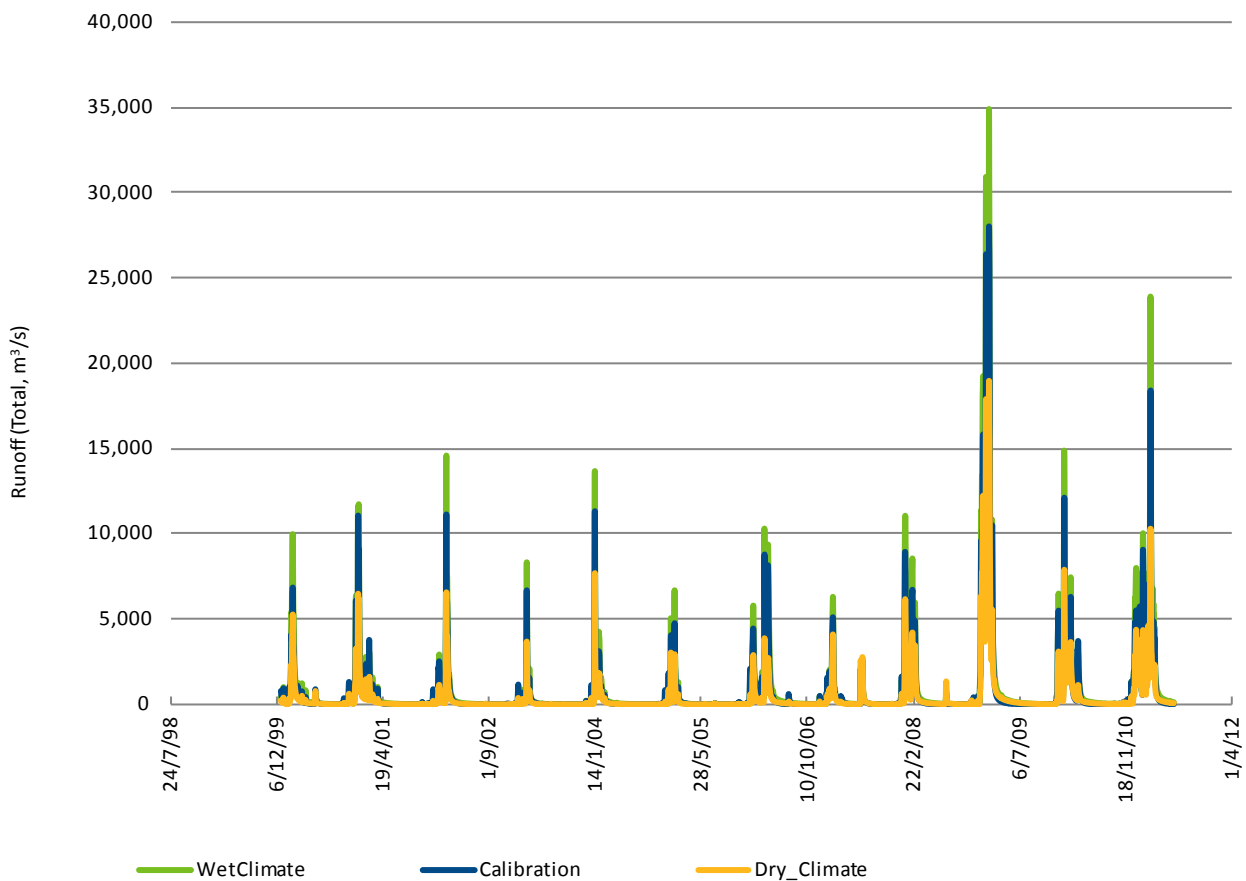


Figure 4.1 Comparison of total runoff within the hydrodynamic modelling domain in the Flinders catchment from 1999 to 2011 (period over which hydrodynamic model was calibrated and validated under scenarios A, Cwet and Cdry)

Figure 4.2 shows the projected changes in the runoff in the Gilbert catchment under scenarios A, Cwet and Cdry from 1999 to 2011.

It shows that under Scenario Cwet, the total annual catchment average runoff increased by 7% and average peak runoff increased by 47%. Under Scenario Cdry, annual runoff decreased by 2% and average peak runoff decreased by 2%. The highest peak in 2009 increased by 47% under Scenario Cwet and decreased by 2% under Scenario Cdry.

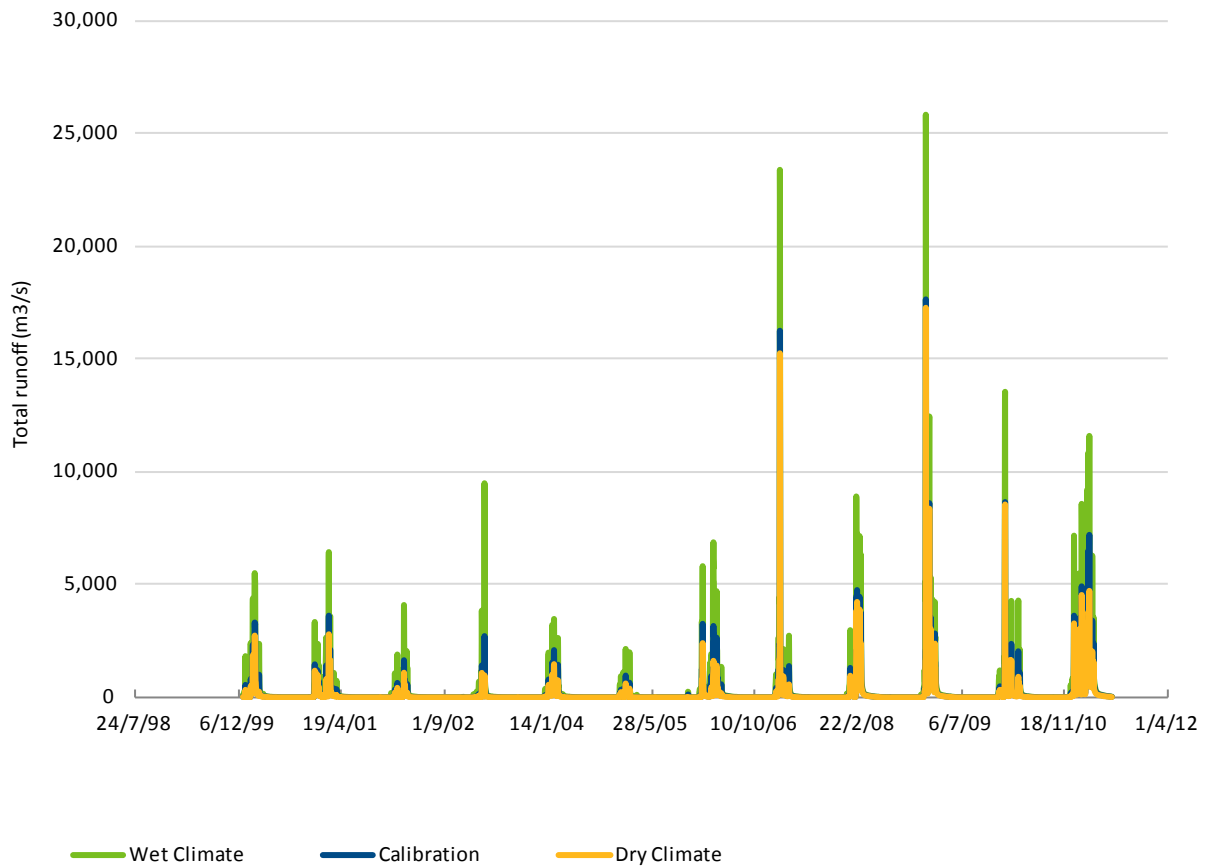


Figure 4.2 Comparison of total runoff within the hydrodynamic modelling domain of the Gilbert catchment during the periods of calibration and validation (1999-2011) of the hydrodynamic model for a) current climate, b) future climate, Cwet, c) future climate, Cdry.

A multiplication factor was used to adjust the local runoff generated by the Sacramento model in the calibrated Flinders floodplain hydrodynamic model. The same factor was used to adjust the local runoff in inundation modelling for the future climate scenarios.

The calibrated river system models of the Flinders and Gilbert catchments (see companion technical report on river system modelling, calibration; Lerat et al., 2013) were used to simulate streamflow under future climate scenarios (Cwet and Cdry) for the upstream boundary conditions to the two-dimensional hydrodynamic models for the future climate scenarios. Figure 4.3 compares the simulated discharge under the current and future climates for the Gilbert river system model at the end of the system for the 2001, 2009 and 2011 flood events. It shows large changes in peak and total discharge under scenarios Cwet and Cdry compared Scenario A. For example, peak discharge is decreased by 30%, 21% and 44% under Cdry climate for the 2001, 2009 and 2011 flood events, respectively.

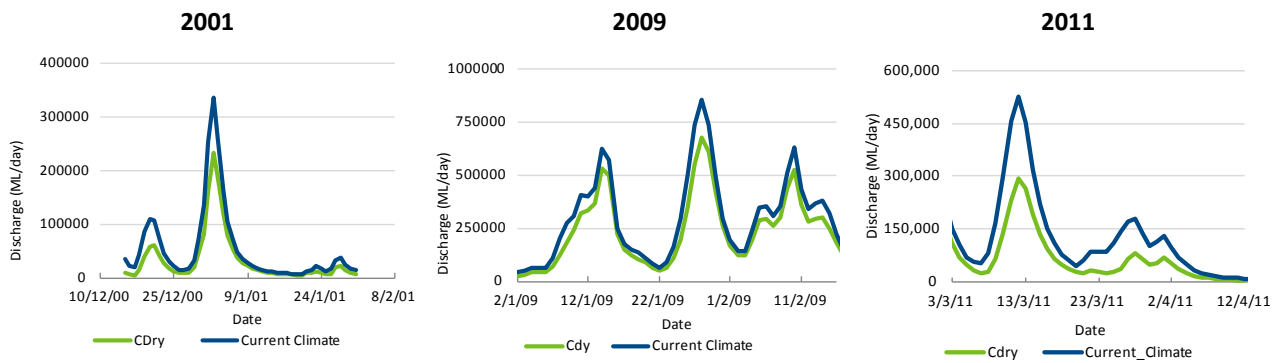


Figure 4.3 Simulated streamflow by the Gilbert river system model at the end of the system for the periods of three different flood events (2001, 2009 and 2011) for current and future climate

4.2.2 FUTURE DEVELOPMENT SCENARIOS

Cave Hill Dam in the Flinders catchment

The potential Cave Hill dam site is on the Cloncurry River, which is one of the main tributaries of the Flinders River. The potential dam site has an approximate catchment area of 5,265 km² (Figure 4.4) and has a mean annual rainfall which varies from 350 to 400 mm per year across the catchment.

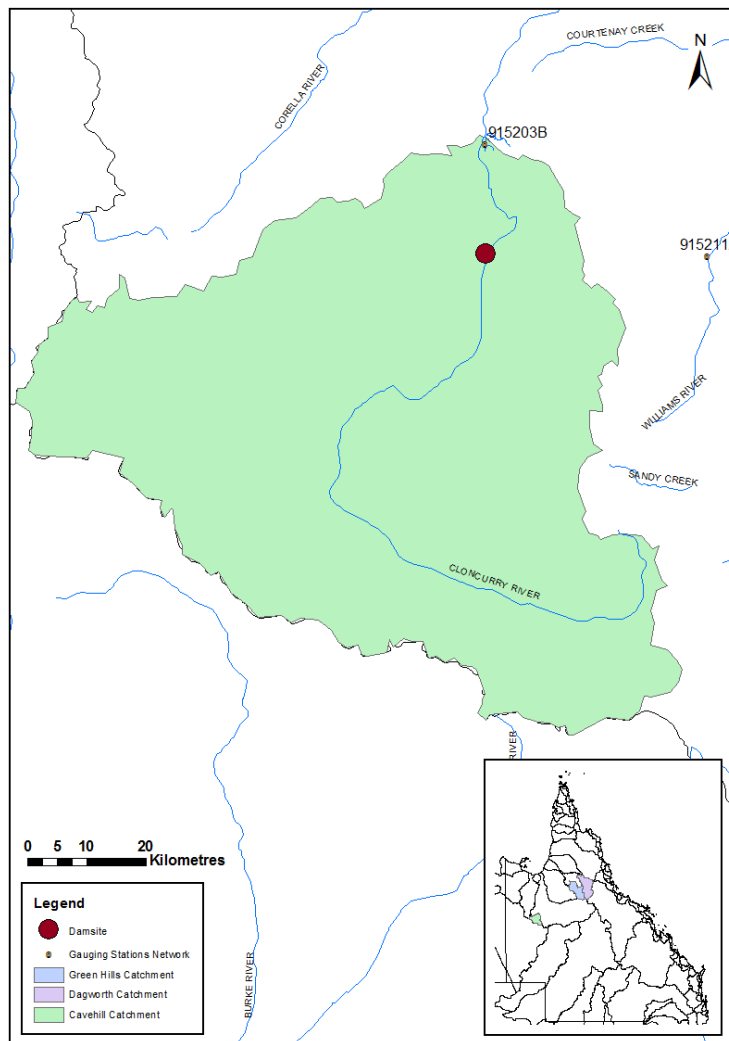


Figure 4.4 Cave Hill catchment area, streamflow gauging station and location of proposed dam site (Source: Lee et al., 2013)

Dagworth and Greenhills dam sites in the Gilbert catchment

The potential Dagworth dam site is on the Einasleigh River, one of the main tributaries of the Gilbert River. The potential dam site has a total catchment area of approximately 15,318 km² (Figure 4.5) and has a mean annual rainfall which varies from 650 to 800 mm across the catchment.

Greenhills potential dam is on the Gilbert River. The potential dam site is to the west of the Dagworth catchment. It has a total catchment area of approximately 8,400 km² (Figure 4.5) and the mean annual rainfall varies between 650 and 750 mm across the catchment.

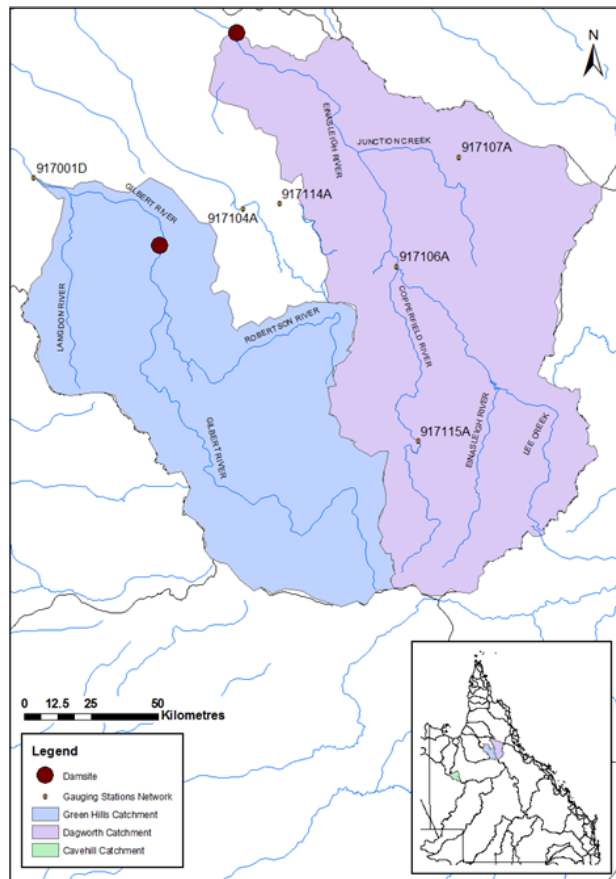


Figure 4.5 Dagworth and Greenhills catchments, streamflow gauging stations and location of proposed dam sites (Source: Lee et al., 2013)

Under the future development scenarios, the calibrated river system models for the Flinders and Gilbert catchments (see companion technical report on river system modelling, calibration; Lerat et al., 2013) were used to generate boundary conditions for reservoir empty condition for Cave Hill, Dagworth and Greenhills potential dam sites at the start of the three selected flood events (2001, 2009 and 2011). In assessing the impact of a reservoir on the inundation of downstream wetlands an empty reservoir condition was deemed to represent the worst case scenario.

The calibrated hydrodynamic model of the Gilbert floodplain was run with the updated boundary conditions obtained from the Gilbert river system model to simulate inundation for the 2001, 2009 and 2011 flood events under the empty reservoir conditions of the Dagworth and Greenhills dams. This was undertaken by updating the only upstream inflow boundary condition, i.e. the end-of-the-system simulated streamflow by the Gilbert river system model. The remaining input data sets and boundary conditions in the calibrated hydrodynamic model were kept the same.

The inflow boundary condition of the calibrated hydrodynamic model of the Flinders floodplain was updated at Canobie (915212A) for the reservoir empty condition of the Cave Hill dam using the simulated streamflow by the Flinders River system model.

Porcupine Creek potential dam site was too small to make any difference to flooding on the mid to lower Flinders floodplain. Similarly O’Connell Creek off-stream storage was not assessed as it does not retard flow events. Figure 4.6 shows the discharge simulated by the Gilbert River system model with the potential Dagworth dam reservoir empty for the periods of 2001, 2009 and 2011 flood events. It shows significant changes in total and peak discharge under this condition. For example, peak discharge decreased by 40%, 4% and 25% under Dagworth reservoir empty condition for 2001, 2009 and 2011 flood events, respectively. Similar impact was found for the Greenhills dam reservoir empty condition as well.

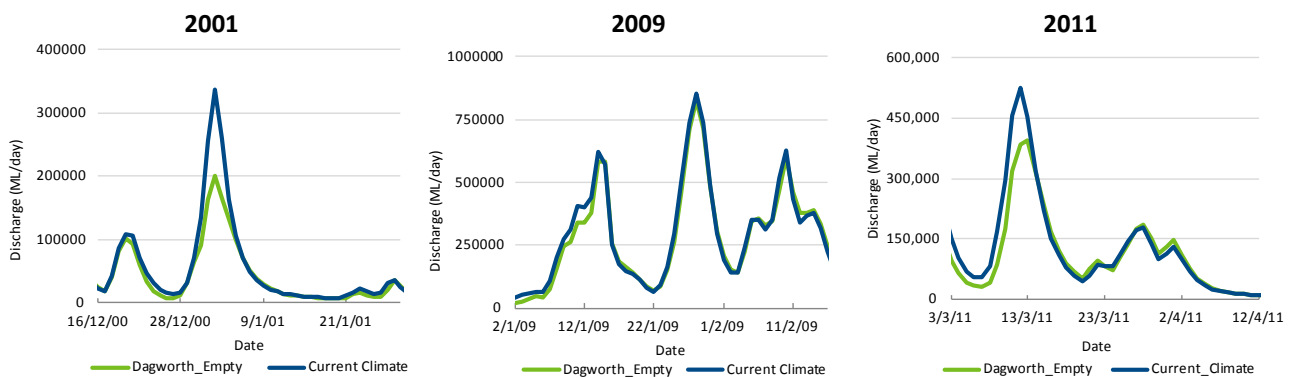


Figure 4.6 Simulated streamflow by the Gilbert river system model at the end of the system for the periods of 2001, 2009 and 2011 flood events under current condition and Dagworth dam reservoir empty scenario

4.2.3 SEA LEVEL RISE SCENARIOS

Based on available literature, the projected rise of mean sea level was considered as 80 cm (including increased storm surge by 20 cm) for the worst case scenario in 2070. This was incorporated into the hydrodynamic model by raising the observed daily tidal data at Karumba by 80 cm. The other input data and boundary conditions in the calibrated model remained fixed. The calibrated Flinders and Gilbert floodplain hydrodynamic models were run for the 2001, 2009 and 2011 flood events using the updated downstream boundary condition incorporating the projected SLR.

4.2.4 FUTURE CLIMATE AND DEVELOPMENT SCENARIOS

Under scenario D (i.e. future climate and development), the combined condition of Cdry and empty reservoirs were investigated as this represents the worst reduction in upstream inflow. The Flinders and Gilbert river system models were run with the projected rainfall and PET data for Cdry scenario (see section 4.2.1) and empty reservoir condition of the proposed dams (see section 4.2.2) to generate upstream inflow boundary conditions for the Flinders and Gilbert floodplain hydrodynamic models. The upstream inflow boundary conditions of the Flinders and Gilbert hydrodynamic models used under Scenario Cdry were updated using Scenario Cdry streamflow simulated by the river system models under an empty reservoir scenarios.

4.3 Results of Scenario Analyses

4.3.1 FUTURE CLIMATE SCENARIOS

Flinders floodplain

Figure 4.7 presents the 6-hourly time series of the number of inundated cells during the flood events of 2001, 2009 and 2011 under scenarios A, Cwet and Cdry. Table 4.2 summaries the changes in total areas of flooding and average depth under these scenarios.

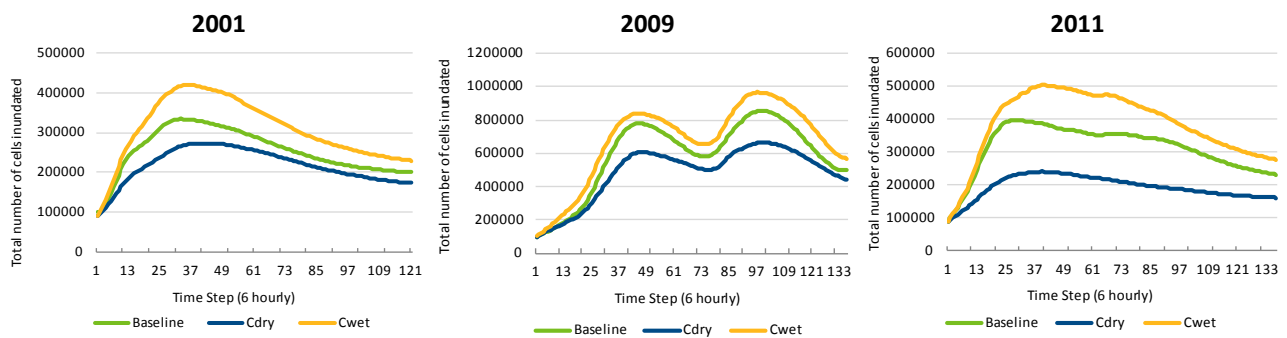


Figure 4.7 6-hourly time series of number of cells inundated in the Flinders floodplain during the 2001, 2009 and 2011 flood events under scenarios A, Cwet and Cdry

Under Scenario Cwet the maximum inundation extent in the Flinders floodplain increased by 13 to 27% and the average inundation area during each event increased by 14 to 23% with the larger percentage increase occurring during the lower magnitude flood events. Relative to the change in extent of inundation, the change in average inundation depth under Scenario Cwet was small (< 4%), due to flat topography in the floodplain area. For 2009 and 2011 events the percentage change of maximum area of inundation and average area of inundation was modelled to be larger than under Scenario Cdry than Scenario Cwet. (Table 4.2).

Table 4.2 Impact of future climate (Cdry and Cwet) on inundation area and depth for flood events of different magnitudes in the Flinders floodplain

CHANGE COMPARED TO BASELINE	2001 (Cdry)	2001 (Cwet)	2009 (Cdry)	2009 (Cwet)	2011 (Cdry)	2011 (Cwet)
Maximum area of inundation	-18.2%	25.5%	-22.4%	13.1%	-39%	27%
Average area of inundation	-14.7%	21.1%	-17.8%	14.5%	-38%	23%
Average inundation depth	-2.5%	3.5%	-2.5%	2.5%	-2.5%	2.6%

Gilbert floodplain

Figure 4.8 compares the temporal variation in the total number of inundated cells during the flood events of 2001, 2009 and 2011 under scenarios A, Cwet and Cdry. A summary of changes in peak and average inundation extents and average inundation depth under the future climate scenarios compared to the current climate is presented in Table 4.3.

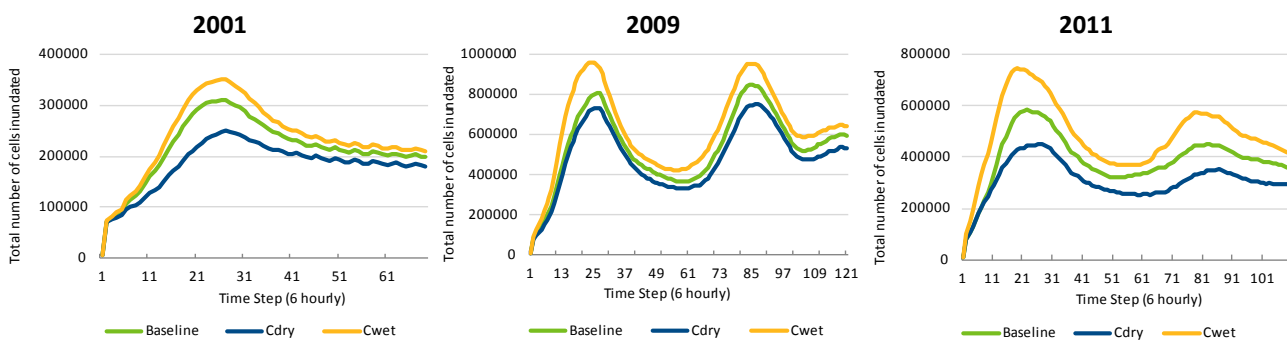


Figure 4.8 6-hourly time series of the number of cells inundated in the Gilbert floodplain during the 2001, 2009 and 2011 flood events under scenarios A, Cwet and Cdry.

Under the Scenario Cwet the maximum extent of inundation in the Gilbert floodplain increased by 13 to 27% and the average inundation extent increased by 9 to 24%. However, the change in average inundation depth was small, increasing by only 2.7%, due to the flat floodplain topography. Under Scenario Cdry the maximum extent of inundation decreased by 11 to 27% and the average inundation extent decreased by 9

to 21%. The decrease in average inundation depth under Scenario Cdry was 7.2% during the 2011 event, which is relatively small compared to the percentage change in inundation extent.

Table 4.3 Impact of future climate (Cdry and Cwet) on inundation area and depth for flood events of different magnitudes in the Gilbert floodplain

CHANGE COMPARED TO BASELINE	2001 (Cdry)	2001 (Cwet)	2009 (Cdry)	2009 (Cwet)	2011 (Cdry)	2011 (Cwet)
Maximum area of inundation	-19.6%	13.0%	-11.5%	13.1%	-22.4%	27.9%
Average inundation area	-15.2%	9.4%	-9.9%	15.7%	-20.9%	24.4%
Average inundation depth	-4.6%	1.7%	-0.6%	1.2%	-7.2%	2.7%

4.3.2 FUTURE DEVELOPMENT SCENARIOS

Flinders floodplain

The 6-hourly time series of number of inundated cells during the flood events of 2001, 2009 and 2011 under baseline and Cave Hill reservoir empty condition are presented in Figure 4.9. Table 4.4 presents the summary of the impact of the empty reservoir condition on inundation extents and depth for the three flood event.

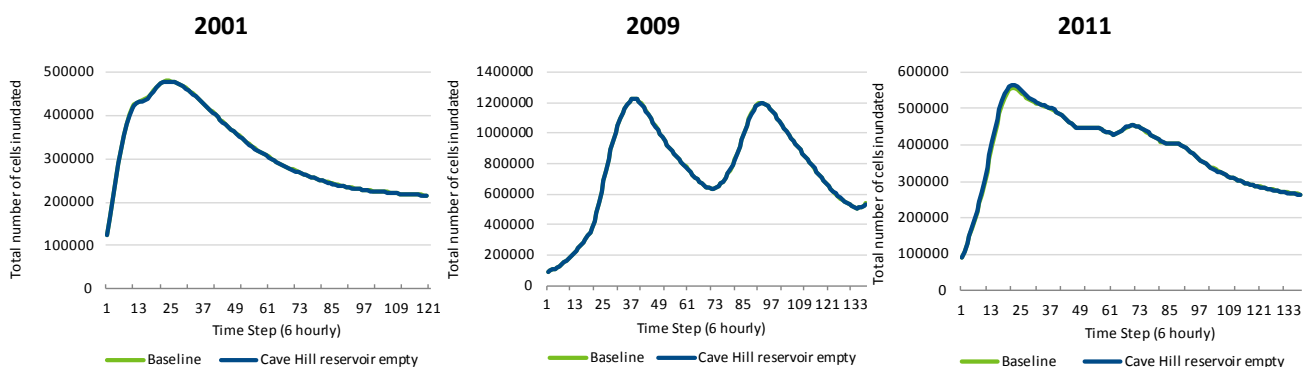


Figure 4.9 6-hourly time series of number of cells inundated during the 2001, 2009 and 2011 flood events under current condition and Cave Hill reservoir empty scenario in the Flinders floodplain

The impact of Cave Hill reservoir empty scenario on total and peak inundation extents and average inundation depth is negligible with a reduction of less than 1%. This is mainly due to two reasons, firstly, the inundation in Flinders floodplain is largely influenced by local runoff and the impact of Cave Hill reservoir empty condition is not too high on the total inflow entering to the Flinders floodplain from the headwater catchments.

Table 4.4 Impact of the Cave Hill dam on inundation area and depth for flood events of different magnitude in the Flinders floodplain

REDUCTION COMPARED TO BASELINE	Cave Hill (2001)	Cave Hill (2009)	Cave Hill (2011)
Maximum area of inundation	0.1%	0%	0.86%
Average inundation area	0.2%	0.01%	0.51%
Average inundation depth	0.1%	0%	0.15%

Gilbert floodplain

Figure 4.10 shows the temporal variation at 6-hourly interval in the number of inundated cells in the Gilberts floodplain for the flood events of 2001, 2009 and 2011 under the baseline condition and the scenario of empty reservoirs of the Dagworth and Greenhills dams. Table 4.5 compares the changes in inundation characteristics due to the development scenarios compared to the baseline condition for the three selected flood events.

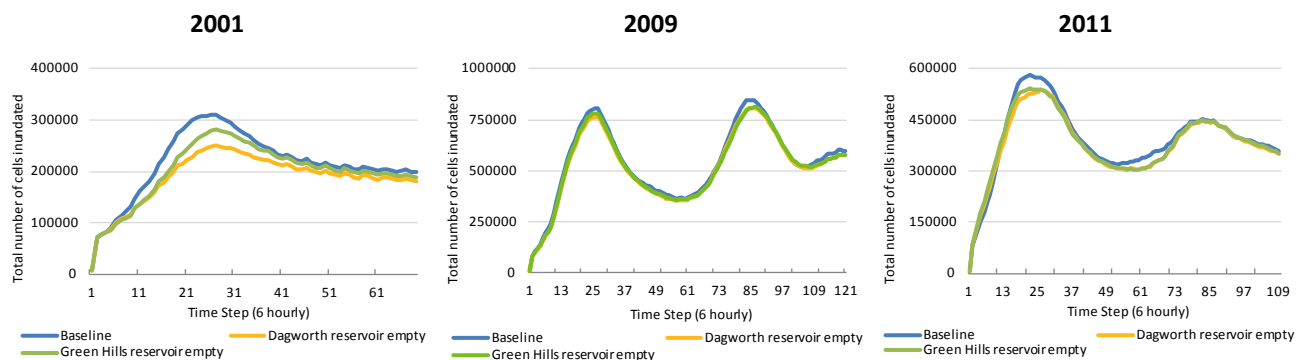


Figure 4.10 6-hourly time series of number of cells inundated during 2001, 2009 and 2011 flood events under current condition and Dagworth and Greenhills reservoirs empty scenarios in the Gilbert floodplain

Table 4.5 Impacts of Dagworth and Greenhills dams on inundation area and depth for flood events of different magnitudes in the Gilbert floodplain

REDUCTION COMPARED TO BASELINE	DAGWORTH (2001)	GREENHILLS (2001)	DAGWORTH (2009)	GREENHILLS (2009)	DAGWORTH (2011)	GREENHILLS (2011)
Maximum area of inundation	19.5%	9.7%	4.6%	4.3%	7.8%	7.1%
Average inundation area	13.0%	7.4%	3.5%	2.7%	3.5%	2.5%
Average inundation depth	3.3%	1.8%	0.07%	0.05%	0.6%	0.8%

The impact of Dagworth dam on inundation extent is relatively larger compared to the Greenhills dam. For example, the maximum area of inundation during the 2001 flood event reduced by 19.5% under Dagworth reservoir empty scenario compared to 14.8% reduction under Greenhills reservoir empty scenario. Similarly, average inundation depth of 2001 flood event reduced by 3.7% and 2.2% under Dagworth and Greenhills reservoir empty scenarios, respectively. The impact of the two dams is the highest during the lowest magnitude flood (2001) and the least during the highest magnitude flood (2009). For example, the maximum area of inundation reduced by 19.4% during the 2001 flood under the Dagworth reservoir empty scenario, and by 9.5% and 4.7% during the 2011 and 2009 flood events, respectively. The impact of the two dams on average inundation depth of the 2009 flood event is less than 1%.

4.3.3 SEA LEVEL RISE SCENARIOS

Flinders floodplain

Figure 4.11 compares the total number of pixels inundated due to the projected SLR compared to the current condition during the flood events of 2001, 2009 and 2011 in the floodplain of the Flinders Catchment. Table 4.6 summarises the changes in inundation characteristics of the three events under the SLR scenario.

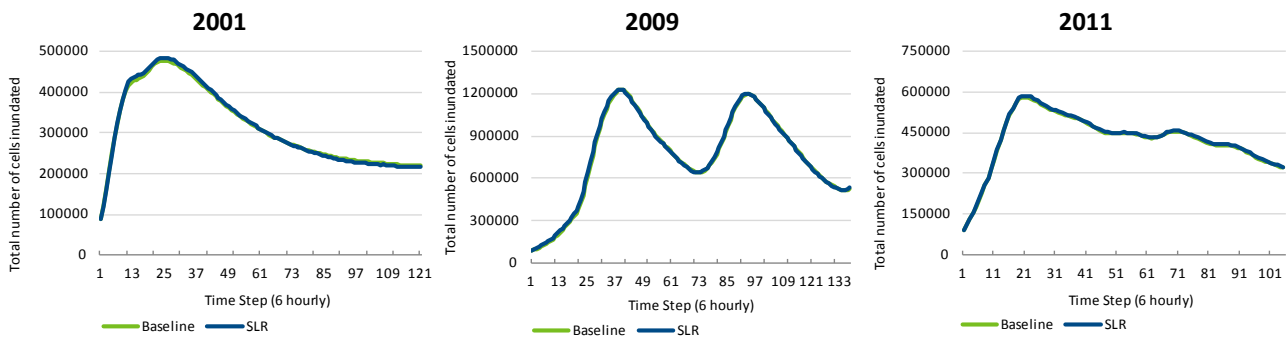


Figure 4.11 6-hourly time series of number of cells inundated during 2001, 2009 and 2011 flood events under current condition and SLR scenario in the Flinders floodplain

Table 4.6 Impact of the SLR on inundation area and depth for flood events of different magnitudes in the Flinders floodplain

CHANGES COMPARED TO BASELINE	FLOOD EVENT OF 2001 WITH SLR	FLOOD EVENT OF 2009 WITH SLR	FLOOD EVENT OF 2011 WITH SLR
Maximum area of inundation	1.4%	0.2%	1.0%
Average inundation area	0.3%	0.5%	0.6%
Average inundation depth	2.7%	1.0%	1.6%

The results show that the projected SLR will cause only small increase in both inundation extent and depth in the Flinders floodplain. The increase in the maximum area of inundation varies between 0.2 to 1.4% with the highest increase occurred in 2001 and the lowest increase in 2009, which is the largest magnitude flood event. The increase in average inundation depth varies between 1 to 2.7% with the highest increase in 2001 and the lowest in 2009. The coastal floodplain with tidal influence in the Flinders catchment is only a small part of the total floodplain (see Figure 3.21) and because of that the impact of SLR is limited on the Flinders floodplain inundation.

Gilbert floodplain

Figure 4.12 presents 6-hourly time series of number of inundated cells during the flood events of 2001, 2009 and 2011 under the baseline condition and the projected SLR scenario in the Gilbert floodplain. Table 4.7 summarises the changes in inundation characteristics of the three events due to the projected SLR.

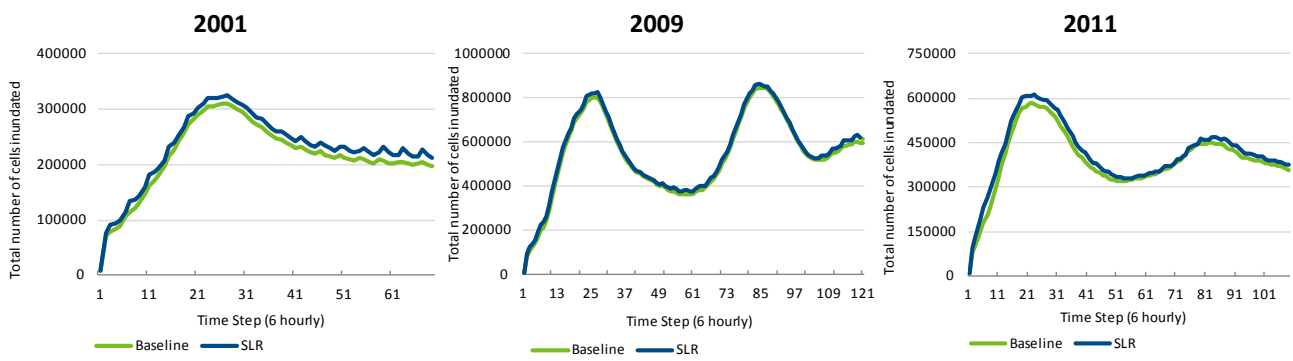


Figure 4.12 6-hourly time series of number of cells inundated during 2001, 2009 and 2011 flood events under current condition and SLR scenario in the Gilbert floodplain

Table 4.7 Impact of SLR on inundation area and depth for flood events of different magnitude in the Gilbert floodplain

CHANGES COMPARED TO BASELINE	FLOOD EVENT OF 2001 WITH SLR	FLOOD EVENT OF 2009 WITH SLR	FLOOD EVENT OF 2011 WITH SLR
Increase in maximum inundation area	4.8%	1.7%	5.3%
Increase in average inundation area	5.9%	2.7%	5.3%
Increase in average depth	25.2%	9.7%	12.7%

The impact of the projected SLR is much more prominent in the Gilbert floodplain compared to the Flinders floodplain as the significant part of the floodplain of the Gilbert catchment is located along the coastal line and influenced by tide (see Figure 3.26). The increase in the maximum area of inundation varies between 1.7 to 5.3% with the highest increase occurred in 2011 and the lowest increase in 2009. The increase in average inundation depth varies between 9.7 to 25.2%.

4.3.4 SCENARIO ANALYSIS UNDER FUTURE CLIMATE AND DEVELOPMENT

As the impact of Cave Hill empty reservoir condition was found to be negligible on Flinders floodplain inundation, the combined scenario of Cdry climate and empty reservoirs was not undertaken for the Flinders floodplain.

Gilbert floodplain

The 6-hourly time series of number of inundated cells during the flood events of 2001, 2009 and 2011 in the Gilbert floodplain under baseline condition and the combined scenario of Cdry climate and Dagworth reservoir empty are shown in Figure 4.13. Table 4.8 summaries the impact of the combined scenario on the maximum and average inundation areas and average inundation depth during the three selected flood events.

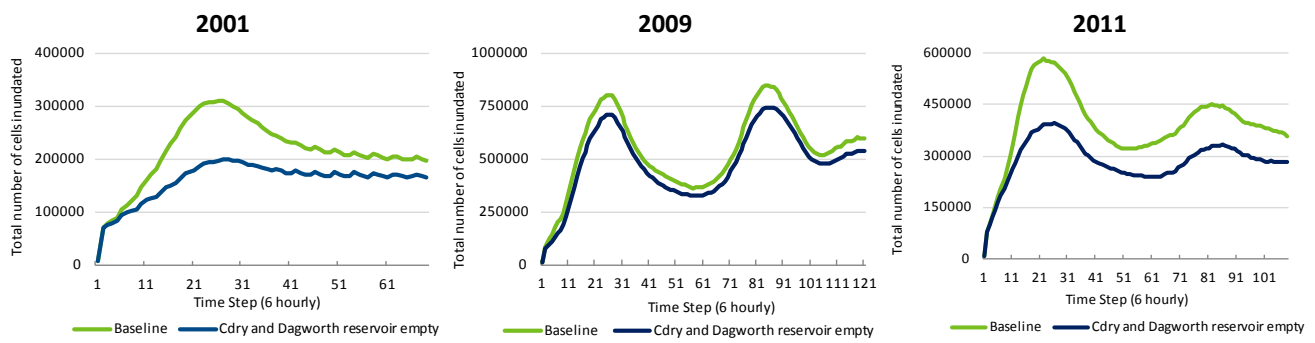


Figure 4.13 6-hourly time series of number of cells inundated during 2001, 2009 and 2011 flood events under current condition and Cdry and Dagworth reservoir empty scenario in the Gilbert floodplain

Table 4.8 Impacts of the Cdry and Dagworth dam on inundation area and depth for flood events of different magnitudes in the Gilbert floodplain

REDUCTION COMPARED TO BASELINE	2001 FLOOD EVENT WITH CDRY+DAGWORTH EMPTY	2009 FLOOD EVENT WITH CDRY+DAGWORTH EMPTY	2011 FLOOD EVENT WITH CDRY+DAGWORTH EMPTY
Maximum area of inundation	35.3%	12.2%	31.8%
Average inundation area	25.7%	11.2%	26.7%
Average inundation depth	8.3%	0.9%	8.3%

The impact of the combined scenario is the highest on both inundation area and depth for all flood events compared to all other scenarios. Under the combined scenario of Cdry and the empty reservoir of Dagworth dam, the maximum area of inundation will be reduced by between 12.2 to 35.3% and average inundation area by between 11.2 to 26.7%. The reduction of average inundation depth would be up to 8.3%.

5 Assessment of Wetland connectivity

5.1 Rationale

Hydrological connectivity is a crucial determinant of ecosystem structure and functioning in freshwater habitats (Ward 1989; Pringle 2001; Hughes et al., 2009) and drives linkages among ecosystem elements in space and time (Fullerton et al., 2010). Habitat quality and the ecological integrity of floodplain wetlands depends on many factors, but a key determinant is how the wetland is hydrologically connected to the main river channel over time (Bunn and Arthington, 2002). In a wet tropical region, permanent flows often provide continuous in-stream connectivity; however, off-stream wetlands may be isolated for significant periods when low flows are constrained to the main stream channels. Flood flows provide the opportunities for these off-stream wetlands to be connected with the main streams. During floods there is an exchange of water, sediments, chemicals and biota between the main channels and floodplain wetlands (Thoms, 2003). The importance of overbank flow connection for the productivity and exchanges of major aquatic biota in river-floodplain systems has been emphasized in many studies (e.g. Junk et al., 1989; Welcomme et al., 2006). The single most important factor for the persistence of the fish assemblage in an isolated wetland is the flow connection between the wetland and a main stream (Lasne et al., 2007). A high connectivity level is needed to conserve native fish diversity because the number of protected and native species increases with connectivity and the number of alien species and individual can increase with isolation (Bunn and Arthington, 2002; Lasne et al., 2007).

Floodplain wetlands in the wet-dry tropics are under increasing pressure from water resource development, and there is a need for methods to assess the biophysical dynamics of these extensive and often remote ecosystems (Ward et al., 2013). These systems are characterized by strong seasonality in precipitation, with high river flows and extensive floodplain inundation occurring over an often brief wet season, followed by low to zero flows and waterbody contraction and isolation during the dry season (Cresswell et al., 2009; McDonald & McAlpine, 1991). The timing, extent, duration, and inter-annual variability of inundation control the exchanges of water and biota between rivers and their floodplains and the degree of seasonal isolation and desiccation of waterbodies determine the distribution of aquatic refugia that persist during the dry season (Junk et al., 1989). Wet-dry tropical savannas that are subject to seasonal inundation exhibit large differences in the length of the wet season and the amount of rainfall over the dry season (Warfe et al., 2011).

The Flinders and Gilbert Rivers are unregulated river systems and they support a large number of off- and on-stream wetlands of distinct ecology and environmental value. An important issue for the management of these wetlands under present and future climate and development is to know the extent, timing and duration of their connectivity to drive ways to maintain or even enhance an optimal level of connection and biophysical exchanges between off-stream wetlands and a main channel. This information is scarce for majority of the Australian floodplains including the Flinders and Gilbert catchments since field based monitoring of connectivity for numerous individual wetlands is both difficult and time consuming. Several studies have used a combination of remotely sensed inundated area and concurrent river flow to predict how flooded area changes with river flow (Townsend and Walsh, 1998). The same approach has also been used to quantify how the number of inundated wetlands changes with river flow (Shaikh et al., 2001; Frazier et al., 2003). However, this approach is not dynamic and only gives information on potential wetland inundation when flow is not changing rapidly (due to the time difference between when the remote sensing images can be obtained and the peak of inundation) and it is not possible to define the duration of wetland connectivity, which can have an important influence on wetland ecology. In this study hydrodynamic modelling is used, which can quantify the time course of flood inundation and, by combing this with high resolution topography, the duration, frequency and timing of connectivity between wetlands and the main streams.

5.2 Water assets for connectivity assessment

A series of ecologically important wetlands and water bodies are located in the Flinders and Gilbert River catchments that provide important aquatic habitat for a broad range of species. In a companion technical report on Ecological responses to changes in flow, Waltham et al., 2013 compiled a map of the important ecological assets across the Assessment region combining information obtained from the Ramsar list of wetlands, the Dictionary of Important Wetlands in Australia, the Register of National Estate, nature reserves/protection areas, wetlands and springs and Regional Ecosystem (V7) data from the Queensland Government, the list of wetland and springs located across the region mapped by Department of Sustainability, Environment, Water, Population and Communities (DSEWPaC), the Register of National Estate is compiled by the Australian Heritage Commission (AHC), list of the declared Fish Habitat Areas (FHA) by the Department of Agriculture, Fisheries and Forestry (DAFF), Queensland Government, discussion with local community members and Northern Gulf NRM Group, published reports and other local expert knowledge (Figure 5.1). Characteristics of these assets are presented in Waltham et al., 2013.

Based on above sources 119 water assets were identified in the Flinders and seven in the Gilbert catchments, including bores and springs. The above list was found to have some repetitions of water assets between sources. Given the very large number of water assets in the Flinders catchment, several 'spring' water bodies located within close proximity to one another were excluded from connectivity analysis. Finally, 85 wetlands were selected in the Flinders catchment and seven wetlands in Gilbert for the connectivity analysis. Brief summaries of the physical properties of individual wetlands in the Flinders and Gilbert catchments are presented in Table 5.1 and Table 5.2, respectively. The selected wetlands include both on- and off-stream wetlands and are located across the floodplain ranging from 0 to 45 km from a major stream. Some wetlands are located outside the boundary of overbank inundation. These wetlands however could be connected to the river through floodplain creeks.

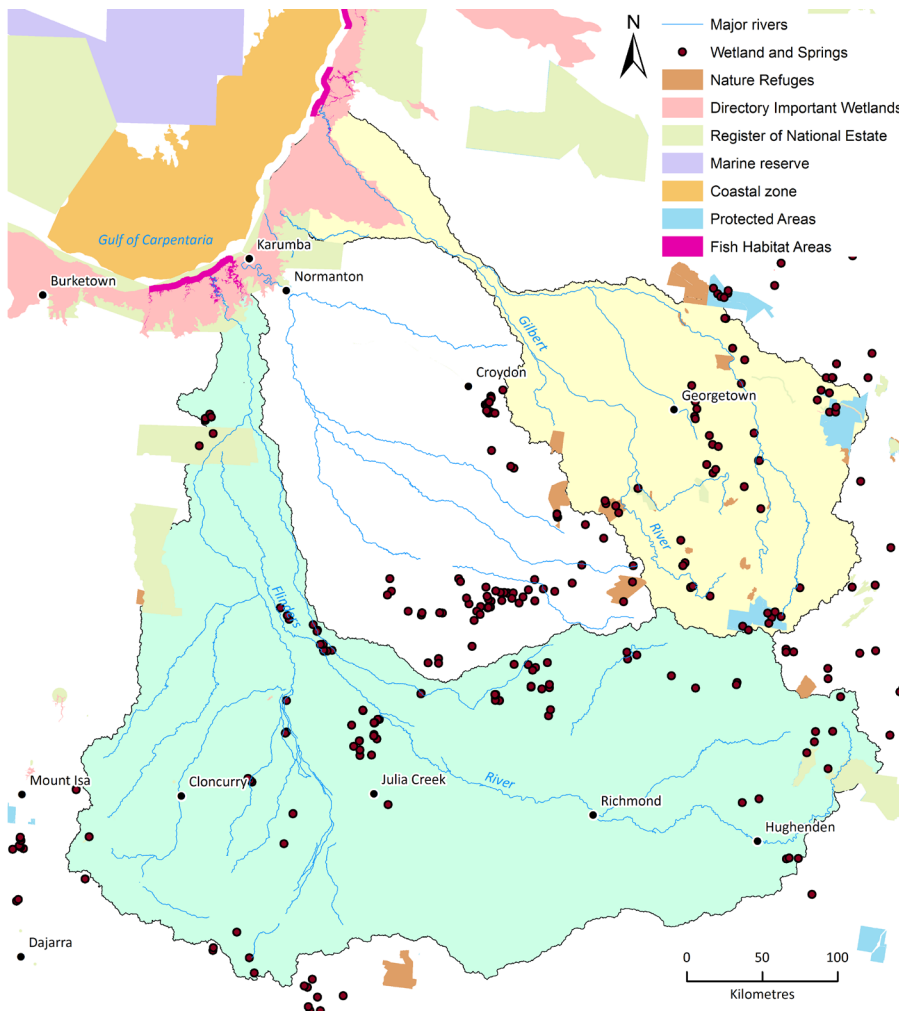


Figure 5.1 Spatial representation of important ecological assets across the Assessment region

Table 5.1 List of wetlands in the Flinders and their physical properties.

ID	WETLAND NAME	SOURCE	LOCATION	NEAREST STREAM	DISTANCE FROM STREAM (M)
1	Walker's Creek Weir	Fish Studies	Off-stream	Walker Creek	466
2	Mutton Hole Wetland	Register of National Estate	Off-stream	Norman River	785
3	Stranded Fish Lake	DIWA coastal small	Off-stream	Flinders River	5,664
4	Shady Lagoon	Fish Studies	Off-stream	Norman River	979
5	Glenore Weir	Fish Studies	On-stream	Norman River	0
6	Burketown crossing	Fish Studies	On-stream	Flinders River	0
7	Burke & Wills monument	Fish Studies	Off-stream	Flinders River	2,784
8	Buffalo Lake Aggregation	DIWA coastal small	Off-stream	Flinders River	30,577
9	The Sisters	Fish Studies	On-stream	Clarina Creek	0
10	Cremeries Waterhole	Fish Studies	Off-stream	Clarina Creek	491
11	Wallabadah Waterhole	Fish Studies	On-stream	Clarina Creek	0
12	Homeward Bound Dam	Register of National Estate	Off-stream	Clarina Creek	45,717
13	Big Mosquito Lagoon	Fish Studies	Off-stream	Norman River	924
14	Walker's Bend	Fish Studies	On-stream	Flinders River	0
15	40 Mile Lagoon	Fish Studies	On-stream	Norman River	0
16	Margaret Vale	Wetlands and Springs	Off-stream	Armstrong Creek	5,920

17	Magowra	Wetlands and Springs	Off-stream	Armstrong Creek	5,493
18	Bloodwood	Wetlands and Springs	Off-stream	Armstrong Creek	9,486
19	Sydney Harbour	Wetlands and Springs	Off-stream	Armstrong Creek	9,931
20	BangBang	Wetlands and Springs	Off-stream	Cloncurry River	7,866
21	Dead Calf Lagoon	Fish Studies	Off-stream	Norman River	2,265
22	Christies	Wetlands and Springs	Off-stream	Cloncurry River	7,814
23	Iffley Homestead	Fish Studies	On-stream	Spear Creek	0
24	Off channel	Fish Studies	On-stream	Dismal Creek	0
25	Earls Camp	Fish Studies	On-stream	Saxby River	0
26	12 Mile Lagoon	Fish Studies	On-stream	Mundjuro Creek	0
27	Saxby Rounup	Fish Studies	Off-stream	Spear Creek	2,167
28	10 Mile Waterhole	Fish Studies	Off-stream	Cloncurry River	1,015
29	TrentonI	Wetlands and Springs	Off-stream	Norman River	7,111
30	Seaward Waterhole	Fish Studies	Off-stream	Cloncurry River	4,919
31	SandySpr	Wetlands and Springs	Off-stream	Mundjuro Creek	5,340
32	Muk Quibunya	Wetlands and Springs	On-stream	Mundjuro Creek	0
33	Lyrian Waterhole	Fish Studies	On-stream	Saxby River	0
34	Tailing yard sps	Wetlands and Springs	Off-stream	Mundjuro Creek	2,904
35	PlainSpr	Wetlands and Springs	Off-stream	Norman River	19,607
36	Cattle Camp Sp	Wetlands and Springs	Off-stream	Norman River	22,181
37	Stanley Waterhole	Fish Studies	On-stream	Cloncurry River	0
38	Cooradine WH	Wetlands and Springs	On-stream	Mundjuro Creek	0
39	Middle Sps	Wetlands and Springs	Off-stream	Mundjuro Creek	16,240
40	boxhole-mud,p	Wetlands and Springs	Off-stream	Flinders River	2,588
41	Cooradin	Wetlands and Springs	Off-stream	Mundjuro Creek	4,650
42	Mt Fort Bowen Sps	Wetlands and Springs	Off-stream	Flinders River	4,302
43	mudsoda,p	Wetlands and Springs	Off-stream	Flinders River	1,996
44	Crocodile Waterhole	Fish Studies	On-stream	Saxby River	0
45	Crocodile Sps	Wetlands and Springs	Off-stream	Saxby River	569
46	The Lake	Fish Studies	Off-stream	Spear Creek	2,227
47	mud,p	Wetlands and Springs	On-stream	Saxby River	0
48	mud,s(Mt Brown/Little)	Wetlands and Springs	Off-stream	Saxby River	2,160
49	Lower Sps(Mt.BorownD)	Wetlands and Springs	Off-stream	Flinders River	1,597
50	Washpool Crk Sps	Wetlands and Springs	Off-stream	Saxby River	534
51	mudsoda,s	Wetlands and Springs	Off-stream	Flinders River	1,050
52	Reedy Crk Sps	Wetlands and Springs	Off-stream	Flinders River	2,681
53	Upper Sps(Mt.BorownC)	Wetlands and Springs	Off-stream	Flinders River	1,116
54	BundaB1	Wetlands and Springs	Off-stream	Mundjuro Creek	1,041
55	BundamudSps	Wetlands and Springs	On-stream	Mundjuro Creek	0
56	Sedan dip	Fish Studies	On-stream	Cloncurry River	0
57	Berinda 2	Wetlands and Springs	Off-stream	Saxby River	180
58	Berinda Sps	Wetlands and Springs	Off-stream	Saxby River	330
59	Berindabaremudcratersx	Wetlands and Springs	Off-stream	Saxby River	540

60	N-GilliatBore	Wetlands and Springs	Off-stream	Gilliat River	2,581
61	Dalgonally Waterhole	Fish Studies	On-stream	Julia Creek	0
62	LaraBoreE,p	Wetlands and Springs	Off-stream	Flinders River	7,783
63	RuthvenBore,p	Wetlands and Springs	Off-stream	Alick Creek	2,863
64	BoonookeBoreNo7	Wetlands and Springs	Off-stream	Alick Creek	3,994
65	StudPaddBoreNo3,p	Wetlands and Springs	Off-stream	Alick Creek	6,557
66	WindmillBoreNo1-A	Wetlands and Springs	Off-stream	Alick Creek	7,200
67	Rocky Waterhole	Fish Studies	On-stream	Alick Creek	0
68	mud,s	Wetlands and Springs	On-stream	Gilliat River	67
69	Fullarton Bore	Wetlands and Springs	Off-stream	Gilliat River	845
70	Bauhinia	Wetlands and Springs	Off-stream	Julia Creek	4,077
71	SpringsBoreNo4	Wetlands and Springs	On-stream	Julia Creek	0
72	mound,p	Wetlands and Springs	Off-stream	Julia Creek	283
73	PigeonCrkBore	Wetlands and Springs	Off-stream	Julia Creek	7,581
74	mud,s	Wetlands and Springs	On-stream	Julia Creek	0
75	Punchbowl Waterhole	Fish Studies	Off-stream	Alick Creek	3,756
76	Rockvale Station	Fish Studies	Off-stream	Flinders River	2,277
77	Fort Const-1	Wetlands and Springs	On-stream	Williams River	0
78	Fort Const-main	Wetlands and Springs	Off-stream	Williams River	1,006
79	Eddington Waterhole	Fish Studies	On-stream	Eastern Creek	0
80	2 Mile Waterhole	Fish Studies	On-stream	Cloncurry River	0
81	Southern Gulf MIN	DIWA coastal large	On-stream	Flinders River	0
82	Lignum Swamp	DIWA	Off-stream	Cloncurry River	5,460
83	Fish Habitat (Flinders River mouth)	Fish Habitat	Off-stream	Flinders River	11,036
84	Fish Habitat (Bynoe River mouth)	Fish Habitat	Off-stream	Bynoe River	137
85	Fish Habitat (Spring Creek mouth)	Fish Habitat	Off-stream	Flinders River	3,648

Table 5.2 List of wetlands in the Gilbert catchment and their physical properties.

ID	WETLAND NAME	SOURCE	LOCATION	NEAREST STREAM	DISTANCE FROM STREAM (M)
1	Macaroni Swamp	DIWA coastal small	Off-stream	Gilbert River	11,139
2	Unnamed	Fish Studies	Off-stream	Gilbert River	849
3	Gilbert River	Fish Studies	On-stream	Gilbert River	0
4	Mutton Hole Wetland Conservation Park	Register of National Estate	Off-stream	Wills Creek	3,977
5	Southeast Karumba Plain	DIWA coastal large	Off-stream	Smithburne River	5,956
6	Smithburne - Gilbert Fan	DIWA coastal large	On-stream	Smithburne River	97
7	Fish Habitat - Gilbert River mouth	Fish Habitat	Off-stream	Gilbert River	1,134

5.3 Method of Connectivity Analysis

Wetland connectivity analysis was undertaken in the floodplain hydrodynamic modelling domains of the Flinders and Gilbert catchments (refer to Figure 1.10). Connectivity of the selected wetlands with the major streams was considered through floodplain flows (i.e. overbank flooding). Hydrological connection

and disconnection during overbank flooding were computed by identifying contiguous flow paths at every 6-hr time step. For this purpose, it was required to define a threshold water depth to ensure continuous water connection across minor topographic variations in the landscape. Considering low resolution of the topographic data used in the inundation modelling and the high roughness of floodplain landscape due to vegetation cover, a threshold water depth of 30 cm was considered to suitable (Karim et al., 2012). While deciding the threshold height, it was also noted that movement of fish can be impeded at low water depths (Bunn and Arthington, 2002). Based on the outputs of the two-dimensional hydrodynamic model, time series information on wet or dry cells were first identified at each wetland and along the intervening floodplain pathways. This information was used to compute the timing and duration of hydrologic connection of the wetlands with other water bodies and/or the main streams. A wetland was considered hydrologically connected to other water bodies when it started receiving water from overbank flow and was considered disconnected when water receded below its bank level as shown in Figure 5.2.

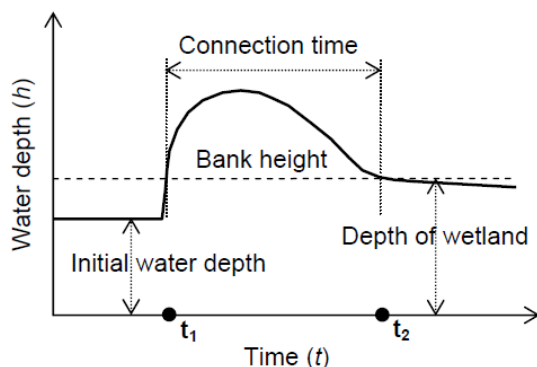


Figure 5.2 A schematic representation of wetland connectivity based on water depth and wetland bank height. Connection to the flood waters and surrounding water bodies starts at time t_1 and ends at t_2 when the depth of inundation falls below the wetland bank height.

In this figure, t_1 and t_2 represent the start and the end of hydrologic connection, respectively. The difference between t_2 and t_1 is the duration of the hydrologic connection. Connection time and duration of connection are different for floods of different magnitudes. In general, large flood events produce early and longer duration of hydrologic connection. Connection time of a particular wetland to the river system was computed based on the time series of water depths derived from the two-dimensional hydrodynamic model at six-hourly time steps. An algorithm was developed to uniquely identify areas of contiguous water during each time step, by tagging all water bodies and river sections which were contiguous in that time step. The same procedures were repeated for all time steps and the results were accumulated to obtain the temporal sequence of connection and disconnection. The analysis technique is described in Karim et al. (2012).

Most of the wetlands in the Flinders and Gilbert floodplains (except those located in the coastal fringes) are small in size and these small wetlands are considered as “point” wetlands for connectivity analysis. Each of these wetlands was represented by a single grid in the hydrodynamic modelling. Polygon wetlands (mostly DIWA) were represented by a number of model grids encompassing the areal extent of the wetlands. Figure 5.3 and Figure 5.4 show the location of wetlands within the hydrodynamic modelling domains in the Flinders and Gilbert catchments, respectively. Connectivity of wetlands was investigated for the flood events of 2001, 2009 and 2011.

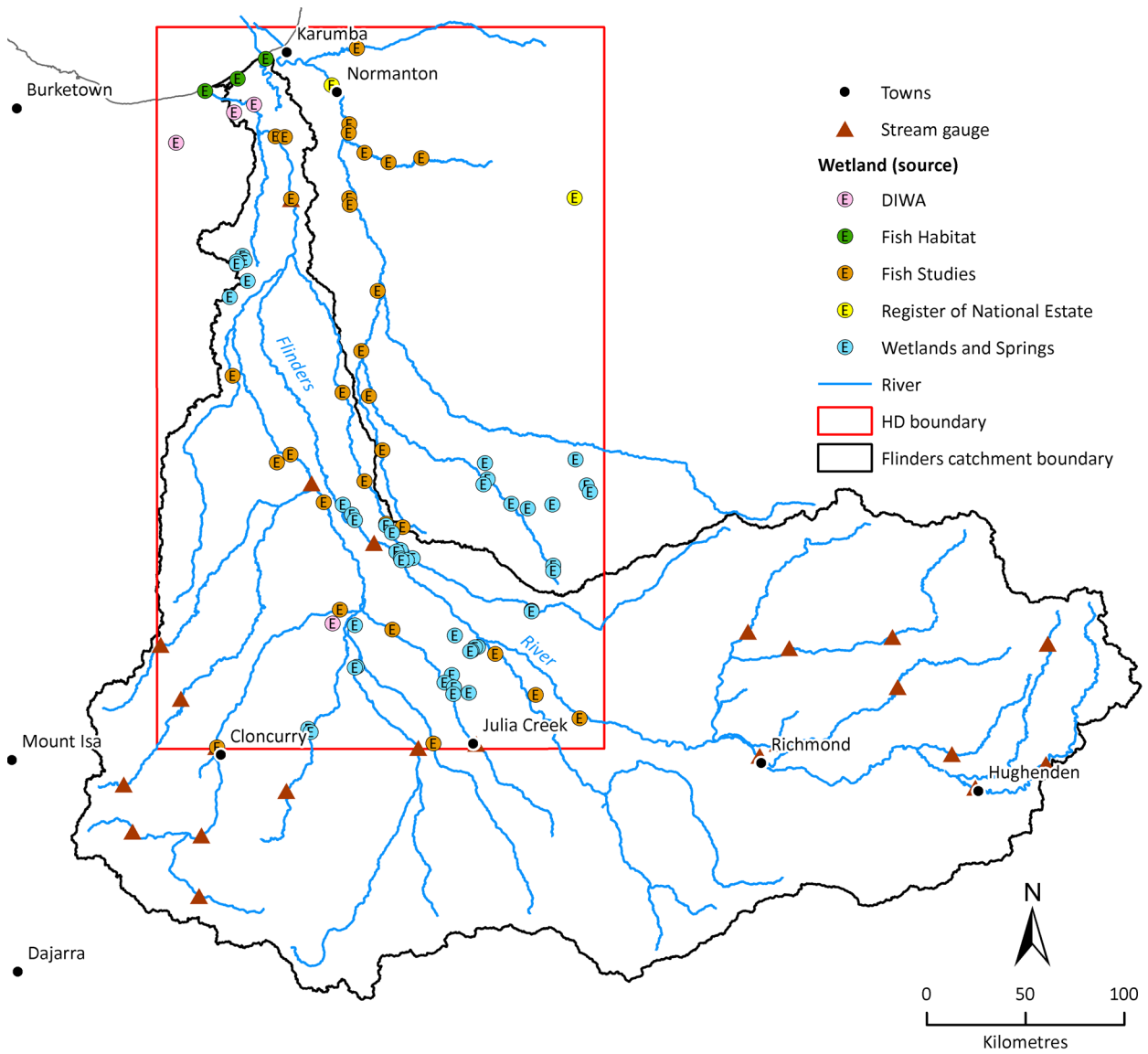


Figure 5.3 Map showing locations of the wetlands and major streams in the Flinders Catchment. The red rectangle shows the hydrodynamic modelling boundary.

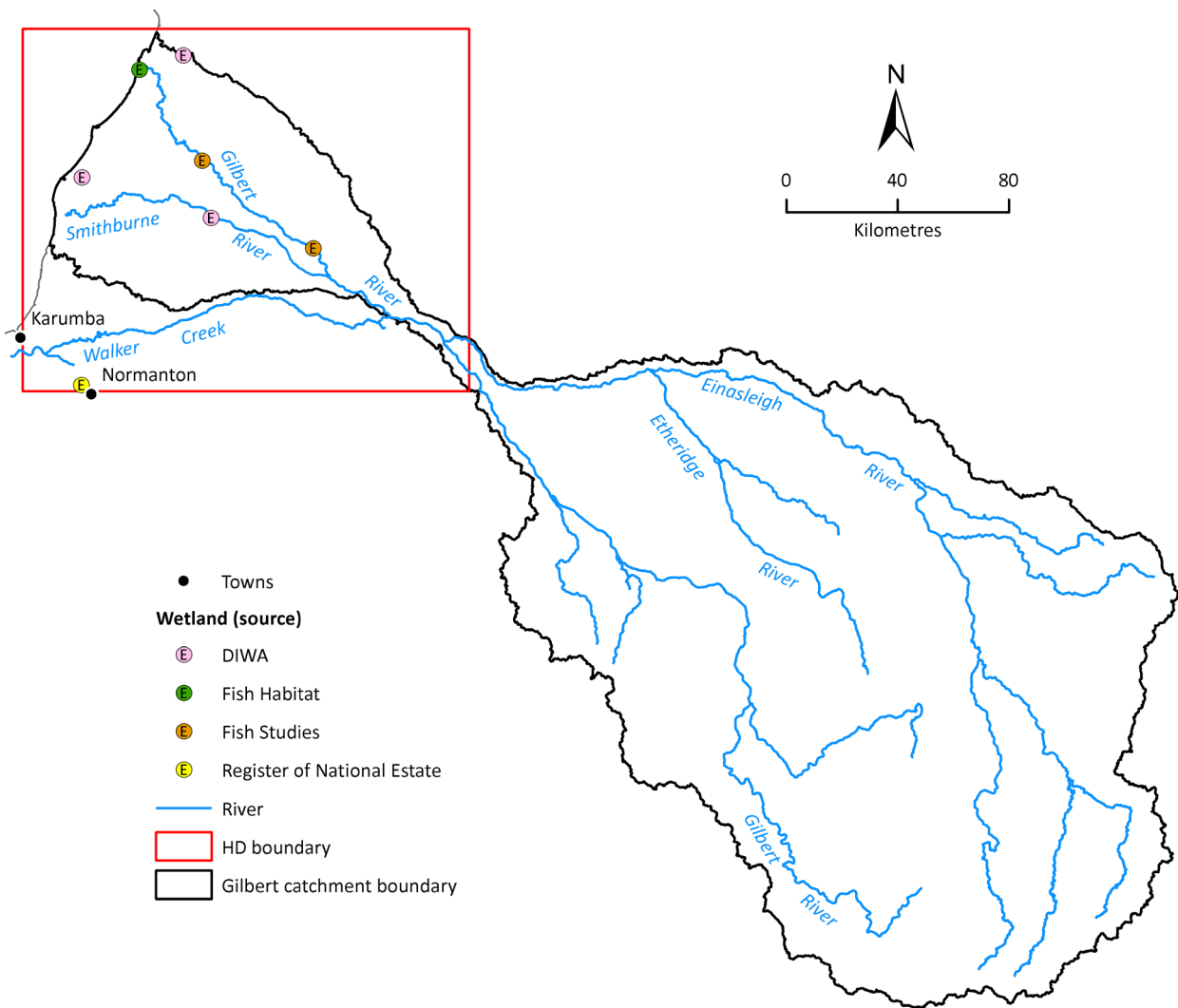


Figure 5.4 Map showing location of the wetlands and major streams in the Gilbert Catchment. The hydrodynamic study (red rectangle) was limited to lower Gilbert floodplain only.

The Flinders is a large catchment and it consists of several large rivers including Flinders, Cloncurry and Saxby Rivers (Figure 5.3). The Gilbert catchment is relatively small and it consists of two large rivers, Gilbert and Einasleigh, in the upper catchment and Smithburne River and Walker Creek in the lower catchment (Figure 5.4). During floods, off-stream wetlands on the floodplain connect to those streams by overbank flows. Table 5.3 shows the list of streams (e.g. rivers and creeks) that were used to estimate connectivity of individual wetlands in the Flinders and Gilbert catchments.

Table 5.3. List of streams that were used to assess connectivity with wetlands in Flinders and Gilbert catchments.

STREAM NAME	TYPE	CATCHMENT
Alick	Creek	Flinders
Bynoe	River	Norman
Clarina	Creek	Norman
Cloncurry	River	Flinders
Corella	River	Flinders
Dugald	River	Flinders
Flinders	River	Flinders
Gilbert	River	Gilbert
Gilliat	River	Flinders

Julia Creek	Creek	Flinders
Mundjuro	Creek	Norman
Norman	River	Norman
Saxby	River	Flinders
Spear	Creek	Norman
Smithburne	River	Gilbert
Walker	Creek	Gilbert
Williams	River	Flinders

5.3.1 FLINDERS FLOODPLAIN

Duration of Inundation

The time series of simulated inundation depths at 6-hourly interval by the two-dimensional hydrodynamic model were used to compute the inundation duration. By accumulating this information for the entire period of simulation, the total inundation duration at each computational grid was estimated. Figure 5.5 shows an example of inundation duration map for the flood event in 2009 (2nd largest in records). In general, duration of inundation is longer in the lower part of the floodplain. This is primarily due to the flat land topography in this region compared to the upper part of the floodplain. The results also show longer duration of inundation on both sides of the Flinders River. Large inflow from the upper catchment produced several kilometres of floodplain inundation across the Flinders River on both banks. It is noticed that floodplains of Flinders and Norman merged together at the lower part of the catchments and produced relatively longer duration of inundation. The area and duration of inundation are small along the Cloncurry River and Julia Creek in the upper part. This is mainly due to the small catchment area above.

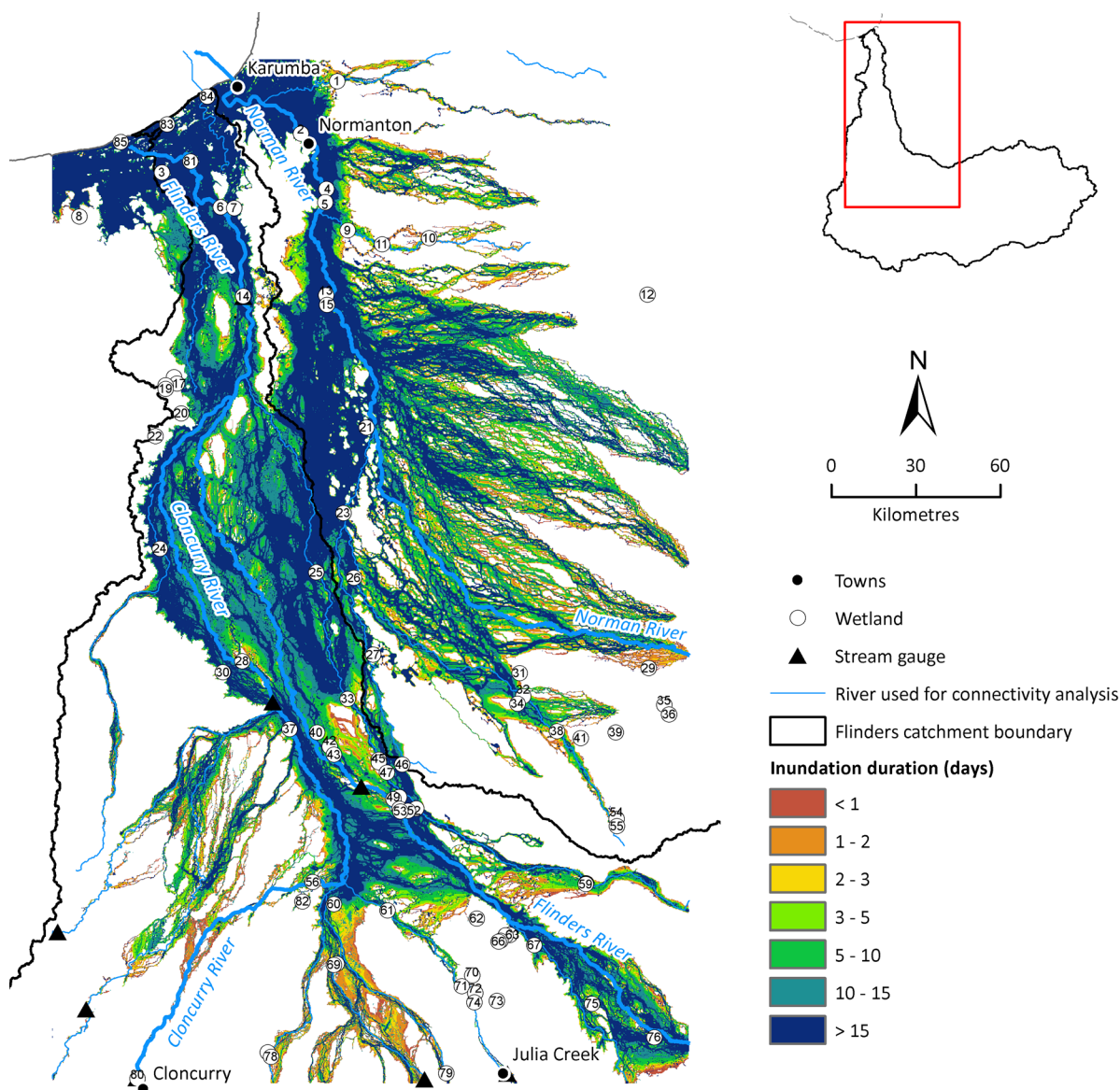
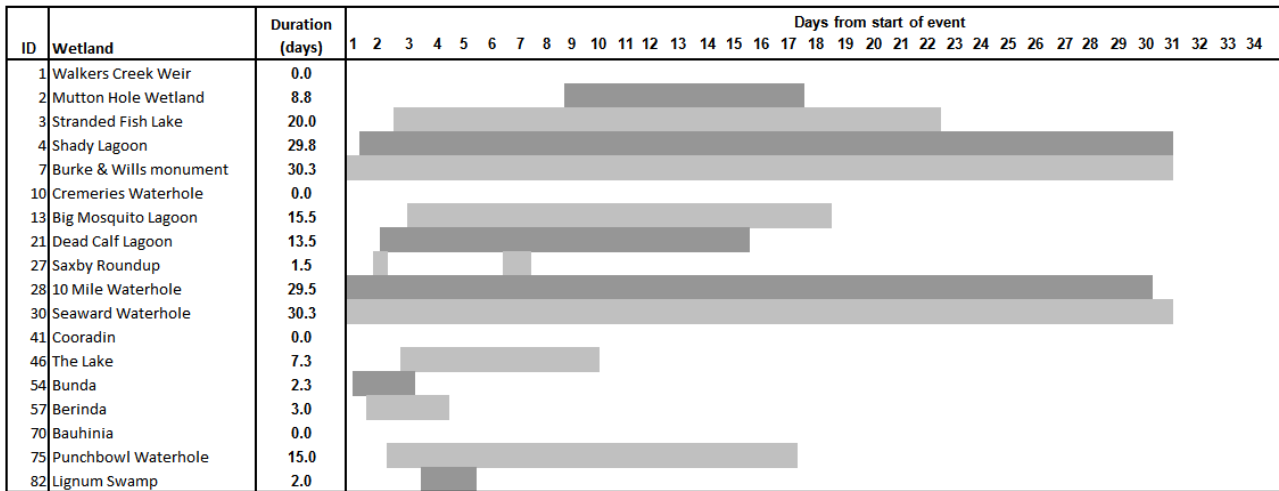


Figure 5.5 Typical example of spatial variation in inundation duration across the floodplain for the flood in 2009.

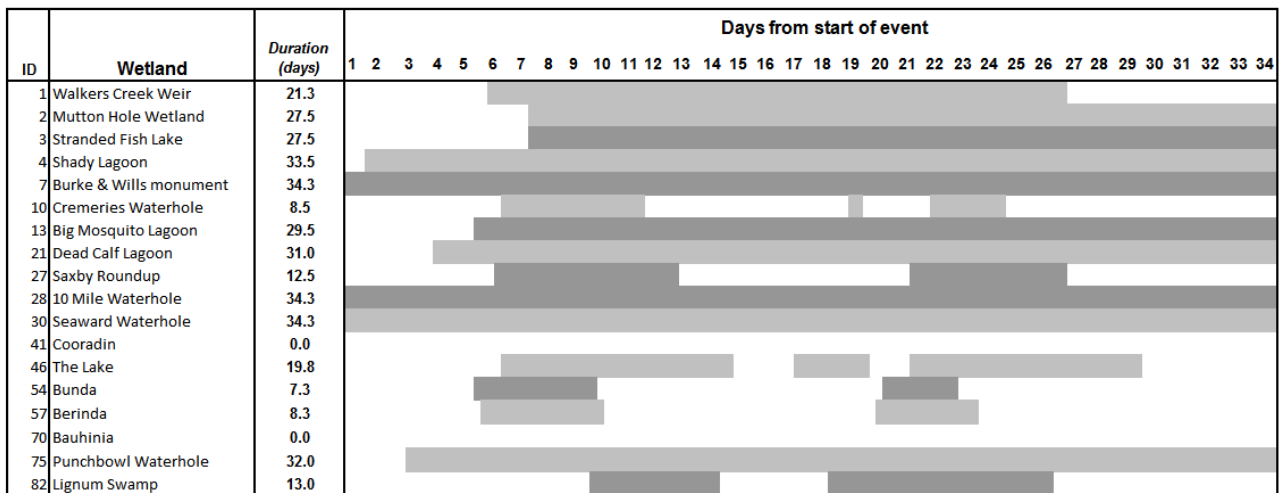
Wetland Connectivity

Figure 5.6 shows the timing and duration of hydrologic connection of the wetlands to the rivers for a number of selected wetlands (ecologically important off-stream wetlands only) during the flood events of 2001, 2009 and 2011. Four wetlands (e.g. Shady Lagoon, Burke & Wills monument, 10 Mile Waterhole, Seaward Waterhole) showed continuous connection with streams during the three flood events. These are large wetlands and located close proximity to rivers. For other wetlands, connectivity varies from 0 to 30 days depending on their locations on the floodplain and the magnitudes of floods. The flood event of 2009 (which is the second biggest flood in record) produced the highest duration of connectivity. As expected, large flood produced longer duration of connection. However local variation in runoff and inflow from upstream can produce different results. For example, the flood event in 2001 is bigger than the 2011 flood event in terms of its duration and the magnitude of the peak. However, due to local variations in flow, connectivity for some wetlands (e.g. Walker Creek Weir, Mutton Hole wetland) in 2011 is longer than in 2001.

a) Flood 2001



b) Flood 2009



c) Flood 2011

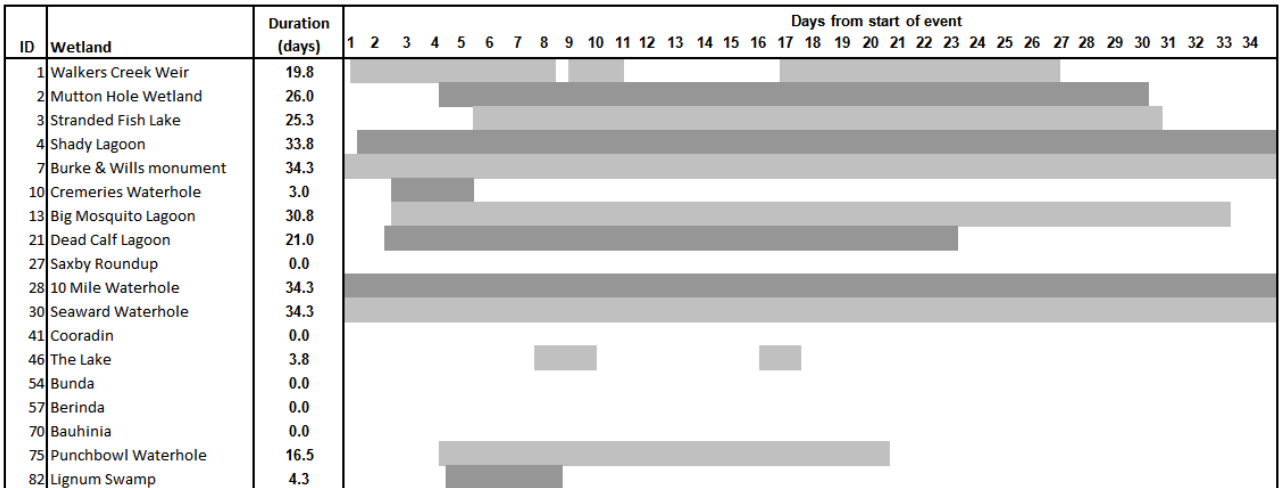


Figure 5.6 Timing and duration of connectivity of selected wetlands in the Flinders Catchment for (a) 2001, (b) 2009 and (c) 2011 flood events.

The level of connectivity of individual wetland was categorised into low (0 to 10 days), medium (11 to 20 days) and high (greater than 20 days). Table 5.4 presents a summary of the overall connectivity of 85 water assets in the Flinders catchment. The quantitative estimates of connectivity for different flood events are presented in Table D1 of Appendix D . It can be seen that large number of water bodies produced high level of connections with the rivers. It is important to note that the wetlands investigated in this analysis included on-stream water assets as well. As shown in Figure 5.6, only four off-stream wetlands have high level of connectivity.

Table 5.4. Summary of connectivity status for 85 wetlands studied in the Flinders catchment. Results are presented as a percentage of total wetlands

CONNECTIVITY	% OF WETLAND CONNECTED WITH RIVERS		
	2001	2009	2011
Low	60	49	58
Medium	8	8	5
High	32	43	37

(Low: 0-10 days; Medium: 11-20 days; high: >20 days)

5.3.2 GILBERT

Duration of Inundation

Figure 5.7 shows the duration of inundation across the lower Gilbert floodplain for the 2009 flood event (2nd largest in records). The Gilbert River and Walker creek produced large area of inundation on both banks. Large inflow from the upper catchment and flat land topography produced this nature of inundation. The floodplain close to the coast also experienced longer period of inundation.

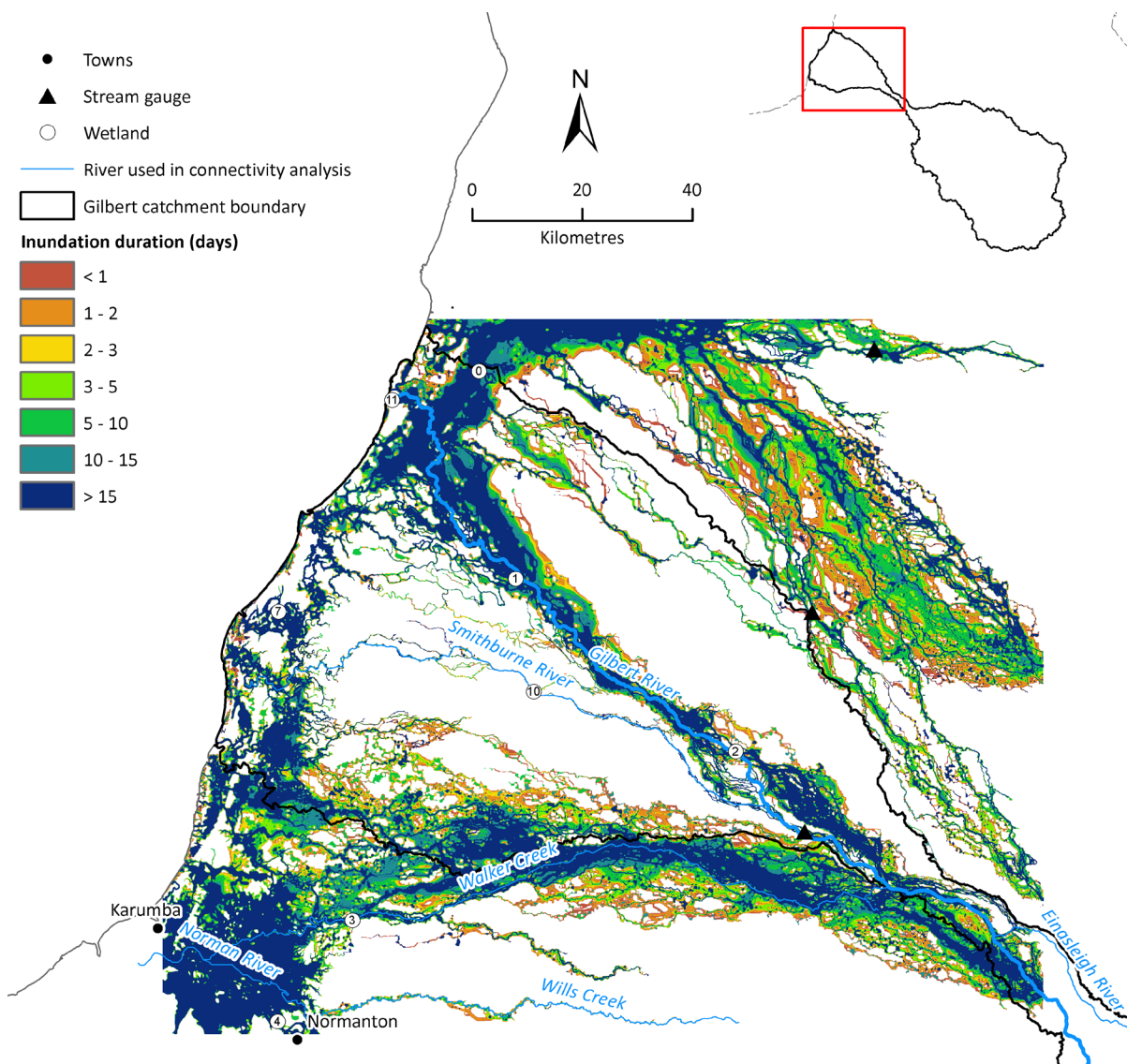


Figure 5.7 Typical example of spatial variation in inundation duration across the lower Gilbert floodplain for the flood in 2009.

Wetland Connectivity

Figure 5.8 summarises the timing and the duration of connection of the wetlands to the main rivers during the flood events of 2001, 2009 and 2011. As indicated previously, larger floods inundated more of floodplain, and they also created longer duration of connectivity. It shows all wetlands were connected to the river by overbank flows during the flood events of 2001, 2009 and 2011. All wetlands connected to the rivers during the 2009 flood event for longer period of time. This was the second largest flood on record. Only the Habitat 1 (which is located upstream) showed relatively less connectivity between the wetlands investigated. This wetland also showed a pattern of connection and disconnection in 2009 and 2011 floods. As can be seen from the flood hydrograph (see Figure 4.10), these two events have a secondary but small peak that produced reconnection after the first connection.

Table 5.6 Summary of connectivity for flood events studied for the current climate.

WETLANDS	CONNECTIVITY (DAYS)		
	2001	2009	2011
Macaroni Swamp	6.8	26.5	23.3
Fish Studies 1 (Gilbert River)	4.8	25.3	15.5
Fish Studies 2 (Gilbert River)	16.0	30.0	27.0
Walker's Creek Weir	16.0	30.0	27.0
Mutton Hole Wetland	14.0	29.3	26.5
Southeast Karumba Plain	14.8	28.8	24.8
Smithburne - Gilbert Fan	14.3	28.3	25.5
Fish Habitat 3 (Gilbert River mouth)	17.0	30.0	26.8

5.4 Changes in Wetland Connectivity under future climate and development scenarios

5.4.1 FLINDERS CATCHMENT

The effects of climate change and future development on hydrological connectivity of floodplain wetlands were investigated. A brief summary of predicted changes in connectivity for Cwet and Cdry climate, SLR and an empty reservoir condition at Cave Hill dam is presented in Table 5.7. Wet climate increased the duration of connectivity and dry climate reduced the connectivity. The effect of climate change is significant for both wet climate (~10%) and dry climate (~20%). It is noticed that the effect of climate change is disproportionate between wetlands. For example, off-stream wetlands are more affected by climate change than on-stream wetland. The effect of SLR on connectivity is small and is limited to coastal wetlands only. The effect of the proposed dam at Cave Hill is also very small. A quantitative measure of connectivity changes to individual wetlands is given in Table D2 of Appendix D .

Table 5.7 Predicted changes in connectivity for different floods due to climate change and future development

EVENT MAGNITUDE	% CHANGES OF CONNECTIVITY DUE TO			
	Wet climate	Dry climate	SLR	Empty dam (Cave Hill)
2001	+5.6	-5.5	+1.1	-0.5
2009	+3.5	-3.9	+0.7	-0.3
2011	+7.1	-17.7	+1.1	-0.1

(Note: + sign indicates increase and – indicates decrease in connectivity duration)

5.4.2 GILBERT CATCHMENT

A brief summary of predicted changes in connectivity for wet/dry climate, SLR and an empty reservoir conditions in the Gilbert catchment is presented in Table 5.6. Similar to the Flinders catchment, wet climate increased the duration of connectivity and dry climate reduced the connectivity, however, the effect is not uniform across the wetlands. For example, Fish Habitat 1 is more affected comparing with others. The reason could be due to its location. The effect of SLR on connectivity is small and limited to the coastal wetlands only. The effect of the proposed dams at Dagworth and Greenhills is also small. The effect of climate change and/or development scenarios is relatively small in terms of connectivity duration. The main reason is that the wetlands investigated are either on-stream or well connected with the main rivers through floodplain stream. A quantitative measure of connectivity changes to individual wetlands is given in Table 5.6.

Table 5.8 Predicted overall changes in connectivity for different flood magnitudes due to climate change and SLR

EVENT MAGNITUDE	% CHANGES OF CONNECTIVITY DUE TO				
	Wet climate	Dry climate	SLR	Empty dam (Dagworth)	Empty dam (Greenhills)
2001	+1.2	-2.2	+1.5	-0.9	-0.3
2009	+2.4	-3.6	+0.7	-1.7	-0.8
2011	+3.1	-12.7	+1.3	-2.0	-1.3

(Note: + sign indicates increase and – indicates decrease in connectivity duration)

Table 5.9 Effect of climate change and land development scenarios on connectivity for individual wetlands

WETLANDS	% CHANGES OF CONNECTIVITY DUE TO				
	Wet climate	Dry climate	SLR	Empty dam (Dagworth)	Empty dam (Greenhills)
Macaroni Swamp	1.4%	-7.5%	0.6%	-0.8%	0%
Fish Habitat 1 (Gilbert River)	6.7%	-17.2%	0.8%	-3.9%	-1.9%
Fish Habitat 2 (Gilbert River)	0.6%	-0.6%	0.0%	0.0%	0.0%
Walker’s Creek Weir	1.1%	-0.3%	0.0%	0.0%	0.0%
Mutton Hole Wetland Conservation Park	1.9%	-1.7%	0.6%	0.0%	0.0%
Southeast Karumba Plain	0.3%	-0.8%	3.6%	0.0%	0.0%
Smithburne - Gilbert	0.3%	-0.6%	2.8%	0.0%	0.0%
Fish Habitat 3 (Gilbert River mouth)	0.0%	-0.3%	0.3%	0.0%	0.0%

(Note: ‘+’ indicates increase and ‘-’ indicates decrease in connectivity duration)

6 Summary and Conclusions

6.1 Summary

The Flinders and Gilbert catchments have large floodplains in the low-lying middle and lower parts, where floods occur frequently. Many wetlands with high biodiversity are located in these floodplains. While flooding can be catastrophic to agricultural production in terms of loss of stock, fodder and topsoil and damage to crops and infrastructure, the wetland ecosystems in these areas are thought to be largely dependent on “flood pulses”. Hydrological connectivity between floodplain wetlands and rivers is the principal mechanism for the diversity, productivity and interactions of the major biota in river-floodplain systems.

This report addresses the flooding characteristics and hydrological connectivity between floodplain wetlands and streamflow and the potential impacts of upstream irrigation development and climate change on flood regime and wetland connectivity in the Flinders and Gilbert Catchments. The main aim of this floodplain mapping and modelling activity of the Flinders and Gilbert Agricultural Resource Assessment Project, which is part of the North Queensland Irrigated Agriculture Strategy (NQIAS), was to map and model floods in the mid-to-lower reaches of the Flinders and Gilbert catchments for the purpose of:

1. Identifying lands susceptible to flooding;
2. Estimating inundation across the floodplains under future climate and development scenarios;
3. Quantifying hydrological connectivity of wetlands in terms of
 - a. extent, timing and duration of connection of off-stream wetlands to main river channels
 - b. changes in connectivity as a result of changes to flow regime
4. Establishing a relationship between streamflow and floodplain inundation to be used by the river system models for long term simulations.

In this assessment, a combination of hydrodynamic modelling and remote sensing was used to quantify floodplain inundation, the connectivity (in terms of extent, timing and duration) of the main river channels to off-stream wetlands and assess how connectivity may change as a result of upstream regulation and climate change. The following are the major tasks that were performed:

- Task 1: use remote sensing techniques to map flood hazard in the Flinders and Gilbert catchments.
- Task 2: use a hydrodynamic model to simulate floodplain inundation under future climate and development scenarios.
- Task 3: use a hydrodynamic model and geographical information system (GIS) techniques to quantify the hydrological connectivity (in terms of extent, timing and duration) of the main river channels to off-stream wetlands and assess how this connectivity may change as a result of changes to flow regime.
- Task 4: use a hydrodynamic model to derive relationships between streamflow and floodplain inundation for river system modelling in floodplain reaches.

MODIS and Landsat imagery were used for producing maps of surface water extents to identify areas subject to flooding in the Flinders and Gilbert catchments as well as to help calibrate and validate the two-dimensional hydrodynamic models used to simulate flood events in the lower part of the two catchments. MODIS satellite data of 500 m resolution acquired at daily interval from November 2000 until March 2011 were used for producing daily maps of surface water using Open Water Likelihood (OWL) algorithm. Landsat data of 30 m resolution at 16 days interval were also used to produce water maps using the Canonical Variates Analysis tool. Composite maps of average, maximum and inundation duration were produced from daily MODIS water maps for each year from 2000 to 2011. Event based inundation maps were produced for a selected number of flood events between 2000-2011 for the calibration and validation

of the two-dimensional hydrodynamic models. Cloud cover was a problem when producing event based inundation maps, particularly for the Gilbert catchment.

MIKE 21 two-dimensional and MIKE 11 one-dimensional hydrodynamic models of the MIKEFLOOD package were used in the project. MIKE 21 was used for inundation modelling in the floodplains of the Flinders and Gilbert catchments. The total area of the hydrodynamic modelling domain of the Flinders floodplain is 82,403 km² and that of the Gilbert floodplain is 20,886 km². The spatial resolution of the hydrodynamic model was 150m and 90m for the Flinders and Gilbert floodplains, respectively.

Based on the historical records and availability of data, several flood events over the past 12 years were selected for the calibration and validation of the two-dimensional model. In the Flinders catchment two events were used for calibrating the model and two events were used for validating the model. Flood maps derived from MODIS imagery were used to compare spatial metrics of inundation area across the floodplain. In addition, gauged water heights at key locations were used. In the Gilbert catchment, with the majority of the MODIS and Landsat imagery during the flood events obscured by cloud, only two events were found to be suitable and the model was calibrated to one and validated to the other (2011 flood event).

The results of the MIKE21 model were used in conjunction with the MIKE 11 and the river system models to establish relationships between streamflow and floodplain inundation. These relationships can be applied to the output of the long term simulations from the river system model to assess how inundation extent may vary over the Assessment timeframe. In the Flinders floodplain, the relationships were derived for 5 sub-catchments located within the floodplain. A single relationship was derived for the entire Gilbert floodplain. The best fitted relationships for most were linear functions for rising limb and power functions for falling limb of the hydrograph.

One-dimensional hydrodynamic modelling was undertaken in the Flinders catchment using MIKE 11 hydrodynamic model. The one-dimensional hydrodynamic model network was setup to mirror the river system model network. The simulated headwater and ungauged runoff by the Flinders river system model was used to define the initial and boundary conditions of the hydrodynamic model. The period of calibration was from 1981-1999 and validation was from 2000-2011.

A number of data sources were explored to identify floodplain water bodies in the Flinders and Gilbert catchments. 85 wetlands were selected in the Flinders catchment and eight wetlands in Gilbert. Wetland connectivity analysis was undertaken for the two-dimensional hydrodynamic modelling domains of the Flinders and Gilbert Catchments. Connectivity of wetlands with the major rivers was considered through floodplain flows (i.e. overbank flooding). Connection and disconnection during overbank flooding were identified using a threshold water depth of 30 cm. Time series information on wet or dry cells were first identified at each wetland and along the intervening floodplain pathways, from which the timing and duration of connection with surrounding water bodies and/or with the main stream were estimated.

The calibrated two-dimensional hydrodynamic models for the Flinders and Gilbert floodplains were used to undertake scenario modelling to analyse the impacts of future climate and potential reservoir developments on floodplain inundation and resulted changes in wetland connectivity in the two catchments. A number of scenarios were investigated in each catchment. These were:

- three future climate scenarios in two catchments (Scenario C);
- three future development scenarios in the Flinders catchment and six in the Gilbert catchment (Scenario B);
- three sea level rise (SLR) scenarios in two catchments (Scenario C); and
- three future climate and development scenarios in Gilbert catchment (Scenario D).

Three historical flood events of different magnitudes (2001, 2009 and 2011 flood events) were selected as the base-line events. The local runoff and upstream and downstream boundary conditions of the calibrated Flinders and Gilbert floodplain hydrodynamic models for the three selected events were updated representing the selected scenarios. The Sacramento rainfall-runoff model was used for generating local

runoff under future climate. The Flinders and Gilbert river system models were used to generate upstream boundary conditions under future climate and potential development scenarios.

6.2 Conclusions

The Gilbert and Flinders floodplains show very similar flood patterns in both the MODIS OWL and the Landsat water maps. The statistical summaries of the MODIS OWL water highlight the large flood in January/February 2009 (during the 2008-2009 wet season) for the Flinders and Gilbert catchments compared to the other years. The lower parts of the two catchments were inundated for more than 10 days during the large flood in February/March 2009 (2008-2009 wet season). The 2010-2011 wet season was also reasonably wet for the two catchment, and the 2005-2006 and 2009-2010 wet seasons for the Flinders Catchment only. The 2001-2002 and 2002-2003 wet seasons appear to have been particularly dry compared to the others, as was the 2006-2007 wet season except to the north of the lower Gilbert catchment

There were significant variations in flooded areas with different OWL thresholds. The area of the water mapped from the MODIS imagery in the Flinders floodplain with 1% OWL threshold was larger by over 2 and 3.5 times the area with 5% and 10% thresholds, respectively. Similarly for the Gilbert floodplain, water area mapped with 1% OWL was larger by over 2 and 2.5 times than that with 5% and 10% thresholds, respectively. The differences between 5% and 10% threshold flood maps are considerably smaller than the differences using the 1% and 5% threshold maps. A 10% threshold of the OWL percentage water is more similar to the Landsat water maps than the 1% and 5% thresholds.

Soil colour and type appear to have an influence on the MODIS OWL for low percentage water values. Overhead vegetation was another problem, particularly for the lower Gilbert catchment where the flooding was expected to be more extensive than was showing in the water maps. Even though the MODIS sensors were imaging at a sub-daily interval, cloud cover is still a major problem when mapping flood events, particularly before the flood peak. The lower Gilbert catchment appeared to be covered in cloud more often than the Flinders catchment.

When the QIFAO (Queensland Interim Floodplain Assessment Overlay) flood map is compared to the MODIS flood map the QIFAO is showing much larger extent than the MODIS. There are a number of reasons for this: the QIFAO map is showing narrow drainage channels, many covered in vegetation, which are too fine for the MODIS to detect; the QIFAO appears to include the whole lower floodplain rather than what is visible to the satellite. There are also a few areas where the MODIS flood map is showing water, while the QIFAO is not. These areas are also mapping as water in the Landsat DERM imagery – although not as extensive as the MODIS flood map. They appear to be in very flat areas, which are not part of the drainage channels. The water mapped in these areas is likely to be very shallow, and possibly confused with moist soil in parts.

The pattern of simulated inundation extents by the hydrodynamic model is similar to the MODIS flood maps in the two catchments. The 1% threshold MODIS flood maps produced much larger flooded areas compared to the hydrodynamic model. MODIS flood maps with 5% and 10% thresholds have better agreement with the hydrodynamic model results. The cell-cell matching of the inundation areas between the hydrodynamic model and the MODIS flood maps with 5% OWL threshold over two events was up to 66% and with 10% threshold up to 72% during the calibration. In the validation period, the cell-to-cell agreement between the simulated flood maps and the MODIS flood maps with 5% threshold was up to 60% and with 10% threshold up to 66%. For the Gilbert floodplain, cell-to-cell agreement between the simulated and MODIS flood maps were above 60% with both 5% and 10% thresholds for the calibration and validation events. The main difference between the inundation maps produced by the hydrodynamic model and MODIS flood map was that the MODIS flood maps were unable to capture the fine scale flow paths, some of which were a single pixel in width. Considering the cloud covers, difference in resolution of MODIS imagery (500m) and hydrodynamic model (150m in the Flinders and 90m in the Gilbert), the cell-to-cell matching between the simulated flood maps by the hydrodynamic model and the MODIS flood maps with 5% and 10% thresholds are reasonably good.

The simulated stage heights had reasonably good agreement with the observed stage heights at the gauges located within the Flinders floodplain during the calibration and validation periods.

The performance of the one-dimensional hydrodynamic model at simulating flood discharge in the Flinders catchment was excellent in terms of percentage bias (PBIAS) at all streamflow gauging stations. NSE values for all streamflow gauging stations were good ranging between 0.58-0.70. The model also performed well at simulating stage height, with low values of MAE and RMSE at all streamflow gauging stations except Etta Plains. In the validation period, the NSE values of the model in discharge simulation were similar to the calibration period. Similar to the calibration period, the model performed well at simulating stage height at all streamflow gauging stations with low MAE and RMSE except in Etta Plains.

In the Flinders floodplain, the relationships between streamflow and floodplain inundation were derived for five sub-catchments within the floodplain. A single relationship was derived for the entire Gilbert floodplain. The best fitted relationships for most were linear functions for rising limb and power functions for falling limb of the hydrograph.

In the Flinders catchment, duration of inundation is longer in the lower part of the floodplain. Large inflow from the upper catchment produced several kilometres of floodplain inundation across the Flinders River on both banks. A large number of wetlands show long periods of connection with streams. Some wetlands were not connected to the streams at all during the flood. These are mostly bores and are located significant distant away from the streams.

In the Flinders floodplain, all investigated wetlands get connected to the rivers, some for short and some for longer period of time during the three selected flood events. A majority of wetlands maintain a high level of connectivity during big floods.

The impact of future climate is significant on the maximum inundation area in the floodplains of the two catchments. Under Cwet Scenario, the maximum inundation extent increased by up to 27% in the floodplains of the Flinders and Gilbert catchments. Compared to the extent of inundation, variation in average inundation depth is less significant. The impact is less prominent on wetland connectivity. Under the Cwet Scenario, wetland connectivity increased by up to 8% in the Flinders floodplain and 3% in the Gilbert floodplain with more increase in connectivity during lower magnitude flood events.

Under Cdry Scenario, the maximum inundation extent decreased by up to 39% in the Flinders floodplain and 27% in the Gilbert floodplain. Similar to Cwet Scenario, variation in average inundation depth is less significant with reduction. Under the same scenario, wetland connectivity decreased by up to 18% in the Flinders floodplain and 13% in the Gilbert floodplain with more reduction in connectivity during lower magnitude flood events.

Projected SLR will cause only small increase in inundation extent, depth and wetland connectivity in the Flinders floodplain. The impact of projected SLR rise is more prominent in the Gilbert floodplain as the significant part of the floodplain of the Gilbert catchment is located along the coastal line and influenced by tide.

The impact of Cave Hill reservoir empty scenario on inundation extent and depth in the Flinders floodplain is negligible. The impact of the proposed Dagworth reservoir and Greenhills reservoir empty scenarios on the Gilbert floodplain is much more significant. The impact of Dagworth reservoir empty scenario on inundation extent is relatively larger compared to impact of the Greenhills reservoir empty scenario.

The impact of the combined scenario Cdry climate and empty reservoir is the largest on both inundation area and depth for all flood events compared to all other scenarios.

7 References

- Abbott MB, Damsgaard A and Rodenhuis GS (1973). A design system for two-dimensional nearly-horizontal flows, *Journal of Hydraulic Research*, 1(1):1-28.
- ABC (2009a). Queensland Flood Update. An ABC Landline TV program broadcast on Sunday 22/02/2009. (<http://www.abc.net.au/landline/content/2008/s2509719.htm>).
- ABC (2009b). Marooned. An ABC Landline TV program broadcast on Sunday 8/03/2009. (<http://www.abc.net.au/landline/content/2008/s2509719.htm>).
- Arcement GJ and Schneider VR (1989). Guide for Selecting Manning's Roughness Coefficients for Natural Channels and Flood Plains, USGS Water-Supply Paper 2339, 44p.
- Bales JD, Wagner CR, Tighe KC and Terziotti S (2007). LiDAR-derived flood-inundation maps for real-time flood-mapping applications, Tar River basin, North Carolina: U.S. Geological Survey Scientific Investigations Report 2007-5032, 42 p.
- Bates PD, Horritt MS, Smith CN and Mason D (1997). Integrating remote sensing observations of flood hydrology and hydraulic modelling, *Hydrological Processes*, 11:1777-1795.
- BOM (2009). Gulf Rivers Floods, January and February 2009, Water Information, Bureau of Meteorology, Australian Government (http://www.bom.gov.au/qld/flood/fld_reports/gulf_floods_jan_mar_2009.pdf) visited on 26 April 2013.
- BoM (2012). Australian Hydrological Geospatial Fabric (Geofabric), Product Guide, Bureau of Meteorology, Australia.
- BTE (2001). Economic Costs of Natural Disasters in Australia, Bureau of Transport Economics, Commonwealth of Australia, Canberra.
- Bullock A and Acreman M (2003). The role of wetlands in the hydrological cycle, *Hydrology and Earth System Sciences*, 7(3):358-389.
- Bunn SE and Arthington AH (2002). Basic principles and ecological consequences of altered flow regimes for aquatic biodiversity. *Environmental Management*, 30: 492-507.
- Burnash RJC, Ferral RL, McGuire RA (1973). A Generalised Streamflow Simulation System e Conceptual Modelling for Digital Computers. Joint Federal and State River Forecast Center, Sacramento, Technical Report, 204 p.
- Chen Y, Huang C, Ticehurst C, Merrin L and Thew P (2013). An evaluation of MODIS daily and 8-day composite products for floodplain and wetland inundation mapping. *Wetlands*, 33:823-835.
- Cresswell R, Petheram C, Harrington G, Buettikofer H, Hodgen M and Davies PM (2009). Chapter 1: Water resources in northern Australia. In Northern Australia Land and Water Science Review. Final Report to the Northern Australia Land and Water Taskforce, Stone P (ed). Canberra, Australia: CSIRO.
- CSIRO (2008). Sea level rise: Understanding the past-Improving projections for the future, CSIRO Marine and Atmospheric Research, Canberra http://www.cmar.csiro.au/sealevel/sl_about_intro.html
- DHI (2007). MIKEFLOOD: Modelling of River Flooding: A Step-by-Step training Guide, DHI: Denmark; 12p.
- DHI (2009a). MIKE 11: A Modelling System for Rivers and Channels: Reference Manual, version 2009, DHI: Denmark, 534p.
- DHI (2009b). MIKE 21 Flow Model: Scientific Documentation, DHI: Denmark; 60p.

- Dutta D (2012). Flood Hazard Mapping using Hydrodynamic Modelling Approach, In: Flood Risk and Flood Management, Chapter 5 (ed by Prof. T. Wong, Nanyang Technological University, Singapore). Nova Science Publishers, ISBN: 978-1-62081-220-4.
- Frazier, P. Page, K., Louis, J., Briggs, S. and Robertson, A. 2003. Relating wetland inundation to river flow using landsat TM data. *International Journal of Remote Sensing*, 24 (1), pp. 1-16.
- Fullerton AH, Burnett KM, Steel EA, Flitcroft RL, Pess GR, Feist BE, Torgersen CE, Miller DJ and Sanderson BL (2010). Hydrological connectivity for riverine fish: measurement challenges and research opportunities. *Freshwater Biology*, 55:2215–2237.
- Gallant JC and Dowling TI (2003). A multiresolution index of valley bottom flatness for mapping depositional areas, *Water Resources Research*, 39(12):1347.
- Gao B-C (1996). NDWI A Normalized Difference Water Index for Remote Sensing of Vegetation Liquid Water from Space, *Remote Sensing of Environment*. 58:257-266.
- Guerschman JP, Warren G, Byrne G, Lymburner L, Mueller N and Van-Dijk A (2011). MODIS-based standing water detection for flood and large reservoir mapping: algorithm development and applications for the Australian continent, Water for a Healthy Country National Research Flagship Report, Canberra.
- Guha-Sapir D and Santos I (2013) (edited). The Economic Impacts of Natural Disasters, Oxford University Press, 368 pages.
- Horritt MS and Bates PD (2002). Evaluation of 1D and 2D numerical models for predicting river flood inundation, *Journal of Hydrology*, 87-99.
- Hughes JM, Schmidt DJ and Finn DS (2009). Genes in streams: using DNA to understand the movement of freshwater fauna and their riverine habitat, *BioScience*, 59:573–585.
- IPCC (2007). Climate Change 2007: Synthesis Report. Contribution of Working Groups I, II and III to the Fourth Assessment Report of the Intergovernmental Panel on Climate Change [Core Writing Team, Pachauri, RK and Reisinger, A (eds.)]. IPCC, Geneva, Switzerland, http://www.ipcc.ch/pdf/assessment-report/ar4/syr/ar4_syr.pdf
- Jeffrey SJ, Carter JO, Moodie KB, Beswick AR (2001). Using spatial interpolation to construct a comprehensive archive of Australian climate data. *Environmental Modelling and Software*, 16:309–330.
- Junk WJ, Bayley PB and Sparks RE (1989). The flood pulse concept in river–floodplain systems. *Canadian Special Publications in Fisheries and Aquatic Sciences*, 110–127.
- Karim F, Kinsey-Henderson A, Wallace J, Arthington A and Pearson R (2012). Modelling wetland connectivity during overbank flooding in a tropical floodplain in north Queensland, Australia, *Hydrological Processes*, 26(18): 2710–2723.
- Land and Water Australia (2009). An Australian handbook of stream roughness coefficients. Land and Water Australia, Canberra. 28p.
- Lasne E, Lek S and Laffaille P (2007). Patterns in fish assemblages in the Loire floodplain: The role of hydrological connectivity and implications for conservation, *Biological Conservation*, 139: 258-268.
- Lee A, Voogt S, Harding P and Loy A (2013) Design Flood Hydrology for selected dam sites in the Flinders and Gilbert catchments. A technical report to the Australian Government from the CSIRO Flinders and Gilbert Agricultural Resource Assessment, part of the North Queensland Irrigated Agriculture Strategy. CSIRO Water for a Healthy Country and Sustainable Agriculture flagships, Australia.
- Lerat J, Egan C, Kim S, Gooda M, Loy A, Shao Q and Petheram C (2013) Calibration of river models for the Flinders and Gilbert catchments. A technical report to the Australian Government from the CSIRO Flinders and Gilbert Agricultural Resource Assessment, part of the North Queensland Irrigated Agriculture Strategy. CSIRO Water for a Healthy Country and Sustainable Agriculture flagships, Australia.

- Lymburner L and Burrows D (2008). A Landsat TM Inventory of Waterbody Permanence and Clarity in Catchments of the Southern Gulf of Carpentaria, North Queensland. ACTFR Report No 09/10.
- McDonald NS, McAlpine JM (1991). Floods and droughts: the northern climate. In Monsoonal Australia – Landscape, Ecology and Man in the Northern Lowland, Haynes CD, Ridpath MG, Williams MAJ (eds). Blakema Publishers: Rotterdam; 19–30.
- Muir JS and Danaher T (2008). Mapping water body extent in Queensland through time series analysis of Landsat imagery, Proceedings of the 14th ARSPC conference, Darwin. ARSPC.
- Nicholas AP and Mitchell CA (2003). Numerical simulation of overbank processes in topographically complex floodplain environments. *Hydrological Processes*, 17: 727–746.
- Petheram C and Yang A (2013). Climatic data and their characterisation for hydrological and agricultural scenario modelling across the Flinders and Gilbert catchments. A technical report to the Australian Government from the CSIRO Flinders and Gilbert Agricultural Resource Assessment, part of the North Queensland Irrigated Agriculture Strategy. CSIRO Water for a Healthy Country and Sustainable Agriculture flagships, Australia.
- Petheram C, Rogers L, Eades G, Marvanek S, Gallant J, Read A, Sherman B, Yang A, Waltham N, McIntyre-Tamwoy S, Burrows D, Kim S, Tomkins K, Poulton P, Bird M, Atkinson F, Gallant S, Lerat J (2013b). Assessment of water storage options in the Flinders and Gilbert catchments. A technical report to the Australian Government from the CSIRO Flinders and Gilbert Agricultural Resource Assessment, part of the North Queensland Irrigated Agriculture Strategy. CSIRO Water for a Healthy Country and Sustainable Agriculture flagships, Australia.
- Pringle CM (2001). Hydrologic connectivity and the management of biological reserves: a global perspective. *Ecological Applications*, 11:981–998.
- Shaikh, M., Brady, A.T., and Sharma, P. 1998. Applications of remote sensing to assess wetland inundation and vegetation response in relation to hydrology in the Great Cumbung Swamp, Lachlan Valley, NSW, Australia. *Wetlands for the Future* (Eds. A.J. McComb and J.A. Davis) pp. 595-606. Gleneagles Publishing.
- Smith LC (1997). Satellite remote sensing of river inundation area, stage, and discharge: a review. *Hydrological Processes* 11:1427-1439.
- Teng J, Vaze J and Dutta D (2013). Simplified methodology for floodplain inundation modelling using LiDAR DEM, In: *Climate and land surface changes in hydrology*, IAHS Red Book (ed by Eva Boegh), IAHS Publication.
- Townsend PA and Walsh SJ (1998). Modeling floodplain inundation using an integrated GIS with radar and optical remote sensing, *Geomorphology*, 21(3-4):295-312.
- Waltham N, Burrows D, Butler B, Brodie J, Thomas C and Wallace J (2013) Ecological responses to changes in flow. A technical report to the Australian Government from the CSIRO Flinders and Gilbert Agricultural Resource Assessment, part of the North Queensland Irrigated Agriculture Strategy. CSIRO Water for a Healthy Country and Sustainable Agriculture flagships, Australia.
- Ward JV (1989). The four-dimensional nature of lotic ecosystems, *Journal of the North American Benthological Society*, 8, 2–8.
- Ward DP, SK Hamilton, TD Jardine, NE. Pettit, EK Tews, JM Olley and SE Bunn (2013). Assessing the seasonal dynamics of inundation, turbidity, and aquatic vegetation in the Australian wet–dry tropics using optical remote sensing, *Ecohydrology*. 6, 312–323.
- Warfe DM, Pettit NE, Davies PM, Pusey BJ, Hamilton SK, et al. (2011). The ‘wet–dry’ in the wet–dry tropics drives river ecosystem structure and processes in northern Australia. *Freshwater Biology* 56: 2169–2195.
- Welcomme RL, Winemiller KO, Cowx IG (2006). Fish environmental guilds as a tool for assessment of ecological condition of rivers. *River Research and Applications*, 22: 377–396

Appendix A IDL programs used to produce water maps

A copy of all the IDL programs used to produce water maps – in alphabetical order

ENVI_same_size.pro

```
pro ENVI_same_size

; This program reads in multiple images output from erdas_to_envi_multi.pro and resizes them all to
; the same image size.

; Written in August 2012

Files=dialog_pickfile(filter='*_ENVI', /multiple_files, path='H:\', title='Please select the ENVI files to resize')
NumIm=n_elements(Files)

if (Files[0] eq '') then begin
  print,'no files selected'
  return
end

; Create the mask image to match all other images to (use info from ERDAS_to_ENVI.pro)

; Get relevant information about mask file (assumption that it is same UTM projection as other Landsat data)
Msamples = 9000 ; these dimensions need to be large to cover south western area of Landsat scenes
Mlines=8000
Mmap_location_x = 253185.00 ; details from ERDAS_to_ENVI.pro (Northeastern most point of all Landsat images)
Mmap_location_y = 8031415.0 ; Remember Northing decreases downwards
MPixSizeX = 30.0
MPixSizeY = 30.0

; Read in mask image
Mask=bytarr(Msamples,Mlines) ; assume data is byte

for J=0,NumIm -1 do begin

  print,'Processing file ',J+1,' of ', NumIm

  ENVIfile=Files[J]

; Open the new ENVI file to subset
  file_information= read_envi_hdr(ENVIfile + '.hdr')
  IF (file_information[1,0] NE 'NaN') THEN Esamples = LONG(file_information[1,0]) ELSE Esamples = 'NaN'
  IF (file_information[1,1] NE 'NaN') THEN Elines = LONG(file_information[1,1]) ELSE Elines = 'NaN'
  IF (file_information[1,16] NE 'NaN') THEN Emap_location_x = DOUBLE(file_information[1,16]) ELSE Emap_location_x = 'NaN'
  IF (file_information[1,17] NE 'NaN') THEN Emap_location_y = DOUBLE(file_information[1,17]) ELSE Emap_location_y = 'NaN'

  ENVI_Im=bytarr(Esamples,Elines)
  OpenR, In, ENVIfile, /get_lun
  ReadU, In, ENVI_Im
  free_lun, In

; Work out pixel offset between mask and Image
  X_off=round((Emap_location_x-Mmap_location_x)/MpixSizeX)
  Y_off=round((Mmap_location_y-Emap_location_y)/MpixSizeY) ; Northing decreases downwards

  if ((X_off lt 0) or (Y_off lt 0)) then print, ' x or y offset is negative', X_off, Y_off
  if ((X_off lt 0) or (Y_off lt 0)) then stop

  print,'X_off Y_off=',X_off, Y_off
  print,'Emap_location =',Emap_location_x, Emap_location_y

  if Msamples-X_off ge Esamples then begin

    if Mlines-Y_off ge Elines then begin
      print,'X_off+Esamples-1 Esamples=',X_off+Esamples-1, Esamples
      print,'Y_off+Elines-1 Elines=',Y_off+Elines-1, Elines
      print,'size mask=',size(Mask)
      Mask[X_off:X_off+Esamples-1,Y_off:Y_off+Elines-1]=ENVI_Im[*,*] ; ie whole ENVI file fits within mask
    endif else begin
      print,'X_off+Esamples-1 Esamples=',X_off+Esamples-1, Esamples
      print,'Y_off Mlines-1 (Mlines-1)-Y_off+1=',Y_off, Mlines-1, (Mlines-1)-Y_off
      print,'size mask=',size(Mask)

      Mask[X_off:X_off+Esamples-1,Y_off:Mlines-1]=ENVI_Im[*;0:(Mlines-1)-Y_off]
    endelse

  endif else begin

    if Mlines-Y_off lt Elines then begin
      Mask[X_off:Msamples-1,Y_off:Y_off+Elines-1]=ENVI_Im[0:(Msamples-1)-X_off,*] ; ie whole ENVI file fits within mask
    endif else begin
      Mask[X_off:Msamples-1,Y_off:M_lines-1]=ENVI_Im[0:(Msamples-1)-X_off,0:(Mlines-1)-Y_off]
    endelse

  endelse

; output the new ENVI image mosaicked on the mask file
  OpenW, Out, ENVIfile+'_M', /get_lun
  WriteU, Out, Mask
  free_lun, Out
```

```
Mask[*,*]=0B
```

```
endfor
```

```
end
```

```
-----  
; Function written by Garth Warren 2012  
FUNCTION read_envi_hdr, filenames  
[SEE ERDAS_to_ENVI_multi.pro for this function]
```

ERDAS to ENVI_multi.pro

```
pro ERDAS_to_ENVI_multi
```

```
; This program reads in multiple .img (compressed ERDAS images) and converts them to ENVI using  
; GDAL translate. It also determines the north and eastern most points from all images (for use in  
; envi_same_size.pro)
```

```
; Written in August 2012
```

```
Files=dialog_pickfile(filter='*.img', /multiple_files, path='H:\', title='Please select the .img files')  
NumIm=n_elements(Files)
```

```
if (Files[0] eq '') then begin  
print,'no files selected'  
return  
end
```

```
Mmap_location_x= 10000000 ; These are dummy values that are too large to be realistic coordinates  
Mmap_location_y= 0
```

```
for J=0,NumIm -1 do begin
```

```
print,'Processing file ',J+1,' of ', NumIm
```

```
infile=Files[J]  
ENVIfilename=strmid(infile, 0, strlen(infile)-4)+'_ENVI'
```

```
; Convert to ENVI file  
SPAWN, 'gdal_translate -of ENVI ' + infile + ' ' + ENVIfilename
```

```
; Open the new ENVI header file to get top-left coordinates
```

```
file_information= read_envi_hdr(ENVIfilename + '.hdr')  
IF (file_information[1,16] NE 'NaN') THEN Emap_location_x = DOUBLE(file_information[1,16]) ELSE Emap_location_x = 'NaN'  
IF (file_information[1,17] NE 'NaN') THEN Emap_location_y = DOUBLE(file_information[1,17]) ELSE Emap_location_y = 'NaN'
```

```
If Emap_location_x lt Mmap_location_x then Mmap_location_x=Emap_location_x  
If Emap_location_y gt Mmap_location_y then Mmap_location_y=Emap_location_y  
print,'Mmap_location xy =' ,Mmap_location_x, Mmap_location_y
```

```
endfor
```

```
end
```

```
-----  
; Function written by Garth Warren 2012  
FUNCTION read_envi_hdr, filenames
```

```
file_information = MAKE_ARRAY(1+N_ELEMENTS(filenames), 20, /STRING)  
file_information[0,*] = ['samples', $  
    'lines', $  
    'bands', $  
    'headeroffset', $  
    'filetype', $  
    'datatype', $  
    'interleave', $  
    'sensortype', $  
    'byteorder', $  
    'wavelengthunits', $  
    'fillvalue', $  
    'datum', $  
    'projection', $  
    'map units', $  
    'cell_location_x', $  
    'cell_location_y', $  
    'map_location_x', $  
    'map_location_y', $  
    'cellsize_x', $  
    'cellsize_y']
```

```
FOR i=0, N_ELEMENTS(filenames)-1 DO BEGIN
```

```
OPENR, lun, filenames[i], /GET_LUN ; Open the current HDR file.
```

```
j = 0 ; Set the while loop counter.
```

```
WHILE NOT EOF(lun) DO BEGIN
```

```
text = ''
```

```
READF, lun, text
```

```
information = STRJOIN(STRSPLIT(text, ' ', /EXTRACT), ' ')
```

```
IF (WHERE (STRMATCH(information, '*samples*', /FOLD_CASE)) NE -1) THEN samples = STRSPLIT(information, 'samples ', /EXTRACT,  
/REGEX)
```

```
IF (WHERE (STRMATCH(information, '*lines*', /FOLD_CASE)) NE -1) THEN lines = STRSPLIT(information, 'lines ', /EXTRACT, /REGEX)
```

```
IF (WHERE (STRMATCH(information, '*bands*', /FOLD_CASE)) NE -1) THEN bands = STRSPLIT(information, 'bands ', /EXTRACT, /REGEX)
```

```
IF (WHERE (STRMATCH(information, '*header offset*', /FOLD_CASE)) NE -1) THEN headeroffset = STRSPLIT(information, 'header offset ',  
/EXTRACT, /REGEX)
```

```
IF (WHERE (STRMATCH(information, '*file type*', /FOLD_CASE)) NE -1) THEN filetype = STRSPLIT(information, 'file type ', /EXTRACT,  
/REGEX)
```

```
IF (WHERE (STRMATCH(information, '*data type*', /FOLD_CASE)) NE -1) THEN datatype = STRSPLIT(information, 'data type ', /EXTRACT,  
/REGEX)
```

```
IF (WHERE (STRMATCH(information, '*interleave*', /FOLD_CASE)) NE -1) THEN interleave = STRSPLIT(information, 'interleave ',  
/EXTRACT, /REGEX)
```

```
IF (WHERE (STRMATCH(information, '*sensor type*', /FOLD_CASE)) NE -1) THEN sensortype = STRSPLIT(information, 'sensor type ',  
/EXTRACT, /REGEX)
```

```
IF (WHERE (STRMATCH(information, '*byte order*', /FOLD_CASE)) NE -1) THEN byteorder = STRSPLIT(information, 'byte order ',  
/EXTRACT, /REGEX)
```

```
IF (WHERE (STRMATCH(information, '*wavelength units*', /FOLD_CASE)) NE -1) THEN wavelengthunits = STRSPLIT(information, 'wavelength  
units ', /EXTRACT, /REGEX)
```

```

    IF (WHERE (STRMATCH (information, '*data ignore value*', /FOLD_CASE)) NE -1) THEN fillvalue = STRSPLIT (information, 'data ignore
value ', /EXTRACT, /REGEX)
    IF (WHERE (STRMATCH (information, '*map info*', /FOLD_CASE)) NE -1) THEN mapinfo = information
    j = (j + 1)
ENDWHILE

IF (N_ELEMENTS (samples) GT 0) THEN file_information [1+i,0] = samples ELSE file_information [1+i,0] = 'NaN'
IF (N_ELEMENTS (lines) GT 0) THEN file_information [1+i,1] = lines ELSE file_information [1+i,1] = 'NaN'
IF (N_ELEMENTS (bands) GT 0) THEN file_information [1+i,2] = bands ELSE file_information [1+i,2] = 'NaN'
IF (N_ELEMENTS (headeroffset) GT 0) THEN file_information [1+i,3] = headeroffset ELSE file_information [1+i,3] = 'NaN' ;'0'
IF (N_ELEMENTS (filetype) GT 0) THEN file_information [1+i,4] = filetype ELSE file_information [1+i,4] = 'NaN'
IF (N_ELEMENTS (datatype) GT 0) THEN file_information [1+i,5] = datatype ELSE file_information [1+i,5] = 'NaN'
IF (N_ELEMENTS (interleave) GT 0) THEN file_information [1+i,6] = interleave ELSE file_information [1+i,6] = 'NaN'
IF (N_ELEMENTS (sensortype) GT 0) THEN file_information [1+i,7] = sensortype ELSE file_information [1+i,7] = 'NaN'
IF (N_ELEMENTS (byteorder) GT 0) THEN file_information [1+i,8] = byteorder ELSE file_information [1+i,8] = 'NaN' ;'0'
IF (N_ELEMENTS (wavelengthunits) GT 0) THEN file_information [1+i,9] = wavelengthunits ELSE file_information [1+i,9] = 'NaN'
;'Unknown'
IF (N_ELEMENTS (fillvalue) GT 0) THEN file_information [1+i,10] = fillvalue ELSE file_information [1+i,10] = 'NaN'

IF (N_ELEMENTS (mapinfo) GT 0) THEN BEGIN
start = STRPOS (mapinfo, '(') + 1
length = (STRPOS (mapinfo, ')') - start)
mapinfo = STRMID (mapinfo, start, length)
mapinfo = STRSPLIT (mapinfo, ',', /EXTRACT)
IF (N_ELEMENTS (mapinfo) GE 8) THEN BEGIN
file_information [1+i,11] = mapinfo [7] ; Assign the datum.
file_information [1+i,12] = mapinfo [0] ; Assign the projection name.
file_information [1+i,13] = mapinfo [8] ; Assign the projection units (map_units).
file_information [1+i,14] = mapinfo [1] ; Assign the x-axis pixel location corresponding to the x-axis map location
(cell_location_x).
file_information [1+i,15] = mapinfo [2] ; Assign the y-axis pixel location corresponding to the y-axis map location
(cell_location_y).
file_information [1+i,16] = mapinfo [3] ; Assign the x-axis map location corresponding to the x-axis pixel location
(map_location_x).
file_information [1+i,17] = mapinfo [4] ; Assign the y-axis map location corresponding to the y-axis pixel location
(map_location_y).
file_information [1+i,18] = mapinfo [5] ; Assign the x-axis pixel size of the image (cellsize_x).
file_information [1+i,19] = mapinfo [6] ; Assign the y-axis pixel size of the image (cellsize_y).
ENDIF ELSE BEGIN
file_information [1+i,11] = 'NaN' ; Assign the datum.
file_information [1+i,12] = 'NaN' ; Assign the projection name.
file_information [1+i,13] = 'NaN' ; Assign the projection units (map_units).
file_information [1+i,14] = 'NaN' ; Assign the x-axis pixel location corresponding to the x-axis map location (cell_location_x).
file_information [1+i,15] = 'NaN' ; Assign the y-axis pixel location corresponding to the y-axis map location (cell_location_y).
file_information [1+i,16] = 'NaN' ; Assign the x-axis map location corresponding to the x-axis pixel location (map_location_x).
file_information [1+i,17] = 'NaN' ; Assign the y-axis map location corresponding to the y-axis pixel location (map_location_y).
file_information [1+i,18] = 'NaN' ; Assign the x-axis pixel size of the image (cellsize_x).
file_information [1+i,19] = 'NaN' ; Assign the y-axis pixel size of the image (cellsize_y).
ENDIFELSE
ENDIF

free_lun, lun ; Close the current HDR file.
close, lun
ENDFOR

; Return the hdr information to the main procedure.
RETURN, file_information

END
;-----

```

MODIS_OWL_frequency_stats.pro

```
pro MODIS_OWL_frequency_stats
```

```

; This program reads in multiple MODIS OWL images and calculates some simple summary statistics using all of the images:
; maximum flooding, average flooding, maximum length of time that a pixel was flooded

; Need to define the % of water to define a wet pixel, and the number of letter to chop off input file for output filename

; Read in the OWL file
; Use Dialog pick file to get the files of interest.
path='\\file-wron\Working\work\cjt\MODIS_Gulf\Daily_OWLs\Processed'
FileNames=dialog_pickfile (/read, path=path, /multiple_files, filter='M*D09*OWLv2p4*max.dat')

; check for any errors
if (FileNames[0] eq '') then begin
print, 'No files selected'
result=widget_message ("No files selected: TERMINATE", /error)
return
endif

; Define image size (hardwired - they all must be the same size)
nsamp=3512 ;4963 ;2965 ;1801
nline=2130 ;2787 ;1801

Band=bytarr (nsamp,nline)
MaxBand=Band
NullMsk=Band

OWL_Total=fltarr (nsamp,nline)
OWL_Num=intarr (nsamp,nline)
ONE=bytarr (nsamp,nline)
ONE[*,*]=1B

MaxWet=intarr (nsamp,nline)
CurrentWet=intarr (nsamp,nline)
TempCloudyWet=intarr (nsamp,nline)
lastWetDays=intarr (nsamp,nline)
Parray=intarr (nsamp,nline)

Thresh=10 ; % of water that defines a wet pixel
Namecut=0 ; the number of letters in the name

for P=0,n_elements (FileNames)-1 do begin
print, 'Processing file ',P+1,' of ',n_elements (FileNames)

```

```

OpenR, In, Filenames[P], /get_lun
ReadU, In, Band
free_lun, In

; Calculate maximum % water value for each pixel
where_max=where((Band gt MaxBand) and (Band lt 200))
if where_max[0] ne -1 then MaxBand[where_max]=Band[where_max]
if where_max[0] ne -1 then NullMsk[where_max]=1B ; determine which pixels are permanent nulls
where_max=0B

; Calculate average water value
where_OK=where((Band ge 0) and (Band le 100))
if where_OK[0] ne -1 then begin
    OWL_Total[where_OK]=OWL_Total[where_OK]+Band[where_OK]
    OWL_Num[where_OK]=OWL_Num[where_OK]+ONE[where_OK]
endif
where_OK=0B

; Calculate the maximum number of consecutive wet days (define 50% or 20%?? water as a wet pixel)
where_wet=where((Band ge thresh) and (Band le 100))
where_dry=where(Band lt thresh)
if where_wet[0] ne -1 then CurrentWet[where_wet]=CurrentWet[where_wet]+ONE[where_wet]
where_wet=0B

; if a pixel is wet before and after a series of cloud images, then assume it has remained wet
; first add to a temporary array recording number of cloudy days following a wet pixel
where_cloudy_wet=where((Band ge 250) and (CurrentWet ne 0)) ; ie find where there is cloud/null but the last cloud-free day had
a wet pixel
if where_cloudy_wet[0] ne -1 then TempCloudyWet[where_cloudy_wet]=TempCloudyWet[where_cloudy_wet]+ONE[where_cloudy_wet]
where_cloudy_wet=0B

; if the pixel is no longer cloudy, but it is still well, then add the number of wet days to CurrentWet and reset TempCloudyWet
where_still_wet=where((Band ge thresh) and (Band le 100) and (TempCloudyWet gt 0))
if where_still_wet[0] ne -1 then CurrentWet[where_still_wet]=CurrentWet[where_still_wet]+TempCloudyWet[where_still_wet]
if where_still_wet[0] ne -1 then TempCloudyWet[where_still_wet]=0

; if the pixel is no longer cloud, but is dry, just reset TempCurrentWet
where_dried_off=where((Band lt thresh) and (TempCloudyWet gt 0))
if where_dried_off[0] ne -1 then TempCloudyWet[where_dried_off]=0

; check if it is a maximum number of consecutive wet days
where_max=where(CurrentWet gt MaxWet)
if where_max[0] ne -1 then MaxWet[where_max]=CurrentWet[where_max]
Parray[*,*]=P+1
if where_max[0] ne -1 then lastWetDays[where_max]=Parray[where_max] ; this records the last day of the maximum wet days - for
debugging only
where_max=0B

; reset the dry pixels back to zero in CurrentWet
if where_dry[0] ne -1 then CurrentWet[where_dry]=0
where_dry=0B

endifor

; Open the Total Output image
OpenW, Out, strmid(Filenames[0],0,strlen(Filenames[0])-Namecut)+'Max'+string(strcompress(Thresh))+'.dat', /get_lun
WriteU, Out, MaxBand
free_lun, Out

; Calculate the average OWL for the entire period
OWL_Total=OWL_Total/OWL_Num

; Open the Average Output image
OpenW, Out, strmid(Filenames[0],0,strlen(Filenames[0])-Namecut)+'Av'+string(strcompress(Thresh))+'.dat', /get_lun
WriteU, Out, OWL_Total
free_lun, Out

; Divide MaxWet into classes
; 0=no wet days or permanent nulls
; 1=1 wet days in a row
; 2= 2-5 wet days in a row
; 3= 5-10 wet days in a row
; 4= >10 wet days in a row
MaxWetClasses=Bytarr(nsamp,nline)
where_0=where(MaxWet eq 0)
if where_0[0] ne -1 then MaxWetClasses[where_0]=0
where_1=where((MaxWet gt 0) and (MaxWet le 1))
if where_1[0] ne -1 then MaxWetClasses[where_1]=1
where_2=where((MaxWet gt 1) and (MaxWet le 5))
if where_2[0] ne -1 then MaxWetClasses[where_2]=2
where_3=where((MaxWet gt 5) and (MaxWet le 10))
if where_3[0] ne -1 then MaxWetClasses[where_3]=3
where_4=where(MaxWet gt 10)
if where_4[0] ne -1 then MaxWetClasses[where_4]=4

; Open the Maximum Consecutive Wet Days Classes Output image
OpenW, Out, strmid(Filenames[0],0,strlen(Filenames[0])-Namecut)+'MaxWetClasses'+string(strcompress(Thresh))+'.dat', /get_lun
WriteU, Out, MaxWetClasses
free_lun, Out

print, 'Finished!'

end

```

MODIS_OWLv2p4.pro

pro MODIS_OWLv2p4

; This program reads in Daily MOD09GA reflectance and State images (all of same size) and calculates the OWL (masking
; Clouds using the state band).

Path='C:\'

Files=dialog_pickfile(/READ, /MUST_EXIST, path=path, /MULTIPLE_FILES, filter='*h30v10*_b01_1.dat')

```

nsamp=3615 ; number of samples
nline=2130 ; number of lines

; band state=uintarr(nsamp-1,nline) ; Range seems to be one sample less than rest of image for some tiles
band_state=uintarr(nsamp,nline)
Red=intarr(nsamp,nline) ; red
NIR=intarr(nsamp,nline) ; NIR
green=intarr(nsamp,nline) ; green
SWIR2=intarr(nsamp,nline) ; SWIR2
SWIR3=intarr(nsamp,nline) ; SWIR3

; **** Read in associated MrVBF file
OpenR, InMr, 'C:\Projects\NASY\Data\Gulf\SRTM_DEM_3s_01_MrVBF_Aust_500m_H30V10', /get_lun
MrVBF=fltarr(nsamp,nline)
ReadU, InMr, MrVBF
free_lun, InMr

; Read in blue-white reversed colour table for PNG files (created through ENVI)
OpenR, InCT, 'C:\Program Files\ITT\IDL_programs\colors_blueWhite.txt', /get_lun
ColourTable=bytarr(256,3)
RGB='' ;intarr(3)
for K=0,255B do begin
  ReadF, InCT, RGB, format='(A)';format='(I3,"",I3,"",I3)'
  ColourTable[k,0]=strmid(RGB,0,3)
  ColourTable[k,1]=strmid(RGB,5,3)
  ColourTable[k,2]=strmid(RGB,10,3)
endfor
Free_Lun, InCT

if (Files[0] eq '') then return
NumFiles=n_elements(Files)

for X=0,NumFiles-1 do begin

print,'processing ',X+1, ' of ',NumFiles

; Open and read in the reflectance and State bands
OpenR, InState, strmid(Files[X],0,strlen(Files[X])-18)+'state_lkm_1.dat', /get_lun
; OpenR, InState, strmid(Files[X],0,strlen(Files[X])-7)+'state_500m.dat', /get_lun
ReadU, InState, band_state
state=congrid(band_state,nsamp,nline)
print,'size state=',size(state)
OpenR, InB1, Files[X], /get_lun
ReadU, InB1, red
OpenR, InB2, strmid(Files[X],0,strlen(Files[X])-7)+'2_1.dat', /get_lun
ReadU, InB2, NIR
OpenR, InB4, strmid(Files[X],0,strlen(Files[X])-7)+'4_1.dat', /get_lun
ReadU, InB4, green
OpenR, InB6, strmid(Files[X],0,strlen(Files[X])-7)+'6_1.dat', /get_lun
ReadU, InB6, SWIR2
OpenR, InB7, strmid(Files[X],0,strlen(Files[X])-7)+'7_1.dat', /get_lun
ReadU, InB7, SWIR3

Free_lun, InState, InB1, InB2, InB4, InB6, InB7

; Calculate the OWL after applying the cloud/cloud shadow mask (Written by Peter Dyce 2009)

; ; code from Garth Warren to apply a cloud mask
Cloud_Msk = MAKE_ARRAY(N_ELEMENTS(Red), VALUE=1, /INTEGER)
FillIndex = WHERE(State EQ 65535, CountFill) ; Fill cells
IF (N_ELEMENTS(FillIndex) GT 1) THEN Cloud_Msk[FillIndex] = 0
CloudIndex = BITWISE_OPERATOR_AND(State, 1, 1, 2, 0, 1) ; Cloud cells ["Cloud"= 0000000000000001]; STATE = ((1033 AND 1) EQ 1) AND
((1033 AND 2) EQ 0)
print,'cloudindex=',N_ELEMENTS(CloudIndex)
IF (N_ELEMENTS(CloudIndex) GT 1) THEN Cloud_Msk[CloudIndex] = 0
ShadowIndex = BITWISE_OPERATOR(State, 4, 0, 0) ; Cloud shadow cells ["Cloud_Shadow"= 000000000000100]
IF (N_ELEMENTS(ShadowIndex) GT 1) THEN Cloud_Msk[ShadowIndex] = 0
InternalIndex = BITWISE_OPERATOR(State, 1024, 0, 0) ; Internal cloud cells
IF (N_ELEMENTS(InternalIndex) GT 1) THEN Cloud_Msk[InternalIndex] = 0

Matrix_Mask = MAKE_ARRAY(N_ELEMENTS(Red), VALUE=1, /INTEGER)
FillIndexRed = WHERE(Red LE -20000, CountFill) ; Fill cells
IF (N_ELEMENTS(FillIndexRed) GT 1) THEN Matrix_Mask[FillIndexRed] = 0
FillIndexNIR = WHERE(NIR LE -20000, CountFill) ; Fill cells
IF (N_ELEMENTS(FillIndexNIR) GT 1) THEN Matrix_Mask[FillIndexNIR] = 0
FillIndexSWIR2 = WHERE(SWIR2 LE -20000, CountFill) ; Fill cells
IF (N_ELEMENTS(FillIndexSWIR2) GT 1) THEN Matrix_Mask[FillIndexSWIR2] = 0
FillIndexSWIR3 = WHERE(SWIR3 LE -20000, CountFill) ; Fill cells
IF (N_ELEMENTS(FillIndexSWIR3) GT 1) THEN Matrix_Mask[FillIndexSWIR3] = 0

; NEW ALGORITHM
; define beta for calculating OWL
B=[-3.41375620,-0.000959735270,0.004179553330,14.1927990,-0.430407140,-0.0961932990]

; New OWL using update from Garth/JP
Z=B[0]+B[1]*SWIR2+B[2]*SWIR3+B[3]*([float(NIR-RED)]/[float(NIR+RED)])+B[4]*([float(NIR-SWIR2)]/[float(NIR+SWIR2)])+B[5]*MrVBF
Fw=1./[1.+exp(Z)]
mNDWI=float(green-SWIR2)/float(green+SWIR2)
where_highmNDWI=where(mNDWI ge 0.8) ; Apply Garth's mNDWI mask
if (where_highmNDWI[0] ne -1) then Fw[where_highmNDWI]=1.
OWL=byte([fw+0.005]*100.)

where_cloud=where(cloud_msk eq 0) ; where there are clouds and nulls
if (where_cloud[0] ne -1) then OWL[where_cloud]=255
where_nulls=where(matrix_mask eq 0) ; where there are clouds and nulls
if (where_nulls[0] ne -1) then OWL[where_nulls]=255

; Write OWL to file

OpenW, Out, strmid(Files[X],0,strlen(Files[X])-19)+'_OWLv2p4', /get_lun
WriteU, Out, OWL
Free_lun, Out

; Output OWL image as a png

```

```

Rd = OWL
Gr = OWL
Bl = OWL
;Apply colour table
for K=0,255 do begin
  where_DN=where(OWL eq K)
  if where_DN[0] ne -1 then begin
    Rd[where_DN]=ColourTable[K,0]
    Gr[where_DN]=ColourTable[K,1]
    Bl[where_DN]=ColourTable[K,2]
  endif
endifor

; Change Nulls and clouds from black to grey
where_cloud = where(cloud_msk eq 0.0)
if where_cloud[0] ne -1 then begin
  Rd[where_cloud]=192
  Gr[where_cloud]=192
  Bl[where_cloud]=192
endif
if where_nulls[0] ne -1 then begin
  Rd[where_nulls]=92
  Gr[where_nulls]=92
  Bl[where_nulls]=92
endif

; ;make a png file of the OWL
array_png = bytarr (3, nsamp, nline)
array_png [0,*,*] = temporary(Rd)
array_png [1,*,*] = temporary(Gr)
array_png [2,*,*] = temporary(Bl)

WRITE_PNG, strmid(Files[X],0,strlen(Files[X])-19)+'_OWLv2p4.png', Temporary(array_png), red,green,blue, /order;;

; Output Bands 721 image as a png (scaled from 0-255)
SWIR3=SWIR3*Matrix_Mask ; convert null values to 0
Rd = byte((1.*(SWIR3-min(SWIR3))/(max(SWIR3)-min(SWIR3)))*255.)
NIR=NIR*Matrix_Mask
Gr = byte((1.*(NIR-min(NIR))/(max(NIR)-min(NIR)))*255.)
Red=Red*Matrix_Mask
Bl = byte((1.*(Red-min(Red))/(max(Red)-min(Red)))*255.)

; ;make a png file of the RGB image
array_png = bytarr (3, nsamp, nline)
array_png [0,*,*] = temporary(Rd)
array_png [1,*,*] = temporary(Gr)
array_png [2,*,*] = temporary(Bl)

WRITE_PNG, strmid(Files[X],0,strlen(Files[X])-19)+'_B721.png', Temporary(array_png), red,green,blue, /order;;

endifor

print, 'Finished!'

END

;-----
FUNCTION BITWISE_OPERATOR, Data, Binary1, Match1, WhereValue
State = ((Data AND Binary1) EQ Match1) ; Apply bit statement.
Index = WHERE(State EQ WhereValue, Count) ; Get the count of cells that conform to the statement.
RETURN, [Index] ; Return index.
END
;-----

;-----
FUNCTION BITWISE_OPERATOR_AND, Data, Binary1, Match1, Binary2, Match2, WhereValue
State = ((Data AND Binary1) EQ Match1) AND ((Data AND Binary2) EQ Match2) ; Apply bit statement.
Index = WHERE(State EQ WhereValue, Count) ; Get the count of cells that conform to the statement.
RETURN, [Index] ; Return index.
END
;-----

```

MODIS stitch OWL

```

pro MODIS_stitch_OWL

; This program reads in two OWL images from tiles H31v10 and H31v11 and stitches them together
; as well as subset for the area of interest (Gulf region). It also outputs a png file
; Written March 2012

; Read in the OWL files (H31v10)
; Use Dialog pick file to get the files of interest.
path='E:'
FileNames=dialog_pickfile(/multiple_files, /read, path=path, filter='MYD09*h31v10*OWLv2p4')

; check for any errors
if (FileNames[0] eq '') then begin
  print,'No files selected'
  result=widget_message("No files selected: TERMINATE", /error)
  return
endif

; Define image sizes (hardwired)
nsamp1=3615
nline1=2130

nsamp2=4963
nline2=2130

Band1=bytarr(nsamp1,nline1)
Band2=bytarr(nsamp2,nline2)

;define mosaic subset dimensions (subset to cover area of interest)
subSampStart=1200

```

```

subLineStart=1200
subSampEnd=3000
subLineEnd=3000
mosaicOffset=1350

mosSamp=subSampEnd-subSampStart+1
MosLine=subLineEnd-subLineStart+1
MosaicSub=bytarr (MosSamp,MosLine)

BigMSamp=3100
BigMLine=3100
BigMos=bytarr (BigMSamp,BigMLine)
BigMos[*,*]=255B

; Read in blue-white reversed colour table for PNG files (created through ENVI)
OpenR, InCT, 'C:\Program Files\ITT\IDL_programs\colors_blueWhite.txt', /get_lun
ColourTable=bytarr (256,3)
RGB='' ;intarr (3)
for K=0,255B do begin
  ReadF, InCT, RGB, format='(A)';format='(I3," ",I3," ",I3)'
  ColourTable[k,0]=strmid (RGB,0,3)
  ColourTable[k,1]=strmid (RGB,5,3)
  ColourTable[k,2]=strmid (RGB,10,3)
endfor
Free_Lun, InCT

; Loop through each OWL file, stitching it to the tile below
for I=0,n_elements (FileNames)-1 do begin
print,'Processing File ',I+1,' of ',n_elements (FileNames)

; Open the OWL files (H31v10 and H31v11)
OpenR, In1, FileNames[I], /get_lun
ReadU, In1, Band1
free_lun, In1

file_part=strmid (FileNames[I],0,strlen (FileNames[I])-27)
file_part=file_part+'1.005.*OWLv2p4'

Im2_name=file_search (file_part)
print,'Im2_name=',im2_name

OpenR, In2, Im2_name, /get_lun
ReadU, In2, Band2
free_lun, In2

; Stitch the two together (this is hardwired in)
BigMos[*,0:nline1-1]=Band1[0:BigMSamp-1,*]
print,'sample=',mosaicOffset,mosaicOffset,BigMSamp-1,BigMSamp-mosaicOffset-1
print,'line=',nline1,BigMLine-1,BigMLine-nline1
BigMos[mosaicOffset-1:BigMSamp-1,nline1-1:BigMLine-1]=Band2[0:BigMSamp-mosaicOffset,0:BigMLine-nline1]

; Subset the mosaic to the area of interest
MosaicSub[*,*]=BigMos[SubSampStart:SubSampEnd,SubLineStart:SubLineEnd]

; Output mosaic
OpenW, Out, Im2_name+'_MOS', /get_lun
WriteU, Out, MosaicSub
free_lun, Out
print,'size mos sub=',size (MosaicSub)

; Output OWL mosaic image as a png
Rd = MosaicSub
Gr = MosaicSub
Bl = MosaicSub
;Apply colour table
for K=0,255 do begin
  where_DN=where (MosaicSub eq K)
  if where_DN[0] ne -1 then begin
    Rd[where_DN]=ColourTable[K,0]
    Gr[where_DN]=ColourTable[K,1]
    Bl[where_DN]=ColourTable[K,2]
  endif
endfor

; Change Nulls and clouds from black to grey
where_cloud = where (MosaicSub eq 250)
if where_cloud[0] ne -1 then begin
  Rd[where_cloud]=192
  Gr[where_cloud]=192
  Bl[where_cloud]=192
endif
where_nulls = where (MosaicSub eq 255)
if where_nulls[0] ne -1 then begin
  Rd[where_nulls]=92
  Gr[where_nulls]=92
  Bl[where_nulls]=92
endif

; make png file of RGB image
array_png = bytarr (3, MosSamp, MosLine)
array_png [0,*,*] = temporary (Rd)
array_png [1,*,*] = temporary (Gr)
array_png [2,*,*] = temporary (Bl)

WRITE_PNG, Im2_name+'_MOS.png', Temporary (array_png), red,green,blue, /order,,

; continue loop until finished
endfor

print,' Finished!'
end

```

MODIS_tile_OWL_Daily.pro

```
pro MODIS_tile_OWL_Daily

; This program reads in multiple MOD and MYD OWLs for MODIS tiles and calculates the best OWL
; image for each day by combining MOD and MYD based on maximum OWL value (with exception of nulls).

; Written January 2013

; define tile size (H31V10 - 3615 x 2130, H31V11 - 4963 x 2130)
samp=3512 ;4963 ;3615
line=2130
BandO=bytarr(samp,line)
BandY=bytarr(samp,line)

; Select the MOD files in the folder for combining daily MOD and MYD OWLs. The file names are assumed to be in
; the following format MOD09GA.AYYYYDD.hXXvYY.005.NNNNNNNNNNNNN_OWLv2p4
filter='MOD09GA*_OWLv2p4'
Files=dialog_pickfile(path='C:', /multiple_files, filter=filter)
NumDates=n_elements(Files)

; loop through for each MOD file
for X=0,NumDates-1 do begin
print,'processing file no. ',X+1,' of ',NumDates

; Open the MOD file
OpenR, InO, Files[X], /get_lun
ReadU, InO, BandO
free_lun, InO

; find the MYD file for the same day - assume it is in the same folder
MYD_filt_start=strmid(Files[X],0,strlen(Files[X])-48)
MYD_filt_end=strmid(Files[X],strlen(Files[X])-47,25)
MYD_filt=MYD_filt_start+'Y'+MYD_filt_end+'*_OWLv2p4'
print,'MOD file=',Files[X]
print,'MYD filter=',MYD_filt
Result=file_search(MYD_filt)
print,'result=',result

if n_elements(Result) gt 1 then begin
print, ' Error - more than one MYD file found for this day !'
return
endif

if ((n_elements(Result) eq 0) or (Result eq '')) then begin ; output MOD file as the daily OWL for this date
Outname=MYD_filt_start+'OY'+MYD_filt_end+'.OWLv2p4_max.dat'
OpenW, Out, Outname, /get_lun
WriteU, Out, BandO
free_lun, Out
endif

if ((n_elements(Result) eq 1) and (Result ne '')) then begin ; Combine MOD and MYD file as the daily OWL for this date
OpenR, InM, Result, /get_lun
ReadU, InM, BandY
free_lun, InM

where_OK = where(BandO gt 200) ; replace nulls from MOD with MYD
if where_OK[0] ne -1 then BandO[where_OK]=BandY[where_OK]

where_max=where((BandO lt 200) and (BandY lt 200) and (BandY gt BandO))
if where_max[0] ne -1 then BandO[where_max]=BandY[where_max]

Outname=MYD_filt_start+'OY'+MYD_filt_end+'.OWLv2p4_max.dat'
OpenW, Out, Outname, /get_lun
WriteU, Out, BandO
free_lun, Out
endif

endifor

print, 'Finished!'
end
```

MODIS_tile_OWL_Daily_Pt2

```
pro MODIS_tile_OWL_Daily_Pt2

; This program reads follows MODIS_tile_OWL_Daily which fills in the missing days that werent processed due
; to missing days in the MOD OWLs, and uses the MYD OWLs as the daily OWL (when they exist).

; Written January 2013

; define tile size (H31V10 - 3615 x 2130, H31V11 - 4963 x 2130)
samp=3512 ;4963 ;3615
line=2130
BandY=bytarr(samp,line)

; Select the MYD OWLs to be used (based on missing MOD OWLs) - currently done manually. The file names are assumed to be in
; the following format MOD09GA.AYYYYDD.hXXvYY.005.NNNNNNNNNNNNN_OWLv2p4
filter='MYD09GA*_OWLv2p4'
Files=dialog_pickfile(path='\\WRON\Working\work\cjt\MODIS_Gulf\Daily_OWLs\'', /multiple_files, filter=filter)
NumDates=n_elements(Files)

; loop through for each MOD file
for X=0,NumDates-1 do begin
print,'processing file no. ',X+1,' of ',NumDates

; Open the MYD file
OpenR, InY, Files[X], /get_lun
ReadU, InY, BandY
free_lun, InY

; extract output file name
MYD_filt_start=strmid(Files[X],0,strlen(Files[X])-48)
MYD_filt_end=strmid(Files[X],strlen(Files[X])-47,25)
```

```

; Output MYD as the daily OWL
Outname=MYD_filt_start+'OY'+MYD_filt_end+'.OWLv2p4_max.dat'
OpenW, Out, Outname, /get_lun
WriteU, Out, BandY
free_lun, Out

endfor

end

```

MRT_multiple_resample

```

pro MRT_Multiple_resample
  compile_opt idl2

; This program reads in multiple MODIS MOD09GA images (*.hdf files) and runs the MODIS MRT program
; to output the state band and the reflectance bands required for calculating the OWI in MODIS_OWL.pro
; DONT FORGET TO USE THE CORRECT PARAMETER FILE (.prm)
; Written February 2011

; Use Dialog pick file to get the files of interest.
path='C:'
FileNames=dialog_pickfile(/multiple_files, /read, path=path, filter='M*D09GA*h29v10*.hdf') ; MYD or MOD

; check for any errors
if (FileNames[0] eq '') then begin
  print,'No files selected'
  result=widget_message("No files selected: TERMINATE", /error)
  return
endif

for X=0,n_elements(FileNames)-1 do begin
  print,'X=',X

  ;Run MODIS MRT
  Out_FileName=strmid(FileNames[X],0,strlen(FileNames[X])-3)+'hdr'
  print,'Processing :',FileNames[X]

  SPAWN, 'C:\Documents_CT\Program_Files\MODIS\MRT\Modis\bin\resample -p C:\Projects\GARA\MODIS\MRT_Test_parameterFile_H29V10.prm -i '
+ FileNames[X] + ' -o ' + Out_FileName

  endfor

  print,' Finished! '

end

```

Multi_Image_Stats.pro

```

pro Multi_Image_Stats

; This program reads in a selection of Landsat water images and outputs the maximum and average values (ignoring nulls).
; Written August 2012

compile_opt IDL2

; Read in the files using Dialog pick file.
FileNames=dialog_pickfile(/multiple_files, /read, path='//FILE-WRON/Working/Work/cjt/', filter='*_ENVI_M')

; check for any errors
if (FileNames[0] eq '') then begin
  print,'No files selected'
  result=widget_message("No files selected: TERMINATE", /error)
  return
endif

; Define image size (hardwired - they all must be the same size)
nsamp=9000
nline=8000

Band=bytarr(nsamp,nline)
MaxBand=bytarr(nsamp,nline)
AvBand=fltarr(nsamp,nline)
AvNum=fltarr(nsamp,nline)
AvNum[*,*]=0.
BandOne=bytarr(nsamp,nline)
BandOne[*,*]=1B
; NullMsk=bytarr(nsamp,nline)

; Loop through each Landsat file, calculating the maximum and average water value
for I=0,n_elements(FileNames)-1 do begin

  print,'Processing File ',I+1

  ; Open the OWL file
  OpenR, In, FileNames[I], /get_lun
  ReadU, In, Band
  free_lun, In

; Find water pixels (ignoring clouds/nulls)
  where_water=where(Band eq 2) ; 2 = water
  print,'n_elements where_water=',n_elements(where_water)
  if where_water[0] ne -1 then MaxBand[where_water]=1B

; Calculate average water value (1=non-water 2=water, so just calculating average number of water days in a pixel)
  where_OK=where(Band ne 0) ; 0=nulls
  if where_OK[0] ne -1 then begin
    Band[where_OK]=Band[where_OK]-BandOne[where_OK] ; convert land=0 and water=1
    AvNum[where_OK]=AvNum[where_OK]+BandOne[where_OK]
    AvBand[where_OK]=AvBand[where_OK]*(AvNum[where_OK]-BandOne[where_OK])/AvNum[where_OK] + (Band[where_OK]/AvNum[where_OK])
  endif

```

```
; continue loop until finished
endfor

; Output the images as a flat binary

OpenW, Out, strmid(FileNames[0],0,strlen(FileNames[0])-22)+'_Max', /get_lun
WriteU, Out, MaxBand
free_lun, Out

OpenW, Out, strmid(FileNames[0],0,strlen(FileNames[0])-22)+'_Av', /get_lun
WriteU, Out, AvBand
free_lun, Out

OpenW, Out, strmid(FileNames[0],0,strlen(FileNames[0])-22)+'_AvNum', /get_lun
WriteU, Out, AvNum
free_lun, Out

print, 'Finished!'

end
```

Appendix B Locations of the river where cross-sections were measured

LOCATION		WIDTH	MAX DEPTH	FLOW CONDITION
		(m)	(m)	
DAY 1				
1	Galah/Porcupine CK	70.0	6.5	dry
2	Flinders River at Hughenden	150.0	12.0	dry
3	Walker Ck near Richmond	25.0	3.5	dry
4	Flinders River at Richmond	80.0	25.0	dry
5	Alick Creek	48.0	3.5	dry
DAY 2				
6	Gauging Station on Julia CK	120.0	4.5	
7	D/s of Julia Ck Bridge	38.0	2.5	
8	Gilliat River on Flinders Highway	28.0	4.0	dry
9	Gilliat River on Wills development road	34.0	5.2	dry
10	Cloncurry River on Wills development road	160.0	12.0	dry
11	Corella River	20.0	6.8	dry
12	Dugald River on Wills development road	32.0	7.2	dry
13	Junction of 3 rivers (1 big, 2 small)	130.0	10.0	dry
14	Dismal Ck on Wills development road	10.0	1.5	dry
From Burke development road to Wondoola				dry
15	Unknown creek (possibly Sandy)	30.0	5.5	dry
16	Unknown River (possibly Flinders)	120.0	15.0	dry
17	Saxby Ck	35.0	6.5	dry
18	Name unknown	28.0	3.5	dry
19	Name unknown	45.0	5.5	dry
20	Flinders River	190.0	11.0	dry
21	Norman River	140.0	10.0	water
DAY 3				
22	Smith Burne River			dry
23	Small Ck before Gilbert	22.5	2.5	dry
24	Gilbert River	150.0	6.5	water
25	Vanrook Ck (perhaps outside Gilbert catchment)	15.0	3.5	dry
26	unknown (possibly Middle Ck)	12.0	2.5	dry
27	unknown (a creek immediately after the Gilbert River)	30.0	2.5	dry

28	Fitzmaurice Ck	3.0	1.2	dry
30	unknown	22.0	2.5	dry
31	Walker Ck	90.0	6.5	dry
32	Twelve mile Ck	25.0	1.8	dry
33	Melvil Ck	32.0	2.0	dry
35	Norman River	250.0	6.5	dry
36	Catchment boundary			
37	Balmore Ck	45.0	6.5	dry
41	Carron River	42.0	7.0	dry
42	Little River	26.0	3.5	dry
43	Pleasant Ck			
44	Gilbert River	240.0	5.5	dry
45	Chinaman Ck	18.0	2.5	dry
46	Stockmans Ck	25.0	5.0	dry
DAY 4				
47	Sandy Ck	80.0	4.8	
48	Etheridge River	315.0	7.5	
49	unknown ck			
50	Gilbert River	150.0	15.0	
51	Branch Ck	60.0	2.5	
52	Delaney River	45.0	5.0	
53	Copperfield River	160.0	8.0	
56	Einasleigh River	110.0	4.5	water

Appendix C

Apx Table C.1 Statistical measures used to evaluate model performance (Moriassi et al., 2007)

Measure	Acronym	Formula
Nash-Sutcliffe modelling efficiency	NSE	$\frac{\sum_{i=1}^n (O_i - \bar{O})^2 - \sum_{i=1}^n (S_i - O_i)^2}{\sum_{i=1}^n (O_i - \bar{O})^2}$
Goodness of fit	R^2	$\left[\frac{\sum_{i=1}^n (O_i - \bar{O})(S_i - \bar{S})}{\sqrt{\sum_{i=1}^n (O_i - \bar{O})^2} \sqrt{\sum_{i=1}^n (S_i - \bar{S})^2}} \right]^2$
% of deviation from observed	PBIAS	$\frac{\sum_{i=1}^n (O_i - S_i)}{\sum_{i=1}^n O_i} \times 100$
Mean absolute error	MAE	$\frac{\sum_{i=1}^n O_i - S_i }{n}$
Root mean square error	RMSE	$\sqrt{\frac{\sum_{i=1}^n (S_i - O_i)^2}{n}}$

where, O_i : observed data; S_i : simulated data; \bar{O} : mean observed data during evaluation period.

NSE ranges between $-\infty$ and 1.0 (1 inclusive), with NSE = 1 being the optimal value. Values between 0.0 and 1.0 are generally viewed as acceptable levels of performance, whereas values <0.0 indicates that the mean observed value is a better predictor than the simulated value, which indicates unacceptable performance. An NSE value greater than 0.85 is considered “excellent”, between 0.85-0.75 is considered “good”, values between 0.75 and 0.36 are considered “satisfactory” and values below 0.36 are considered “not satisfactory”.

Percent bias (PBIAS) measures the average tendency of the simulated data to be larger or smaller than their observed counterparts (Gupta et al., 1999). The optimal value of PBIAS is 0.0, with low-magnitude values indicating accurate model simulation. Positive values indicate model underestimation bias, and negative values indicate model overestimation bias (Gupta et al., 1999). An absolute value for PBIAS of less than 10% is considered “excellent”, between 10-20% is considered “good”, values between $\pm 20\%$ and $\pm 40\%$ are considered “satisfactory”, and those greater than $\pm 40\%$ are considered “not satisfactory”.

Mean absolute error (MAE) and root mean square error (RMSE) are valuable because they indicate error in the units (or squared units) of the constituent of interest, which aids in analysis of the results. MAE and RMSE values of 0 indicate a perfect fit.

Appendix D

Apx Table D.1 Estimates of connectivity (number of days) of wetlands to streams in the Flinders floodplain for the flood events of 2001, 2009 and 2011

ID	WETLAND	2001	2009	2011
1	Walker's Creek Weir	0.0	21.3	19.8
2	Mutton Hole Wetland Conservation Park	8.8	27.5	26.0
3	Stranded Fish Lake	20.0	27.5	25.3
4	Shady Lagoon	29.8	33.5	33.8
5	Glenore Weir	30.0	34.0	34.0
6	Burketown crossing	30.3	34.3	34.3
7	Burke & Wills monument	30.3	34.3	34.3
8	Buffalo Lake Aggregation	0.0	0.0	0.0
9	The Sisters	17.5	33.0	33.5
10	Cremeries Waterhole	0.0	8.5	3.0
11	Wallabadah Waterhole	12.5	34.0	34.0
12	Homeward Bound Mine Battery Dam, Croydon	0.0	0.0	0.0
13	Big Mosquito Lagoon	15.5	29.5	30.8
14	Walker's Bend	30.3	34.3	34.3
15	40 Mile Lagoon	30.0	34.0	34.0
16	Margaret Vale	0.0	0.0	0.0
17	Magowra	0.0	0.0	0.0
18	Bloodwood	0.0	0.0	0.0
19	Sydney Harbour	0.0	0.0	0.0
20	BangBang	0.0	0.0	0.0
21	Dead Calf Lagoon	13.5	31.0	21.0
22	Christies	0.0	0.0	0.0
23	Iffley Homestead	30.0	34.0	34.0
24	Off channel	13.8	29.0	18.0
25	Earls Camp	30.3	34.3	34.3
26	12 Mile Lagoon	28.5	30.0	31.0
27	Saxby Rounup	1.5	12.5	0.0
28	10 Mile Waterhole	29.5	34.3	34.3

29	TrentonI	0.0	0.0	0.0
30	Seaward Waterhole	30.3	34.3	34.3
31	SandySpr	0.0	0.0	0.0
32	Muk Quibunya	26.0	33.5	30.5
33	Lyrian Waterhole	30.3	34.3	34.3
34	Tailing yard sps	1.0	5.8	0.0
35	PlainSpr	0.0	0.0	0.0
36	Cattle Camp Sp	0.0	0.0	0.0
37	Stanley Waterhole	30.3	34.3	34.3
38	Cooradine WH	21.3	33.5	25.5
39	Middle Sps	0.0	0.0	0.0
40	boxhole-mud,p	0.0	12.0	0.0
41	Cooradin	0.0	0.0	0.0
42	Mt Fort Bowen Sps (mudsoda,p)	11.3	27.8	15.3
43	mudsoda,p	27.0	28.5	27.0
44	Crocodile Waterhole	30.3	34.3	34.3
45	Crocodile Sps (Mt.Brown E)	3.8	13.3	0.0
46	The Lake	7.3	19.8	3.8
47	mud,p	30.3	34.3	34.3
48	mud,s (Mt Brown/Little)	23.0	31.5	27.0
49	Lower Sps (Mt.BorownD)	2.0	10.3	0.0
50	Washpool Crk Sps (Mt.BorownA)	22.3	34.3	27.5
51	mudsoda,s	6.3	25.5	6.8
52	Reedy Crk Sps (Mt.BorownB)	30.3	34.3	34.3
53	Upper Sps (Mt.BorownC)	30.3	34.3	34.3
54	BundaB1	2.3	7.3	0.0
55	BundamudSps (Cudray Spr?Maitland)	2.3	8.3	0.8
56	Sedan dip	30.3	34.3	34.3
57	Berinda 2	3.0	8.3	0.0
58	Berinda Sps	2.8	7.3	0.0
59	Berindabaremudcratersx2	3.0	9.0	0.0
60	N-GilliatBore	0.0	15.8	5.5
61	Dalgonally Waterhole	30.3	34.3	34.3
62	LaraBoreE,p	0.0	0.0	0.0
63	RuthvenBore,p	0.0	0.0	0.0

64	BoonookeBoreNo7	0.0	0.0	0.0
65	StudPaddBoreNo3,p	0.0	0.0	0.0
66	WindmillBoreNo1-A	0.0	0.0	0.0
67	Rocky Waterhole	30.3	34.3	34.3
68	mud,s	0.0	2.5	0.0
69	Fullarton Bore	0.0	1.5	0.0
70	Bauhinia	0.0	0.0	0.0
71	SpringsBoreNo4	30.3	34.3	34.3
72	mound,p	0.0	3.5	0.0
73	PigeonCrkBore	0.0	0.0	0.0
74	mud,s	0.0	2.5	0.0
75	Punchbowl Waterhole	15.0	32.0	16.5
76	Rockvale Station, Flinders River crossing	30.3	34.3	31.0
77	Fort Const-1	6.5	33.8	13.0
78	Fort Const-main (Alice Sps?)	0.0	2.3	0.0
79	Eddington Waterhole	30.3	34.3	34.3
80	2 Mile Waterhole	30.3	34.3	34.3
81	Southern Gulf	30.3	34.3	0.0
82	Lignum Swamp	2.0	13.0	4.3
83	Fish Habitat - Flinders River mouth	30.3	34.3	34.3
84	Fish Habitat - Bynoe River mouth	30.3	34.3	34.3
85	Fish Habitat - Spring Creek mouth	11.3	28.3	12.8

ApX Table D.2 Estimates of connectivity of wetlands to streams in the Gilbert floodplain for the flood events of 2001, 2009 and 2011

ID	WETLAND	% CHANGE OF CONNECTIVITY DUE TO			
		Wet climate	Dry climate	SLR	Dam empty
1	Walker's Creek Weir	0.6%	-5.8%	23.4%	0.0%
2	Mutton Hole Wetland Conservation Park	9.9%	-27.8%	30.5%	0.0%
3	Stranded Fish Lake	12.1%	-19.0%	31.6%	0.0%
4	Shady Lagoon	0.0%	-0.6%	4.4%	0.0%
5	Glenore Weir	0.0%	0.0%	4.4%	0.0%
6	Burketown crossing	0.0%	0.0%	4.4%	0.0%
7	Burke & Wills monument	0.0%	0.0%	4.4%	0.0%
8	Buffalo Lake Aggregation	0.0%	0.0%	8.8%	0.0%
9	The Sisters	0.0%	-7.7%	6.6%	-0.3%
10	Cremeries Waterhole	0.0%	-4.7%	9.1%	-0.6%
11	Wallabadah Waterhole	0.0%	-8.0%	14.3%	-0.3%
12	Homeward Bound Mine Battery Dam, Croydon	0.0%	0.0%	0.0%	0.0%
13	Big Mosquito Lagoon	7.7%	-27.5%	15.4%	0.0%
14	Walker's Bend	0.0%	0.0%	4.4%	0.0%
15	40 Mile Lagoon	0.0%	-1.4%	4.4%	0.0%
16	Margaret Vale	0.0%	0.0%	0.0%	0.0%
17	Magowra	0.0%	0.0%	0.0%	0.0%
18	Bloodwood	0.0%	0.0%	0.0%	0.0%
19	Sydney Harbour	0.0%	0.0%	0.0%	0.0%
20	BangBang	0.0%	0.0%	0.0%	0.0%
21	Dead Calf Lagoon	17.3%	-23.9%	18.2%	0.0%
22	Christies	0.0%	0.0%	0.0%	0.0%
23	Iffley Homestead	0.0%	-0.8%	4.4%	0.0%
24	Off channel	16.5%	-1.4%	19.8%	-0.6%
25	Earls Camp	0.0%	-3.9%	4.4%	0.0%
26	12 Mile Lagoon	1.1%	-10.2%	3.6%	0.0%
27	Saxby Rounup	3.9%	-5.2%	14.3%	0.0%
28	10 Mile Waterhole	20.6%	-2.8%	11.3%	0.0%
29	TrentonI	0.0%	0.0%	0.0%	0.0%
30	Seaward Waterhole	0.0%	0.0%	4.4%	0.0%
31	SandySpr	0.0%	0.0%	0.0%	0.0%

32	Muk Quibunya	5.8%	-13.2%	4.4%	0.0%
33	Lyrian Waterhole	0.0%	0.0%	4.4%	0.0%
34	Tailing yard sps	0.0%	0.0%	6.3%	0.0%
35	PlainSpr	0.0%	0.0%	0.0%	0.0%
36	Cattle Camp Sp	0.0%	0.0%	0.0%	0.0%
37	Stanley Waterhole	0.0%	0.0%	4.4%	0.0%
38	Cooradine WH	9.6%	-15.1%	4.1%	0.0%
39	Middle Sps	0.0%	0.0%	0.0%	0.0%
40	boxhole-mud,p	4.7%	-4.4%	12.9%	0.0%
41	Cooradin	0.0%	0.0%	0.0%	0.0%
42	Mt Fort Bowen Sps(mudsoda,p)	9.4%	-17.9%	18.4%	0.0%
43	mudsoda,p	3.3%	-28.9%	3.9%	0.0%
44	Crocodile Waterhole	0.0%	0.0%	4.4%	0.0%
45	Crocodile Sps(Mt.Brown E)	6.9%	-6.1%	12.7%	0.0%
46	The Lake	16.8%	-5.5%	14.9%	0.0%
47	mud,p	0.0%	0.0%	4.4%	0.0%
48	mud,s(Mt Brown/Little)	9.1%	-20.6%	6.6%	0.0%
49	Lower Sps(Mt.BorownD)	7.2%	-2.5%	11.0%	0.0%
50	Washpool Crk Sps(Mt.BorownA)	10.2%	-28.9%	11.6%	0.0%
51	mudsoda,s	20.4%	-7.2%	20.9%	0.0%
52	Reedy Crk Sps(Mt.BorownB)	0.0%	-10.7%	4.4%	0.0%
53	Upper Sps(Mt.BorownC)	1.7%	-11.8%	6.1%	0.0%
54	BundaB1	0.0%	-2.8%	7.2%	0.0%
55	BundamudSps(Cudray Spr?Maitland)	0.0%	-7.7%	9.1%	0.0%
56	Sedan dip	0.0%	0.0%	4.4%	0.0%
57	Berinda 2	3.6%	-5.0%	9.1%	0.0%
58	Berinda Sps	1.7%	-1.9%	8.0%	0.0%
59	Berindabaremudcratersx2	3.0%	-6.1%	9.6%	0.0%
60	N-GilliatBore	3.3%	-7.7%	17.6%	0.0%
61	Dalgonally Waterhole	0.0%	0.0%	4.4%	0.0%
62	LaraBoreE,p	0.0%	0.0%	0.0%	0.0%
63	RuthvenBore,p	0.0%	0.0%	0.0%	0.0%
64	BoonookeBoreNo7	0.0%	0.0%	0.0%	0.0%
65	StudPaddBoreNo3,p	0.0%	0.0%	0.0%	0.0%
66	WindmillBoreNo1-A	0.0%	0.0%	0.0%	0.0%

67	Rocky Waterhole	0.0%	0.0%	4.4%	0.0%
68	mud,s	0.6%	-0.6%	3.0%	0.0%
69	Fullarton Bore	0.0%	0.0%	2.5%	0.0%
70	Bauhinia	0.0%	0.0%	0.0%	0.0%
71	SpringsBoreNo4	0.0%	0.0%	4.4%	0.0%
72	mound,p	0.0%	3.6%	3.9%	0.0%
73	PigeonCrkBore	0.0%	0.0%	0.0%	0.0%
74	mud,s	0.6%	-0.6%	3.0%	0.0%
75	Punchbowl Waterhole	7.2%	-19.3%	20.9%	0.0%
76	Rockvale Station, Flinders River crossing	6.1%	-20.1%	8.3%	0.0%
77	Fort Const-1	11.3%	-0.3%	32.7%	0.0%
78	Fort Const-main(Alice Sps?)	1.7%	-0.6%	2.5%	0.0%
79	Eddington Waterhole	0.0%	0.0%	4.4%	0.0%
80	2 Mile Waterhole	0.0%	0.0%	3.0%	0.0%
81	Southern Gulf MIN	0.0%	0.0%	4.4%	0.0%
82	Lignum Swamp	3.3%	-7.7%	13.8%	-3.3%
83	Fish Habitat - Flinders River mouth	0.0%	0.0%	4.4%	0.0%
84	Fish Habitat - Bynoe River mouth	0.0%	0.0%	4.4%	0.0%
85	Fish Habitat - Spring Creek mouth	15.7%	-5.0%	64.6%	0.0%

CONTACT US

t 1300 363 400
+61 3 9545 2176
e enquiries@csiro.au
w www.csiro.au

YOUR CSIRO

Australia is founding its future on science and innovation. Its national science agency, CSIRO, is a powerhouse of ideas, technologies and skills for building prosperity, growth, health and sustainability. It serves governments, industries, business and communities across the nation.

FOR FURTHER INFORMATION

Water for a Healthy Country Flagship

Dushmanta Dutta
t +61 2 6246 5858
e dushmanta.dutta@csiro.au
w csiro.au/Organisation-Structure/Flagships/Water-for-a-Healthy-Country-Flagship.aspx

Fazlul Karim
t +61 2 6246 4526
e Fazlul.karim@csiro.au
w csiro.au/Organisation-Structure/Flagships/Water-for-a-Healthy-Country-Flagship.aspx

Catherine Ticehurst
t +61 2 6246 5842
e Catherine.ticehurst@csiro.au
w csiro.au/Organisation-Structure/Flagships/Sustainable-Agriculture-Flagship.aspx

Steve Marvanek
t +61 8 8303 8440
e steve.marvanek@csiro.au
w csiro.au/Organisation-Structure/Flagships/Sustainable-Agriculture-Flagship.aspx

Cuan Petheram
t +61 2 6246 5987
e cuan.petheram@csiro.au
w csiro.au/Organisation-Structure/Flagships/Sustainable-Agriculture-Flagship.aspx